

RECOMBINANT HUMAN GROWTH HORMONE PRODUCTION BY  
*Pichia pastoris* AND DETERMINATION OF ITS INTERACTION WITH  
PEPTIDE LIGANDS

A THESIS SUBMITTED TO  
THE GRADUATE SCHOOL OF NATURAL AND APPLIED SCIENCES  
OF  
MIDDLE EAST TECHNICAL UNIVERSITY

BY

BAHAR İNANKUR

IN PARTIAL FULFILLMENT OF THE REQUIREMENTS  
FOR  
THE DEGREE OF MASTER OF SCIENCE  
IN  
CHEMICAL ENGINEERING

JULY 2010

Approval of the thesis:

**RECOMBINANT HUMAN GROWTH HORMONE PRODUCTION BY  
*Pichia pastoris* AND DETERMINATION OF ITS INTERACTION WITH  
PEPTIDE LIGANDS**

submitted by **BAHAR İNANKUR** in partial fulfillment of the requirements for the degree of **Master of Science in Chemical Engineering Department, Middle East Technical University** by,

Prof. Dr. Canan Özgen  
Dean, Graduate School of **Natural and Applied Sciences**

\_\_\_\_\_

Prof. Dr. Gürkan Karakaş  
Head of Department, **Chemical Engineering Dept.,**

\_\_\_\_\_

Prof. Dr. Pınar Çalık  
Supervisor, **Chemical Engineering Dept.,**

\_\_\_\_\_

Prof. Dr. Burak Erman  
Co-supervisor, **Chemical and Biological Eng. Dept., Koç U.**

\_\_\_\_\_

**Examining Committee Members:**

Prof. Dr. Ali Çulfaz,  
Chemical Engineering Dept., METU

\_\_\_\_\_

Prof. Dr. Pınar Çalık  
Chemical Engineering Dept., METU

\_\_\_\_\_

Prof. Dr. İsmail Hakkı Boyacı  
Food Engineering Dept., Hacettepe University

\_\_\_\_\_

Assoc. Prof. Dr. Nihal Aydoğan  
Chemical Engineering Dept., Hacettepe University

\_\_\_\_\_

Assist. Prof. Dr. A. Elif Erson Bensan  
Biological Sciences Dept., METU

\_\_\_\_\_

**Date:**

19.07.2010

**I hereby declare that all information in this document has been obtained and presented in accordance with academic rules and ethical conduct. I also declare that, as required by these rules and conduct, I have fully cited and referenced all material and results that are not original to this work.**

Name, Last name : Bahar İnankur

Signature :

## ABSTRACT

### RECOMBINANT HUMAN GROWTH HORMONE PRODUCTION BY *Pichia pastoris* AND DETERMINATION OF ITS INTERACTION WITH PEPTIDE LIGANDS

İnankur, Bahar

M.Sc., Department of Chemical Engineering

Supervisor : Prof. Dr. Pınar Çalık

Co-supervisor : Prof. Dr. Burak Erman

July 2010, 207 pages

In this study, the aim was to achieve high concentration of recombinant human growth hormone (rhGH) production by recombinant *Pichia pastoris* by investigating the effects of various operation parameters and to determine the suitable peptide ligand sequence that shows affinity and specificity to hGH. In this context, firstly the effect of temperature and Tween-20/80 addition on production and cell growth were investigated. While at T=30 and 32°C, there was no difference, at 27 and 25°C cell growth slowed down and production decreased significantly. The addition of Tween-20/80 in existence of co-substrate sorbitol did not affect the bioprocess while in absence of sorbitol Tween alone did not show the same positive effect on product formation and cell growth.

Thereafter at T=30°C, without addition of Tween, three sets of pilot scale bioreactor experiments were performed. In the first set, the effect of

methanol feeding rate on bioprocess characteristics were investigated at the specific growth rates of  $\mu=0.02$ ,  $0.03$  and  $0.04 \text{ h}^{-1}$ . While the highest cell concentration was achieved at  $\mu=0.04 \text{ h}^{-1}$ , the highest rhGH concentration was achieved at  $\mu=0.03 \text{ h}^{-1}$ . Secondly, conducting methanol feeding at  $\mu=0.03 \text{ h}^{-1}$ , pH=5.5 experiment was conducted. The highest cell concentration,  $45 \text{ g L}^{-1}$  and maximum rhGH concentration  $0.25 \text{ g L}^{-1}$  were achieved at  $t=18 \text{ h}$  of the process. Finally, the effect of batch sorbitol feeding on bioprocess was observed by the addition of  $50 \text{ g L}^{-1}$  sorbitol at  $t=0$ ,  $14$  and  $31 \text{ h}$  of the production phase. It was shown that sorbitol addition to the medium increased process duration; hence cells enter stationary phase after a longer production phase. However, the protease concentration continued increasing with respect to time and at the end of the process reached twice the concentration it was obtained with single sorbitol addition case decreasing the rhGH concentration.

In selection of the peptide sequence that shows affinity towards hGH, phage display method was conducted. Additionally the sequences from literature and computational design were used as alternatives. The interaction between these peptides and hGH was investigated by isothermal titration calorimetry and surface plasmon resonance.

**Keywords:** Recombinant human growth hormone, *Pichia pastoris*, feeding strategy, peptide, phage display

## ÖZ

### *Pichia pastoris* İLE REKOMBİNANT İNSAN BÜYÜME HORMONU ÜRETİMİ VE PEPTİT LİGANDLARLA ETKİLEŞİMİNİN İNCELENMESİ

İnankur, Bahar

Yüksek Lisans, Kimya Mühendisliği Bölümü

Tez Yöneticisi : Prof. Dr. Pınar Çalık

Ortak Tez Yöneticisi : Prof. Dr. Burak Erman

Temmuz 2010, 207 sayfa

Bu çalışmada, *Pichia pastoris* ile çeşitli üretim parametrelerinin rekombinant insan büyüme hormonu (rhGH) üretimine etkileri yüksek derişimde ürün üretimini sağlamak amacıyla araştırılmış ve insan büyüme hormonuna afinite ve spesifiklik gösteren peptit dizinlerinin belirlenmesi amaçlanmıştır. Bu bağlamda, çalışmanın ilk bölümünde sıcaklığın ve üretim ortamına Tween-20/80 eklenmesinin rhGH üretimi ve hücre çoğalmasına etkileri araştırılmıştır. T=30 ve 32°C koşulları arasında bir fark görülmezken, 27 ve 25°C'de hücre çoğalmasının yavaşladığı ve dolayısıyla üretimin belirgin düzeyde azaldığı görülmüştür. Sorbitolün ikinci karbon kaynağı olarak kullanıldığı durumda ortama ek olarak Tween-20/80 eklenmesinin biyoprosesi etkilemediği ve sorbitolün ortamda bulunmadığı durumlarda yalnızca Tween eklenmesinin, sorbitol eklenmesi ile aynı pozitif etkiyi yapmadığı gözlemlenmiştir.

Bu çalışmanın sonrasında  $T=30^{\circ}\text{C}$ 'de ve Tween ilavesi yapılmadan, üç set laboratuvar ölçekli biyoreaktör deneyi yapılmıştır. İlk sette, metanol besleme hızının biyoproses karakteristiklerine etkisi  $\mu=0.02, 0.03$  ve  $0.04\text{st}^{-1}$  spesifik hücre çoğalma hızlarında incelenmiştir. En yüksek hücre derişimine  $\mu=0.04\text{st}^{-1}$  koşulunda ulaşılırken, en yüksek ürün derişimi  $\mu=0.03\text{st}^{-1}$  koşulunda elde edilmiştir. İkinci olarak,  $\mu=0.03\text{st}^{-1}$  e bağlı olarak belirlenen methanol besleme profili kullanılarak,  $\text{pH}=5.5$  koşulu denenmiştir. En yüksek hücre derişimine,  $45\text{g L}^{-1}$ , ve maksimum rhGH derişimine,  $0.25\text{g L}^{-1}$ ,  $t=18\text{st}$ 'te ulaşılmıştır. Son olarak, kesikli olarak sorbitol eklenmesinin biyoprosese etkisi  $50\text{g L}^{-1}$  sorbitolun üretim fazının  $t=0, 14$  ve  $31\text{st}$ 'lerinde kesikli olarak eklenmesi ile araştırılmıştır. Ortama sorbitol eklenmesinin üretim süresini uzattığı, böylelikle hücrelerin durağan faza daha geç ulaştığı gösterilmiştir. Ancak, üretim süresi uzadıkça artmaya devam eden proteaz derişimi, proses sonunda tek sefer kesikli sorbitol eklendiği koşuldaki ile proses sonunda görülen proteaz miktarının iki katına çıkmış; proses sonunda elde edilen rhGH derişiminde azalma görülmüştür.

hGH'ye afinite gösterebilecek peptit dizinlerinin seçiminde faj display yöntemi kullanılmıştır. Buna ek olarak, literatürde bulunan ve bilgisayar ortamında dizayn edilen peptitler de alternatif dizinler olarak kullanılmıştır. Peptitler ve hGH etkileşimi izotermal titrasyon kalorimetre ve yüzey plasmon rezonans cihazları ile incelenmiştir.

**Anahtar Kelimeler:** Rekombinant insan büyüme hormonu, *Pichia pastoris*, besleme stratejisi, peptit, faj display

*To my beloved family,*

## ACKNOWLEDGMENTS

I wish to express my sincere gratitude to my supervisor Prof. Dr. Pınar Çalık for her support, guidance and help, in all the possible way, throughout this study.

I am thankful to my co-supervisor Prof. Dr. Burak Erman for designing the peptide ligands and to Prof. Dr. İsmail Hakkı Boyacı for giving me the opportunity to use the Food Engineering Department's laboratories in Hacettepe University and to Assist.Prof.Can Özen and Dr.Deniz Yücel (METU, Molecular Biology and Biotechnology Research Center) for their valuable advices and critics.

I would like to especially thank to Emre Büküşoğlu for loving, encouraging and giving me extreme support in any way possible and also to Tolga Gürol and Serkan Esiner for making me laugh all the time. Moreover, I am thankful for the days spent with Berk, Eda, Sena, Emre Y. and all my friends in Chemical Engineering Department. Without them these 2 years would be harder.

I am grateful to Ceyda Dudak for her friendship and generosity in sharing her invaluable experiences; without her I would not have improved my skills on the use of different analysis tools. It is also a great chance for me to have Elif Soyaslan, Hatice Taşpınar, Merve Şahin in my research group; without their great friendship and support even in sleepless nights, I would not have carried out the requirements of this thesis with success. I am also thankful to Dr. Eda Çelik Akdur, Eda Açıık, Eda Bayraktar, Erdem Boy and Vahideh Anghardi for their advices and support. Additionally, I would like to thank to lab group of Prof.Dr. İsmail Hakkı Boyacı for their friendship and support, making me feel like I was in my own laboratory.

I would like to thank to all academic, administrative and technical staff of Department of Chemical Engineering, METU, for their help and support throughout my education.

My M.Sc. scholarship provider Scientific and Technical Research Council of Turkey (TUBITAK BİDEB-2228) is greatly acknowledged. This work was supported by the Middle East Technical University Research Fund Project and Scientific and Technical Research Council of Turkey (TÜBİTAK-109R015).

Above all, I would like to deeply thank to my family; Cansel, Cihan and İpek İnankur for loving, supporting and encouraging me all through my life.

## TABLE OF CONTENTS

ABSTRACT .....	iv
ÖZ.....	vi
ACKNOWLEDGMENTS.....	ix
TABLE OF CONTENTS.....	xi
LIST OF TABLES .....	xiv
LIST OF FIGURES .....	xvi
LIST OF SYMBOLS AND ABBREVIATIONS .....	xix
CHAPTERS	
1. INTRODUCTION.....	1
2. LITERATURE SURVEY.....	4
2.1 Target Protein: Human Growth Hormone .....	4
2.1.1 Properties of Human Growth Hormone .....	4
2.1.2 Structure of Human Growth Hormone.....	5
2.2 Microorganisms for rhGH Production.....	9
2.2.1 Expression host: <i>Pichia pastoris</i> .....	10
2.2.2 Carbon Source Utilization Pathways of <i>P.pastoris</i> .....	12
2.2.3 Alcohol Oxidase Promoter and Methanol Utilization Phenotypes.....	15
2.2.4 Post-translational Modifications and Protein Secretion .....	17
2.2.5 Proteolytic Degradation.....	18
2.3 Bioreactor Operation Parameters and Medium Composition .....	19
2.3.1 Medium Composition and Feeding Strategy.....	19
2.3.2 Bioreactor Operation Parameters .....	24
2.3.2.1 Temperature .....	24
2.3.2.2 pH .....	25
2.3.2.3 Oxygen Transfer .....	26
2.4 Computation of Bioprocess Characteristics.....	27
2.4.1 Oxygen Transfer Characteristics.....	27
2.4.2 Yield Coefficients and Specific Rates.....	30
2.5 Purification of Human Growth Hormone.....	35
2.5.1 Types of Ligands Used for Affinity Separations .....	37
2.5.2 Peptide Selection .....	43
2.5.2.1 Phage Display .....	43
2.5.2.2 Computational Methods .....	46
2.6 Thermodynamic Interpretation of Protein Ligand Interactions.....	46
2.6.1 Surface Plasmon Resonance (SPR) .....	46
2.6.2 Isothermal Titration Calorimetry (ITC).....	57
3. MATERIALS AND METHODS.....	70

3.1 Chemicals .....	70
3.2 Buffers and Stock Solutions .....	70
3.3 Production .....	70
3.3.1 Microorganism.....	70
3.3.2 Growth Medium and Storage of Microorganisms.....	71
3.3.2.1 Solid Medium.....	71
3.3.2.2 Glycerol Stock Solution and Precultivation Medium.....	71
3.3.2.3 Production Medium .....	73
3.3.3 Recombinant Human Growth Hormone Production.....	75
3.3.3.1 Precultivation .....	75
3.3.3.2 Laboratory Scale Air Filtered Shake Bioreactors.....	76
3.3.3.3 Pilot Scale Bioreactor .....	76
3.3.3.3.1 Bioreactor Operation Parameters.....	78
3.3.3.3.2 Precultivation, Co-Substrate Addition and Methanol Feeding Rate in Fed-Batch Pilot Scale Bioreactor Operations.....	79
3.3.4 Ultrafiltration .....	82
3.3.5 Production Analyses.....	83
3.3.5.1 Cell Concentration .....	83
3.3.5.2 Protein Concentration .....	83
3.3.5.2.1 Total Protein Concentration.....	83
3.3.5.2.2 rhGH Concentration .....	84
3.3.5.2.3 SDS-Polyacrylamide Gel Electrophoresis (SDS-PAGE) .....	84
3.3.5.2.4 Staining the SDS-PAGE Gels.....	85
3.3.5.3 Glycerol, Methanol, Sorbitol Concentrations.....	86
3.3.5.4 Organic Acids Concentrations.....	87
3.3.5.5 Amino Acids Concentrations .....	88
3.3.5.6 Protease Activity .....	89
3.3.5.7 AOX Activity .....	90
3.3.5.8 Oxygen Uptake Rate and Liquid Phase Mass Transfer Coefficient.....	92
3.3 Ligand Selection .....	95
3.4.1 Phage Display .....	95
3.5 Thermodynamic Interpretation of Protein Ligand Interactions.....	107
3.5.1 Surface Plasmon Resonance (SPR) .....	107
3.5.2 Isothermal Titration Calorimetry (ITC).....	112
4. RESULTS AND DISCUSSION.....	115
4.1 Effect of Temperature on Cell Growth and Protein Production.....	116
4.2 Effect of Tween-20/80 addition on Cell Growth and Production.....	119
4.3 Production of Human Growth Hormone by <i>Pichia pastoris</i> in Pilot Scale Bioreactor.....	122
4.3.1 Bioreactor Operation Parameters .....	122
4.3.2 Effect of Methanol Feeding Rate on Bioprocess Characteristics of <i>P.pastoris</i> Producing rhGH .....	123
4.3.2.1 Effect of Methanol Feeding Rate on Sorbitol Consumption Rate.....	124
4.3.2.2 Effect of Methanol Feeding Rate on Cell Growth .....	127
4.3.2.3 Effect of Methanol Feeding Rate on rhGH Production.....	127
4.3.2.4 Effect of Methanol Feeding Rate on Alcohol Oxidase Enzyme Production..	129
4.3.2.5 Effect of Methanol Feeding Rate on Protease Production .....	130
4.3.2.6 Effect of Methanol Feeding Rate on Amino Acid and Organic Acid Concentration Profiles.....	131
4.3.2.7 Effect of Methanol Feeding Rate on Oxygen Transfer Characteristics of the Bioprocess .....	135
4.3.2.8 Effect of Methanol Feeding Rate on Yield Coefficients of the Bioprocess ....	138

4.3.3 Effect of pH on Bioprocess Characteristics of <i>P.pastoris</i> Producing rhGH	139
4.3.3.1 Cell Growth and Sorbitol Consumption Profiles at pH=5.5	140
4.3.3.2 rhGH Production, AOX Activity and Protease Concentration Profiles at pH=5.5	141
4.3.3.3 Organic Acid Concentrations at pH=5.5	143
4.3.3.4 Oxygen Transfer Characteristics of the rhGH Production Process at pH=5.5	144
4.3.4 Effect of Sorbitol Feeding Strategy on Bioprocess Characteristics of <i>P.pastoris</i> Producing rhGH	145
4.3.4.1 Sorbitol Consumption and Cell Growth Profiles	146
4.3.4.2 rhGH Production, AOX Activity and Protease Activity Profile	149
4.3.5.3 Organic Acid Concentration	151
4.3.5.4 Oxygen Transfer Characteristics	152
4.4 Determination of peptides having affinity and selectivity towards hGH	154
4.4.1 Experimental determination of hGH specific peptides: Phage Display	154
4.4.2 Isothermal Titration Calorimetry Studies	157
4.4.3 Surface Plasmon Resonance Studies	160
5. CONCLUSION	164
REFERENCES	168
APPENDICES	
A. BUFFERS AND STOCK SOLUTIONS	187
B. CALIBRATION CURVES	191
C. ELECTROPHEROGRAM OF hGH STANDARD	195
D. MOLECULAR WEIGHT MARKER	196
E. PROPERTIES OF SELECTED PEPTIDES	197
F. ISOTHERMAL TITRATION CALORIMETRY RUNS	199
G. HPLC RESULTS FOR hGH-PEPTIDE BINDING	205
H. SURFACE PLASMON RESONANCE RUNS	206

## LIST OF TABLES

### TABLES

<b>Table 2.1</b> Definition of overall yield coefficients .....	34
<b>Table 3.1</b> The composition of the YPD, solid medium.....	71
<b>Table 3.2</b> The composition of YPD, the first precultivation medium.....	72
<b>Table 3.3</b> The composition of the glycerol stock solution .....	72
<b>Table 3.4</b> The composition of BMGY, second precultivation medium. ....	72
<b>Table 3.5</b> The composition of PTM1 .....	74
<b>Table 3.6</b> The composition of the defined production medium.....	74
<b>Table 3.7</b> The composition of Basal Salt Medium (BSM) .....	75
<b>Table 3.8</b> Parameters of Equation (3.1) for Glycerol and Methanol Fed-Batch Feeding.....	81
<b>Table 3.9</b> Procedure for silver staining .....	86
<b>Table 3.10</b> Conditions for HPLC system for methanol and sorbitol analyses .....	87
<b>Table 3.11</b> Conditions for HPLC system for organic acids analysis .....	88
<b>Table 3.12</b> Conditions for HPLC system for amino acid analyses .....	89
<b>Table 3.13</b> ITC operating conditions .....	114
<b>Table 4.1</b> Variations in specific rates throughout of the fermentation for MS-0.02, MS-0.03 and MS-0.04 conditions. ....	126
<b>Table 4.2</b> Variations in amino acid concentrations with respect to time for different specific growth rates.....	132
<b>Table 4.3</b> Variations in organic acid concentrations with respect to time for different specific growth rates.....	134
<b>Table 4.4</b> Variations in oxygen transfer parameters throughout the bioprocess for different growth rates.....	136
<b>Table 4.5</b> Overall yield coefficients for different specific growth rates.....	139
<b>Table 4.6</b> Variations in specific rates throughout of the fermentation at pH=5.5 .....	141
<b>Table 4.7</b> Variations in oxygen transfer parameters with the cultivation time at pH=5.5 .....	144
<b>Table 4.8</b> Variations in specific rates throughout of the fermentation.....	148
<b>Table 4.9</b> Organic acid concentrations throughout the process .....	152
<b>Table 4.10</b> Oxygen transfer parameters characteristics of the bioprocess .....	154

<b>Table 4.11</b> Amino acid sequences of peptides that show affinity to hGH in phage-ELISA.....	155
<b>Table 4.12</b> Amino acid sequences of computationally designed peptides.	156
<b>Table 4.13</b> Amino acid sequences of literature and modified peptides .....	156
<b>Table 4.14</b> Experiments conducted by ITC and SPR and their computationally estimated ( $\Delta G$ ) values.....	157
<b>Table E.1</b> Properties of selected peptides for interaction determination towards hGH.....	197
<b>Table G.1</b> Conditions for HPLC system for interaction analyses .....	205
<b>Table G.2</b> Preliminary HPLC study for detection of hGH and phage display selected peptides' interaction .....	205

## LIST OF FIGURES

### FIGURES

<b>Figure 2.1</b> Primary and secondary structure of hGH.....	7
<b>Figure 2.2</b> The tertiary structure of hGH .....	8
<b>Figure 2.3</b> Microscopic view of <i>P.pastoris</i> .....	11
<b>Figure 2.4</b> Glycerol utilization pathways in <i>P. pastoris</i> .....	13
<b>Figure 2.5</b> Methanol metabolism in <i>P.pastoris</i> .....	14
<b>Figure 2.6</b> Sorbitol and mannitol metabolism of yeasts.....	15
<b>Figure 2.7</b> Steps involved in oxygen transport from a gas bubble to the cell.....	28
<b>Figure 2.8</b> Schematic view of affinity chromatography.....	38
<b>Figure 2.9</b> Phage Display Procedure.....	45
<b>Figure 2.10</b> Schematic representation of SPR .....	49
<b>Figure 2.11</b> 11-MUA on gold surface .....	52
<b>Figure 2.12</b> An example of a one site binding experiment at different ligand concentrations .....	55
<b>Figure 2.13</b> Schematic diagram of ITC instrument.....	60
<b>Figure 2.14</b> Diagram of ITC equipment; the syringe rotates to provide continuous mixing.....	61
<b>Figure 2.15</b> ITC data. Top: Raw interaction data; bottom: binding curve .....	62
<b>Figure 2.16</b> Effect of $K_a$ on the shape of the titration curve.....	64
<b>Figure 3.1</b> Scale up steps and the pilot scale bioreactor system. ....	77
<b>Figure 3.2</b> Variation in cell concentration with cultivation time in the precultivation phases.....	80
<b>Figure 3.3</b> The predetermined feeding profile for glycerol, calculated for specific growth rate ( $\mu_o$ ) of $0.18 \text{ h}^{-1}$ .....	81
<b>Figure 3.4</b> The predetermined feeding profile for methanol, calculated for specific growth rate ( $\mu_o$ ) of $0.04 \text{ h}^{-1}$ .....	82
<b>Figure 3.5</b> Variation of dissolved oxygen concentration with time in dynamic measurement of $K_{La}$ .....	93
<b>Figure 3.6</b> Evaluation of $K_{La}$ using the Dynamic Method.....	94
<b>Figure 3.7</b> Panning procedure for selection of peptides specific to target protein .....	97
<b>Figure 3.8</b> Sensogram for steps of SPR before analyte injection .....	111
<b>Figure 3.9</b> Binding of ligand to the protein.....	112
<b>Figure 4.1</b> Cell growth profiles at different temperatures.....	117
<b>Figure 4.2</b> Silver stained SDS-PAGE gel view of extracellular proteins produced by <i>Pichia pastoris</i> in laboratory scale air filtered shake bioreactor to observe the effect of temperature on rhGH production at different times of the bioprocesses.....	118

<b>Figure 4.3</b> Silver stained SDS-PAGE gel view of extracellular proteins produced by <i>Pichia pastoris</i> in laboratory scale air filtered shake bioreactor to observe the effect of temperature on final rhGH concentration.....	119
<b>Figure 4.4</b> The effect of Tween-80/20 surfactants on cell growth profiles of <i>P.pastoris</i> producing rhGH in air filtered shake flask bioreactors.....	120
<b>Figure 4.5</b> Silver stained SDS-PAGE gel view of extracellular proteins produced by <i>Pichia pastoris</i> in laboratory scale air filtered shake bioreactor to observe the effect of Tween 20/80 on rhGH production.....	121
<b>Figure 4.6</b> The predetermined feeding profile for methanol, calculated for specific growth rates $\mu_0=0.02 \text{ h}^{-1}$ .....	124
<b>Figure 4.7</b> Variation in cell and sorbitol concentrations with fermentation time for different methanol feeding rates.....	125
<b>Figure 4.8</b> Variation in rhGH concentrations with fermentation time for different methanol feeding rates .....	128
<b>Figure 4.9</b> Silver stained SDS-PAGE gel view of extracellular proteins for different methanol feeding rates. Lane M: protein marker; Lane1: MS-0.02 Lane2: MS-0.03; Lane3: MS-0.04.....	128
<b>Figure 4.10</b> Variation in AOX activity with fermentation time for different methanol feeding rates.....	130
<b>Figure 4.11</b> Variation in total protease concentration activity with fermentation time for different methanol feeding rates .....	131
<b>Figure 4.12</b> Variation in cell and sorbitol concentration with fermentation time for pH=5.5 condition.....	140
<b>Figure 4.13</b> Variation in rhGH concentration and AOX activity with fermentation time for pH=5.5 condition .....	142
<b>Figure 4.14</b> Silver stained SDS-PAGE gel view of extracellular proteins for different pH values.....	142
<b>Figure 4.15</b> Variation in protease concentration with fermentation time for pH=5.5 condition .....	143
<b>Figure 4.16</b> Sorbitol consumption profile for <i>P.pastoris</i> producing rhGH .	147
<b>Figure 4.17</b> Cell growth profile for <i>P.pastoris</i> producing rhGH .....	147
<b>Figure 4.18</b> Variation in rhGH concentration with fermentation time.....	149
<b>Figure 4.19</b> Silver stained SDS-PAGE gel view of extracellular proteins for different feeding strategies .....	150
<b>Figure 4.20</b> Variation in protease concentration and AOX activity (dashed lines) with fermentation time .....	151
<b>Figure 4.21</b> Phage clones that bind to hGH in ELISA.....	154
<b>Figure 4.22</b> ITC diagram for titration of 15 $\mu$ M hGH with 1.07mM peptide	158
<b>Figure 4.23</b> Dilution experiments for literature peptide.....	159
<b>Figure 4.24</b> Data fitting for hGH-peptide binding at pH=9.0.....	160
<b>Figure 4.25</b> SPR sensogram showing steps involved prior to peptide binding .....	161
<b>Figure 4.26</b> SPR sensogram for peptide 3/19 at different peptide concentrations .....	162
<b>Figure 4.27</b> $k_{\text{obs}}$ vs peptide 3/19 concentrations.....	163

<b>Figure B.1</b>	Standard curve for Bradford Assay.....	191
<b>Figure B.2</b>	HPLC Analysis: calibration curve obtained for methanol concentration .....	191
<b>Figure B.3</b>	HPLC Analysis: Calibration curve for sorbitol concentration.....	192
<b>Figure B.4</b>	Calibration curve for succinic acid concentration.....	192
<b>Figure B.5</b>	Calibration curve for maleic acid concentration .....	192
<b>Figure B.6</b>	Calibration curve for glutaric acid concentration.....	193
<b>Figure B.7</b>	Calibration curve for lactic acid concentration.....	193
<b>Figure B.8</b>	Calibration curve for formic acid concentration .....	193
<b>Figure B.9</b>	Calibration curve for citric acid concentration.....	194
<b>Figure B.10</b>	Calibration curve for fumaric acid concentration.....	194
<b>Figure B.11</b>	Calibration curve for formaldehyde concentration .....	194
<b>Figure C.1</b>	Electropherogram of 0.05 g L <sup>-1</sup> hGH standard .....	195
<b>Figure D.1</b>	PageRuler™ Prestained Protein Ladder.....	196
<b>Figure F.1</b>	(a) 20μM hGH+500 μM P-1, in pH=7, 10mM Phosphate Buffer..	199
	(b) 20μM hGH+500 μM P-3, in 10mM PB.....	199
	(c) 15μM hGH+450 μM P-4, in pH=7, 10mM PB+100mM NaCl..	199
	(d) Dilution B.+450 μM P-4, in pH=7, 10mM+100mM NaCl.....	199
<b>Figure F.2</b>	(a) 20μM hGH+600μM P-5, in pH=7 10mM PB+100mM NaCl..	200
	(b) 15μMhGH+450μM P-4, in pH=3.5 10mM CB+100mM NaCl..	200
	(c) 15μMhGH+450μM P-4, in pH=4.5 10mM CB+100mM NaCl..	200
	(d) 15μMhGH+450μM P-4, in pH=5.5 10mM CB+100mM NaCl..	200
<b>Figure F.3</b>	(a) 15μM hGH+450μM L, in pH=7.5 PBS Buffer.....	201
	(b) 18 μM hGH+450 μM L, in pH=7.5 30mM HEPES Buffer .....	201
	(c) 18 μM hGH+395 μM L, in pH=5.5 30mM HEPES .....	201
	(d) 15 μM hGH+450 μM L, in pH=6.5 30mM Tris- Buffer .....	201
<b>Figure F.4</b>	(a) 15μM hGH+1.3mM 3/8, in pH=7.5mM HEPES+50mM NaCl..	202
	(b) 15μM hGH+1mM 3/6, in pH=7.5 10mM Tris+50mM NaCl..	202
	(c) 18μM hGH+1.15mM 3/7, in pH=7.5 10mMTris+50mMNaCl..	202
	(d) 15μM hGH+1.27mM 3/, in pH=7.5 10mMTris+50mM NaCl..	202
<b>Figure F.5</b>	(a) 15μM hGH+1 mM 3/8, in pH=8.5 30mM Tris+50mM NaCl....	203
	(b) 20μM hGH+1.34mM 3/8, in pH=7.5 TBS .....	203
	(c) 20μM hGH+1.34mM 3/5, in pH=7.5 TBS.....	203
	(d) 15μM hGH+1.275mM 2/2-3/9, in pH=7.5 TBS .....	203
<b>Figure F.6</b>	(a) 15μM hGH+1.115 mM 3/29, in pH=7.5 TBS.....	204
	(b) 15μM hGH+1.035mM 3/16, in pH=7.5 TBS.....	204
	(c) 15μM hGH+1.153mM 3/31, in pH=7.5 TBS.....	204
	(d) 15μM hGH+0.756mM 3/31, in pH=7.5 TBS.....	204
<b>Figure H.1</b>	Sensogram for P-1 binding to hGH.....	206
<b>Figure H.2</b>	Sensogram for P-1 binding to hGH.....	206
<b>Figure H.3</b>	Sensogram for P-2 binding to hGH.....	206
<b>Figure H.4</b>	Sensogram for 3/8 binding to hGH.....	207
<b>Figure H.5</b>	Sensogram for 2/2-3/9 binding to hGH .....	207
<b>Figure H.6</b>	Sensogram for 2/2-3/9 binding to hGH .....	207
<b>Figure H.7</b>	Sensogram for 2/2-3/9 binding to hGH .....	207

## LIST OF SYMBOLS AND ABBREVIATIONS

C	Concentration in the medium	$\text{g L}^{-1}$ or $\text{mol m}^{-3}$
$C_0^*$	Saturated dissolved oxygen concentration	$\text{mol m}^{-3}$
Da	Damköhler number ( $=\text{OD}/\text{OTR}_{\text{max}}$ ; Maximum possible oxygen utilization rate per maximum mass transfer rate)	
DO	Dissolved oxygen	%
E	Enhancement factor ( $=K_{L,a} / K_{L,a_0}$ ); mass transfer coefficient with chemical reaction per physical mass transfer coefficient	
$K_{L,a}$	Overall liquid phase mass transfer coefficient	$\text{s}^{-1}$
$K_{L,a_0}$	Physical overall liquid phase mass transfer coef.	$\text{s}^{-1}$
N	Agitation rate	$\text{min}^{-1}$
OUR	Oxygen uptake rate	$\text{mol m}^{-3} \text{sec}^{-1}$
OTR	Oxygen transfer rate	$\text{mol m}^{-3} \text{sec}^{-1}$
OD	Oxygen demand	$\text{mol m}^{-3} \text{sec}^{-1}$
Q	Feed inlet rate	$\text{L h}^{-1}$
q	Specific formation or consumption rate	$\text{g g}^{-1} \text{h}^{-1}$
r	Formation or consumption rate	$\text{g L}^{-1} \text{h}^{-1}$
t	Cultivation time	h
T	Bioreaction medium temperature,	$^{\circ}\text{C}$
U	One unit of an enzymatic activity	
V	Volume of the bioreactor	L
Y	Yield (overall)	$\text{g g}^{-1}$
R	Response	
$\Delta H$	Enthalpy of binding	$\text{kcal mol}^{-1}$
$\Delta G$	Free energy of binding	$\text{kcal mol}^{-1}$
$\Delta S$	Entropy of binding	$\text{kcal mol}^{-1} \text{K}^{-1}$
$\Delta C_p$	Specific heat of binding	$\text{kcal mol}^{-1} \text{K}^{-1}$

### Greek Letters

$\rho$	Density	$\text{g L}^{-1}$
$\eta$	Effectiveness factor ( $=\text{OUR}/\text{OD}$ )	
$\mu_0$	Desired specific growth rate	$\text{h}^{-1}$
$\mu_{s,\text{max}}$	Maximum specific growth rate on sorbitol	$\text{h}^{-1}$
$\mu_t$	Total specific growth rate	$\text{h}^{-1}$
$\lambda$	Wavelength	nm

## **Subscripts**

0	initial condition
AOX	alcohol oxidase
G	Glycerol
M	Methanol
O	Oxygen
pro	protease
S	Sorbitol or substrate
P	Product
X	Cell
rp	Recombinant protein
A	association
D	dissociation
fwd	forward
rev	reverse
T	total

## **Abbreviations**

CDW	Cell dry weight
EPO	Human erythropoietin hormone
hGH	Human growth hormone
rhGH	Recombinant human growth hormone
SDS-PAGE	Sodium dodecylsulfate-polyacrylamide gel electrophoresis
HPCE	High pressure capillary electrophoresis
HPLC	High pressure liquid chromatography
ITC	Isothermal titration calorimetry
SPR	Surface plasmon resonance

# CHAPTER 1

## INTRODUCTION

Starting from the 20<sup>th</sup> century, especially in the last few decades, the increasing demand for medical, agricultural and food products lead to studies that combine biological sciences and engineering disciplines (such as computer, food, chemical, environmental, electronics and material engineering) in order to improve human health and environment. With the advances in biological process engineering, new methods began to be developed in order to first produce and then optimize the production and downstream processing of the bio-products to overcome the demand in the market.

The human based therapeutic drugs are derived from natural biomolecules in the body such as hormones, enzymes, antibodies and lymphokines. With the advances in recombinant DNA technology, it is now possible to produce these biomolecules in an organism other than its natural source (Nielsen et al., 2003) by cloning targeted gene responsible for the production of the desired bio-molecules into the genome of a different organism depending on required characteristics of production and target biomolecule

There are a number of well-known recombinant therapeutic proteins in the market such as erythropoietin (EPO), interferon  $\alpha$ , human growth hormone (somatotropin or hGH), human insulin, rec. hepatit B vaccine, gronulocyte colony stimulating factor (G-CSF) and tissue plasminogen activator (tPA). As one of these therapeutic proteins, human growth

hormone (hGH) is a non-glycosylated hormone with various functions such as cell production and regeneration, protein, lipid and carbohydrate metabolisms (Tritos and Mantzoros, 1998). hGH is widely used in treatments of various diseases like hypo-pituitary dwarfism, injuries, bleeding ulcers, bone fractures, and burns (Roehr, 2003). Moreover, it is useful in treatment of children with long stature, chronic kidney failure, Turner's syndrome, adults with growth hormone deficiency or HIV syndrome (Baulieu et al., 1990; Binkley., 1994; Trevino et al., 2000).

In 1956 hGH was isolated from human pituitaries for the first time. Later, recombinant production of hGH by *Escherichia coli* was first achieved by Goeddel et al (1979). Then, production by *E. coli* was further developed by the studies of Gray et al. (1985), Becker et al. (1986), Kato et al. (1987), Hsiung et al. (1989), Shin et al. (1998b) and Tabadeh et al. (2004). In addition to *E. coli* other expression host *Bacillus subtilis* (Nakayama et al., 1988; Franchi et al., 1991; Kajino et al., 1997; Özdamar et al., 2009), and eukaryote hosts baker's yeast-*Saccharomyces cerevisiae* (Tokunaga et al., 1985) and methylotropic yeast *Pichia pastoris*, with the capability of performing posttranslational modifications and high secretion capacity, (Trevino et al., 2000; Eurwilaichitr et al., 2002; Orman, 2008) were used to produce rhGH.

The recombinant therapeutic proteins produced by various microorganisms need to be prepared in large quantities with almost 100% purity in order to be used clinically. Hence, the major goal in recombinant protein production can only be achieved with an efficient purification method with high yields. Generally for purification of proteins, combinations of different methods, that are hard to control and often provide low efficiencies, need to be applied (Cautrecasas et al., 1968). For purification purpose one or more steps of affinity chromatography applications are one of the most commonly used methods. The first step for affinity purification is to select the ligand that binds specifically to the target protein. For that

purpose among various ligand options such as antibodies, metal ions, dyes, aptamers; peptides are new and advantageous options as they do not require any modification on the target, bind specifically with high affinity, allow recovery of specific proteins with low elution conditions and usually are lower in cost. The selection of these peptides can be done using several tools such as in vitro phage display or computational design.

In this context, first aim of the study was to increase rhGH production by *Pichia pastoris* through investigating the effects of various operation parameters; and second aim was to determine the suitable peptide ligand sequence that shows affinity and specificity to hGH by experimentally using phage display technology and by using the computationally designed peptides.

## CHAPTER 2

### LITERATURE SURVEY

For efficient recombinant protein production, the properties of the target protein, characteristics of the host microorganism and optimum production conditions, should be investigated in detail. For understanding effect of production conditions on the microorganism in terms of growth, protein and by product formation, oxygen consumption, the yield coefficients, oxygen transfer characteristics and the specific production and consumption rates should be defined.

Moreover, the efficient purification of the target protein is as important as its production. Hence, suitable separation method and tools should be selected and the dynamics of the separation process should be well understood.

In this context, this chapter reviews the literature on the product, hGH; effect of bioprocess operation parameters on the selected microorganism, *Pichia pastoris*; protein separation methods and thermodynamic techniques for the analysis of hGH and peptide ligand interaction.

#### **2.1 Target Protein: Human Growth Hormone**

##### **2.1.1 Properties of Human Growth Hormone**

Most of the hormones are the proteins that are specialized to serve as chemical messengers from a cell or a group of cells and as a signal to the

target cells. They have wide effects on human body such as stimulation or inhibition of growth, induction or suppression of apoptosis, activation or inhibition of the immune system, regulation of the metabolism and preparation for a new activity or phase of life (Baulieu and Kelly, 1990; Binkley, 1994). One of the crucial hormones produced by human body is growth hormone (GH). It is secreted by the somatotroph cells of the anterior pituitary gland. This pituitary gland derived growth hormone was first described in 1921 by Evans and Long (1921). Then Li and Evans (1944) isolated the pituitary human growth hormone (hGH). The isolation of the hormone was a big improvement for treatment of the people who are suffering from hypopituitary dwarfism, Turner's syndrome, human immune deficiency syndrome (HIV) and for treatment of children with chronic renal failure and with short stature. Moreover, hGH is used in the treatment of burns, bleeding ulcers and bone fractures (Tritos and Mantzoros, 1998; Trevino et al., 2000; Krysiak et al., 2007). Therefore, after its isolation hGH was used for the first time in 1960s for treatment of hGH deficient children (Kopchick, 2003). However, as the hGH for clinical use could only be obtained from the pituitary glands of limited number of cadavers, the extended need for hGH necessitated the production of this hormone using genetic engineering techniques. By genetic engineering, the genes responsible for hGH production are isolated and the cDNA encoding hGH was cloned to bacteria as host microorganism for recombinant production (Martial et al., 1979). In 1979, Goeddel et al. achieved production of recombinant hGH for the first time and Gray et al. (1985) produced hGH in the native form, by the host microorganism *E. coli*. Also in 1985, recombinant hGH was approved for clinical use (Kopchick, 2003).

### **2.1.2 Structure of Human Growth Hormone**

hGH is a non-glycosylated polypeptide chain produced by the pituitary glands. Having the genes located in q22-24 region of chromosome

17 of human, the native form of hGH is composed of 191 amino acids with a molecular mass of approximately 22 kDa (Kasimova et al., 2002). The net charge of hGH at pH=7.0 is -4.9 and pI ranges between 4.9-5.1 (Binkley, 1994). The ratio of the hydrophilic residues to total number of residues is 45% (www.innovagen.se).

The structure of hGH was determined by circular dichroism studies at different pH values (Bewley et al., 1969; Bewley and Li, 1972). In those studies,  $\alpha$ -helix content of hGH was calculated and pH=8.2 was found to have slightly higher  $\alpha$ -helix content than pH=3.6 condition. After these first attempts, the crystal structure of hGH was first given in the study by Abdel-Meguid et al. (1987). It was found that hGH is composed of four- $\alpha$ -helix structure in which the helices are arranged in up-up-down-down topology in addition to the two disulfide bonds. The four helices are located between amino acid residues of 9-34,72-92,106-128 and 155-184. Three shorter connective  $\alpha$ -helices are also present in hGH: two of them 1-2 and two between alpha helices 2-3. hGH also contains hydrophobic central core that is composed of approximately 20 hydrophobic amino chains (Kopchick, 2003). Moreover, the disulfide bridges link the residues Cys<sup>53</sup>-Cys<sup>165</sup>, Cys<sup>182</sup>-Cys<sup>189</sup>. The protein data bank code for this native form of hGH is 1HGU (www.pdb.org/pdb/explore.do?structureId=1HGU). For 1HGU, the amino acid sequence as well as the disulfide bridges and helices; i.e. both primary and secondary structure are indicated in Figure 2.1.

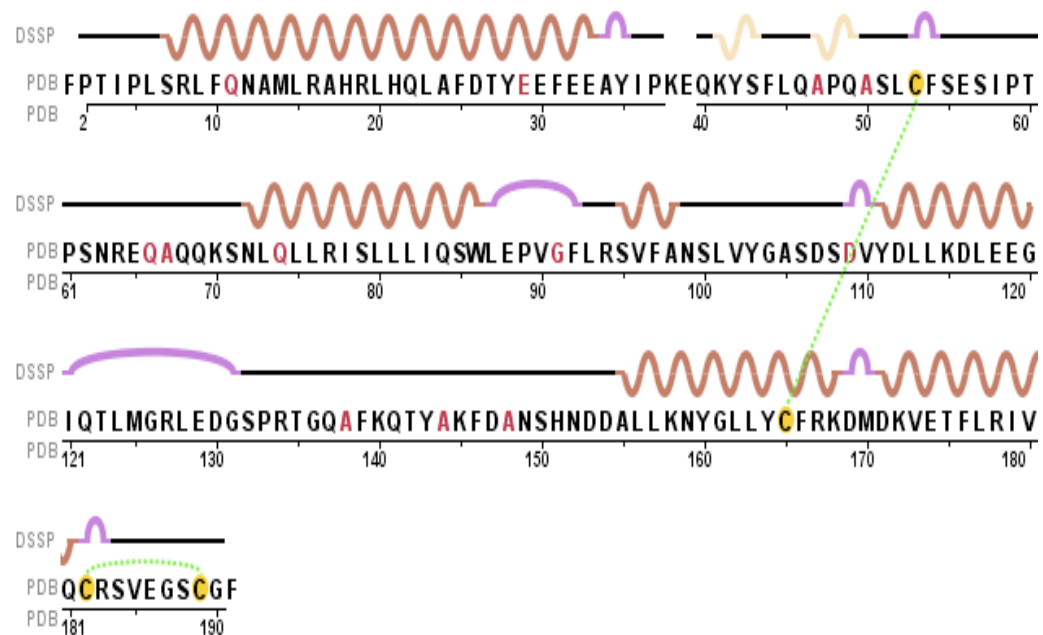


**Figure 2.1** Primary and secondary structure of hGH; the brown and purple curves indicate the major  $\alpha$ -helices; pale pink curves are shorter connective  $\alpha$ -helices; green dashed lines show the disulfide bridges between Cys residues.(<http://www.pdb.org/pdb>)

The positions of the  $\alpha$ -helices and disulfide bonds are important for determination of tertiary structure of hGH which is useful for understanding the interaction of hGH with other molecules. The tertiary structure of hGH is given schematically in Figure 2.2.

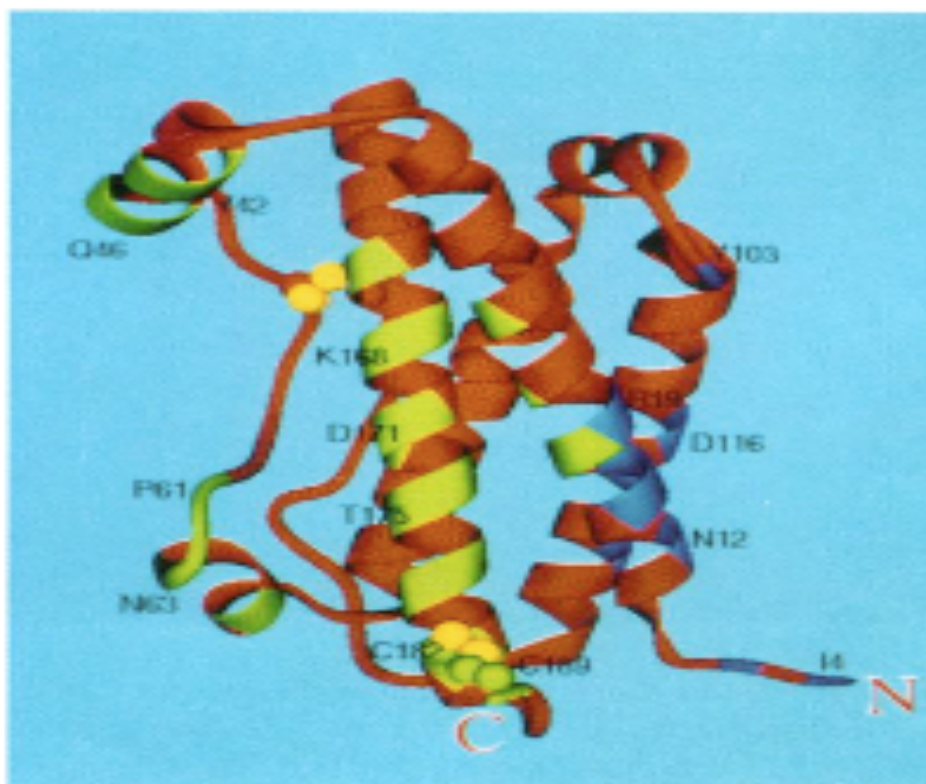


**Figure 2.2** The tertiary structure of hGH; C and N represents carboxyl and amino terminus of the protein respectively; Green and blue regions indicate the interface regions of the protein with its two receptors (de Vos et al., 1992).

The further investigations of hGH revealed that the protein forms complex with its receptors. The examination by de Vos et al., (1992) under 2.8 Å resolution showed that the complex consists of two identical receptors binding to one growth hormone from two different sites. Moreover, Sunstrom et al. (1996) and Clackson et al. (1998) conducted the structural and functional analysis of 1:1 growth hormone by forming a variant of hGH which the mutation prevents 2<sup>nd</sup> receptor's binding in order to understand the role of each side chain of hGH receptors. Moreover, in all these three studies the amino acids that get in contact with each other are determined as the active sides for complex formation (Figure 2.2).

## 2.2 Microorganisms for rhGH Production

As mentioned previously, in order to supply the demand for human growth hormone, recombinant production is required. In bioprocesses, the selection of host microorganism for production of industrial proteins is critical for the process. Potential hosts should give sufficient yields, be able to secrete large amounts of protein, be suitable for industrial fermentations; should be cheap on medium components, be considered as safe, and should not produce harmful substances or any other undesirable products (Kirk and Othmer, 1994). For that purpose, until now several host microorganisms were employed for production of rhGH. The first and most extensively used microorganism was *Escherichia coli* (*E.coli*) (Goeddel et al., 1979; Gray et al., 1985; Hsiung et al., 1986; Kato et al., 1987; Shin et al., 1998; Patra et al., 2000; Tabandeh et al., 2004; Singh et al., 2009). While some of the productions are intercellular some are extracellular and as most of hGH productions takes place in inclusion bodies, the subsequent purification of hGH is hard to achieved. Moreover, although *E.coli* fermentations are cheap in terms of medium requirements and due to their fast growth rate fermentation processes are fast, as *E.coli* is not capable of post-translational modifications, which are very important for the protein to take its active form, such as glycosylation and disulfide bond formation.

One alternative to *E.coli* is the *Bacillus subtilis* (*B. subtilis*) that is used for rhGH production (Nakayama et al., 1988; Franchi et al., 1991; Özdamar et al., 2009). One very important problem that arises related with *B.subtilis* is the high protease production rate. As the proteases lead to breaking-down of proteins in order to reach high production efficiencies protease formation should be reduced. For that purpose either protease inhibitors are added (Özdamar et al., 2009) or protease deficient strains are used.

Other than prokaryotic organisms, being eukaryotic cells; yeasts also provide higher fermentation efficiencies (high density production) and are

additionally capable of performing post-translation modifications. Therefore, for rhGH production the use of yeasts is a better option. The methylotropic yeast *P.pastoris* has been started to be used widely as an expression host for heterologous recombinant production of various proteins (Macauley-Patrick et al., 2005). Related with rhGH production, the first study was conducted by Trevino et al. (2000). In this study, they achieved 49mg L<sup>-1</sup> production of mature and active rhGH using 2L bioreactor. Eurwilaichitr et al. (2002) produced rhGH by using three different vectors and determined the optimum medium condition for production as complex medium with 3% (v/v) methanol concentration and obtained the highest rhGH concentration of 190 mg L<sup>-1</sup> after 3 days of induction. In another study, Çalık et al. (2008) and Orman et al. (2009), firstly constructed the plasmid, *pPICZαA::hGH*, then integrated the plasmid into two different strains of *P.pastoris*. In the second part of the study, the batch cultivations for the two strains Mut<sup>+</sup> and Mut<sup>-</sup> were optimized and the highest rhGH concentration was obtained as 110 mg L<sup>-1</sup> by Mut<sup>+</sup> strain in defined medium with 1% (v/v) methanol and 30 g L<sup>-1</sup> mixed substrate concentrations. Moreover, Açık (2009) and Bayraktar (2009) conducted methanol fed-batch experiments on Mut<sup>+</sup> strain and investigated the effect of carbon sources and pH on the effect of rhGH production respectively. They achieved 301 mg L<sup>-1</sup> and 270 mg L<sup>-1</sup> product concentrations. In a recent study, while the our study was continuing, Apte-Deshpande et al. (2009) added Tween-20 to fermentation medium while conducting linear methanol fed-batch process and that increased the rhGH expression to 500 mg L<sup>-1</sup>.

### **2.2.1 Expression host: *Pichia pastoris***

*P.pastoris* is a methylotropic, facultative anaerobic, chemo-heterotroph yeast. It has the typical structure of yeast with a width of 1-5µm and a thick cell wall (Figure 2.3). *P. pastoris* is a mesophilic microorganism as it is able to live at mild temperatures around 25-35 °C (Macauley-Patrick

et al., 2005). One advantage of *P.pastoris* is that it can also grow at a very wide range of pH between 3.0-7.0 (Cereghino and Cregg, 1999).



**Figure 2.3** Microscopic view of *P.pastoris*  
([www.fz-juelich.de/ibt/ferm/cuvers/htm](http://www.fz-juelich.de/ibt/ferm/cuvers/htm))

*P.pastoris* has many advantages over other microorganisms. It combines the ability of growing on minimal medium at very high cell densities. The production medium for *Pichia* processes are mainly simple chemically defined media with inexpensive formulation (Cos et al., 2005). It is capable of producing proteins extracellularly at high levels, facilitating the subsequent purification (Macauley-Patrick et al., 2005). It has advantages of eukaryotic cell; it is genetically easy to manipulate and has eukaryotic protein synthesis pathway that enables this yeast to perform many post-translational modifications (Cereghino et al., 2002). Moreover, it is non-pathogenic and does not have endotoxin problems (Daly and Hearn, 2005). On the other hand, one important disadvantage of *Pichia* fermentations is the slower growth rate of the yeast compared with bacteria; hence the

cultivation durations are longer. The other disadvantage is the necessity to use the petrochemical hazardous substance, methanol, as a carbon source.

The most important feature of *P. pastoris* is the alcohol oxidase one promoter (AOX1), the strongest and tightly regulated promoter known (Cereghino and Cregg, 2000). As methanol induces protein production through AOX1 promoter, it acts both as a carbon source and inducer. Working on this property of *P. pastoris*, The Phillips Petroleum Company was the first to develop media and procedure for growing *Pichia pastoris* during 1970s (Cereghino and Cregg, 2000). Thereafter, hundreds of proteins have been produced by *P.pastoris*.

### **2.2.2 Carbon Source Utilization Pathways of *P.pastoris***

As a standard protocol, *P. pastoris* fermentations are realized in two phases; growth and production. Before protein production (methanol induction) in order to reach high cell densities glycerol is used as a sole carbon source. The reason for using glycerol instead of methanol is due to the higher specific growth rate on glycerol ( $0.18 \text{ h L}^{-1}$ ) (Cos et al., 2006). Once glycerol is depleted, a production phase is initiated by methanol feeding. The glycerol pathway is shown schematically in Figure 2.4.

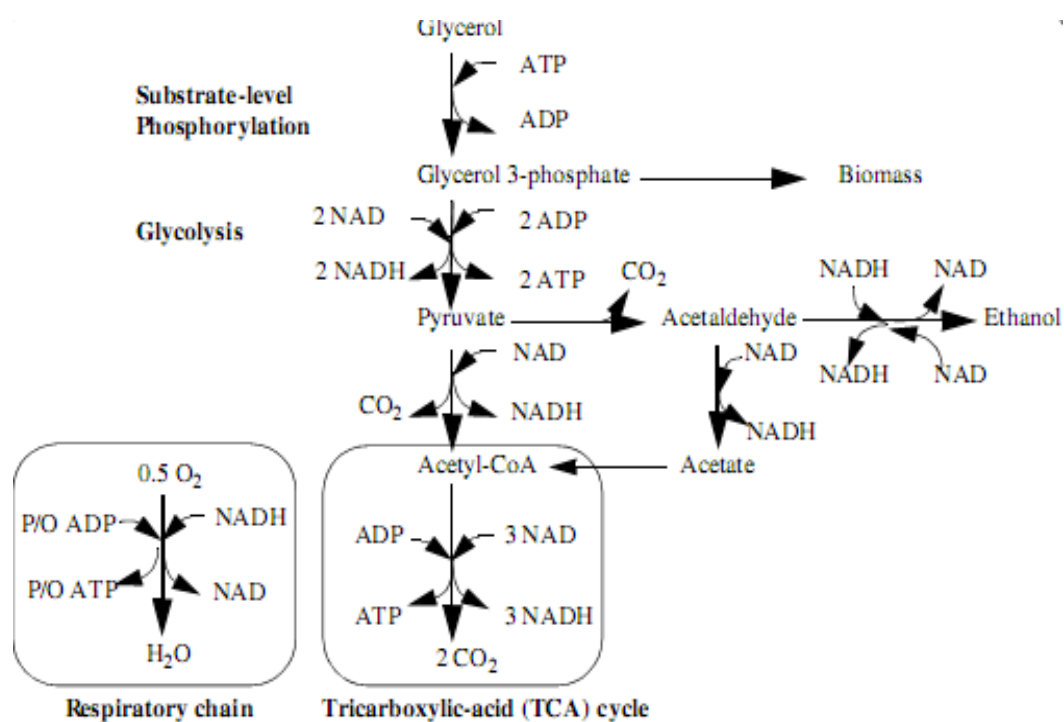


**Figure 2.4** Glycerol utilization pathways in *P. pastoris* (Ren et al., 2003).

The basis for the *P. pastoris* expression procedure arises from the finding that some of the enzymes that are required for methanol utilization pathway are only present at substantial amounts only if the cells were grown on methanol. The first reaction in the metabolism begins with the help of AOX, which catalyzes the oxidation of methanol to formaldehyde and hydrogen peroxide. By catalase the hydrogen peroxide formed in the first reaction is converted to oxygen and water. While some portion of formaldehyde leaves peroxisome and is further oxidized to formate and carbondioxide, the remaining portion reacts by xylulose-5-monophosphate forming glyceraldehyd-3-phosphate and dihydroxyacetone. These two products enter the cytoplasmic pathway for reproduction of xylulose 5-monophosphate and other cell materials. Methanol utilization pathway that is shown by the Figure 2.5 is the pathway through which product formation takes place.

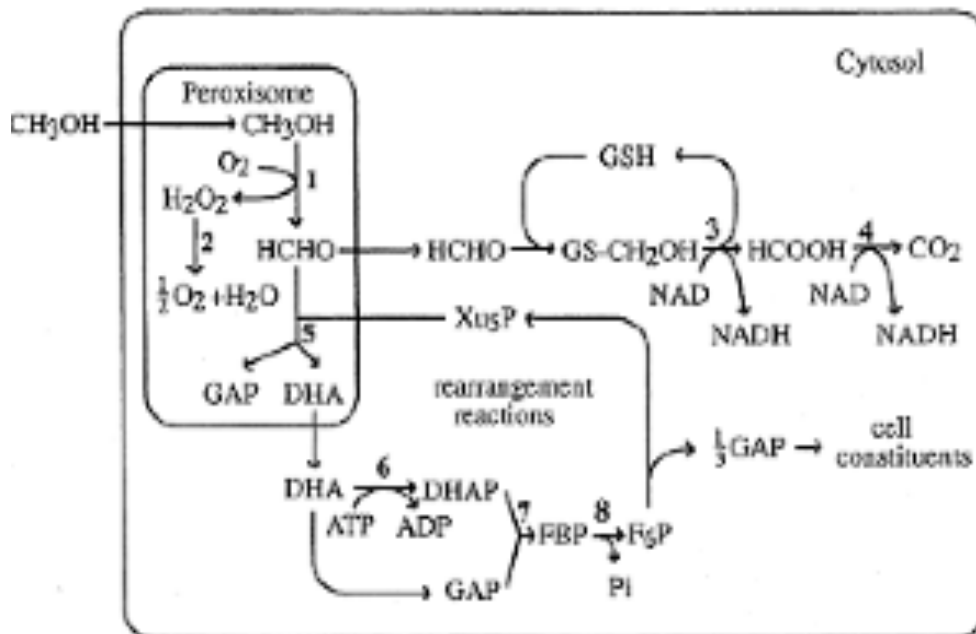


**Figure 2.5** Methanol metabolism in *P.pastoris*. Numbers indicate the enzymes: 1- AOX; 2- Catalase; 3- formaldeyhde dehydrogenase; 4- formate dehydro-genase; 5-dihydroxyacetone synthase;6- dihydroxyacetone kinase; 7-fructose 1,6 biphosphate aldolase; 8-fructose 1,6-biphosphatase (Cereghino and Cregg, 2000).

Recently, for the improvement of production efficiency reaching higher recombinant protein concentrations, during production phase the use of several other carbon sources on addition to methanol has been investigated (Cos et al., 2006). As in this study the sorbitol is used as the co-substrate the sorbitol utilization pathway is given in Figure 2.6.

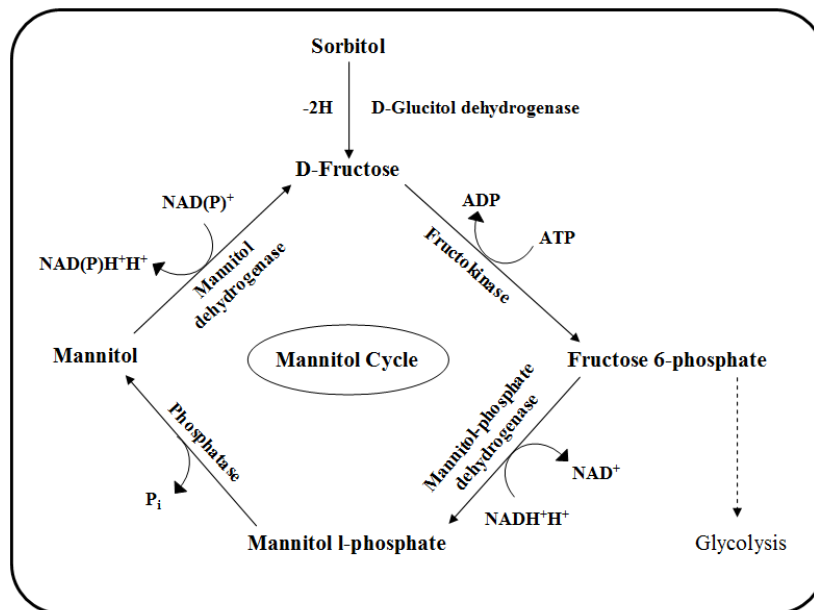


**Figure 2.6** Sorbitol and mannitol metabolism of yeasts (Walker, 1998)

### 2.2.3 Alcohol Oxidase Promoter and Methanol Utilization Phenotypes

As mentioned, the production of recombinant proteins is desirable under the control of strong and tightly regulated AOX1 promoter (Jahic et al., 2006). AOX1 is advantageous since the protein transcription is tightly regulated by depression/redepression mechanism; high levels of production can be achieved; the repression of transcription by the initial carbon source (glycerol) provides higher cell concentration before production begins. The increase in cell concentration when cells are not producing product is directly related with the shift of the metabolic reactions toward growth reactions. On the other hand, the major problem related with *P.pastoris* is the use of methanol, which is a hazardous chemical. One other challenge is the monitoring problems related with methanol (Cereghino and Cregg, 2000).

In fact, one other promoter, AOX2, also exists in *P.pastoris*. While AOX1 gene regulates 85% of the alcohol oxidase activity, AOX2 gene yields 10-20 times less activity (Zhang et al., 2000).

*P. pastoris* uses methanol as a sole carbon and sole energy source. There are three phenotypes of *P. pastoris* host strains with respect to methanol utilization;

- **Methanol utilization plus phenotype (Mut<sup>+</sup>):** Grow on methanol at wild type rate since it uses AOX1, but it requires high feeding rates of methanol, a petroleum by-product, in large-scale fermentations (Cereghino and Cregg, 2000). The maximum specific growth rate for Mut<sup>+</sup> strain is 0.14h<sup>-1</sup> (Jungo et al., 2006). In literature there are several studies in which Mut<sup>+</sup> strain was used for recombinant protein productions (Sinha et al., 2003; Jungo et al., 2006; Çelik et al., 2007; Wu et al., 2008; Orman et al., 2009a; Wang et al., 2010).

- **Methanol utilization slow phenotype (Mut<sup>s</sup>):** Has a disruption in the AOX1 gene. Therefore, the cells use the weaker promoter AOX2 for methanol metabolism, the strain grows and utilizes methanol at a slower rate compared with Mut<sup>+</sup>. By cultivating these strains on methanol, two strains are easily differentiated among transformed colonies since growing rates of two phenotypes on methanol differs from each other. The maximum specific growth rate of Mut<sup>s</sup> on methanol is 0.04 h<sup>-1</sup> (Cregg et al., 1987). Thorpe et al., 1999; Ramon et al., 2007, Orman et al., 2009 selected *Pichia pastoris* Mut<sup>s</sup> strain as the expression host for recombinant protein production in their studies.

- **Methanol utilization minus phenotype (Mut<sup>-</sup>):** Is unable to grow on methanol since both of the AOX genes in this phenotype are deleted. One of the advantages of this phenotype is that low growth rates may be desirable for production of certain recombinant products (Macauley-Patrick et al., 2005).

#### 2.2.4 Post-translational Modifications and Protein Secretion

In most of the microorganisms the protein production can only be performed intracellularly (Mukhija et al., 1995; Özdamar et al., 2009). Therefore in order to obtain the target protein as the first step of purification, cell lysis becomes necessary. Different from other microorganisms i.e. prokaryotes; one other advantage of *P.pastoris* is its capability of producing proteins extracellularly, which facilitates the subsequent purification (Macauley-Patrick et al., 2005). For the extracellular production, a signal sequence, usually a short amino-terminal pre-sequence that contains a charged amino-terminal region followed by hydrophobic residues, is necessary. When translation is completed, the signal sequence mediates the translocation into endoplasmic reticulum and then the sequence is recognized by signal peptidases and prior to extracellular secretion they are cleaved. Then proteins are transported into golgi body for packing into the secretory vesicles and then sent to the cell surface (Romanos et al., 1992; Daly and Hearn; 2005). One of the most common native signals of *Saccharomyces cerevisiae*, is acid phosphatase signal sequence, invertase signal sequence and alpha-mating factor pre-loader sequence that is composed of a pre-loader sequence of 19-amino acids and following that 60-amino acid pro-region (Li et al., 2001; Macauley-Patrick et al., 2005). For the extracellular production of the native protein, the signal sequence and pro-region are cleaved by is cleaved by signal peptidase and kex2 protease respectively (Raemaekers et al., 1999).

As mentioned earlier, one of the most advantageous features of *P.pastoris* is its capability of performing post-translational modifications such as disulphide bond formation, O- and N- linked glycosylation, lipid addition, correct folding. These post-translation modifications are important for the heterologous proteins to take their native forms (Cereghino and Cregg, 2000; Macauley-Patrick et al., 2005).

Since the tertiary structure determines the properties of a protein, in order to show activity properly, the most crucial step in production is correct folding (Holst et al.,1996; Hohenblum et al., 2004). After translation and formation of the secondary structure, in endoplasmic reticulum, the disulfide bonds are formed. In a prokaryotic organism, usually misfolded disulfide bonds are formed as a result of the reducing environment of cytoplasm. Conversely, a eukaryotic microorganism *P.pastoris* has been shown to be successful in formation of correct disulfide bonding (White et al., 1994). As human growth hormone contains two disulfide bonds, correct bonding is important for hGH to keep its native structure and show activity.

The other important post-translational modification is glycosylation. Glycosylation is the enzymatic process in which the carbohydrate groups forms glycans that are attached to proteins. There are two types of glycosylations that can be performed by *P.pastoris*; O-linked and N-linked glycosylation (Macauley-Patrick et al., 2005). Although glycosylation is important for some proteins to ensure their biological activity, some other non-glycosylated proteins such as hGH glycosylation needs to be prevented. *P.pastoris* is also advantageous for this purpose, since rhGH does not have a recognition site for glycosylation; thus there is no need for the cleavage of glycans (Daly and Hearn, 2005). In previous studies on rhGH production by *P.pastoris*, Trevino et al. (2000), Eurwilaichtr et al. (2002), Orman et al., (2009), Aık (2009) and Bayraktar (2009) reported production of rhGH without glycans.

### **2.2.5 Proteolytic Degradation**

Although *P.pastoris* is one of the most advantageous for recombinant protein production, similar to *Bacillus* species proteolytic degradation is a major challenge that needs to be overcome (Kobayashi et al., 2000; Sinha et al., 2004; zdamar et al., 2009). In *P.pastoris* high-density fermentations, proteolytic degradation leads to loss of biological activity of protein and

hence reduction in product yield (Kobayashi et al., 2000). In *P.pastoris* both vacuolar and extracellular proteases exist. Although the proteases are not well characterized, Jahic et al., (2006) indicated that secretion of extracellular proteases is at low levels. Therefore the main reason of proteolytic degradation can be shown as vacuolar proteases. In order to prevent the vacuolar proteases to be released out to fermentation medium, cells should be kept viable i.e. do not lyse. The reasons for yeast lysis could related with different carbon sources, temperature, pH; starvation or toxic chemicals (Hilt and Wolf, 1992). To deal with this problem addition of protease inhibitors is one of the solutions (Kobayashi et al., 2000; Sinha et al., 2004). One other strategy could be the use of protease deficient strains (Sreekrishna et al., 1997). Instead of these, operation conditions; pH, temperature and medium compositions; carbon, nitrogen sources can be optimized so that protease activity can be reduced.

### **2.3 Bioreactor Operation Parameters and Medium Composition**

In fermentation processes, production and process yields are affected tremendously by the medium components and operation conditions of the bioprocess. Thus, the effect of operation conditions; pH, temperature, oxygen transfer and medium composition; carbon sources, feeding strategy on metabolic pathways leading to changes in yields and process kinetics should be investigated (Çalık et al., 1999).

#### **2.3.1 Medium Composition and Feeding Strategy**

Cell Growth and metabolite production by an organism in a bioprocess are results of the interactions between intracellular and extracellular effectors. In design of the medium composition, the first step is to determine the necessary components that enhance energy generation, enzymatic activity inside the cell, membrane transport, induce the required pathways for growth and product formation. Then, the concentrations of the

medium constituents can be decided (Scragg, 1988). A well-designed fermentation medium for recombinant production contains carbon, nitrogen and energy sources, mineral sources; the medium should be in consistent quality and constituents should be readily available; the medium components should result in minimum downstream processing (Nielsen and Villadsen, 1994). The nutrients that need to be added to the bioprocess medium can be grouped under two titles; Macronutrients-compounds that are found in the medium at concentrations higher than 0.1 mM and micronutrients- compound needed in the medium at concentrations less than 0.1mM, in trace amounts. The macronutrients are can be listed as carbon, nitrogen, oxygen, magnesium, potassium, sulfur etc.; while major micronutrients, trace elements, are  $Zn^{2+}$ ,  $Cu^{2+}$ ,  $Mn^{2+}$ ,  $Fe^{2+}$ ,  $Ca^{2+}$ ,  $Na^{2+}$ ,  $Cl^{-}$  (Shuler and Kargı, 2002).

The growth media can be grouped into two according to the medium composition; defined and complex medium. The complex medium components are naturally obtained without the knowledge of exact compositions, such as yeast extract. In defined medium, on the other hand, the exact amounts of the constituents are known. The decision of which media to use depends on the purpose. While in complex medium higher cell growth rate can be achieved, the effect of concentration of each component in the medium can be understood and manipulated accordingly. Therefore, in most of the studies in literature for precultivation steps complex media are preferred while, defined media is used for production phases (Hohenblum et al., 2004; Guo et al., 2007; Orman et al., 2009; Wang et al., 2010).

As the medium components and their concentration are directly effective on the cell metabolism, it is very important to determine the amount of macro- and micronutrients in proper ratio. For production in defined medium with high cell density fermentation process, the most common used medium is the basal salt medium together with the trace salts

(PTM1) (Jungo et al., 2006; Çelik et al., 2007; Ramon et al., 2007). As an alternative to BSM medium, Stratton et al., (1998), d' Anjou et al., (2000), Kobayashi et al., (2000) and Sinha et al., (2004) used modified BSM or other medium compositions. Additionally, the effect of each component in the medium was investigated in detail by Plantz et al., (2007). Conversely, in another study Lin et al., (2007) investigated the effect of different salt supplementation on fed-batch *P.pastoris* fermentation in defined medium. Higher product concentrations were achieved in no salt conditions.

Another essential medium component is the nitrogen. The most commonly used nitrogen source is ammonium hydroxide. Due to the hydroxide groups in ammonium hydroxide, it is also used for pH adjustment (Cos et al., 2005; Hao et al., 2007; Çelik et al., 2009; Wang et al., 2010). Although the use of ammonium hydroxide is advantageous in terms of application as it avoids nitrogen accumulation that might inhibit growth and protein expression (Yang et al., 2004); the main disadvantage is the possibility of nitrogen starvation. If the amount of ammonium hydroxide that is used to adjust pH is not enough as a nitrogen source, nitrogen starvation occurs increasing the protease secretion (Werten et al., 1999; Kobayashi et al., 2000). As another strategy to adjust pH and add nitrogen source to the medium can be achieved by adding batchwise  $\text{NH}_4\text{Cl}$  as the nitrogen source and adjusting pH by potassium hydroxide or phosphoric acid depending on the desired pH (Jungo et al., 2006; Lin et al., 2007).

The most important medium component that plays a crucial role in *P.pastoris* is the carbon source. As mentioned the metabolic pathways for different carbon sources are different. In *P.pastoris* fermentations, due to the existence of AOX1 promoter in Mut<sup>+</sup> and Mut<sup>s</sup> strains, which is induced by methanol, methanol can be used both as a carbon source and inducer. However, when methanol is used as the sole carbon source growth is inhibited above 4g L<sup>-1</sup> methanol concentration (Zhang et al., 2000) Therefore, in order to keep concentration below the toxic limit, fed-batch

feeding strategy with a three or four stage feeding process is employed (Stratton et al., 1998; Zhang et al., 2000; Sinha et al., 2004). In a three-stage process first in order to accumulate cells, the engineered strain is cultured in medium containing glycerol, a non-fermentable but repressing carbon source. Second, a glycerol fed-batch transition phase is applied at limiting glycerol levels to further increase cell concentration without repressing growth. Another purpose of the second stage is to prepare the cells for another carbon source. In third stage, methanol is added to the fermentation medium fed-batch, starting induction. In a four-stage process, an additional stage of batch-methanol addition was employed in between 2<sup>nd</sup> and 3<sup>rd</sup> stages to prepare the cells prior to fed-batch operation (transition phase). Kobayashi et al., (2000), Zhang et al., (2005), Ohya et al. (2005), and Çelik et al., (2009) showed that the specific growth rates have influence on production. Jungo et al. (2007), in their study, indicated that maximum specific growth rate on methanol was  $\mu_{\max}=0.14 \text{ h}^{-1}$ , and conducted two fed-batch bioreactor experiments at  $\mu_0=0.03 \text{ h}^{-1}$  and  $\mu_0=0.05 \text{ h}^{-1}$  using 43% methanol and 57% sorbitol ( $\text{C-ml C-mol}^{-1}$ ) for recombinant avidin production and reported that at  $\mu=0.05 \text{ h}^{-1}$ , and pointed out that for  $\mu$  values larger than  $0.02 \text{ h}^{-1}$ , productivity increases slightly with  $\mu$ . It was also shown that above  $\mu=0.032 \text{ h}^{-1}$  dual carbon source limitations would occur. Moreover, in a more recent study Çelik et al., (2009) investigated the effect of batch-wise sorbitol addition in the fed-batch production phase for glycosylated protein, human erythropoietin, at different methanol feeding rates and obtained slightly higher product yield at  $\mu_0=0.03 \text{ h}^{-1}$  where the highest cell concentration was achieved at  $\mu=0.02 \text{ h}^{-1}$  in the presence of co-substrate sorbitol.

In order to decrease the process time and to increase product yields, in literature on *P.pastoris* fermentation processes, there are several studies conducted using various co-carbon sources such as methanol, glycerol, sorbitol, mannitol, trehalose, glucose and alanine. Sreekrishna et al., (1997)

implemented the use of sorbitol/methanol mixed substrates on Mut<sup>-</sup>. Inan and Meagher, (2001) investigated the effect of alanine, sorbitol, mannitol, glycerol, ethanol, acetate and trehalose; showing that sorbitol, mannitol, alanine and trehalose are the non-repressing carbon sources for Mut<sup>-</sup> strain. The use of glycerol as the co-substrate is one of the most common strategy (Zhang et al., 2003; Jungo et al., 2007a; Orman et al., 2009). However, Xie et al., (2005) represented that the excess glycerol in medium represses the AOX1 promoter, i.e. protein production. As an alternative to glycerol/methanol co-feeding strategy using the sorbitol, non-repressing carbon source, as co-substrate many other studies are conducted with different feeding strategies (Jungo et al 2007b; Çelik et al., 2009; Açıık , 2009; Wang et al., 2010). While Jungo et al., (2007d) used fed-batch feeding strategy using 43% methanol and 57% sorbitol (C-ml C-mol<sup>-1</sup>) under two different feeding rates, Çelik et al., (2009) showed that below 50 g L<sup>-1</sup> did not repress growth or production and hence added 50 g L<sup>-1</sup> batch-wise sorbitol in the beginning of production phase. Moreover, Açıık (2009) in her recent work added sorbitol for the second time t=9h, in which highest AOX activity was reached, such that 50 g L<sup>-1</sup> sorbitol was achieved once again. As a result the process duration increased 30 h and reaching higher cell and rhGH concentrations (~1.3 and ~1.2-fold respectively).

*P.pastoris* is an advantageous microorganism as it is capable of performing high-density fermentation. With the increasing cell and product concentrations aggregation of recombinant proteins may arise. Surfactants Tween-20 and Tween-80 has been started to be added to *P.pastoris* fermentations recently (Hao et al., 2007; Apte-Deshpande et al., 2009). While Hao and coworkers (2007) could not obtain any significant differences on biomass and protein concentration between with and without Tween-20 they observed that aggregation of cIFN could be greatly inhibited by Tween-20 at lower temperatures. In a recent study Apte-Deshpande and co-workers (2009) reported that both Tween-20 and -80 enhanced the expression levels

in shake flask experiments and further showed the addition of 0.1% (v/v) Tween-20 to pilot scale bioreactor increased the product concentration up to 500 mg L<sup>-1</sup>.

## **2.3.2 Bioreactor Operation Parameters**

### **2.3.2.1 Temperature**

Temperature is one of the critical parameters that affects the cellular metabolism and hence cell growth and production pathways. Actually, temperature does not only affect the cellular reactions but also the nutrients and product stability will be affected. Therefore, in determination of the optimum temperature both the cell growth profiles and product formation rates should be taken into account. The optimal temperature can increase carbon flux toward protein formation and excess biomass generation.

As the secondary and tertiary structures of the protein will be influenced by temperature and fermentations at higher temperatures might lead to misfolding affecting the activity of the protein (Georgiou and Valax, 1996). Also, the effect of temperature on specific growth rate is similar to its effects on enzyme activity. The growth rate increases with the increasing temperature up to a certain point above which protein denaturation starts decreasing the intracellular reaction rates (Nielsen, 2003).

In literature most of the studies are conducted at 30°C, considering the growth profiles of *P.pastoris* (Wegner, 1983; Cos et al., 2005; Thorpe et al., 1999; Çelik et al., 2007; Orman et al., 2009). However, when the productivity is considered, the differences in optimum temperature were seen in literature studies. It was shown that at temperatures above 32°C can inhibit protein expression and lead to cell death resulting in cell lysis and higher protease activity in the extracellular medium (Inan et al., 1999; Invitrogen 2002).

In their studies, Li et al., (2001), Hong et al., (2002) and Macauley-Patrick et al. (2005) observed that the proteolytic activity decreases with decreasing temperature. Lin et al. (2007) investigated the effect of temperature on Fc fusion protein production in Fed-batch *Pichia pastoris* fermentation at 20, 25 and 30°C. Temperature showed a strong correlation with the specific growth rate; higher growth rates were achieved, as the temperature was increased. Li et al. (2001) showed that decreasing the temperature from 30 to 20°C was effective in achieving higher lactase activity.

Moreover, Hong et al, (2001) achieved higher antifreeze proteins and increased cell viability by decreasing temperature from 30°C to 20°C. Jahic et al. (2003) and then Surribas et al. (2007) used temperature limited fed-batch technique and tried to lower protease activity and higher AOX activity was seen. Moreover, in both studies as the temperature was adjusted according to the dissolved oxygen level in the medium, the oxygen limitation was not the case, preventing cell lysis and proteolytic activity.

### **2.3.2.2 pH**

The pH of the medium is one of the most important parameters of the bioprocesses as it shows the hydrogen ion concentration in the medium. The intracellular and extracellular reactions such as energy production, enzymatic activities and transport mechanisms are all influenced by the concentration of the hydrogen ions (pH).

Microorganisms are capable of maintaining their intracellular pH at desired value; but the more difference between the medium pH and desired intracellular pH, the more maintenance energy requirement. As the cells try to maintain the proton gradient across the membrane, Gibbs free energy is necessary (Nielsen and Villadsen, 1994).

*Pichia pastoris* can tolerate a broad pH range between pH=3.0-7.0 (Macauley-Patrick et al., 2005). However the pH should be determined

mostly according to the production yields and stability of the product; i.e. final product concentrations can be achieved by decreasing the protease activity, which is related to the medium pH to a higher extent (Sreekrishna et al., 1997).

As the isoelectric point, the pH at which the net charge of the protein is zero, depends on the nature of the protein and hence affects its stability, different pH values are optimum for different proteins in literature studies (Macauley-Patrick et al., 2005). Kobayashi et al. (2000) investigated the effect of pH on human serum albumin production and obtained pH=5.6 as the pH at which less proteolytic activity was observed; Clare et al. (2001) reported pH=3.0 as the optimum pH for on insulin like growth factor-I production. In another study Lin et al. (2007) studied Fc-fusion protein production at five different pH values. At pH=3.0, 4.0, 5.0 and 6.0 the protein concentrations in the fermentation medium were undetectable. Referring to the study of Inan et al. (1999), the reason for undetectable concentrations were associated with higher level of protease activity at lower pH. Hence pH=7.2 at which Fc-fusion protein was detected in the medium was used for subsequent studies. On the other hand, Cos et al. (2006) stated that the use of BSM medium at pH higher than pH=5.0 leads to precipitation and operational problems such as starvation of nutrients and problems in OD<sub>600</sub> measurement.

### **2.3.2.3 Oxygen Transfer**

*Pichia pastoris* is a facultative anaerobic microorganism that uses oxygen up to a certain level throughout the fermentation processes. Oxygen is effective on influencing metabolic pathways and hence fluxes. Oxygen requirement varies between each microorganism as it depends on metabolism of the organism and medium conditions.

Being a yeast, *P. pastoris* uses oxygen both as the terminal acceptor in respiration (oxidative phosphorylation) for energy formation and as an

essential growth factor for fatty acid and sterol biosynthesis (Walker, 1998). *P.pastoris* is an advantageous expression host prefers respiratory pathways rather than fermentation and it does not highly produce ethanol and acetic acid (Cereghino et al., 2002). However, as the oxygen is also used in oxidation of methanol to formaldehyde as a side-reaction, higher oxygen transfer rates are required for methanol utilization pathway, which leads to product formation (Sibirny et al. 1990). To provide required amount of oxygen, transfer resistances are minimized by high agitation and usually oxygen enriched air is used (Çelik et al., 2009).

In most of the *P.pastoris* fermentation processes the dissolved oxygen was kept around 20-30% (Thorpe et al., 1999; Xie et al 2005; Surribas et al., 2007; Horstkotte et al., 2008; Çelik et al., 2009; Wang et al., 2009). Additionally, Pla et al., (2006) and Lin et al. (2007) kept dissolved oxygen at 40%; while Kobayashi et al. (2000) used 10% dissolved oxygen in fermentation studies.

Moreover, oxygen is used as a method for controlling methanol concentrations. When a rapid increase in the dissolved oxygen level occurs due to exhaustion of carbon source, methanol is added (Lin et al., 2000).

## **2.4 Computation of Bioprocess Characteristics**

### **2.4.1 Oxygen Transfer Characteristics**

The effect of oxygen transfer in the medium and through the microbial cell during aerobic fermentation of the microorganism is one of the factors that strongly affects the metabolic fluxes through the pathways and hence affects the cell growth and production (Çalık et al., 1999). The methanol metabolism, which is responsible for the production of recombinant protein, is dependent on the oxygen utilization. The transfer of oxygen from the fermentation medium to the cell involves several steps (Bailey and Ollis, 1986) (Figure 2.7).

- 1-Transfer from bulk gas to gas-liquid interface
- 2- Diffusion across the interface
- 3- Movement through the stagnant region
- 4- Transport within the bulk liquid
- 5-Transport through the 2<sup>nd</sup> stagnant region
- 6-Diffusion into the cell aggregate
- 7-Transport across the cell and into reaction

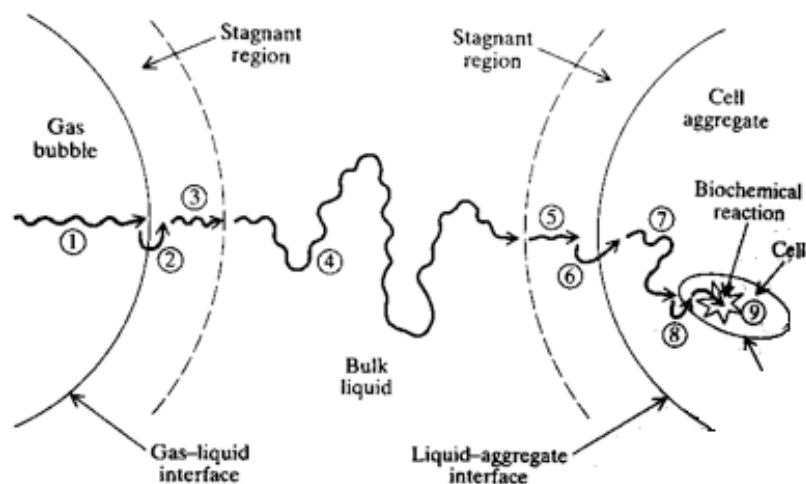


**Figure 2.7** Steps involved oxygen transport from a gas bubble to the cell (Bailey and Ollis, 1986)

When the cells do not form aggregates, i.e. they are dispersed in the liquid, and the fermentation medium is well mixed, the major resistance to oxygen transfer is the liquid film surrounding the gas bubbles (region 2 in Figure 2.7). At steady state, the oxygen transfer rate to the gas-liquid interface equals its transfer rate through the liquid side film.

$$\text{Oxygen flux} = (\text{molO}_2 / \text{cm}^2 \cdot \text{s}) = k_g (c_{g_o} - c_{g_{oi}}) - k_l (c_{l_{oi}} - c_{l_o}) \quad (2.1)$$

where;  $-c_{go}$  and  $c_{lo}$  are oxygen concentrations in the gas and bulk liquid respectively

$-c_{goi}$  and  $c_{loi}$  are oxygen concentrations in the gas and liquid interface respectively.

Moreover, since the interfacial concentrations are not measurable, transfer equation is written in terms of overall mass transfer coefficient  $K_L$  and overall concentration driving force ( $C_o^* - C_o$ ) as shown below,

$$OTR = K_L a (C_o^* - C_o) \quad (2.2)$$

where;

- $C_o$  is the actual dissolved oxygen concentration in the broth.
- $a$  is the gas-liquid interfacial area.
- $C_o^*$  is saturated dissolved oxygen concentration; i.e. liquid phase concentration which is in equilibrium with the bulk gas with the following equation:

$$C_{go} = H C_o^* \quad (2.3)$$

$H$  is the partition constant.

Defining the overall mass transfer coefficient in terms of gas and liquid phase mass transfer coefficients;

$$\frac{1}{K_L} = \frac{1}{k_L} + \frac{1}{H k_g} \quad (2.4)$$

Since solubility of oxygen in aqueous solutions is very low,  $H$  is much larger than unity and hence, the liquid phase mass transfer resistance dominates. Therefore, the overall liquid phase mass transfer coefficient,  $K_L$  is approximately equal to liquid phase mass transfer coefficient,  $k_L$  (Cussler, 1997).

Additionally, the maximum possible mass transfer rate can be defined as,

$$OTR_{\max} = K_L a C_o^* \quad (2.5)$$

Another important parameter that defines the oxygen transfer characteristics of the bioprocess is the Oxygen uptake rate (OUR),  $-r_o$  expressed as,

$$OUR = -r_o = -q_o C_X \quad (2.6)$$

where,  $q_o$  is the specific rate of oxygen consumption and  $C_X$  is the cell concentration (Shuler and Kargi, 2002).

$K_L a$  values in the oxygen transfer expressions, OTR and OUR should be determined experimentally. Among the various methods, one of the widely used is the dynamic method (Bandyopadhyay and Humprey, 1967). The details of the method are described in Section 3.3.5.8 in detail.

#### **2.4.2 Yield Coefficients and Specific Rates**

To understand the characteristics and evaluate the effect of operation parameters on the fermentation process, specific rates and yield coefficients are one of the most important terms. By defining those, the bioprocess parameters can be optimized.

##### Specific rates

Although the final concentration of the metabolites, cell, product concentrations in the medium are important, for the optimization of the process “rates” and “rates per cell” are more important as they provide insight for further experiments. Specific rate of consumption/production at a certain time can be defined as the change in the concentration of a substance per unit time per cell concentration at that instant.

Microbial growth can be considered as an increase in the number of individuals in the population as a result of both replication and change in cell size due to the chemical reactions occur inside the cell (Nielsen and Villadsen, 1994; Scragg, 1988). The rate of microbial growth is characterized by the specific growth rate,  $\mu$ . Assuming that the losses through sampling can be neglected, general mass balance for biomass in a fed-batch reactor can be written as:

$$\frac{d(C_X V)}{dt} = r_X V \quad (2.7)$$

where  $r_X$ , the biomass formation rate, is defined as the product of specific cell growth rate ( $\mu$ ), and cell concentration ( $C_X$ ), i.e.,

$$r_X = \mu C_X \quad (2.8)$$

Then combination of (2.7) and (2.8) gives the equation for  $\mu$  as,

$$\frac{d(C_X V)}{dt} = \mu C_X V \quad (2.9)$$

As the medium is fed- to the reactor fed-batchwise, volume changes throughout the process. Therefore  $Q$  is defined as the variation of volume within time is (2.10).

$$Q = \frac{dV}{dt} \quad (2.10)$$

Then evaluating (2.9) and inserting (2.10) ;

$$\begin{aligned} C_X \frac{d(V)}{dt} + V \frac{d(C_X)}{dt} &= \mu C_X V \\ C_X Q + V \frac{d(C_X)}{dt} &= \mu C_X V \end{aligned} \quad (2.11)$$

Hence, for known cell concentration ( $C_X$ ) and volume ( $V$ ) data throughout the bioprocess,  $\mu$  can be calculated for all times by rearranging;

$$\mu = \frac{d(C_X)}{dt} \frac{1}{C_X} + \frac{Q}{V} \quad (2.12)$$

The major substrate methanol is added fed-batch to the fermentation medium. Conducting a mass balance for fed-batch process;

$$\frac{d(C_X V)}{dt} = QC_{Mo} - 0 + r_M V \quad (2.13)$$

where,

$$r_M = q_M C_X \quad (2.14)$$

$r_M$  is the product of specific substrate consumption rate ( $q_M$ ) and cell concentration ( $C_X$ ),

Combining equations (2.13) and (2.14);

$$V \frac{dC_M}{dt} + C_M \frac{dV}{dt} = QC_{Mo} + q_M C_X V \quad (2.15)$$

As known from the previous studies in predetermined feeding strategy the cell consumes all methanol fed to the medium. Therefore, a fed-batch system can be assumed to operate at quasi-steady state. At quasi-steady state, no significant level of the substrate can accumulate (Shuler and Kargi, 2002). Although the terms on the left hand side are mathematically negligible, but physically the first term on the left hand side should be considered carefully. As the methanol is consumed with its predetermined feeding rate only the second term on the left side is neglected.

$$C_M \frac{dV}{dt} \sim 0 \quad (2.16)$$

The specific methanol consumption rate,  $q_M$  can then be calculated by equation (2.17),

$$q_M = \left( -\frac{dC_s}{dt} + \frac{Q}{V} C_{M_o} \right) \frac{1}{C_X} \quad (2.17)$$

Similar derivation can be followed for the co-substrate (Sorbitol) added batch-wise in to fermentation medium. Mass balance of sorbitol for this batch system becomes,

$$\frac{d(C_s V)}{dt} = r_s V - q_s C_X V \quad (2.18)$$

where  $r_s$ , can be defined in terms of specific substrate consumption rate,  $q_s$  and cell concentration,  $C_X$ ;

Rearranging gives;

$$q_s = \left( \frac{dC_s}{dt} - \frac{Q}{V} C_s \right) \frac{1}{C_X} \quad (2.19)$$

Using similar mass balance equations, the recombinant protein balance for fed batch system becomes,

$$q_{rp} = \left( \frac{dC_{rp}}{dt} + \frac{Q}{V} C_{rp} \right) \frac{1}{C_X} \quad (2.20)$$

#### Overall and Instantaneous Yield Coefficients

Overall yield coefficients are used to define the overall conditions of the bioprocess by relating the concentration change of the metabolites, cell and substrates between the beginning and the end of fermentation process.

Yield coefficients are stoichiometrically related parameters generally defined as;

$$Y_{P/S} = -\frac{\Delta P}{\Delta S} \quad (2.21)$$

where,  $Y_{P/S}$  is the overall yield coefficient with of product formation (mass or moles of product) per substrate consumption(mass of moles of substrate).

Some of the frequently used yield overall coefficients are listen in Table 2.1.

**Table 2.1** Definition of overall yield coefficients

<b>Symbol</b>	<b>Definition</b>	<b>Unit</b>
$Y_{X/S}$	Mass of cells produced per unit mass of substrate consumed	g cell g <sup>-1</sup> substrate
$Y_{P/S}$	Mass of product formed per unit mass of substrate consumed	g product g <sup>-1</sup> substrate
$Y_{P/X}$	Mass of product formed per unit mass of substrate consumed	g product g <sup>-1</sup> cell
$Y_{X/O}$	Mass of cells produced per unit mass of oxygen consumed	g cell g <sup>-1</sup> oxygen
$Y_{S/O}$	Mass of substrate consumed per unit mass of oxygen consumed	g substrate g <sup>-1</sup> oxygen

However, in batch and fed-batch operations, since the yield coefficients may differ during the process for a given microorganism in a given medium, due to the growth rate and metabolic functions of the microorganism, it is sometimes more useful to evaluate the instantaneous yield at a particular point in time which can be computed as given in (2.22). When instantaneous yields for fermentation are reported, the time or time period to which they refer should be stated (Doran, 1995).

$$Y_{P/S}^i = -\frac{dP}{dS} = -\frac{dP/dt}{dS/dt} \quad (2.22)$$

## 2.5 Purification of Human Growth Hormone

As the final aim of rhGH production is to implement the clinical use of this product as a therapeutic agent, it is very important to achieve high purity (~99%). Depending on the host microorganism used for rhGH production the protein can be produced extracellularly (as in *P. pastoris*) or intracellularly (in *E. coli* by inclusion bodies). Therefore, after fermentation processes rhGH is found in either the fermentation broth together with some fermentation by-products (such as proteases and other host cell proteins), salts, organic/amino acids or in an intracellular medium with even more complex constituents. Although desalting and ultrafiltration using proper membranes can remove some of these medium constituents, other purification methods mostly based on affinity separations are necessary.

In previous studies several different methods such as ion exchange chromatography, gel filtration chromatography, hydrophobic interaction chromatography, metal chelate affinity chromatography were used either alone or simultaneously for the purification of rhGH.

In one of the earliest studies on hGH purification Battersby et al., (1995) used the combination of affinity chromatography, in which receptor protein was used as the ligand, and reversed phase HPLC were employed for purification of hGH serum or tissue culture samples. Using this combination; 70% of the protein was recovered with high purity. In the study conducted by Mukhija et al. (1995) without an attempt to reach high recovery, first rhGH was produced by *E. coli* as a fusion protein containing His<sub>6</sub> tag and then was purified by as single step affinity chromatography using Ni<sup>+2</sup>NTA agarose. Liesiene et al. (1997) investigated the effect of ligand density of immobilized metal affinity chromatography for purification of hGH. In the study, Cu(II) charged chelating support was found to exhibit high affinity towards hGH and after 1 step purification resulted in 80% purification. Alam et al. (1998) used gel filtration chromatography in Sephacryl S-200

column and by SDS-page observed changes in hGH concentrations of the fractions collected from the column. Finally by elution with a gradient of 1M NaCl in 0.1M EDTA and 10mM Tris-Cl pH=8.0 a single hGH band with 15% yield was obtained in SDS-PAGE. In order to obtain high-yield, high-purity hGH purification, Oliviera et al. (1999) conducted a six-step (ammonium sulfate fractionation, first gel chromatography, anion exchange chromatography, second gel chromatography, hydrophobic interaction chromatography, high-performance size exclusion chromatography (HPSEC) and reversed phase (RP-HPLC) that provided more than 40% final yield with high-purity. In another study by Patra et al., (2000) rhGH expressed in *E.coli* was first purified by DEAE-Sepharose ion exchange column and then by gel filtration chromatography. Using this two-step purification, 50% yield and 99% purity was achieved as shown in SDS-PAGE. Different from the chromatographic separation studies for rhGH purification Khodabandeh et al. (2003) developed a procedure for acid precipitation (isoelectric precipitation) of the host derived proteins and other impurities in the fermentation medium. As shown by SDS-PAGE and Western blot analyses, high purity (>99%) and 40% recovery was obtained. In the same year, Catzel et al. (2003) published a study on purification of hGH from Chinese hamster ovary cell culture supernatant by Gradiflow preparative electrophoresis using 50mM Tris/HEPES buffer at pH=7.5 with 50 kDa membrane. After 60 min separations hGH was purified to 98% purity with 90% yield. In one of the recent studies Singh et al. (2009) used radial column and axial column anion exchange chromatographies for comparison of purification of rhGH produced by *E. coli* in Inclusion bodies. With faster process time and higher purification rate radial column chromatography resulted in 42% recovery of pure rhGH under mild operation conditions. More recently, Çalık et al. (2010) determined an oligonucleotide sequence (aptamer), that has affinity towards rhGH, by LETEG and investigated the effects of time and pH on aptamer binding to hGH. While the highest binding efficiency was obtained

at pH=7.0, the strongest affinity was disrupted at 85°C. For the aptamer that showed strongest affinity, affinity column experiments were conducted and the adsorption was found to fit Langmuir type isotherm. Using the selected aptamer 99.8% rhGH purification was achieved with 41% recovery.

As mentioned in earlier sections, using peptides as ligands for affinity chromatography has advantages over other methods in terms of cost and application, therefore in this study alternative to all these ligand options for aiming further use in affinity purification of rhGH from *P. pastoris* fermentation medium, peptide ligands are investigated.

### **2.5.1 Types of Ligands Used for Affinity Separations**

Separation and purification of therapeutic proteins from production media are as important as their production. Since downstream processing accounts for 50-80% of the cost of manufacturing a therapeutic product, reductions in the number of steps in the purification in the purification train and increases the yield and purity of the product in each step would effectively decrease production costs. For this reason attention is being given to affinity chromatography as purification method that would result in both a reduction in the number of steps required for purification as well as a higher yield of product mass (Wang et al., 2005).

As conducted very commonly in many biological applications, chromatography is a physical method of separation in which the components to be separated are distributed between two phases one of which is stationary while the other moves in a definite direction. Out of many chromatography techniques, affinity separations comprises a number of highly selective purification techniques in which chemical molecules (ligands) are bonded to a solid support and undergo specific and reversible interaction with a biomolecule to be purified as shown schematically in Figure 2.8. Covalent bonds attach the ligand to an insoluble, porous support medium in a manner that overtly presents the natural biospecific binding of

one molecular species to separate and purify a second species from a mixture.

Affinity chromatography is a very advantageous method as it provides high fold purification, potential for scale-up and good recovery together with simultaneous concentration of the target protein. Moreover, as the ligands are very selective for the target protein, this process can easily be used to pick out small amounts of target protein even from a complex and large amount of crude mixture (Mondal and Gupta, 2006).

Ligands, as mentioned in the previously are the substance that readily bind to their target by non-covalent intermolecular forces such as ionic bonds, hydrogen bonds, Van der Waals forces and form a complex with a biomolecule to serve a biological purpose.

A suitable ligand should; (Clonis ,1990)

1. Form a reversible complex with the molecule to be purified with a dissociation constant value between  $10^{-4}$  and  $10^{-8}$  M.
2. Provide functional group(s), which are not involved in the affinity interaction, via which it can be immobilized.
3. Remain stable during the immobilization procedures that involve chemical treatment.

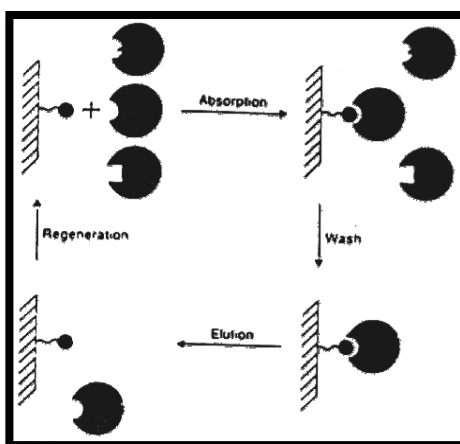


**Figure 2.8** Schematic view of affinity chromatography

The classical applications of biological affinity processes are based upon the *in vivo* relationship between molecules; i.e. receptor-protein binding. Hence for the purification the first attempts were done using natural affinity ligands. Then it was realized that the ligands are not necessarily be the molecules that show affinity toward the target *in vivo*. Therefore, the search for new affinity ligands began such as antibodies, dyes, chelated metal ions, aptamers obtained by systematic evolution of ligands by exponential enrichment (SELEX), peptides obtained by phage display technology and combinatorial synthesis. Moreover, molecular modeling techniques are also used to facilitate the design of biomimetic ligands (Mondal and Gupta, 2006). Together with these developments, high throughput screening methods developed, which made fast search for the probable candidate structure possible (Jayasena, 1999; Yang et al., 2003). Molecular modeling/docking techniques contributed in a complimentary way (Labrou, 2003; Erickson et al., 2004). So today, for a given protein, it is almost possible to design an affinity ligand.

There are several studies in literature conducted using various types of ligands. The strongest and most used ligands are the antibodies. However, as antibodies show very strong interaction towards the target, although adsorption is not a problem desorption arises. In order to break the bonds between these two, the use of harsh elution conditions, low pH values and the use of detergents might be required. Such harsh treatments may harm both the antibody and the target protein (Clonis, 1990). As the antibodies recognize the target molecule due the its tertiary structure in solution, any changes that may result in small changes on the tertiary structure may result in reduction or even loss in affinity. One other disadvantage regarding the use of antibodies is the higher cost. Also as some targets might be toxic or poorly immunogenic the availability of the antibodies for such targets is problematic. Moreover, linkage of antibodies to columns often result in coupling that are not uniform, that leads to reduced capacity and affinity

(Romig et al., 1999). Furthermore, the relatively large size of the antibodies limits the ligand density at the chromatographic surface (Ravelet et al., 2006).

Another alternative is the reactive dyes that began to be used for affinity separations in 80s (Clonis and Lowe, 1981; Clonis et al., 1987; Reya-tonetti and Perotti, 1999; Denizli et al., 1997; Roy and Gupta 2000). These dyes are inexpensive, chemically and biologically stable and they can be easily immobilized, require mild elution conditions and provide good yields. On the other hand, their moderate specificity and performance variation from batch to batch, are the main disadvantages of these ligands (Clonis, 1990).

Some metal ions like  $\text{Ni}^{+2}$ ,  $\text{Cu}^{+2}$ ,  $\text{Zn}^{+2}$ ,  $\text{Co}^{+2}$ ,  $\text{Ca}^{+2}$ ,  $\text{Mg}^{+2}$ ,  $\text{Fe}^{+3}$  can be used as ligands for immobilized metal affinity chromatography. While Ueda et al. (2003) used  $\text{Ni}^{+2}$  for the purification for recombinant human prolactin, Gupta et al. (2003), made comparison about the effect of different metal ions on purification of recombinant ovine growth hormone and obtained higher yield (83%) with  $\text{Ni}^{+2}$ , than 73.5% yield obtained when  $\text{Cu}^{+2}$  is used as a ligand. One single histidine is good enough for binding to  $\text{Cu}^{+2}$  column. Other metal ions require His-(X)n-His topography.  $\text{Fe}^{+3}$  is useful for binding to phosphoproteins (Mbrabet and Vijaylakshmi, 2002). Related with the use of metals ions for affinity chromatography, similar advantages and disadvantages with the dyes exist.

Affinity tags are also one of the most commonly used methods in protein purification studies. While some of the molecules can be used as an affinity tags, recombinant proteins can also be expressed by these affinity tags. As avidin biotin interaction is the strongest molecular interaction (Holmberg et al., 2005), avidin can be used as a ligand for the biotinylated target molecule; i.e. biotin can be used as an affinity tag (Wilchek and Bayer, 1990). Some other affinity tags are, poly arginine tag, poly histidine tag,

strep-tag, cellulose binding domain tag (Terpe, 2003). Çelik et al., (2007) produced recombinant erythropoietin with poly-histidine (His<sub>6</sub>) tag, and for the purification of this protein used Co<sup>+2</sup> based metal resins. Although these tags provide specific purification of the target with high recovery, as the bond are strong harsh elution conditions might be needed. Moreover, the removal of the tags that are expressed within the protein structure need further treatment, which may again affect the structure and recovery of the target protein.

Another ligand that can be used for the purification of proteins from crude mixtures by affinity chromatography is the aptamers. Aptamers are short oligonucleotides, selected for binding molecules of interest (Cao et al., 2005). As aptamers show specificity and affinity for their targets similar to the antibodies, they have been created for a variety of targets (Tombelli et al., 2005). With the use of combinatorial libraries, the combinatorial chemistry technique (Systematic Evaluation of Ligands by Exponential Enrichment-SELEX) for large single stranded oligonucleotide libraries. Romig et al., (1999) showed the effectiveness of human L-selectin specific DNA-aptamer for purification of L-selectin receptor globulin (LS-Rg). In a recent study, Çalık et al., (2010) in addition to human growth hormone specific aptamer selection by SELEX in order to be used by the single step affinity chromatography; they investigated the effect of operation parameters on binding and elution of the protein. The high cost of aptamers is one of the main challenges in such purification experiments.

For purification of therapeutic products 3-25 amino acid peptides on the other hand provide promising alternatives as they can have affinities to target molecules with comparable strength. However, mild elution conditions are sufficient for breaking the bonds between the biomolecule of interest and ligand, so that target molecule can be obtained with higher recovery and loss of activity. As opposed to antibodies, peptides remain much more stable as they do not need to maintain a specific tertiary

structure to show affinity. Also the immune response that might be caused by the linkage of the antibody into the target biomolecules, is less likely for a peptide. In addition to being target specific, these small peptide ligands are advantageous in terms of relatively low costs of manufacture and availability of production in large scale.

Although the use of peptides as ligands is relatively new, there are several studies in literature on the use of peptide ligands for the affinity purification of target molecules from crude mixtures. Koivunen et al. (1999) selected the highly specific peptide ligand for the  $\alpha_1\beta_5$  integrin from C7C cyclic peptide library, obtained the nine-amino acid cyclic peptide as CRRETAWAC the interaction was proved by ELISA and cell attachment assays. Ploug et al. (2001) used combinatorial chemistry to identify 9-mer peptide that binds glycolipid-anchored urokinase receptor (uPAR) using one-bead-one-peptide and obtained  $K_D \sim 0.4 \text{ nM}$  by surface plasmon resonance (SPR) for the selected peptide. Wang et al. (2004) isolated a hexamer peptide ligand that binds to Staphylococcal enterotoxin B (SEB) again from a solid phase one-bead-one-peptide combinatorial library and showed the specific interaction of the selected peptide with SEB by using peptide immobilized column and different targets for control experiments. In another study, Yang et al. (2006) identified hexamer peptide affinity resins that bind the Fc region of human immunoglobulin G (HIgG), using solid peptide libraries as an alternative to many other ligands used for HIgG purification. The affinity screening was done using radiolabeling with  $^{14}\text{C}$  and gel electrophoresis was used to check the purity of the target, after affinity chromatography. Soykut et al. (2008) screened 12-mer phage display peptide library for peptide selection that binds selectively and with high affinity to SEB. The affinities of the phages were determined by SPR and the binding constant of the interaction of SEB with the highest affinity peptide, selected from SPR results, was determined by Isothermal titration calorimetry (ITC) as  $K_A = 4.2 \times 10^5 \text{ M}^{-1}$ . In a recent study, Han et al. (2009)

constructed peptides of 47, 27, 16 and 14-mer length from  $\alpha$ -helical subunits of the Lac repressor protein (LacI) and tailored these designs to achieved desired binding kinetics toward the interaction with plasmid DNA. They employed SPR for detection and characterization of the binding. In literature there is no study conducted for peptide selection that binds hGH with high affinity and specificity so that it could further be used in separation.

## **2.5.2 Peptide Selection**

### **2.5.2.1 Phage Display**

For the use in affinity chromatography, the important thing is to choose an appropriate ligand that shows high affinity towards the target molecule. For that purpose, phage display has been becoming one of the powerful tools in terms of providing opportunities to represent natural protein-peptide interactions. Moreover these developments of phage display, screening of millions of peptide sequences to discover specific peptide that bind to the desired protein become possible. This technique is advantageous as it originated from the incorporation of protein and genetic components into a single phage particle (Smith, 1985; Cwirla et al., 1990; Clackson and Wells, 1994). By using the direct physical link between the expressed protein and the encoding genetic information clones with desirable functional capacities (binding strengths) can be subjected to iterative selection rounds that enriches the number of specific clones with specificity and affinity towards the target so that the final selections can be amplified (Goodyear and Silverman, 2005).

Using this technique peptides were chosen specific to target. The affinity and specificities of the peptides (or the on purpose-modified forms of these peptides) were checked by analysis methods or by affinity column chromatography as is used in several studies published. Wobbe et al. (2001) chose the integrin  $\alpha_5 \beta_1$  specific peptide from CX<sub>7</sub>C cyclic phage display library and modified C terminal of the peptide in order to use in affinity

chromatography column. Similarly, Kelly et al. (2004) used phage display for selection of a cyclic peptide for cGMP production factor VIII by attaching the and before the use of this peptide for affinity chromatography the binding affinity was investigated by isothermal titration calorimetry.

Phage display technique can both be used in vivo and in vitro for several purposes. Jost et al. (2001) applied 7 amino acid length phage display peptide library on airway epithelial cells and obtained THALWHT sequence with high affinity. In another study, Mourez et al. (2001) isolated a peptide from a 12-mer phage display library that binds weakly to heptameric cell-binding sub-unit of anthrax toxin (heptamer was purified for in vivo study) to prevent the interaction between cell binding and enzymatic moieties. Different from the preceding examples, Chen et al. (2006) obtained the synthetic peptide, CSSSPSKHC, which facilitates efficient transdermal insulin delivery through intact skin, by performing in vivo phage display in Male Wistar rats. Soykut et al. (2008) conducted high throughput screening and selection of 12-mer peptides from commercial M13 phage library, in order to find the peptides that recognize staphylococcal enterotoxin B (SEB) and obtained three peptides, without revealing any consensus sequence, that show high affinity to SEB.

### ***The Biology of Phage Display***

In phage display peptide libraries, random oligonucleotides with a known length are generated and then inserted into M13 filamentous bacteriophage gene pIII (Wang et al., 2005). This technique works on the assumption that, when a peptide is fused to the coat protein of the phage, the fused peptide variants will be expressed on the outside of the virion making them accessible to other proteins for subsequent binding interactions; while the genetic material encoding each variant resides on the inside (Goodyear and Silverman, 2005). The peptide coded by the inserted DNA is displayed at the N-terminal of the gene III protein on the phage surface. This protein

pIII modulated phage infectivity by binding to the F-pilus of the recipient bacterial cell, and is present as 5 copies clustered at one end of mature M13 virion (Scott and Smith, 1990). The peptides that selectively bind to the target protein are selected on several rounds of affinity purification. Non-binding phages are washed out and eluted phages are amplified on agar medium the tight binding phages are cloned and propagated in *E. coli*. In order to determine the relative binding strengths of the phages enzyme linked immunosorbent assay (ELISA) is conducted using M13 antibody. Finally the amino acid sequence of the peptide on the selected phage is obtained by isolating the phage DNA in phage gene III and sequencing (Figure 2.9).

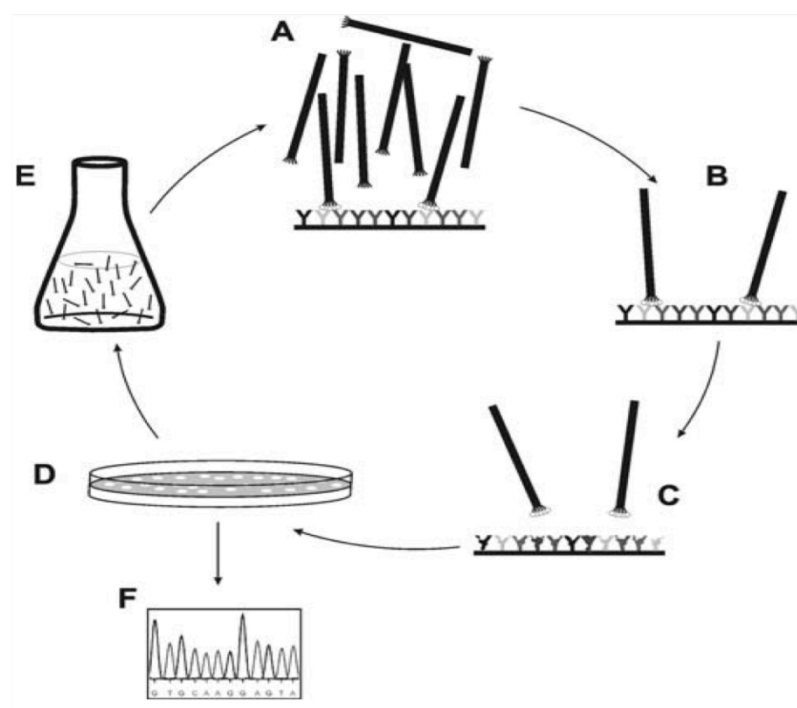


**Figure 2.9** Phage Display Procedure (Bratkovič, 2010) **A:** Phages are incubated over the target immobilized surface **B:** Non-binding clones are washed away **C:** Binding peptides are eluted and collected **D:** The phages and *E. coli* are plated on agar plates for propagation and then phage isolation. **E:** The isolated phages are again propagated in *E. coli* amplified in liquid growth medium. **F:** After amplification the *E. coli* are removed from the medium by several centrifugation and treatment steps and the DNA of selected phage is isolated. The genetic information about the peptide sequence is then obtained by sequencing with the selected primer.

### **2.5.2.2 Computational Methods**

Using computational docking method and considering the strengths of the binding interaction between each selected peptide and active sites of the target molecule, peptide sequence that shows the highest affinity can be selected.

## **2.6 Thermodynamic Interpretation of Protein Ligand Interactions**

One of the main difficulties with affinity chromatography system is the optimization of the operation conditions in order to obtain high purity and recovery of the target from the medium (Roselin et al., 2010). However, the knowledge of binding mechanism and strength between the two interacting molecules at selected parameters such as pH, temperature and buffer conditions, provide in sight into the determination of operation parameters of affinity separation. In order to understand the binding mechanism and strength the information about the thermodynamic characteristics of the affinity binding is important. For that purpose in this study, the two different analysis methods Surface Plasmon Resonance and Isothermal Titration Calorimetry are used as will be explained in detail in the following sections.

### **2.6.1 Surface Plasmon Resonance (SPR)**

Surface Plasmon Resonance (SPR) spectroscopy is a powerful technique that uses an optical method to measure biomolecular interaction between two molecules in real-time and label free (e.g. no radioactivity or fluorescence) environment. Since its first observation by Wood (1902 and 1912), the physical phenomenon of SPR has been developed tremendously and with the introduction of a commercial SPR biosensor in 1990, these optical biosensors became readily available tool for quantitative and qualitative characterization of reversible interactions between biological macromolecules. In advance to solution methods, SPR can detect specific reversible binding of a reactant in a mobile phase to its interacting partner

immobilized on the surface of the sensor (Schuck, 1997). Important aspects investigated by using SPR are binding properties, specificity, association/dissociation kinetics and affinity constants. Moreover, SPR is advantageous over several other analysis methods as it can be applied for determination of interactions within a broad range of affinities from nM to  $\mu$ M, and for detection small sample volumes with comparatively low requirements on the purity of the reactants are sufficient (Gedig, 2008).

With all these advantages, SPR has been used in a large amount of studies involving various molecular interactions. These fields include antibody-antigen (Karlsson et al., 1991; Glaser et al., 1996, Kelly et al 2004; Papalia et al, 2006), receptor-ligand (Boniface et al., 1994; Goldstein et al., 1995; Alam et al., 1996; Komolov et al., 2006;), protein-protein (Edwards et al. 1995; Karlsson et al., 1997; Kim et al., 2006; Chen et al., 2009), protein-phage (Soykut et al., 2008), protein-carbohydrate (MacKenzie et al., 1996) , protein-lipid (Ramsden et al., 1996), protein-DNA (Bondeson et al., 1993; Lin et al., 2009; Dexheimer et al., 2010), and DNA-DNA (Fisher et al., 1994; Yang et al., 1995), interactions involving lipid vesicles, cell adhesion molecules (van der Werve and Barclay, 1996; Li et al., 2009), virus research (Pellequer et al., 1993; Van Regenmortel et al., 1994; Pizarro et al., 2001; Boltovetz et al., 2004) . Therefore, SPR contributes to a wide application area such as molecular engineering, food analysis, clinical diagnosis, proteomics, environmental monitoring, bacteriology, virology, cell biology and drug discovery (Shankonan et al., 2007).

In this study, SPR is used to investigate the association/dissociation kinetics of hGH and designed/selected peptide interaction as well as to determine the binding affinity constants. Similarly, Wobbe et al. (2001) used SPR for binding experiments between C-terminal modified immobilized peptide and  $\alpha_5\beta_1$ . In another study by Schubert et al. (2003) thermodynamic analysis and determination of affinity constant, of interaction between 26-mer single strand DNA and RPA was conducted at variable temperature and

various ligand concentrations. In a recent study regarding peptide-DNA interaction Han et al. (2009) employed SPR for quantification and characterization of binding of double stranded *E. coli* plasmid DNA (*pUC19*) via LacI-based 47mer, 27mer, 16mer and 14mer peptides. Moreover, Jacobsen et al. (2007) compared the affinity strength of peptide identified via random phage library and monoclonal antibody towards urokinase-type plasminogen activator receptor (uPAR) by SPR and evaluated optimal elution conditions. Soykut et al. (2008) determined the thermodynamic constants of the interaction between Staphylococcal enterotoxin B (SEB) and peptide ligands selected from 12-mer phage display library and compared the affinity of selected peptides with the commercially available antibodies using SPR.

### ***Theory of SPR***

When polarized light is shone through a prism on a sensor chip with a thin metal film on top, the light is reflected by the metal film, usually gold, which acts as a mirror. When the angle of incidence is changed and the intensity of the light reflected is monitored, it is observed that the reflected light passes through a minimum. At this angle of incidence the light causes the excitation of the surface plasmons, the surface electromagnetic waves that propagate in a direction parallel to the metal/dielectric (or metal/vacuum) interface. This induces the surface plasmon resonance causing a dip in the intensity of the reflected light. Photons of the polarized light can interact with the free electrons of the metal layer, inducing a wave-like oscillation of the free electrons, reducing the reflected light intensity. The angle at which the maximum reflected light intensity is observed is called the *resonance angle* or the *SPR angle* (Gedig, 2008; Sambrook and Russell 2001). The working principle of SPR is shown as in Figure 2.10.

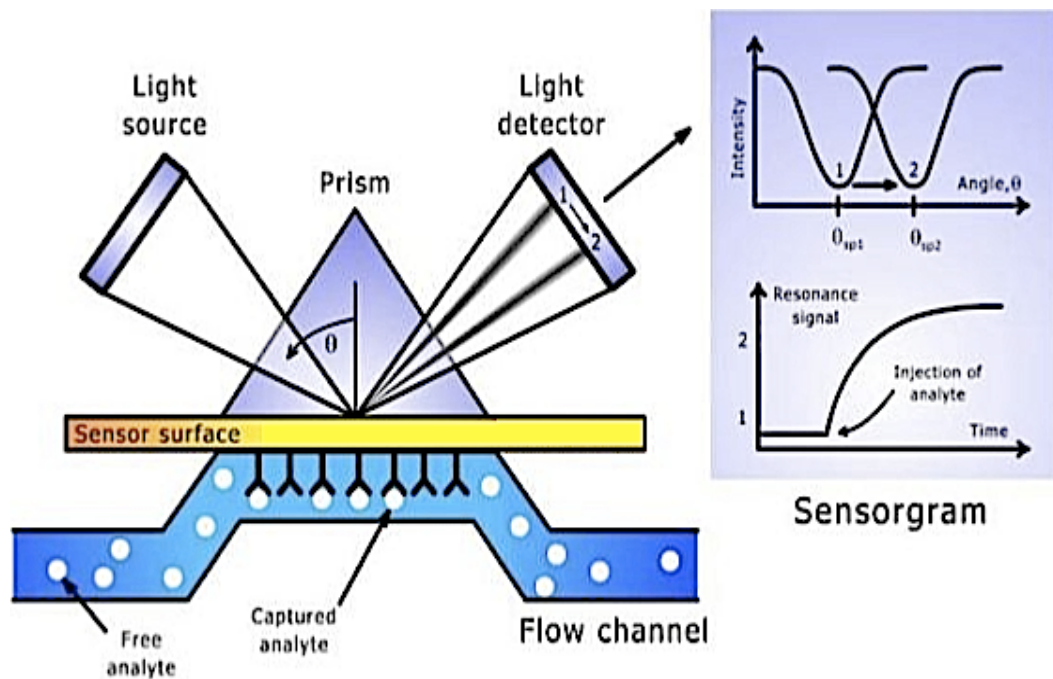


**Figure 2.10** Schematic representation of SPR. Left- SPR sensor chip; Upper right- Change in the minimum intensity angle ; Lower right- Change in response units with respect to time. (Golemis and Adams, 2005)

In SPR system while one of the interacting species is immobilized to the sensor surface, other species is passed over the sensor surface freely. While the refractive index at the prism side is not changing, the refractive index in the proximity (within  $\sim 300\text{nm}$ ) of the metal surface changes when the accumulated mass is absorbed on to the surface. When the refractive index changes, the angle at which the minimum intensity is observed shifts as shown in Figure 2.10 (upper right). This change in the refractive index is measured in real time and the result is plotted as response or resonance units (RU) vs. time in a graph called sensogram (Figure 2.10-lower right). One RU represents the binding of approximately  $1\text{ pg protein mm}^{-2}$ , but in practice for measurement at least  $50\text{ pg mm}^{-2}$  analyte binding is necessary (van der Werve et al., 2001).

The SPR unit is composed of mainly three units ;

- 1-Sensor-chip and the optical interface unit to mount the sensor-chip,
- 2-Micro-fluidics system to precisely deliver the ligand (molecule that is to be attached to the surface of the sensor-chip, and the analyte (the molecule of interest to be adsorbed by the ligand) to the sensor-chip surface,
- 3- Data collection and analysis software.

Although SPR provides fast and easy monitoring of the macromolecule-ligand interactions, in application of an SPR analysis several challenges should be overcome (Schuck, 1997):

- 1- Choice of the immobilization technique that must attach the immobilized species in a native conformation and accessible orientation.
- 2- Selection of concentration of the species such that the interaction on the sensor surface changes the refractive index in observable amounts.
- 3- Preventing non-specific interactions.
- 4- Providing the efficient transportation of the reactants to and from the sensor surface preventing mass transport limitations.

The steps chosen for efficient application of SPR analysis and the uses of the SPR units are explained in detail in the following sections.

### **Surface Modifications**

The initial uses of SPR technology were based on the direct physical adsorption of proteins to an active metal surface (Liedberg et al., 1983). However, gold surface shows high tendency for spontaneous adsorption of proteins and molecules leading to a loss in bioactivity. Thereafter, it was realized that the successful direct and label-free measurement of specific binding events are facilitated by the best possible activity to immobilize the interacting species. Also, it is important to avoid all possible non-specific

binding to the surface in order to get obtain signals of the specific interaction free of irrelevant signals. SPR can be used in a variety of applications, a large range of immobilization methods has been emerged. However, no general application method was accepted (Löfås and Mcwhirter, 2006) The two of the most commonly used surface modification methods for investigating interactions involving peptides are coating the surface with self-assembled monolayers or formation of a dextran layer for achieving ordered and well packed layers without defects within the chains. There are many used of these methods in literature. While Lin et al. (2009) and Han et al. (2009) used gold surfaces to which a carboxymethylated dextran layer is bound, in other studies by Pollet et al. (2009) and Dudak et al. (2010) self-assembled monolayer coating were employed. Similarly, as in this study for detection and quantification of peptide-hGH interaction, self-assembled monolayer surfaces on gold were prepared, the details of this method are discussed.

Self-assembled monolayer (SAM) is a layer of amphiphilic molecules in which one end of the molecule the head group shows a special affinity for a substrate and a tail with a functional group at the terminal end. SAMs are created by the chemisorption of hydrophilic head groups followed by a small organization of hydrophobic tail groups. In the beginning of layer formation on the surface, the molecules get into a disordered form; but over a period of time (8-24h) the hydrophilic groups assemble together on the substrate, while the hydrophobic tail groups assemble far from the substrate. Areas of close-packed molecules nucleate and grow until the surface of the substrate is covered in a single monolayer (Love et al., 2005). In formation of SAMs, different molecules can be selected such as 11-mercaptoundecanoic acid (11-MUA), 3-mercaptopropanoic acid or the mixture of these two (Rusmini et al 2007). In order to reduce steric hindrance and increase the immobilization efficiency in this study 11-MUA was used (Figure 2.11). The thiol head group binds to the gold surface while the Van der Waals forces between alkane chains cause them to lie at a certain angle (Nam et al, 2004).

The acid end group can then be replaced by other functionalized groups (Stettner, 2010).

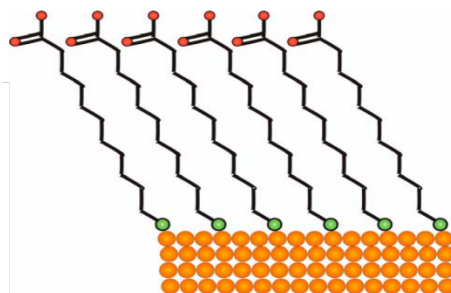


**Figure 2.11** 11-MUA on gold surface (Dots together with chains and dots on the gold surface represent acid end groups and thiol groups respectively.)

### **Ligand immobilization**

Immobilization to the surface can either be direct by covalent coupling or indirect through capture by a covalently coupled molecule.

The major advantage of direct immobilization is that it can be used for any protein provided that it is reasonably pure (>50%) and has a pI above 3.5. However, there are some disadvantages of covalent coupling. Proteins are coupled heterogeneously and often with multiple sites, thus a decrease or even abrogation of binding can be observed. Also, directly coupled proteins are difficult to regenerate (van der Werve et al., 2001). In indirect immobilization, on the other hand, immobilization usually does not affect the binding strength; all the molecules are in a known consistent orientation on the surface and using appropriate buffers, the easier dissociation might be possible. However, this technique can only be used for the proteins that have a suitable binding site or tag for the covalently coupled molecule. Also the covalently coupled molecule would act like a spacer, increasing the distance

of the immobilized molecule from the sensor surface decreasing the signal strength.

In this study as the peptides or the macromolecule hGH do not have special sites indirect binding, direct covalent binding method was applied. For covalent coupling, there are several techniques such as carboxyl chemistry, aldehyde chemistry, epoxy chemistry, thiol chemistry, amine chemistry, photoactive chemistry, ligation and so on (Rusmini et al., 2007). If the protein to be immobilized has a surface exposed disulphide or a free cysteine, thiol chemistry is the method of choice. If the protein is glycosylated aldehyde coupling can be used. If these are not the case, amine coupling should be tried for the first instance (van der Werve et al., 2001). As hGH is a non-glycosylated protein without a free cysteine, in stead of more complex methods amine coupling was applied. In this method, the carboxyl groups are activated by EDC/NHS ((1-Ethyl-3-(3-dimethylamino-propyl)carbodiimide/N-hydroxysuccinimide) creating a highly reactive ester which reacts with amine groups on proteins, forming strong amide bond. The use of NHS chemistry on SAM has been reported by Patel et al. (1997), who determined the effect of accessibility of the thermal carboxylated groups of SAM on the reaction with NHS and immobilization of the protein (catalase). Using the same procedure Karlsson et al. (1997); Wobbe et al. (2001); Han et al. (2009) ; Dudak et al. (2010) immobilized the ligand onto the surface .

After ligand is immobilized, the free carboxyl groups on the surface that are not occupied by immobilized species need to be blocked in order to prevent non-specific interaction. For that purpose bovine serum albumin (BSA) (Xie et al., 2002; Zhang et al., 2004), ethanolamine (Subramanian et al 2006; Han et al 2009; Dudak et al., 2010) or glycine can be used.

### **Interaction with the Analyte**

After ligand immobilization and blocking the free carboxyl groups are completed, the surface is equilibrated with the buffer that the analyte is dissolved in. The analyte is usually dissolved in a low molarity buffer with a low salt concentration at a pH that is chosen for the interaction. For quantitative measurements, in order to determine the association and dissociation rate constants, the concentration of the injected material should be known with a high precision. Moreover, it is important to perform a second injection with control analyte (buffer usually). This helps to rule-out non-specific binding and any other refractive index artifacts.

Additionally, for determination of binding constants, temperature of the medium should be kept constant and experiments at different analyte concentrations should be conducted by measuring the level of binding at equilibrium. Also pH of the buffer, buffer type, ligand density and analyte concentrations, flow rates of each injection (ligand, EDC/NHS, ethanolamine, buffers, analyte) should be optimized considering binding strength and mass transfer limitations.

Analyte is transported to the surface by both convection and diffusion. Convection transport can be increased simply by increasing flow rate. If this is not enough then there is an unstirred 'diffusion' layer near the sensor surface through which transport is solely by diffusion. In such a case, decreasing surface density of the immobilized ligand helps to decrease mass transfer limitations. (van der Werve et al., 2001).

### **Calculation of Affinity Constant Using Raw Data**

Although there are several binding models that can be fit to according to the shape of the binding signal, in this section the equations are written explicitly for bimolecular model for which the response signal is expected to be as shown in Figure 2.12 (Gedig, 2008).

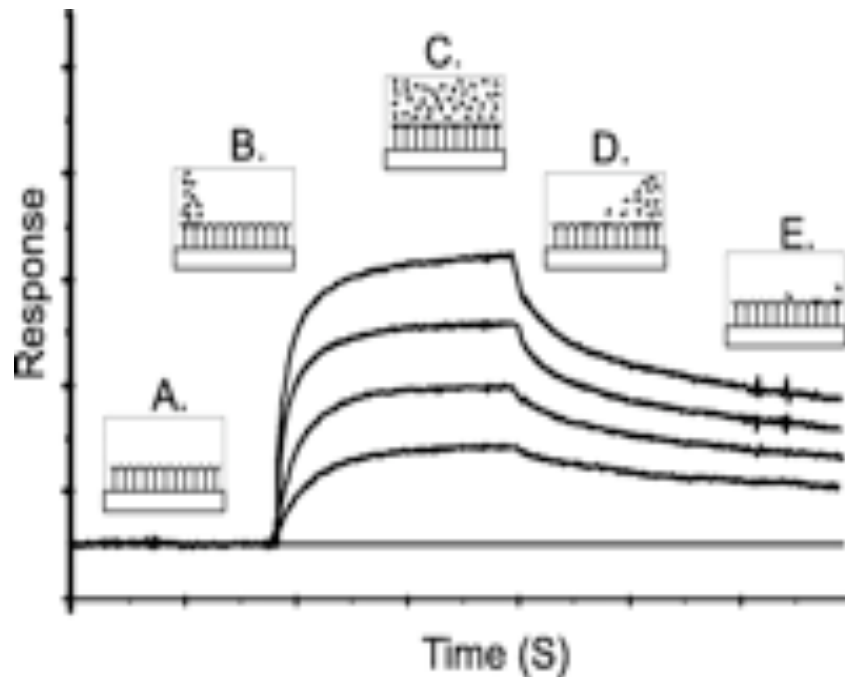
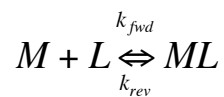


**Figure 2.12** An example of a one site binding experiment at different ligand concentrations, **A:** Macromolecule immobilized surface, **B:** ligand is passed through the sensor surface and starts to interact with macromolecule, **C:** All binding sites are filled reaching equilibrium, **D:** Desorption begins by passing the elution buffer through the sensor surface, **E:** Desorption continues until all ligands are removed from the surface (PNAS)

For a simple binding experiment with one site binding the reaction can be written as;



where  $k_{fwd}$  and  $k_{rev}$  are the rate constants for association and dissociation reactions; M, L, ML represent the macromolecule, ligand and complex respectively.

Hence the equilibrium association constant,  $K_a$  (in  $L \text{ mol}^{-1}$ ), and equilibrium dissociation constant,  $K_d$  (in  $\text{mol L}^{-1}$ ), are;

$$\begin{aligned}
K_A &= \frac{k_{fwd}}{k_{rev}} = \frac{[ML]}{[M][L]} \\
K_D &= K_A^{-1} = \frac{k_{fwd}}{k_{rev}} = \frac{[M][L]}{[ML]}
\end{aligned}
\tag{2.23}$$

where terms in brackets indicate concentrations in mol L<sup>-1</sup>.

As mentioned earlier in SPR, the sensogram signals reflect the amount of species at the surface and is recorded as a function of time (Figure 2.10). In determination of the shift in SPR angle at equilibrium ( $R_{eq}$ ) is given by the evaluation software's supplied by the equipment, the data can be plotted as  $R_{eq}/[L]$  vs.  $R_{eq}$  (Scatchard plot) giving a straight line. However, as low strength binding and low concentrations may lead to large errors in this plot, mainly non-linear regression method is used employing Langmuir binding isotherm (2.24);

$$R_{eq} = \left( \frac{[L]}{[L] + K_D} \right) M_{MAX}
\tag{2.24}$$

where  $M_{max}$  is the maximum binding capacity

The following (2.24) can then be written for an expression of response signal for association ( $R_t$ ) vs. time.

$$R_{tot} = \left( \frac{k_{fwd}[L]M_{max}}{k_{fwd}[L] + k_{rev}} \right) \left( 1 - e^{-(k_{fwd}[L] + k_{rev}).t} \right)
\tag{2.25}$$

In order to lessen the complexity of the previous equation, another parameter is defined as:

$$k_{obs} = k_{fwd}[L] + k_{rev}
\tag{2.26}$$

Hence (2.25) can be simplified as;

$$R_{eq} = \frac{k_{fwd} [L]}{k_{obs}} M_{MAX} \quad (2.27)$$

And,

$$R_t = \left( \frac{k_{fwd} [L] M_{max}}{k_{obs}} \right) (1 - e^{-k_{obs} \cdot t}) \quad (2.28)$$

Therefore fitting  $R_t$  vs. time data gives  $k_{obs}$ .

In order to calculate  $k_{fwd}$  and  $k_{rev}$ , i.e.  $K_A$  and  $K_D$  the experiments are conducted at different ligand concentrations and using (2.26), plot of  $k_{obs}$  vs.  $[L]$  gives  $k_{fwd}$  as the slope and  $k_{rev}$  as the y-axis intercept.  $K_A$  and  $K_D$  values are then calculated from (2.23).

### 2.6.2 Isothermal Titration Calorimetry (ITC)

In investigation of the interaction between two species there are many variables such as; the concentration of the species, the physical conditions; temperature, solvent type, and the kinetics and thermodynamic outcomes of the of the interaction. For understanding the effect of all these parameters on molecular interactions, isothermal titration calorimetry (ITC) is a powerful technique that can directly measure the binding affinity and the thermodynamics between the two molecules. ITC is a very advantageous tool for investigation of the molecular interactions since it simultaneously determines all the binding parameters (binding stoichiometry (n), binding affinity K, enthalpy change  $\Delta H$ ,  $\Delta S$  and  $\Delta G$  at a single experiment.), together with characterization of ligand specificity. In contrast with other methods of molecular interaction analysis, ITC characterizes interactions with native (unmodified) forms of molecules in solution (without immobilization or labeling). Additionally, ITC does not have molecular weight limitations; it can be used with any biomolecule with a wide range of biological buffers, ionic

strengths and pH values (Microcal, VP-ITC Catalogue). One challenge of ITC for the researchers is the sample amount required for one set of analysis.

Being a calorimetry based tool, ITC enables the measurement of binding affinity through the measurement of heat released/absorbed during a biomolecular binding event. This direct yield of enthalpy change yields binding affinity, the free energy of the reaction and entropy change within binding reaction. These information provide insight about the nature of interaction and ease the rationalization of relationships between structure and function of biomolecules. (Golemis and Adams, 2005)

Having such superior features, ITC has been used in large number of studies of various application fields such as investigation of protein-protein (Anderka et al., 2008), protein-peptide (Kelly et al. 2004, Soykut et al., 2008; Hoyer et al., 2008), protein-DNA (Cooper et al., 1994; Buczek and Horvath, 2006; Deleeuw et al., 2008) protein-carbohydrate (Dam and Brewer 2002,2004), protein-lipid (Ek et al., 1997; Abraham et al., 2005; Fang et al., 2006) , antibody-antigen (Braden and Poljak, 1995; Sottriffer et al., 1999; Arouri et al., 2007; Dormitzer et al., 2008; Jakola et al., 2008), protein-small molecule (Aitken et al, 2001; Banerjee and Kshore, 2006; Behbehani et al., 2010) small-molecule-small-molecule, enzyme-inhibitor (Adjuar-Sanchez et al., 2007), enzyme-coenzyme (Wolthers et al., 2007), enzyme-substrate (Mudhivartha et al., 2007) interactions; drug design (Haq, 2002; Bertini et al., 2007), biopolymer interactions (Chatterjee et al., 2002; Yin et al., 2008).

In this study, ITC is used to investigate the binding affinity of the designed/selected peptides towards hGH and to conduct the thermodynamic analysis of interaction by determination of binding parameters binding stoichiometry (n), binding affinity K, enthalpy change  $\Delta H$ ,  $\Delta S$  and  $\Delta G$ . Similarly, Kelly et al., (2004) used ITC for development and validation of affinity between a peptide ligand selected from phage display library and recombinant B-domain deleted factor VIII (BDDrFVIII). The evaluation of the

binding data for titration of BDDrFVIII by the peptides that are found free in solution and peptides that are immobilized on sepharose beads, showed that the immobilization of peptides on beads lead to loss of interaction. In a recent study, Dudak et al. (2010) conducted the thermodynamic analysis of interactions between peptide ligands again selected from phage display library and Staphylococcal Enterotoxin B (SEB) and peptide ligands and compared the binding affinity and hence specificity of these ligand by using bovine serum albumin (BSA) in control experiments. According to the results of this study it was concluded that the interaction between peptides and SEB were driven entropically and the binding was dominated by hydrophobic interactions.

Related with the ITC analysis of interactions involving hGH as macromolecule, Behbehani et al., (2010) performed the thermodynamic study on the interaction of copper ion with hGH at two different temperatures, 300.15 K and 310.15 K. For achieving a detectable enthalpy, 60 $\mu$ M hGH solution in 30mM Tris buffer at pH=7 was used in the cell, while 100mM Cu(NO<sub>3</sub>)<sub>2</sub> solution in the same conditions was titrated. The binding parameters were obtained, and Kd value for the interacting species were found as 1313.4 \*10<sup>-6</sup> and 1648.2 \*10<sup>-6</sup> at 27°C and 37°C respectively; while the enthalpies were almost equal to each other.

### **Theory of ITC**

In 1965, the first calorimetric method for determination of binding constants was developed by Hansen et al., (1965) for the investigation of thermodynamic properties of metal-ligand binding interactions. Since then, several improvements have been made on calorimetry based analysis approaches and isothermal titration calorimetry has been developed. ITC is composed of two identical cells (a reference cell and a sample cell) made of highly efficient conducting material surrounded by an adiabatic jacket as shown schematically in Figure 2.11 (Roselin et al, 2010). These two cells are

kept in thermal equilibrium; i.e  $\Delta T=0$  throughout the experiment. One cell is filled with water to act as a reference, while the other cell is filled with one of the components of the interaction.

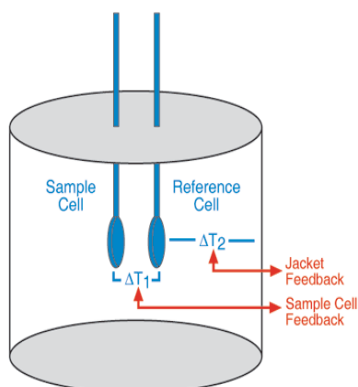


**Figure 2.13** Schematic diagram of ITC instrument ([www.microcal.com](http://www.microcal.com))

The other interacting component is loaded to the injector and the solution is titrated into the cell containing the other component solution at constant temperature (Figure 2.14). If there is an interaction between these two species, as the component in syringe is injected into the cell in series of equal volume of injections, heat is either released or absorbed due to interaction and in direct proportion to the amount of binding. This amount of energy is measured by measuring the heat energy per unit time that must be added/removed to the sample cell in order to maintain the temperature of the sample cell and reference cell equal to each other at the selected temperature for the experiment (Ladbury and Chowdhry, 1996). For measurement of necessary heat and regulation of the constant temperature the device uses a cell feedback network (CFB) ([www.microcal.com](http://www.microcal.com)).

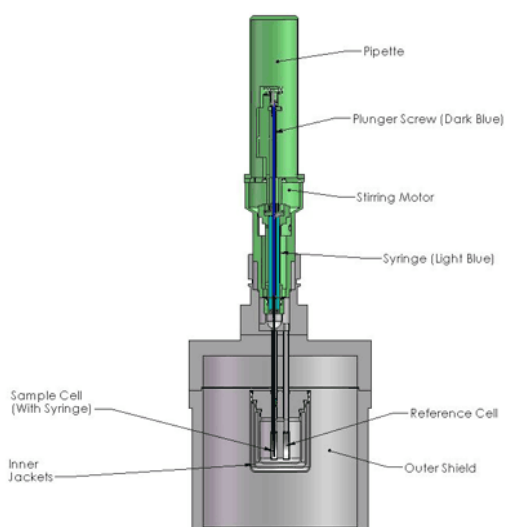


**Figure 2.14** Diagram of ITC equipment; the syringe rotates to provide continuous mixing ([www.microcal.com](http://www.microcal.com))

As the titration continues, the power needed to maintain the cell temperature constant is given as a function of time in seconds. Each power peak corresponds to total heat effect of one ligand injection. The titration experiment is continued until the system reaches saturation; i.e. the heat signals (power peaks) are no longer diminishing. At the end of the experiment, in order to obtain the binding curve, the raw data-power peaks are integrated and heats from each injection vs. the ratio of component in the syringe (ligand) and component in the cell is plotted. Although this plot gives an idea about the strength of binding, before calculation of the thermodynamic parameters, three blank experiments should be conducted. These experiments are:

- 1) *Heat of dilution of ligand*; the ligand is titrated onto buffer in a sample cell.
- 2) *Heat of dilution of macromolecule*; the buffer is titrated onto macro-molecule in the sample cell. The enthalpy change of this system is usually negligible.

- 3) *Instrument blank*; the buffer is titrated into buffer. Again negligible enthalpy change expected to be observed. This is done before the main binding experiment to check whether the device is properly working.

After all these four analysis are conducted, the binding curve for heat of dilution of ligand (this experiment should be conducted with the same ligand concentration as the main binding experiment) is subtracted from the main binding experiment, then the binding curve can be fit to a desired appropriate model (Figure 2.15).

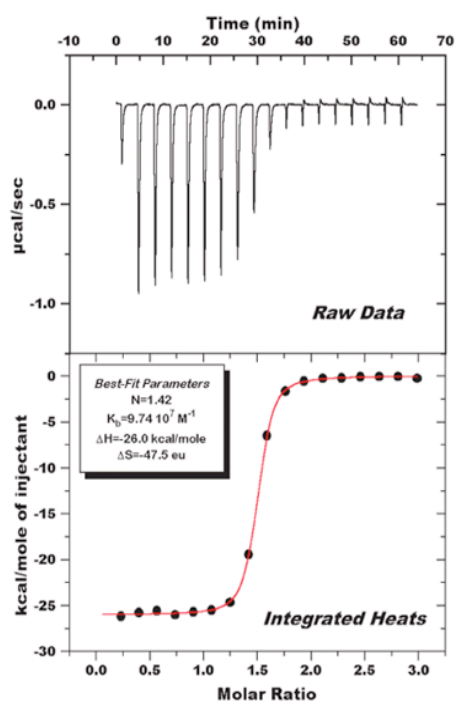


**Figure 2.15** ITC data. Top: Raw interaction data; bottom: binding curve (www.microcal.com)

### **Determination of Macromolecule Concentration**

The figure shows a binding curve for a well-planned experiment. For the planning of the experiments in addition to the physical parameters such as temperature, pH, buffer type and strength and salt concentration, the macromolecule and ligand concentrations should be selected properly so that appropriate binding isotherm can be achieved for data fitting. For that purpose Wiseman et al., (1989) defined a dimensionless constant,  $c$  (2.29), that describes the practical approach to accurately determine the binding constant and then to make a decision for macromolecule/ligand concentrations of the next experiment to obtain better results.

$$c = nK_A [M]_T \quad (2.29)$$

where,  $n$  is the stoichiometry of interaction  $K_a$  is the binding constant and  $[M_T]$  is the macromolecule concentration in the cell.

To obtain accurate estimate of binding affinity and thermodynamic parameters, the values of  $c$  should be between 1 and 1000. Otherwise, when  $c > 1000$  although accurate binding enthalpy can be obtained,  $K_a$  estimation becomes unreliable. When  $c < 1$  determination of both binding affinity and enthalpy are challenging.

Therefore once a preliminary experiment is performed, by looking at the binding diagram one can make a decision on whether it is necessary to increase or decrease the macromolecule concentration to obtain accurate binding constants (Figure 2.16).

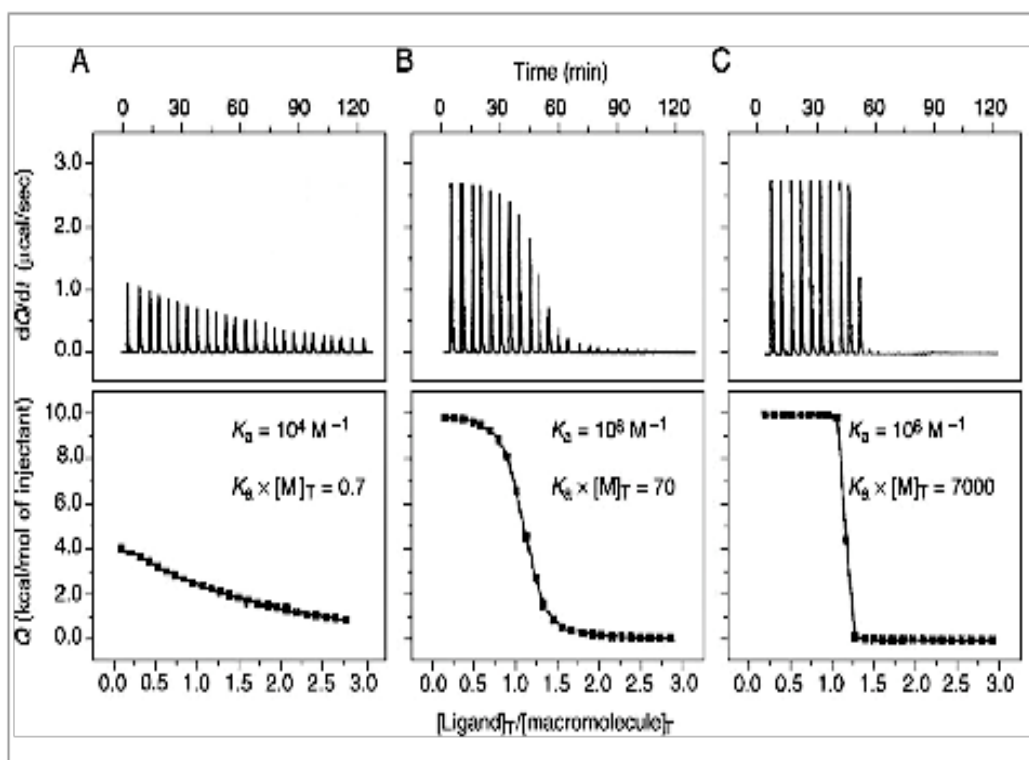


**Figure 2.16** Effect of  $K_a$  on the shape of the titration curve. These experiments are formed at the same conditions, concentrations but has different affinities. A) low affinity; B) intermediate affinity; C) high affinity (Velazquez-Campoy et al., 2004)

### **Determination of Ligand Concentration**

Another important parameter that should be considered is the ligand concentration. In order to obtain the binding curve at the shortest time within a specified number of injections, due to higher volume of the cell, the syringe concentration should be higher than cell concentration, so that for 1:1 stoichiometry, at the end of the experiment, ligand/cell molar ratio is 2-3. Therefore, taking the cell volume ( $\sim 1.5$ ml), single injection volume ( $\sim 10$ ul) and the number of injections ( $\sim 30$ ) into account, around 10-30 times higher than the macromolecule concentration (Velazquez-Campoy et al., 2004).

### **Evaluation of Thermodynamic Constants of Binding**

As mentioned earlier using ITC, one can determine the thermodynamic properties of an interaction. ITC is capable of measuring the  $\Delta H$ , the enthalpy change during binding in  $\text{cal mol}^{-1}$ , and calculating the  $K_a$ , the binding affinity or association constant, from the equilibrium data. Taking  $M$  as the macromolecule in the cell, and  $L$  as the ligand in the syringe the reversible binding reaction can be written as (2.30).



For a single binding site, the association constant is defined earlier as in (2.23).

The relation between Gibbs free energy of binding,  $\Delta G$  (in  $\text{cal mol}^{-1}$ ), and association constant can be given as (Velazquez-Campoy et al., 2004);

$$\Delta G = -RT \ln K \quad (2.31)$$

where  $T$  is the absolute temperature (in  $K$ ) at which the experiment was conducted and  $R$  is the gas constant and equals to  $1.9858775 \text{ cal K}^{-1}\text{mol}^{-1}$ .

Once the binding curve is formed by subtracting the peptide dilution experiment from the binding experiment  $\Delta H$  can be easily calculated by subtracting the lower plateau from the upper plateau molar energy values (Fisher and Singh, 1995). Then knowing  $\Delta G$  and  $\Delta H$  at the temperature of the experiment, from the Gibb's free energy equation (2.32) (Sandler,1999),  $\Delta S$  entropy of binding,  $\text{cal mol}^{-1} \text{K}^{-1}$ , in can be calculated.

$$\Delta G = \Delta H - T\Delta S \quad (2.32)$$

From the derived equations, it is clear that binding affinity is dependent on  $\Delta H$  and  $\Delta S$  of the chemical interaction.

Moreover, another thermodynamic parameter  $\Delta C_p$ , the change in heat

capacity can be defined as the temperature derivative of enthalpy change (Sandler, 1999) and written in 2.33;

$$C_p = \left( \frac{dH}{dT} \right)_p \quad (2.33)$$

As it can be easily understood from (2.33), when a series of experiments are performed at different temperatures, slope of the  $\Delta H$  vs. T plot gives  $\Delta C_p$  value.

### **Interpretation of the Thermodynamic Data**

Specific interactions that are involved in protein-ligand binding are hydrogen bonding, hydrophobic interactions, electrostatic (salt bridge) interactions and proton ionization. After all the thermodynamic data (N,  $K_a$ ,  $\Delta H$ ,  $\Delta G$ ,  $\Delta S$  and  $\Delta C_p$ ) are calculated, in order to understand the characteristics of binding the data extracted from the experiment needs to be understood. N gives the number of binding sites on the macromolecule that ligands bind.  $K_a$  is the binding affinity constant that is usually between  $10^3$  and  $10^9$  (Nienhaus, 2005); the higher the  $K_a$ , the stronger the interaction.  $\Delta G$  value shows whether binding is spontaneous or not, hence for a considerable binding affinity  $\Delta G$  should obviously be negative signed.  $\Delta H$  represents the changes in bond energy that occurred during reaction takes place, whereas  $\Delta S$  represents all other positive and negative driving forces that contribute to the free energy. When (2.31) is considered, for stronger binding  $\Delta G$  is desired to be negative and as small as possible. Therefore, to obtain  $\Delta G$  negative signed, looking at (2.32),  $\Delta H$  is desired to be negative (exothermic), while for  $\Delta S$  positive values are more desirable.

The binding enthalpy majorly reflects the interaction strength (the non-covalent interactions such as van der Waals, hydrogen bonds and electrostatic forces).  $\Delta H$  is actually the resultant value of formation and breaking of individual bonds. As it is difficult to form a bond without

breaking some others, the individual component interactions may produce positive or negative energy. Therefore, the resultant energy of complex formation is expected to be much smaller than some of the individual interactions (Fisher and Singh, 1995).

$\Delta S$  can be defined as the reflection of tendency for disruption of order i.e change in degrees of freedom of all components; moreover it expresses the degree of uncoupling of enthalpic processes from  $\Delta G$  (Fisher and Singh, 1995). Entropy change mainly reflects two changes; in solvation entropy and conformational entropy (D'Aquino et al., 2000). As the ligand binds to the macromolecule, desolvation occurs and the release of water molecules from the binding site produces increase in degrees of freedom, which favorable for binding interactions. On the other hand, as the proteins bind to ligands they lose conformational freedom reducing the conformational entropy term (Velazquez-Campoy et al., 2004). This is unfavorable since high entropy values are desired. As indicated in previous studies, the increase in entropy could be the result of hydrophobic interactions or electrostatic interactions (Krescheck et al., 1995; Jelesarov and Bosshard, 1999; Dudak et al., 2010). In a recent study, Dudak et al., (2010) concluded that the main factor that leads to large favorable entropy for the interaction between peptide ligands and SEB is the release of ordered water in to solution and reduction in the water accessible surface during complex formation which indicates the importance of hydrophobic residues for interaction. In another study conducted by Krescheck et al. (1995), the interaction between horse ferricytochrome c and yeast cytochrome c peroxidase was obtained to be driven by entropy. Although the high value of entropy was thought as a reflection of hydrophobic interactions, due to the low  $\Delta C_p$  value (very close to zero), either van der Waals or electrostatic interactions could be the contributors of entropy. When the experiments were carried out in buffers of different ionic strengths, different binding affinity values were obtained and  $\Delta G$  of binding was extrapolated to infinite ionic strength where electrostatic

interaction should be negligible indicating that electrostatic effects dominated that interaction.

For determination of the binding type according to thermodynamic data obtained, Eftink et al. (1983) proposed the following methodology: 1) Hydrophobic interactions:  $\Delta H=0-2$  kcal mol<sup>-1</sup>/  $\Delta S=0-20$  kcal mol<sup>-1</sup> K<sup>-1</sup>, 2) Electrostatic interactions:  $\Delta H=0$  kcal mol<sup>-1</sup>/  $\Delta S=0-30$  kcal mol<sup>-1</sup> K<sup>-1</sup>, 3) Hydrogen bonding:  $\Delta H=0-3$  kcal mol<sup>-1</sup>/  $\Delta S=0- -7$  kcal mol<sup>-1</sup> K<sup>-1</sup>. Although there are many studies in which for the interaction analysis similar approaches were used, the small range and high overlapping of these values imply that such an interpretation of data would not be accurate.

One other parameter that is important to understand the binding better is  $\Delta C_p$ .  $\Delta C_p$  is the measure of dependence of  $\Delta H$  and  $\Delta S$  on temperature (van der Werve, 2001).  $\Delta C_p$  is usually negative and smaller than 1kcal mol<sup>-1</sup> K<sup>-1</sup> in absolute value (Velazquez-Campoy et al., 2004). However, the high heat capacity of binding,  $\Delta C_p$ , reflects the burial of polar and apolar surfaces as a consequence of binding reaction (Murphy and Freire, 1992). Therefore, similar to entropy, higher  $\Delta C_p$  is an indication for the hydrophobic interactions this time due to protein folding and binding. As mentioned previously, using this approach Kresheck et al. (1995) concluded that even though the binding process was entropically driven as  $\Delta C_p$  was low, while determining the binding, interactions other than hydrophobic are taken into account.

Thermodynamic constants and experimental conditions of many protein-protein and protein-peptide interaction experiments are summarized by Stites (1997).

As formation of protein peptide complex is accomplished usually by net release or uptake of protons, the number of protons given up or taken by the proteins will lead to equal number of protonation or deprotonation events in the buffer. Therefore the experimental binding enthalpy becomes the sum of

binding enthalpy that only arises from complex formation independent of the buffer used,  $\Delta H_{bind}$ , and another term proportional to the enthalpy of ionization of the buffer,  $\Delta H_{ion}$ , and formulated as (Velazquez-Campoy et al., 2004);

$$\Delta H_T = \Delta H_{bind} + N_{H^+} \Delta H_{ion} \quad (2.34)$$

where,  $N_{H^+}$  is the proportionality constant, the number of protons that are exchanged between the complex and the bulk solution.

In order to determine if protonation or deprotonation events take place within binding process,  $\Delta G$  and  $\Delta H$  of binding should be determined for the same experimental conditions using different buffers with different enthalpy of ionizations and at different pH values. (Stites, 1997; Falconer et al., 2010).

## CHAPTER 3

### MATERIALS AND METHODS

#### 3.1 Chemicals

All chemicals and solutions were analytical grade, and obtained from Sigma Aldrich Co., Merck &Co. Inc., New England Biolabs Inc. and Fitzgerald Inc., Peptides are synthesized by Genscript USA Inc.

#### 3.2 Buffers and Stock Solutions

All buffers and stock solutions were prepared with distilled water and sterilized by autoclaving at 121°C for 20 minutes or by filtering with 0.45 µm filters (MF-Millipore, MCE Membrane) and stored at +4°C or room temperature. All buffers and stock solutions used are listed in Appendix A.

#### 3.3 Production

##### 3.3.1 Microorganism

*Pichia pastoris* pPICZαA::hGH::Mut<sup>+</sup> (Orman et al., 2008) were used for rhGH production. The recombinant microorganisms are stored in microbanks (PRO-LAB), by inoculating young colonial growth into cryopreservative fluid present in the vial. After providing the adsorption of microorganisms into the porous beads, excess cryopreservative was aspirated and inoculated into cyrovial stored at -55°C.

### 3.3.2 Growth Medium and Storage of Microorganisms

#### 3.3.2.1 Solid Medium

Recombinant *P. pastoris* strains were stored in microbanks at -55°C or inoculated on YPD agar containing 0.1 ml/L Zeocin as antibiotic. The composition of solid medium is listed in Table 3.1.

**Table 3.1** The composition of the YPD, solid medium.

Compound	Concentration, g L <sup>-1</sup>
Yeast extract	10
Peptone	20
Glucose	20
Agar	20
Zeocin	1 ml

The inoculated solid medium was kept at +4°C and the media were refreshed at least every two months to obtain fresh single colonies.

#### 3.3.2.2 Glycerol Stock Solution and Precultivation Medium

Recombinant *P. pastoris* *Mut<sup>+</sup>* strain grown on YPD agar was first inoculated into precultivation medium, liquid YPD (Table 3.2). If the production was not aimed to continue, the harvested cells from YPD were resuspended in glycerol stock solution (Table 3.3) and stored at -55°C; otherwise after around incubation in solid media, the single colonies were directly inoculated into of BMGY (Buffered Glycerol Complex Medium) as will be described in later, the second precultivation medium and growth is continued in air filtered shake bioreactors. The composition of BMGY is

given in Table 3.4. After sterilization the selective antibiotics, Zeocin or chloramphenicol, were added to the precultivation media with concentrations given in following Tables 3.2, 3.3 and 3.4.

**Table 3.2** The composition of YPD, the first precultivation medium

<b>Compound</b>	<b>Concentration, g L<sup>-1</sup></b>
Yeast extract	10
Peptone	20
Glucose	20
Zeocin	1ml

**Table 3.3** The composition of the glycerol stock solution(Schenk et al., 2007)

<b>Compound</b>	<b>Concentration, g L<sup>-1</sup></b>
NaCl	9
Glycerol	20

**Table 3.4** The composition of BMGY, second precultivation medium.

<b>Compound</b>	<b>Concentration, g L<sup>-1</sup></b>
Yeast extract	10.0
Peptone	20.0
Potassium phosphate buffer pH=6.0	0.1 M
YNB	3.4
(NH <sub>4</sub> )SO <sub>4</sub>	10.0
Biotin	4×10 <sup>-4</sup>
Glycerol (mL)	10.0
Chloramphenicol* (mL)	1

\* Chloramphenicol is prepared as 34mg/ml stock in pure ethanol, kept in sterile dark bottle at -20°C.

### 3.3.2.3 Production Medium

The recombinant *P. pastoris* strain grown on BMGY medium was inoculated into production medium after cells were harvested by centrifugation. For recombinant protein production, a defined medium production medium, which contains sorbitol together with methanol, basal salts solution and nitrogen sources, whose composition was reported by Jungo et al. (2006) was used in air filtered shake bioreactor experiments. However, instead of ammonium chloride in this study ammonium sulfate was used and the amount was calculated such that Carbon/Nitrogen ratio and Methanol/Nitrogen ratio are 4.57 and 2.19 in the medium (Jungo et al, 2006). Methanol and sorbitol were added as optimized in thesis study by Aık, (2009) to production medium in shake flask experiments. Basal salt medium (BSM) was used as a production medium for pilot scale fed-batch bioreactor experiments. The compositions of the PTM1 (trace salt elements) and the defined medium used in shake flask experiments and BSM are listed Table 3.5, 3.6 and 3.7 respectively. All of the medium components were autoclaved at 121°C for 20 min, except chloramphenicol, ammonia and trace salts (sterile filtered and stored at +4°C) were then added to the medium separately.

**Table 3.5** The composition of PTM1 (Sibirny et al.,1987)

<b>Compound</b>	<b>Concentration (g ml<sup>-1</sup>)</b>
CuSO <sub>4</sub> .5H <sub>2</sub> O	0.6
NaI	0.008
MnSO <sub>4</sub> .H <sub>2</sub> O	0.3
Na <sub>2</sub> MoO <sub>4</sub> .2H <sub>2</sub> O	0.02
H <sub>3</sub> BO <sub>3</sub>	0.002
ZnCl <sub>2</sub>	2
FeSO <sub>4</sub> .7H <sub>2</sub> O	6.5
CoCl <sub>2</sub> .6H <sub>2</sub> O	0.09
H <sub>2</sub> SO <sub>4</sub> (mL)	0.5
Biotin*	0.02

\*Biotin was prepared as 0.2g/L stock and stored in dark bottle at +4°C.

**Table 3.6** The composition of the defined production medium (Açık, 2009).

<b>Compound</b>	<b>Concentration, g L<sup>-1</sup></b>
Methanol (mL)	10
Sorbitol	30
Potassium phosphate buffer pH=6.0	0.1M
(NH <sub>4</sub> ) <sub>2</sub> SO <sub>4</sub>	21.75
PTM1 (mL)	4.35
MgSO <sub>4</sub> .7H <sub>2</sub> O	7.30
Ca SO <sub>4</sub> .2H <sub>2</sub> O	0.57
Chloramphenicol (mL from stock)	1

**Table 3.7** The composition of Basal Salt Medium (BSM) (Sibirny et al., 1987)

<b>Compound</b>	<b>Concentration g L<sup>-1</sup></b>
85% H <sub>3</sub> PO <sub>4</sub>	26.7 mL
CaSO <sub>4</sub> .2H <sub>2</sub> O	1.17
MgSO <sub>4</sub> .7H <sub>2</sub> O	14.9
KOH	4.13
K <sub>2</sub> SO <sub>4</sub>	18.2
Glycerol	40.0
Chloramphenicol (mL from stock)	1
10% Antifoam (mL)	1
PTM1 (mL)	4.35

### 3.3.3 Recombinant Human Growth Hormone Production

As mentioned, rhGH production was performed either in batch cultures using laboratory scale air filtered shake bioreactors or pilot scale bioreactors.

#### 3.3.3.1 Precultivation

*P. pastoris* strains carrying human growth hormone gene, was inoculated onto solid medium containing with given composition in Table 3.1 and incubated for t=48-60 h at 30°C, until single colonies are obtained. After that, two or three colonies were inoculated into liquid YPD medium and for glycerol stock preparation the culture was incubated at 30°C and N=225 min<sup>-1</sup> for 19 h in agitation and heating rate controlled orbital shakers (B.Braun, Certomat BS-1) using air-filtered Erlenmeyer flasks of 150 mL in size with a working volume of 10 mL. Then 200µL from liquid culture was added to 800µL glycerol stock. Stock is stored at -55°C. If it was aimed to

continue the production process, two or three colonies from solid medium were inoculated into BMGY medium ( $V_R=15\text{mL}$ ) and grown for 19h of incubation at  $30^\circ\text{C}$  and  $N=225\text{ min}^{-1}$  agitation in shaker until cell concentration reaches  $OD=6-8$  which corresponds to cell concentrations of  $C_X=1.65-2.2\text{ g L}^{-1}$ .

### **3.3.3.2 Laboratory Scale Air Filtered Shake Bioreactors**

In laboratory scale air filtered shake bioreactor experiments, production was achieved in baffled and air filtered Erlenmeyer flasks of 250 mL in volume ( $V$ ) having working volume capacities ( $V_R$ ) of 50 mL. The cells grown in BMGY were harvested by centrifugation (10 min, 4000rpm,  $+4^\circ\text{C}$ ) and cells are resuspended using distilled water and directly transferred to production medium, with composition given in Table 3.6, such that the initial OD for production was 0.3 i.e  $C_X=0.0825\text{ g L}^{-1}$ . Production was performed batchwise again in air filtered shake bioreactors at different temperatures ( $T=25-32^\circ\text{C}$ ) and  $N=225\text{ min}^{-1}$ . For induction 1% methanol was added to the medium in every 24 hours. Production process was performed batchwise and continued for 49 h, in order to get a foresight before starting higher density cultivations in pilot scale bioreactor.

### **3.3.3.3 Pilot Scale Bioreactor**

The production was achieved in  $V=3.0\text{ L}$  bioreactor (Braun CT2-2), having a working volume of  $V_R=1\text{L}$  in pilot scale bioreactor experiments. The major control systems that are used in the reactor are temperature, pH, foam, stirring rate, feed inlet rate and dissolved oxygen controls. Moreover in order to provide homogeneity (prevent precipitation) and to ease the oxygen transfer within reactor, bioreactor was stirred two four-bladed Rushton turbines and consisted of four baffles and a sparger. Sterilization and temperature control were achieved using a jacket around the bioreactor, an external cooler and a steam generator. A compressor and a pure oxygen tubes were employed to supply air or oxygen enriched air. The inlet oxygen

flow rate was adjusted by a mass flow controller and gas inlet pressure was kept at 1 bar with the help of a gas regulator. Feed solutions placed on balances were transferred through inlet ports by using peristaltic pumps. The schematic presentation of the bioreactor and the cultivation steps for production were given in Figure 3.1.

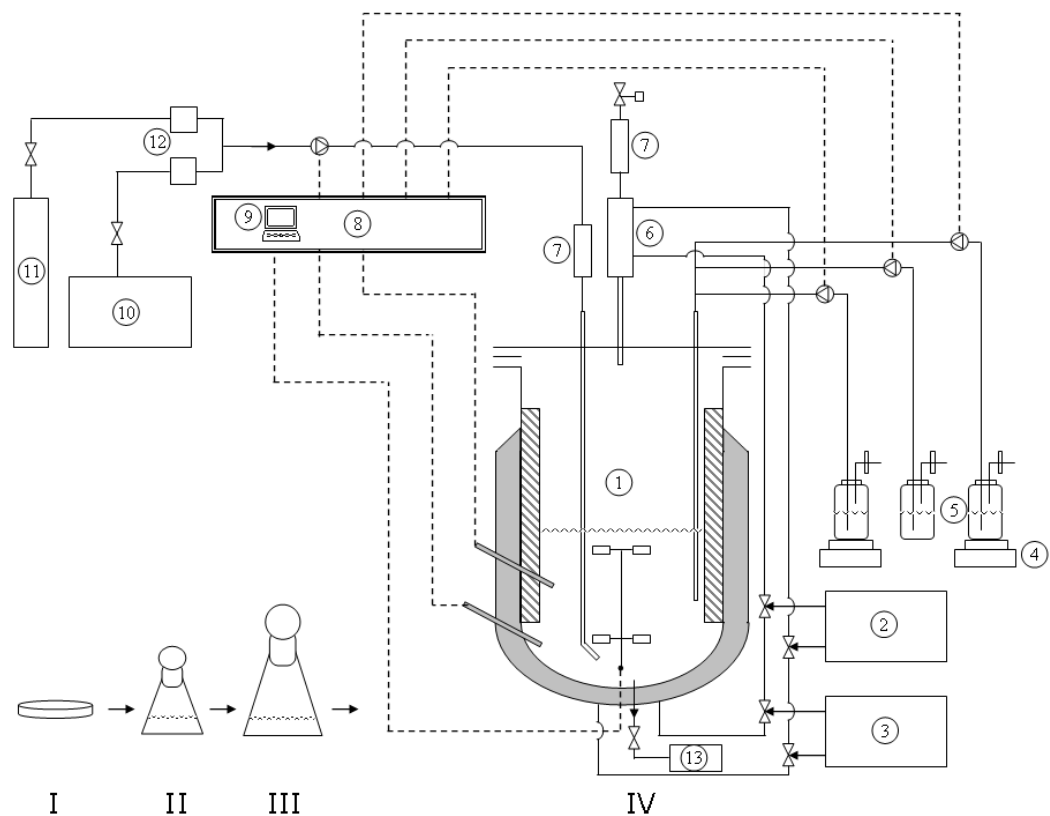


**Figure 3.1** Scale up steps and the pilot scale bioreactor system. I: Solid medium inoculated from stock culture; II: 1st Precultivation medium,  $V = 10$  mL; III: 2nd Precultivation medium,  $V = 50$  mL; IV: Pilot scale bioreactor system,  $V_0=0.9$  L, which is composed of (1) Bioreaction vessel, Biostat CT2-2 (2) Cooling circulator (3) Steam generator (4) Balances (5) Feed, base and antifoam bottles (6) Exhaust cooler (7) Gas filters (8) Controller (9) Biostat CT Software (10) Air compressor (11) Pure  $O_2$  tank (12) Digital mass flow controllers (13) Sampling bottle (Çelik, 2008)

### 3.3.3.3.1 Bioreactor Operation Parameters

In order to construct an efficient bioprocess to obtain high productivity and yields, determining and controlling the ideal bioprocess operation parameters is crucial. Temperature was to be controlled constant using the PI controller of the bioreactor system throughout the process. For adjustment of pH at desired level, ammonium hydroxide solution (25%  $\text{NH}_3\text{OH}$ ) was supplied to the fermentation medium (Çelik et al., 2009). Using the PI controller of the bioreactor system with parameters as  $X_p=30\%$  and  $T_I=30\text{s}$ , and keeping the base-pump-valve open at 10%, the pH of the medium was automatically controlled.

Another important parameter for *P. pastoris* high-density fermentations is the percentage of dissolved oxygen in the media. As methanol is used as the main substrate and the inducer of the bioprocess, and the methanol utilization pathway requires oxygen, high oxygen consumption rates can be seen in high-density production. Taking the previous studies in literature as the reference (Xie et al., 2005; Çelik et al., 2009; Wang et al., 2009) dissolved oxygen (DO) was kept above 20% saturation in all sets of experiments to prevent oxygen limitation. At the beginning of the bioprocess (glycerol batch phase), air was fed to the medium for control; and as the oxygen in the air became insufficient, i.e. the dissolved oxygen was below 20%; enriched air with increasing amount of oxygen controlled by the mass flow controller was fed to the medium. PID controller of bioreactor system was used and adjusting the valve opening with respect to changes in the oxygen requirement of the system, oxygen control was performed.

In order to enhance aeration and prevent aggregation, the agitation rate was maintained constant at  $N=900$  rpm for pilot scale bioreactor experiments and  $N=250$  rpm for laboratory scale shake flask bioreactors (Thorpe et al., 1999; Hao et al., 2007; Çelik et al., 2009). Agitation used in shake flask experiments would not be enough for pilot scale bioreactor since

*P. pastoris* consumes oxygen at a very high rate in high-density fermentations.

To prevent foaming that is mainly seen at the production phase (Methanol fed-batch) antifoam solution (10%(v/v)) was added to the medium to the initial medium (0.01% (v/v)) and very small amounts of usually 1 or 2 mL of 10% antifoam solution was added drop-wise as required during the process.

### **3.3.3.3.2 Precultivation, Co-Substrate Addition and Methanol Feeding Rate in Fed-Batch Pilot Scale Bioreactor Operations**

The *P. pastoris* cells having  $C_x=1.65-2.2$  g L<sup>-1</sup>, were harvested from the BMGY precultivation medium and resuspended in BSM medium which was previously fed to the bioreactor such that the initial  $OD_{600} \sim 1$ ;  $C_x=0.275$  g L<sup>-1</sup>. Although a standard protocol developed by Stratton et al., (1998) was used for the expression of rhGH by *P. pastoris* under the control of the AOX1 promoter; in order to increase the cell density and product concentrations modifications were done.

In this study, a four-phase feeding strategy was employed for rhGH production by *P.pastoris* (Stratton et al., 1998, Sinha et al., 2004). First in order to first glycerol batch (GB) in which the main purpose was to achieve higher cell concentrations, was conducted for around 18 hours until  $C_x$  reached 10 g L<sup>-1</sup>. Second, a glycerol fed-batch transition phase (GFB) was applied at limiting glycerol levels with a pre-determined exponential feeding profile to further increase cell concentration and re-depressing AOX enzyme (necessary for the dissimilation of methanol) by feeding glycerol at limited concentration. This phase was continued until  $C_x=20-23$  g L<sup>-1</sup> and then in order to prepare the cell for the new substrate prior to fed-batch phase methanol transition (MT) phase is applied by the addition of methanol as a pulse such that the concentration is 1.5 g L<sup>-1</sup> (from 100% methanol containing 12mL L<sup>-1</sup>PTM1) (Figure 3.2). The transition phase was continued

for 6 hours and with the increase dissolved oxygen concentration methanol fed-batch phase (MFB) was started with the pre-determined exponential feeding strategy. For every bioreactor experiment performed in this study, the first three phases; GB, GFB and MT the same cell growth was achieved (Figure 3.2). For fed-batch feeding of methanol and glycerol, (3.1) was used with different constants for these two different carbon sources were used as tabulated in Table 3.8.

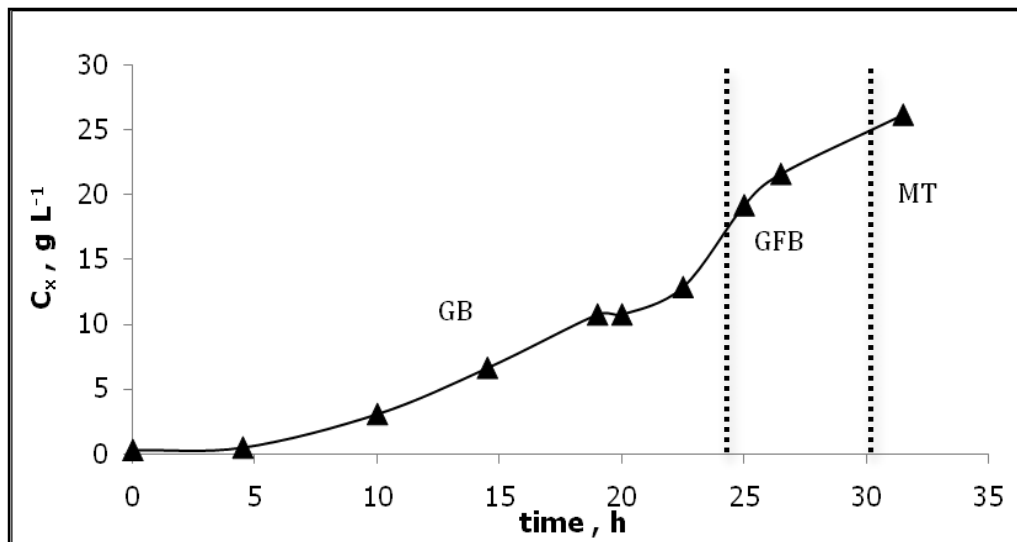


**Figure 3.2** Variation in cell concentration with cultivation time in the precultivation phases: glycerol batch phase (GB), glycerol fed-batch phase (GFB) and methanol transition phase (MT).

In fed-batch fermentations the exponential feeding rate of the limiting substrate was determined due to the specific growth rate of the microorganism. In this context, in this study using (3.1), the rate of exponential methanol (and glycerol) feeding rate is determined prior to feeding (Shuler and Kargi, 2002).

$$F(t) = \frac{\mu_0 V_0 C_{X0}}{Y_{X/S}} \exp(\mu_0 t) \quad (3.1)$$

where,  $\mu_0$  is the specific growth rate ( $\text{h}^{-1}$ ),  $V_0$  is the initial culture volume (L),  $C_{X0}$  is the initial cell concentration ( $\text{g L}^{-1}$ ), and  $Y_{X/S}$  ( $\text{g g}^{-1}$ ) is the cell yield on substrate, which are the limiting substrates glycerol and methanol.

**Table 3.8** Parameters of Equation (3.1) for Glycerol and Methanol Fed-Batch Feeding

Parameter	Glycerol Fed-Batch Phase	Methanol Fed-Batch Phase
$\mu_0$ ( $\text{h}^{-1}$ )	0.18	variable 0.02-0.04
$Y_{X/M}$ ( $\text{g g}^{-1}$ )	0.5 *	0.42**

\* Cos et al., 2005, \*\* Jungo et al., 2006

Using the parameters given in Table 3.8 for GFB phase and MFB phase, sample glycerol and methanol feeding schemes are plotted in Figure 3.3 and Figure 3.4 respectively.

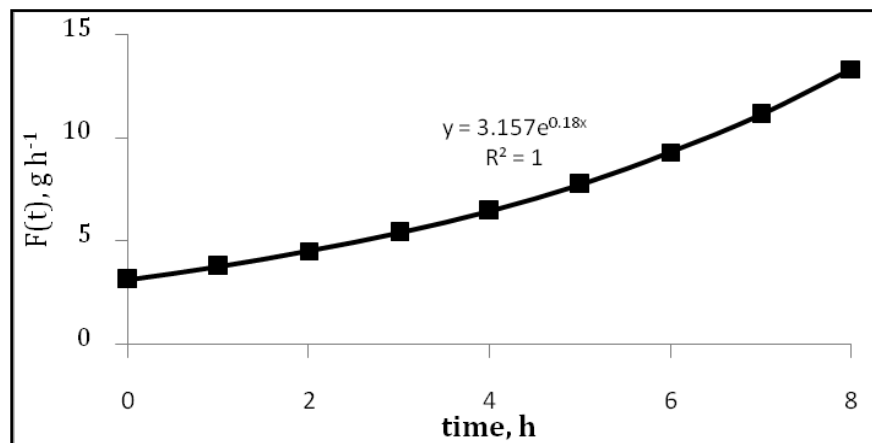


**Figure 3.3** The predetermined feeding profile for glycerol, calculated for specific growth rate ( $\mu_0$ ) of  $0.18 \text{ h}^{-1}$ .

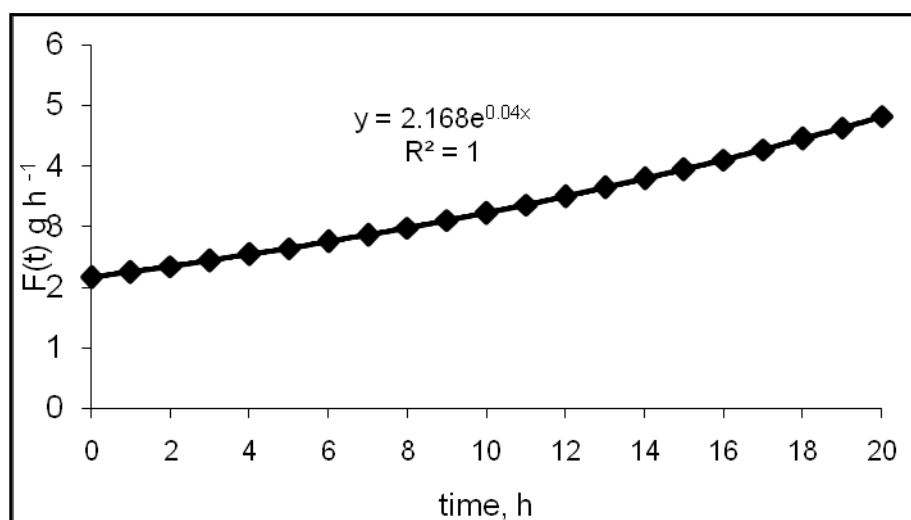


**Figure 3.4** The predetermined feeding profile for methanol, calculated for specific growth rate ( $\mu_0$ ) of  $0.04 \text{ h}^{-1}$ .

At the beginning of MFB phase, the co-substrate sorbitol was added to the medium batch-wise such that its concentration in the medium was  $50 \text{ g L}^{-1}$  (Açık, 2009). Although the process is continuous and the production (induction) phase starts at around  $t=32\text{h}$  of the precultivation period, for simplicity in calculations, beginning of the production phase was taken as  $t=0\text{h}$ .

At the end of the production, the medium was centrifuged (10500 rpm, 11 min,  $4^\circ\text{C}$ ) in order to discard the cells. The supernatant was stored at  $-20^\circ\text{C}$  or for longer time at  $-55^\circ\text{C}$  for further analysis and purification steps of rhGH.

### 3.3.4 Ultrafiltration

In order to remove the salts and concentrate the supernatant, ultrafiltration was performed using 400 mL stirred cells (Amicon) with 10 kDa cut-off regenerated cellulose ultrafiltration membranes (Millipore). The ultrafiltration process was carried out at  $T=4\text{-}8^\circ\text{C}$  in a cold room using  $\text{N}_2$  gas at a pressure of 3.5 bars, and the stirring rate was adjusted to the maximum

value 300-400 rpm such that the membrane was not harmed. Desalting was done by adding filter sterilized ultra pure water of known volume to the cell. The process was continued until at least 10-fold concentrated medium was achieved.

### **3.3.5 Production Analyses**

Throughout the production process, samples were collected with certain time intervals to determine the characteristics of the process. The samples were centrifuged for (11 min, 12000 rpm, 4°C). The cells and the supernatant were stored separately at -55°C for further analysis. The supernatants were used to determine methanol, sorbitol, amino acid, organic acid, total protein, rhGH and protease concentrations. The harvested cells were used to determine AOX activity.

#### **3.3.5.1 Cell Concentration**

Cell concentration was measured using a UV-Vis Spectrophotometer (Thermo Spectronic, Helios $\alpha$ ) at 600 nm. The range is between 0.1 and 0.9 to read OD<sub>600</sub>. Hence, in most of the cases samples taken from medium were diluted with dH<sub>2</sub>O. To convert absorbance to cell concentration, C<sub>x</sub> (g L<sup>-1</sup>), (3.2) was used (Orman et al., 2008)

$$C_x = 0.275 * OD_{600} * \text{Dilution Ratio} \quad (3.2)$$

#### **3.3.5.2 Protein Concentration**

##### ***3.3.5.2.1 Total Protein Concentration***

Total protein concentration was measured spectrophotometrically using Bradford assay (Bradford, 1976). 100  $\mu$ L of sample was mixed with 3 mL of Bradford reagent (BioRad) and incubated in a dark place at room temperature for 10 min. The absorbance was read at 595 nm by UV-spectrophotometer. The calibration curve was obtained using BSA in the concentration range of 0-0.75 mg mL<sup>-1</sup> (Appendix B).

### **3.3.5.2.2 rhGH Concentration**

RhGH concentrations were measured using a high-performance capillary electrophoresis (Agilent CE). Supernatants filtered with 0.45 µm cellulose acetate filters (Millipore) were analyzed at 12 kV and 15°C with a positive power supply using 60cm x 75 µm silica capillary. As the separation buffer 50 mM borate buffer (pH=10.0) containing zwitter ion (Z1-Methyl reagent, Waters) which is used to prevent protein adsorption to the capillary column was used. Proteins were detected by UV absorbance at 214 nm, as mentioned elsewhere (Çalık et al., 1998). A sample electropherogram which belongs to a hGH standard can be seen in Appendix C.

### **3.3.5.2.3 SDS-Polyacrylamide Gel Electrophoresis (SDS-PAGE)**

SDS-PAGE analysis was performed as described by Laemmli (1970). The sample buffer and protein samples were mixed in 1:2 ratio and heated in boiling water for 4 min, then they are vortexed and centrifuged. 3 µL of a dual color prestained protein MW marker (Appendix D) and 15 µL of the samples were loaded to each well of the gel and were run simultaneously at 40 mA of constant current around 45min. The buffers used are given in Appendix A. The protocol is given as follows;

#### Pouring SDS-polyacrylamide Gels:

1. Clean the glasses with ethanol and assemble the glass plates according to the manufacturers' instructions.
2. In an Erlenmeyer flask, prepare appropriate volume of solutions containing the desired concentration of monomer solution (12% for resolving gel and 5% for stacking gel) using the values given in Appendix A. Mix the solutions in order shown. Polymerization will begin as soon as the NNN'N'-Tetramethylethylenediamine (TEMED) and 10% (w/v) ammonium persulfate (APS) have been added.
3. Swirl the mixture rapidly and immediately pour the solution into the gap between the glass plates by micropipette. Leave sufficient space for the

stacking gel. Pour isopropanol into the left space till the top of the glasses to overlay the monomer solution. Leave the gel in a vertical position until polymerization is completed (45min).

4. Pour off the isopropanol and dry the area above the resolving gel with filter paper. Pour the stacking gel, immediately place a comb in the gel sandwich. Allow the gel to polymerize 30 minutes.
5. The gels can be kept +4°C covered with wet towels for 1 week.

#### Preparation of Samples and Running the Gel:

1. Prepare samples by diluting at 1:2 ratio with sample buffer and heated at 95°C for 4 minutes.
2. While the samples are boiling, mount the gels in electrophoresis apparatus and fill the reservoir with running buffer (1x SDS).
3. Load 15µL of each sample into the wells and start running with 40 mA. The usual run time is approximately 45 minutes.

#### ***3.3.5.2.4 Staining the SDS-PAGE Gels***

The gels were silver stained with silver salts using the procedure of Blum et al. (1987) given in Table 3.9.

**Table 3.9** Procedure for silver staining

<b>Step</b>	<b>Solution*</b>	<b>Treatment duration</b>	<b>Application</b>
<b>1</b> Fixing	Fixer	≥ 1 hr	Overnight incubation is acceptable
<b>2</b> Washing	50% Ethanol	3 x 20 sec	Fresh
<b>3</b> Pre-treatment	Pretreatment Solution	1 min	Fresh
<b>4</b> Rinse	Distilled water	3 x 20 sec	
<b>5</b> Impregnate	Silver Nitrate Solution	20 min	
<b>6</b> Rinse	Distilled water	2 x 20 sec	
<b>7</b> Developing	Developing Solution	Time is determined according to the color development	After the color starts to appear water should be added to slow-down the reaction.
<b>9</b> Stop	Stop Solution	-	The gels are stored in this solution.

\*Composition of the buffers are given in Appendix A.

### 3.3.5.3 Glycerol, Methanol, Sorbitol Concentrations

Methanol and sorbitol concentrations were measured with reversed phase HPLC (Waters HPLC, Alliance 2695, Milford, MA) on Capital Optimal ODS-5 $\mu$ m column (Capital HPLC, West Lothian ,UK) (Çelik et al., 2009). The methods were based on reversed phase HPLC, in which their concentrations were calculated from the chromatogram, based on the chromatogram of the standard solutions. The calibration curves for methanol and sorbitol concentrations are given in Appendix B. Samples were filtered with 45  $\mu$ m filters (Millipore) and loaded to the analysis system. For dilution of the samples and washing buffer filter sterilized, ultra pure water was used. Before using the HPLC system, all the buffers were degassed for at least 15

min. The sorbitol and methanol concentration analyses were performed under the specified conditions given in Table 3.10.

**Table 3.10** Conditions for HPLC system for methanol and sorbitol analyses

Column	: Capital Optimal ODS, 5 $\mu$ m
Column dimensions	: 4.6 $\times$ 250 mm
System	: Reversed phase chromatography
Mobile phase	: 5 mM H <sub>2</sub> SO <sub>4</sub>
Mobile phase flow rate	: 0.5 mL/min
Column temperature	: 30°C
Detector type and wavelength	: Waters 2414 Refractive Index detector, 214 nm
Detector temperature	: 30°C
Injection volume	: 5 $\mu$ L
Analysis period	: 10 min
Space time	: 5 min

#### 3.3.5.4 Organic Acids Concentrations

For organic acid concentration determination reversed phase HPLC (Waters HPLC, Alliance 2695, Milford, MA) on Capital Optimal ODS-5 $\mu$ m column (Capital HPLC, West Lothian, UK) was used (Çelik et al., 2009). The method was based on reversed phase HPLC, in which their concentrations were calculated from the chromatogram, based on the chromatogram of the standard solutions. For sample preparation analysis same the preparation steps were employed; samples were filtered with 45  $\mu$ m pore sized filters (Millipore) and loaded to the analysis system. For dilution of the samples and washing buffer filter sterilized, ultra pure water was used. Before using the HPLC system, all the buffers were degassed for at least 15 min. The

calibration curves for organic acid concentrations are given in Appendix B and the working conditions for the analysis are tabulated in Table 3.11.

**Table 3.11** Conditions for HPLC system for organic acids analysis (İleri and Çalık, 2006)

Column	: Capital Optimal ODS, 5 $\mu$ m
Column dimensions	: 4.6 $\times$ 250 mm
System	: Reversed phase chromatography
Mobile phase	: 0.312% (w/v) NaH <sub>2</sub> PO <sub>4</sub> and 0.062% (v/v) H <sub>3</sub> PO <sub>4</sub>
Mobile phase flow rate	: 0.8 mL/min
Column temperature	: 30°C
Detector and wavelength	: Waters 2487 Dual absorbance detector, 210 nm
Injection volume	: 5 $\mu$ L
Analysis period	: 15 min
Space time	: 5min

### 3.3.5.5 Amino Acids Concentrations

Amino acid concentrations were measured with an amino acid analysis system (Waters, HPLC), using the Pico Tag method (Çalık et al., 1998). Again, the method is based on reversed phase HPLC, using a pre-column derivatation technique with a gradient program developed for amino acids. The analyses were performed under conditions specified in Table 3.12.

**Table 3.12** Conditions for HPLC system for amino acid analyses

Column	: Nova-Pak C18, Millipore
Column dimensions	: 3.9 mm x 30 cm
System	: Reversed phase chromatography
Mobile phase	: 6% (v/v) acetonitrile
Mobile phase flow rate	: 1 mL/min
Column temperature	: 38 °C
Detector and wavelength	: UV visible detector, 254 nm
Injection volume	: 4 µL
Analysis period	: 20 min

### 3.3.5.6 Protease Activity

Protease activity was measured by hydrolysis of casein. Hammerstein casein solution (0.5% w/v) was prepared in either 0.05 M borate buffer (pH=10), 0.05 M sodium acetate buffer (pH=5) or 0.05 M sodium phosphate buffer (pH=7). The compositions of these three buffers are given in Appendix A. The samples were then diluted in casein solution at desired dilution and hydrolyzed at T=30°C, 200rpm for 20 min. At the end of these 20min, the reaction was ceased by the addition of 2mL of 10% (w/v) trichloroacetic acid (TCA) to the reaction mixture. The samples were kept on ice for 20 min and then centrifuged at 10500rpm for 10 min, +4°C. Thereafter, the samples with two separated layers were kept the mixture at room temperature for 5 min. Then the absorbance of the supernatant was measured at 275 nm in UV-Vis spectrophotometer using quartz cuvette. The dilutions at the beginning of the assay were decided such that the absorbance was between 0.2-0.6.

In order to convert the absorbance to protease activity, the correlation developed by Moon and Parulekar,(1991) given in (3.3) was used. Accordingly, one unit protease activity was defined as the activity that liberates 4nmole tyrosine per minute. (U cm<sup>-3</sup>) (Çalık et al., 1998).

$$A = \left( \frac{\text{Absorbance}}{0.8 \times 1 / \mu\text{mol} \cdot \text{cm}^{-3}} \right) \left( \frac{1U}{4 \text{nmol} / \text{min}} \right) \left( \frac{1}{20 \text{min}} \right) \left( \frac{1000 \text{nmol}}{1 \mu\text{mol}} \right) \left( \frac{\text{Dilution}}{\text{Ratio}} \right) \quad (3.3)$$

### 3.3.5.7 AOX Activity

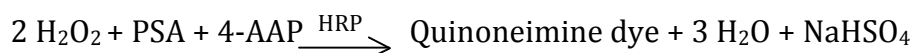
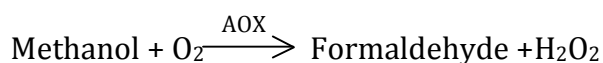
For this assay as the specific AOX activity was to be determined, the cell of 1 mL fermentation medium was used. The samples taken were centrifuged (10 min, 12500 rpm, +4°C) and the supernatant was removed. After the cells were lysed to get the intracellular components (as AOX is an intracellular enzyme), the assay was performed. The steps of the assay are given as follows.

#### Yeast Lysis to Get Intracellular Medium

Intracellular medium of the cells harvested from the fermentation medium should be extracted by using yeast lysis buffer (Appendix A). In order to get the intracellular medium of the cells, 500 µL yeast lysis buffer was added on the cells and these cell are mixed up three times for 20 sec and after each cycle they are kept on ice for 30 sec. Then, one spoonful of glass beads were added to the cells, again these cells are mixed up three times for 20 sec and after each cycle they were kept on ice for 30 sec. After 30sec, cells were centrifuged at 3000rpm for 2 min at +4°C, cells were discarded and the supernatant obtained was centrifuged again at 12500rpm for 5 min at +4°C. The supernatant obtained from this second centrifugation was used for determination of AOX activity.

### Activity Determination

A bi-enzymatic assay comprising alcohol oxidase (AOX) and horseradish peroxidase (HRP) was used to monitor the oxidation of methanol to formaldehyde by AOX enzyme. A colorimetric system based on the combination of phenol-4-sulfonic acid (PSA) and 4-aminoantipyrine (4-AAP) was chosen to measure the concentration of H<sub>2</sub>O<sub>2</sub> produced by AOX. The assays were performed at 25°C using a standard assay reaction mixture, containing 0.4mM 4-AAP, 25mM PSA, and 2U/mL HRP in 0.1M phosphate buffer with pH 7.5. The reactions for this particular system are given as follows.



The quinoneimine dye which is produced at the end of this two step series reaction, has a characteristic magenta color with maximum absorption around 500 nm. Therefore, the activity of AOX was determined by monitoring the associated increase in absorbance at 500 nm with UV-Vis spectrophotometer. The increase in absorbance is proportional to the rate of H<sub>2</sub>O<sub>2</sub> production and, consequently, to the rate of methanol consumption. One unit of activity (U) was defined as the number of μmol of H<sub>2</sub>O<sub>2</sub> produced per minute at 25°C (Azevedo et al., 2004).

The protocol for the analysis is as follows; 3 ml standard assay reaction mixture was put into a cuvette and 30 μL HPR, 375 μL methanol and 75 μL sample are added and mixed with that standard assay reaction mixture. Then increase in absorbance at 500 nm is monitored for 3 min and recorded every 30 sec of time intervals for 4min.

To convert absorbance to specific AOX activity, (3.4) was formed using the calibration curve given in Appendix B.

$$C_{AOX} \left[ \frac{U}{gCDW} \right] = 18.8 \left[ \frac{UmL^{-1}}{absorbance} \right] * OD_{500} * \frac{1}{C_x} \quad (3.4)$$

### 3.3.5.8 Oxygen Uptake Rate and Liquid Phase Mass Transfer Coefficient

The dynamic oxygen transfer experiments were performed at certain cultivation times during production phase in the bioreactor. In determination of the liquid phase mass transfer coefficient ( $k_La$ ), oxygen transfer rate (OTR) and oxygen uptake rate (OUR) defined in Chapter 2, were determined during the fermentation processes by dynamic method (Bandyopadhyay and Humprey, 1967).

The basis of the dynamic method relies upon the material balance on oxygen as in (3.5),

$$K_L a (C_o^* - C_o) + r_o = OTR - OUR = \frac{dC_o}{dt} \quad (3.5)$$

In order find the unknown of the balance at a certain time during the bioprocess; specific time intervals were chosen (i.e. every 3 hours). In each of these time intervals, to simplify the previous mass balance by cancelling out some terms in the previous balance, at some time  $t_0$  the broth was first de-oxygenated by stopping the air flow and lowering the agitation rate from 900 rpm to 100 rpm to prevent surface aeration. Therefore as the cells would continue utilizing the dissolved oxygen in the media (Figure 3.5, Part - II) . Then, the balance directly simplifies to (3.6) ;

$$\frac{dC_o}{dt} = r_o \quad (3.6)$$

As seen, OUR, which is negative, is equal to oxygen accumulation in the fermentation media. By taking and plotting  $C_o$  vs  $t$  data until dissolved oxygen in the media drops below 20%, oxygen utilization profile can be obtained. Taking the derivative provides  $-r_o$  at that certain time.

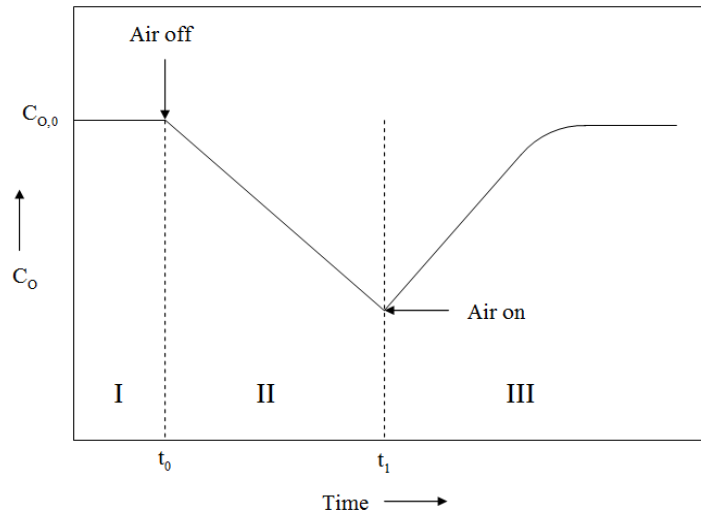


**Figure 3.5** Variation of dissolved oxygen concentration with time in dynamic measurement of  $K_La$

After dissolved oxygen level decreases,  $t_1$ , the air inlet flow and agitation rate were turned back to their initial conditions and the change in  $C_o$  with respect to time was recorded (Figure 3.5 Part-III). For the evaluation of the data in this region, (3.5) is no longer valid; hence (3.6) was used by assuming  $r_o$  is constant and was independent of the dissolved oxygen concentration in the medium.

Moreover,  $r_o$  in part-III was assumed to have the same value as calculated from part-II for the same analysis set. Also,  $C_o^*$  was taken as constant at constant temperature.

Aiming to obtain  $k_{La}$ , (3.5) is rearranged and equation (3.7) is obtained.

$$C_o = -\frac{1}{K_La} \left( \frac{dC_o}{dt} - r_o \right) + C_o^* \quad (3.7)$$

Thus, plotting  $C_o$  versus  $(dC_o/dt - r_o)$ , the slope gives  $K_{La}$  as can be determined understood from (3.7), (Figure 3.6).

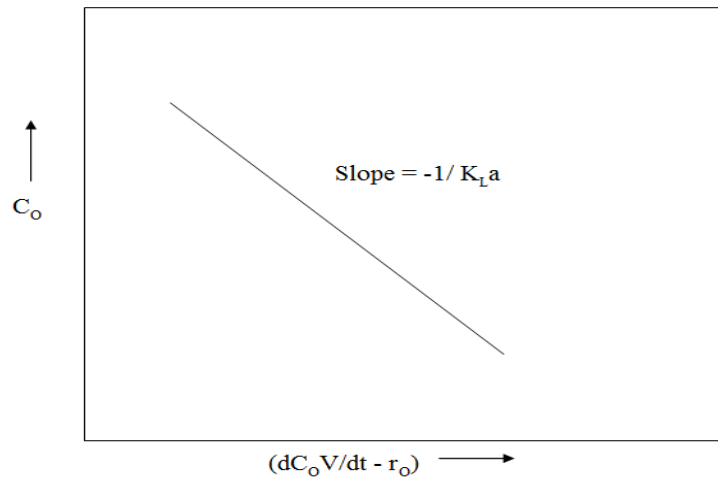


**Figure 3.6** Evaluation of  $K_{La}$  using the Dynamic Method.

The  $k_{La}$  value found in the presence of the microorganism can also be compared with the  $k_{La}$  value found when there is no microorganism in the same medium; i.e. without oxygen uptake rate. This term can be called as  $k_{La0}$ , and is important in order to understand the effect of additional mass transfer resistances in the presence of microorganism. For calculation of  $k_{La0}$ , the medium was de-oxygenated by giving nitrogen as the inlet. Then, air inlet was turned on monitoring the increase in  $C_o$  with respect to time. As there is no rate term (3.7) simplifies to;

$$C_o = -\frac{1}{K_{La}} \frac{dC_o}{dt} + C_o^* \quad (3.8)$$

Hence the slope of a plot of  $C_o$  versus  $d(C_o)/dt$ , determines the value of  $K_{La0}$ , determined.

In addition to  $K_{La}$ , OTR and OUR in order to get a deeper in sight on the oxygen transfer characteristics of the bioprocess maximum possible

oxygen transfer rate ( $OTR_{max}$ ) and maximum possible utilization rate (OD) were also calculated as in (3.9) a and b respectively (Çalık et al., 1998);

$$\begin{aligned} OTR_{MAX} &= K_L a C_o^* \\ OD &= \frac{\mu_{max} C_X}{Y_{X/S}} \end{aligned} \quad (3.9 \text{ a and b})$$

Moreover, effectiveness factor,  $\eta$ , and Damköhler number,  $Da$  were defined in order to compare the characteristics of fermentation process with the estimated maximum values (3.10 a and b).

$$\begin{aligned} Da &= \frac{OD}{OTR_{MAX}} \\ \eta &= \frac{OUR}{OD} \end{aligned} \quad (3.10 \text{ a and b})$$

In ideal conditions, when the mass transfer resistances and biochemical reaction resistances overcome each other,  $\eta$  equals to 1. When  $\eta < 1$  the cells are utilizing oxygen less than the ideal condition (at maximum growth rate). Similarly, when  $Da \gg 1$  mass transfer resistances are effective and when  $Da < 1$  the process can be described as biochemical reaction limited.

### 3.3 Ligand Selection

#### 3.4.1 Phage Display

In order to further purify the produced rhGH from the supernatant with high recovery, it is necessary to choose a ligand that has as high affinity as possible for the target protein, hGH. For that purpose, phage display technique was employed to choose a suitable peptide ligand for hGH. In this technique the 7-aminoacid containing Phage Display Peptide Library was used together with *E. coli* ER2738 strain (New England Biolabs Inc., UK). The library is composed of  $1 \cdot 10^{13}$  pfu/mL (supplied in TBS with 50% glycerol). *E. coli* was grown in LB medium properly. 96-microtiter well plates are first

coated with the protein of interest (Panning) and kept overnight at +4°C. After removing hGH, the wells are coated with phages and after several washing steps the phages that are attached to the hGH coated well surfaces are suspended and stored at +4°C. This procedure was performed at least three times, (but this time using the phages that were selected in the previous panning) to get the phages with the highest binding affinity (Figure 3.2). To determine the number of phage titers that bind to hGH, different dilutions of phage clones were mixed with top agar and were spreaded in LB/IPTG/Xgal agar. After many steps, 40 phages were chosen to bind hGH. These phages were then, amplified in LB medium using *E. coli* as the host microorganism (Figure 3.7).

Before sequencing, to decrease the number of these 40 phages and to compare the binding affinities of these phages to hGH, phage-ELISA assay was conducted. As the target protein, instead of the reactor supernatant (rhGH), pure hGH stock (2g L<sup>-1</sup>) was used, to prevent binding of phage to other supernatant components; hence hGH specific peptide sequences could be achieved. Compositions of all media and solutions used in Phage Display and phage-ELISA are given in Appendix A. The protocol used in conducting the experiment was the direct application of the procedure in phage display library kit producer company, New England Biolabs's, manual ([www.neb.com](http://www.neb.com)) and is as follows;

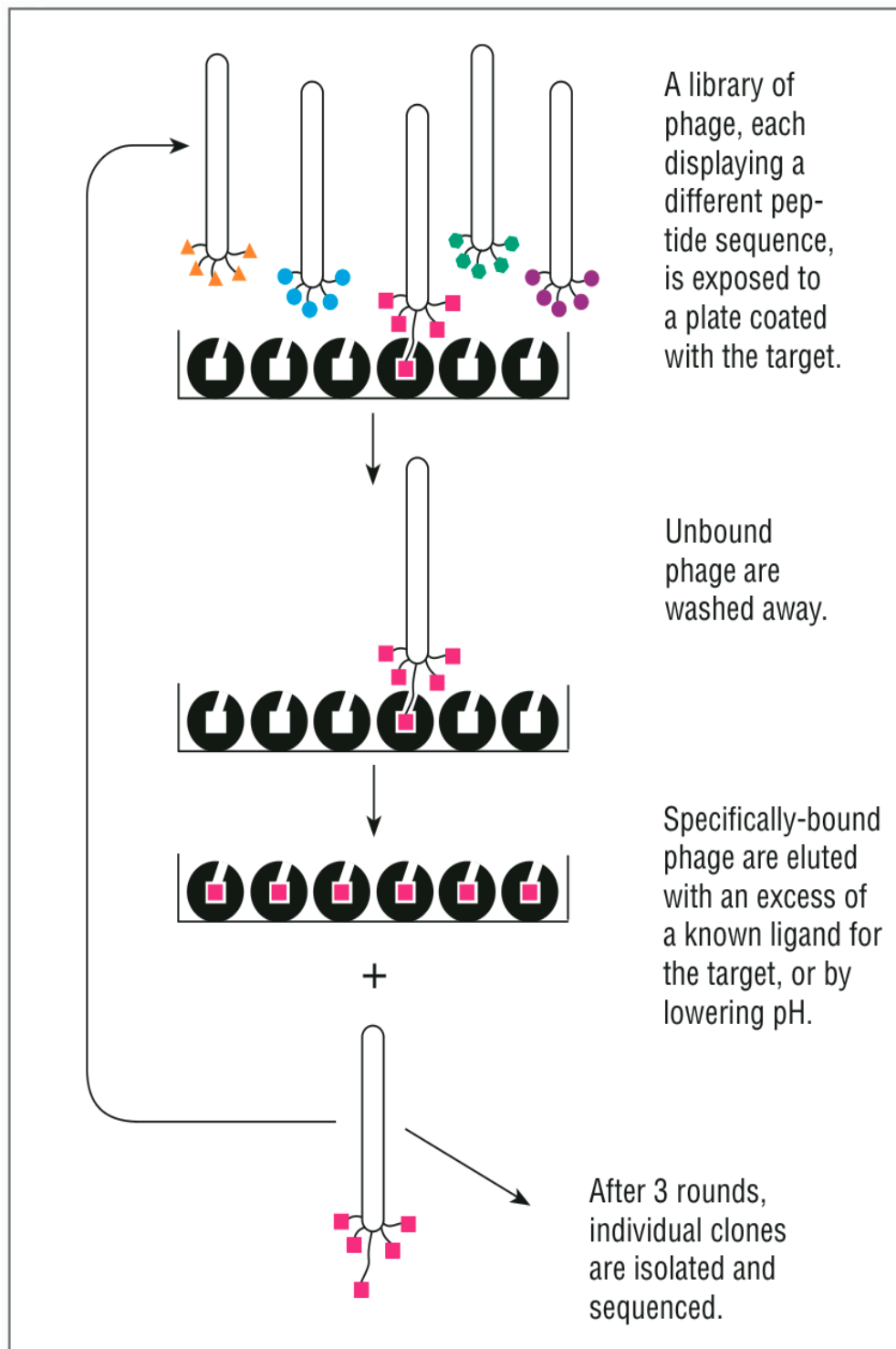


**Figure 3.7** Panning procedure for selection of peptides specific to target protein ([www.neb.com](http://www.neb.com))

### Surface Panning Procedure (Direct Target Coating)

The most straightforward method of panning includes coating a plastic surface directly with the target of interest (by nonspecific hydrophobic and electrostatic interaction), washing away the unbound, and applying the pool of virions over the coated surface (Figure 3.7).

#### ***Day One***

Panning was carried out in 96-well microtiter plates by coating a minimum of 1 individual well per target. It is important to keep the number of phages in each well the same ( $10^{11}$  virions).

1. A solution of  $200 \mu\text{g mL}^{-1}$  of the target was prepared in 0.1 M  $\text{NaHCO}_3$ , pH=8.6.
2. 150  $\mu\text{l}$  of the target solution was added to each well and swirled in order to completely wet the well surface.
3. In order to coat plates with target, overnight incubation was done at  $4^\circ\text{C}$  in a humidified container.

#### ***Day Two***

4. *E. coli*, ER2738 was inoculated in 10 ml of LB. This culture was be used for titering in Step 11. If amplifying the eluted phage on the same day (step 12), *E. coli* was inoculated in 20 ml of LB medium in a 50-ml conical tube. Incubate cultures at  $37^\circ\text{C}$  with shaking. Incubate the culture until needed; make sure that it does not grow beyond early-log phase, for use in Step 12.
5. The coating solution was poured off from each plate and firmly slapped it face down onto a clean paper towel to remove residual solution. Each well was filled completely with blocking buffer. Wells were incubated for at least 1 hour at  $4^\circ\text{C}$ .
6. The blocking solution was discarded as in step 5. The wells were washed

rapidly 6 times with TBST (TBS + 0.1% [v/v] Tween-20). The sides of the wells were coated by swirling, the solution was poured off, and the plate was slapped face down on a clean paper towel each time.

7. A 100-fold representation of the library was diluted with 100 $\mu$ l of TBST. Pipette onto coated plate and rock gently for 10–60 minutes at room temperature.
8. The non-binding phages were discarded by pouring off and slapping plate face-down onto a paper towel.
9. The plates were 10 times with TBST. The paper towel was used each time to prevent cross-contamination.
10. The bound phages were eluted for non-specific disruption of binding interactions in 0.2 M Glycine-HCl (pH 2.2), 1 mg mL<sup>-1</sup> BSA. Eluate was pipetted into a microcentrifuge tube, and neutralize with 15  $\mu$ l of 1 M Tris-HCl, pH 9.1.
11. Titer a small amount ( $\sim$ 1  $\mu$ l) of the eluate. Plaques from the first or second round eluate titering can be sequenced if desired.
12. The rest of the eluate was amplified by addition of the eluate to the 20-ml *E. coli* culture at early-log phase from Step 4 and vigorous shaking was maintained for 4.5 hours incubation at 37°C.

*Note: The remaining eluate can be stored overnight at 4°C at this point, if preferred, and amplified the next day. In this case, inoculate 10 ml of LB with E. coli and incubate with shaking overnight at 37°C. The next day, dilute the overnight culture 1:100 in 20 ml of LB in a 50 ml conical tube and add the unamplified eluate. Incubate with vigorous shaking for 4.5 hours at 37°C and proceed to Step 13.*

13. The culture was transferred to a centrifuge tube and spinned (10 minutes, 12,000 g, 4°C). The supernatant was transferred to a fresh tube and re-

spinned. The pellet was then discarded.

14. The upper the supernatant was transferred to a fresh tube and 1/6 volume of 20% PEG/2.5 M NaCl was added to it. The phage was kept at 4°C for at least 2 hours (or overnight) for precipitation.

### ***Day Three***

15. For PEG precipitation the tubes were centrifuged (30min, 14500rpm, 4°C). The supernatant was then discarded and the tube was re-spinned briefly to remove residual supernatant with a pipette. The phage pellet left was a white finger print sized smear on the side of the tube.
16. The pellet was suspended in 1 ml TBS. This suspension was transferred to a microcentrifuge tube and spinned (14,000 rpm, 5min, 4°C) to pellet residual cells.
17. The supernatant was then transferred to a fresh microcentrifuge tube and re-precipitated by addition of 1/6 volume of 20% PEG/2.5 M NaCl. The tubes were incubated on ice for 60 minutes, then microcentrifuged (14,000 rpm, 10min, 4°C) the supernatant was discarded and by re-spinning briefly the residual supernatant was removed.
18. The pellet was suspended in 200 µl TBS. The tubes were centrifuged for 1 min. to harvest any remaining insoluble material. The supernatant, the amplified phage, was then transferred to a fresh tube.
19. This amplified eluate was titered as described, on LB/IPTG/Xgal plates.
20. The wells were coated for the second round of panning as in Steps 1–3.

### ***Days Four and Five***

21. Blue plaques from the titering were counted and the phage count was taken which should be on the order of  $10^{11-12}$  pfu mL<sup>-1</sup>. If the phage titer of the amplified eluate was too low, succeeding rounds of panning was carried out with as little as  $10^9$  pfu of input phage.

22. The second round of panning was conducted by repeating steps 4–18 using the calculated amount of the first round amplified eluate as input phage, and raising the Tween concentration in the wash steps to 0.5% (v/v).

23. The resulting second round amplified eluate on LB/IPTG/Xgal plates was titered.

24. The wells were coated for the third round of panning as in Steps 1–3.

### ***Day Six***

25. The third round of panning was realized by repeating steps 4–10, using the second round amplified eluate as input phage and again using 0.5% Tween in the washing steps.

26. The unamplified third round eluate were titered as in step 11 on LB/IPTG/Xgal plates.

27. For preparation of individual clones for sequencing or ELISA, a 10 mL overnight culture of *E.coli* was set up and phage amplification was preceded.

### Plaque Amplification for ELISA

Before identification of selected phage clones by DNA sequencing, the target specificity was confirmed by phage ELISA. The phages were amplified to obtain sufficient quantities to work with. The steps of plaque selection and amplification are as follows;

1. The overnight culture of *E. coli* was diluted as 1:100 in LB. 1 mL of the culture were dispensed into culture tubes, one for each clone to be characterized. 2 clones from 1<sup>st</sup>, 2 clones from 2<sup>nd</sup> and 32 clones from the 3<sup>rd</sup> round were used to detect a consensus binding sequence.

2. A sterile wooden stick was used to stab a blue plaque from a titering plate (important: plates should be <1–3 days old, stored at 4°C and have <100

plaques) and transferred to a tube containing the diluted culture.

3. The tubes were incubated at 37°C in a shaker for 4.5 hours.
4. The cultures were transferred to microcentrifuge tubes, and spinned (14,000 rpm, 30 s). The supernatant was transferred to a fresh tube and re-spinned. By a pipette, the upper-part of the supernatant was transferred to a fresh tube. This amplified phage stock was stored at 4°C for several weeks with little loss of titer.

#### Phage-ELISA Binding Assay with Direct Target Coating

It is useful to include a phage ELISA in any panning experiment since artifacts of the panning process cannot always be anticipated or prevented. The following ELISA protocol was used in rapid detection of whether a selected phage clone binds the target, without the need for an antibody specific for the target. In this procedure the wells were coated with the target at 200µg mL<sup>-1</sup>, and each purified phage clone was added to the plate such that each well contains equal number of phages. Bound phages were then detected with anti-M13-HRP conjugate monoclonal antibody (Fitz-Gerald Inc). As the amount of target coated on the plate is not quantifiable, and is present at sufficiently high density to allow multivalent binding to the phage, this method would not determine whether the selected phage binds with high or low affinity. The method was useful for qualitative determination of relative binding affinities for a number of selected clones in parallel, and distinguished true target binding from binding to the plastic wells. The procedure is carried out as given below,

1. After plaque amplification was conducted, after the first centrifugation in Step 5, the phage-containing supernatants were saved at 4°C.
2. For each clone to be characterized, the overnight culture of *E. coli* was diluted as 1:100 in 20 mL of LB.
3. The 5 µl of phage stock from Step 1 were added to a 20 mL culture for

each clone to each culture and incubated with vigorous aeration in a shaker for 4.5–5 hours at 37°C.

4. The culture was then transferred to a centrifuge tube and centrifuged at (12,000 g, 10 min, 4°C), the supernatant was then transferred to a fresh tube and re-spinned to remove the pellet.
5. The upper-part of the supernatant was transferred to a fresh tube and 1/6 volume of 20% PEG/2.5 M NaCl was added. The phages were kept at 4°C for at least 2 hours (or overnight) for precipitation.
6. Spin the PEG precipitation at 14500rpm for 30 min, 4°C. Decant and discard the supernatant, re-spin briefly, and remove residual supernatant with a pipette.
7. The pellet was resuspended in 1 ml TBS. This suspension was then transferred to a micro-centrifuge tube and spin at 14,000 rpm, 5min, 4°C to precipitate residual cells.
8. The supernatant was transferred to a fresh microcentrifuge tube and re-precipitated with 1/6 volume of 20% PEG/ 2.5 M NaCl. The tubes were incubated for 60 minutes on ice. Then microcentrifuging (14,000 rpm, 10 min, 4°C) the supernatant was discarded. By re-spinning briefly the removal of residual supernatant was achieved with a micropipet.
9. The pellet was suspended in 200 µl TBS. The titration was performed such that the concentrations were kept as  $10^{13}$  pfu mL<sup>-1</sup>.
10. The two ELISA plate wells were coated for each clone to be characterized (for parallel reading) with 150 µl of 200 µg/ml of target in 0.1 M NaHCO<sub>3</sub>, pH=8.6. To achieve binding the wells were incubated overnight at 4°C in an air-tight humidified box. Additionally extra-coating was done to the wells for control experiments.

a) Blocking buffer+Phage+ Antibody+Substrate= To test for

binding of the selected phages to BSA-coated plastic.

**b)** hGH+ Blocking buffer +Antibody+Substrate= To test whether the antibodies are only phage specific

**c)** Blocking buffer +Substrate= To examine the color change without the enzyme (zero base for colorimetric measurement)

**d)** Blocking buffer +Antibody+Substrate= To test for binding of the antibody to BSA-coated plastic

Accordingly, hGH coating was also applied to two extra wells for conducting the control in part (b).

- 11.** The unbound hGH solution was removed by slapping plate face-down onto a paper towel. Each well was filled (and wells for control (b)) completely with blocking buffer. In addition to these, six more of uncoated wells were also blocked to perform the controls (a), (c) and (d). The plate was incubated like this for 1–2 hours at 4°C.
- 12.** The blocking buffer was removed and each well was washed 6 times with TBST (TBS+0.1% Tween 20), slapping the plate face-down onto a clean section of paper towel each time.
- 13.** The serial dilutions for the phages were made such that  $1 \times 10^{10}$  phage  $\text{mL}^{-1}$ .
- 14.** Using a multichannel pipettor, 100  $\mu\text{l}$  from each diluted phage was transferred to two wells for each target-coated wells, and to one of the selected phages to two wells of control (a). The remaining control wells were filled with TBST to prevent drying. Incubate at room temperature for 1–2 hours with agitation.
- 15.** The plate was washed 6 times with TBST.
- 16.** HRP-conjugated anti-M13 monoclonal antibody was diluted in 1:20 ratio in blocking buffer as recommended by Fitz-Gerald Inc. Then 200  $\mu\text{l}$  of

diluted antibody was added to each sample well and to wells of (a), (b) and (d) controls. For control (c) the well is filled with TBST to prevent drying. The plate was incubated at RT for 1 hour with agitation.

17. The wells were washed 6 times with TBST.
18. The HRP substrate solution was prepared as described: Immediately prior to the detection step, add 36  $\mu\text{l}$  of 30%  $\text{H}_2\text{O}_2$  to 21 ml of ABTS stock solution per plate to be analyzed.
19. 200  $\mu\text{l}$  of ABTS solution was added to each well, and incubated for 10–60 minutes at 37°C with gentle agitation.
20. The plates were read using a microplate reader set at 405nm (BIO-TEK EL 808, Biotek Instruments, Winooski, VT, USA). For each phage concentration, the signals obtained with and without hGH were compared.

#### Purification of Sequencing Templates of Phage DNA

1. The phage amplifications were conducted as described previously.
2. After 1<sup>st</sup> centrifugation in Step 5, 60  $\mu\text{l}$  from the 200  $\mu\text{l}$  phage solution in TBS was taken.
3. Equal volume of “Phenol/Cholorofom/ isoamylalcohol” mixture was added.
4. The solution was vortexed, waited ~1min vortexed again. The formation of white layer and jel-like part was observed.
5. Solution was centrifuged at maximum speed (13200 rpm) for 10 min at room temperature.
6. 2 phases with a white separation layer in the middle was be formed. Without touching the 2<sup>nd</sup> (white) layer, the aquaeous phase was transferred to another microcentrifuge tube.

7. The aqueous phase was diluted as 1:3 by addition of absolute ethanol, also addition of 1:10 volume of 3M sodium acetate pH=7.1. This mixture was mixed by turning the tubes up-side down, without vortexing.
8. The microcentrifuge tubes were kept at -20°C overnight.
9. The tubes were centrifuged at maximum speed (13200 rpm) for 15 min at +4°C.
10. A very pale color of dot-sized pellet should be seen at the bottom of the tube. If not, the following steps were still continued.
11. The tubes were aspirated by removing the aqueous part first (not by pipette, just turn the tubes up side down on a clean towel.) and then by leaving the tubes open for a few seconds (~30 s).
12. Add 40 µl TE buffer was added for re-suspension of the existing or even unseen existing pellet.
13. The samples were kept at -20°C until use.

### Electrophoresis

#### *Gel preparation:*

1. For 1.2 % solution, 0.6 g agarose was dissolved in 50 mL 0.5 M TBS buffer by heating.
2. When the buffer boils and agarose was completely dissolved, the bottle from the heater was removed and cooled down to ~70°C.
3. 2.5µl ethidium bromide was added and the solution was mixed vigorously until pink color disappears.
4. The solution was poured on apparatus, the comb was inserted and it was waited until the gel formation.
5. Gels could be stored at +4°C for 1-2 days.

#### *Gel loading:*

1. The gel was inserted into the electrophoresis device, the comb was removed and the device was filled with 1x TBS buffer.
2. 5  $\mu$ l Hind  $\lambda$ III ladder was added to one of the wells.
1. 1  $\mu$ l loading buffer was mixed with 3-4  $\mu$ l sample and samples were loaded into the wells.
2. The samples were run at constant voltage 60 V for 1 hour.

### **3.5 Thermodynamic Interpretation of Protein Ligand Interactions**

After selection of peptides selected using either phage display or computational design, in order to understand the characteristics of binding, and its strength several methods could be used. As the strength and properties of binding may not be the same when the interaction takes place in a cell freely and when one of the binding pairs (either ligand or the target protein) more than one method is employed for interpretation of the interaction. In this study, for real time determination of the interaction on a sensor surface, Surface Plasmon Resonance Spectroscopy is employed. Moreover, for the Calorimetry based analysis of protein-peptide interaction Isothermal Titration Calorimetry was used. In the following, both of these methods are explained in detail.

#### **3.5.1 Surface Plasmon Resonance (SPR)**

SPR is a technique that can be used to obtain the kinetic parameters of binding between two interacting species (protein and peptide) in real time and without use of labels. When compared with other methods SPR is a very advantageous method as it enables user to obtain kinetic data i.e.; association and dissociation rate constants with limited sample (Golemis and Adams, 2005).

The SPR experiments mainly involve several steps.

- Prepare the ligand and analyte.
- Insert a suitable sensor chip.
- Prepare the surface so that active sites are available for the immobilization.
- Immobilize the macromolecule or the ligand and prepare the control surface.
- Inject the analyte and control analyte over sensor surface and record the response.
- Wash the sensor surface to remove the unbound analyte and obtain the dissociation profile.
- Regenerate the surface if necessary.
- Analyze data.

The overall method using Spreeta chip developed by Texas Instruments, is tried to be optimized for hGH-peptide binding analysis and given in detail as follows.

#### Sensor Chip and Surface Preparation

1. Before inserting the sensor into the SPR cell, first the gold surface is cleaned by using piranha solution (a mixture of 96% H<sub>2</sub>SO<sub>4</sub> and 30% H<sub>2</sub>O<sub>2</sub> in ratio of 3:1). By using a micropipette 1-2 drops of this solution is applied on to the gold surface without touching. After waiting for a few minutes and the solution on the surface should be rinsed thoroughly with deionized water. Then the surface is left to dry. Lastly, a Kimwipe wetted with ethanol is used to remove the remaining water stains.
2. After it is made sure that surface is cleaned, it is inserted into the SPR cell and the cell is closed tightly avoiding any possible leak during the analysis.
3. For the analysis Spreeta 5 software is employed.
4. After the calibrations, pure ethanol is passed through the surface by 50  $\mu$ l

min<sup>-1</sup> flow rate.

5. Then the surface is first prepared by forming Self-Assembled Monolayer SAM on the gold surface by Mercaptoundecanoic acid (11-MUA; C<sub>11</sub>H<sub>22</sub>O<sub>2</sub>S) by chemisorption. For that purpose 10mM 11-MUA solution in ethanol is prepared and passed through the gold surface for ~18hours. Keeping the gold surface under 11-MUA overnight ensures the formation of ordered and well packed layers that were initially not well ordered and contained many gauche defects within the chains (Sigma-Aldrich Catalogue). After 18 hours the surface formed.
6. After SAM formation, the surface is washed first with pure ethanol, then with deionized water at flow rate of 50 μL.
7. Before binding of protein (or ligand) to the surface, as direct covalent immobilization is selected as a method for immobilization, the surface needs to be activated first, so that protein/ligand can be immobilized.
8. Among the choices of coupling chemistry mentioned previously in Chapter2, amine coupling was selected, which is mostly used as the primary method. As the standard protocol for amine coupling EDC/NHS (1-Ethyl-3-(3-dimethylaminopropyl)carbodiimide / N-hydroxysuccinimide) is used such that in the mixture the concentrations are 0.2M and 0.05M for EDC and NHS respectively. (van der Werve , 2001)
9. This mixture is passed through the channels for 1 hour at a flow rate of 10μL/ min. After this treatment, the surface now has the free carboxyl groups for the amines to bind.
10. During that time the protein (or ligand), the component which is selected for immobilization, is prepared at desired 2 concentrations.
11. In order to remove unbound EDC/NHS water is passed through the surface at a 20 μL min<sup>-1</sup> flow rate, until the steady state response diagram is reached.
12. Then as there are three lines used on the sensor chip, to two lines two different protein (or ligand) concentrations are loaded, where to the

remaining line, as it is selected for control, one of the same concentrations of protein (or ligand) is loaded. The flow rates of these solutions are one of the parameters to be optimized. For this thesis  $20 \mu\text{L min}^{-1}$  is selected.

- 13.** While the particles reach to the surface, an increase in the response units is observed. The feeding is continued until the response units (RU) reach steady state (no longer increasing). By this way it is understood that the surface is saturated.
- 14.** The unbound particles are then removed from the surface by passing water through the lines, and the decrease in RU is seen again until a flat response is observed. The difference of RU before and after the washing indicates whether the particles are bound or not.
- 15.** In order to fill the unbound carboxyl groups on the EDC/NHS treated surface, 3M Ethanolamine is passed at  $20\mu\text{L}/\text{min}$  flow rate again increase in RU reaching a plateau is observed. The high concentration of ethanolamine is also helpful in elution of any non-covalent bound material (van der Werve, 2001).
- 16.** Similar to all previous surface modification steps, step 15 is also continued with washing to remove unbound ethanolamine. After all these steps the sensogram is expected to be as in Figure 3.8.

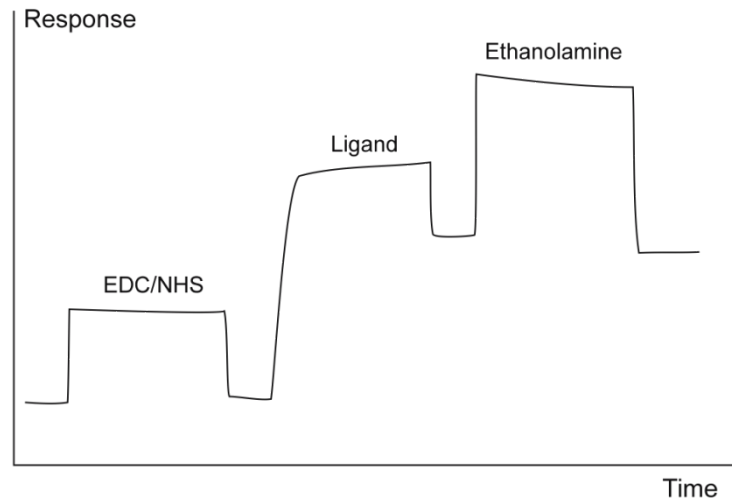


**Figure 3.8** Sensogram for steps of SPR before analyte injection (Löfås and McWhirter, 2006)

17. When the system reaches steady state, if a buffer is selected for the interaction, it is passed through the lines at  $50 \mu\text{L min}^{-1}$  to make the surface ready for the interaction.
18. When the flat lines of response units for all three cases are reached, analyte is injected at a desired concentration to two lines and to the control line buffer is continued to be injected. For the analyte injection the selected flow rate is  $25 \mu\text{L min}^{-1}$ .
19. During the injection, the response unit of the two lines will increase as the analyte reaches to the surface. When the plateau is reached, the association is completed.
20. To observe the dissociation profile, the lines are washed with buffer. The structure of dissociation and the time it takes for a complete dissociation are the important points that determine the characteristic and strength of binding.
21. After analysis is completed, pH is shifted to lower values (Acidic) to regenerate the surface for further analyses allowing the reuse of the ligand in subsequent binding/regeneration cycles.

The last three steps that describe the protein–ligand interaction steps of the SPR analysis are summarized in Figure 3.9.

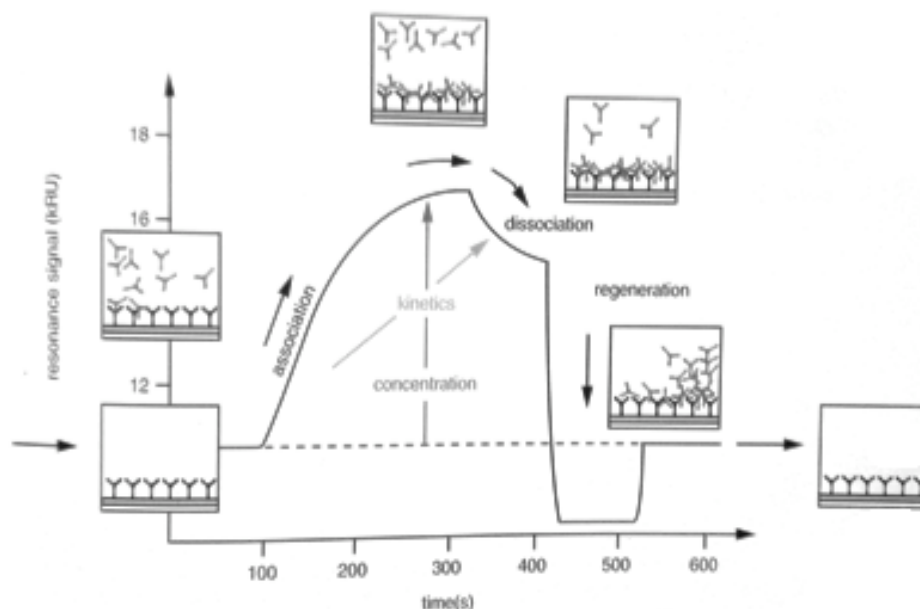


**Figure 3.9** Binding of ligand to the protein. (Golemis and Adams, 2005)

In summary, the analyte (gray particles) binds to the surface attached ligand (black particles) causing an increase in RU, at the end of injection the sample is replaced by the continuous flow of buffer. The decrease in signal reflects the dissociation of the analyte from surface bound complex.

According to the dissociation profile, the binding properties are decided and models fit to the experimental data as explained in Section 2.

### 3.5.2 Isothermal Titration Calorimetry (ITC)

In order to measure the strength of the interaction and determine the binding characteristics, alternative to SPR calorimetry based approach Isothermal Titration Calorimetry (ITC) can be applied. As mentioned in

previous chapter, ITC directly yield the change in enthalpy and the free energy of interaction by directly measuring the heat evolved or absorbed in liquid samples as a result of mixing precise amount of reactants.

ITC is a more precise instrumental analysis tool compared with SPR as both the protein and ligand are found as free in solution without immobilization. On the other hand, one very important disadvantage of ITC is the need to use higher amounts and concentrations of analyte and ligand to achieve detectable levels of interaction.

The ITC analyses are performed with VP-ITC micro calorimeter (MicroCal, LLC) device, with an operating range between 2-80°C. The cell and titrant volume are 1800 $\mu$ L and 400  $\mu$ L respectively.

The protein solution (lyophilized hGH dissolved in buffer/ water at desired pH) was injected into the cell avoiding bubbles. As the titrant ligand is used. Between 20-30 times of the hGH concentration, the ligand concentration is adjusted again by dissolving the lyophilized peptide in the same buffer as hGH. Although the same buffer at same pH is used for dissolving the interacting species, depending on the properties of the peptide /protei, the final pH of the solutions may differ. In such a condition in order to keep the pH difference between the species less than 0.05, 0.1N NaOH or 0.1N HCl is added dropwise one of the desired components. Before the components are injected to the instrument, in order to remove bubbles peptides are degassed for 10 min. Considering that hGH can be affected from the degassing conditions, the buffer that is used to dissolve hGH is degassed prior to hGH solution preparation. Both solutions and the buffer itself were filter sterilized by 0.45 $\mu$ m Durapore PVDF (Millipore) and 0.45 $\mu$ m cellulose acetate sterile filters (Millipore) respectively.

The operating conditions for the ITC analyses are as given in Table 3.13.

**Table 3.13** ITC operating conditions

---

Cell Temperature	: 30°C
Total Number of Injections	: 25-35
Injection Volume	: 10µL
Syringe Concentration	: 300-1000µM
Cell Concentration	: 15-25 µM
Buffer concentration	: various buffers btw. 1-50 mM
Salt concentration	: max. 10mM NaCl
pH	: varies between 6.5 and 9
Stirring Speed	: 150- 300 rpm
Reference power	: 5-10 µcal
Injection duration	: 20 sec
Spacing	: 240-420 sec
Initial delay	: 60 sec
Filter period	: 2 sec

---

## CHAPTER 4

### RESULTS AND DISCUSSION

In this study, the effects of different operation parameters on recombinant human growth hormone production (hGH) by *Pichia pastoris* to increase product concentration and the interaction kinetics of peptide ligands with hGH were investigated. In the production part of the study, the effect of temperature and Tween-20/80 concentration on *P. pastoris* hGH-Mut<sup>+</sup> phenotype were studied in laboratory scale air-filtered shake bioreactors. At the selected conditions, the effect of methanol feeding rates on recombinant protein production, cell growth, oxygen transfer, by-product formation and co-substrate utilization were investigated and overall yields and the specific rates were calculated in order to understand the characteristics of the bioprocess using pilot scale bioreactor. In two additional pilot scale bioreactor experiments; the optimum pH and co-substrate sorbitol feeding strategy were determined. Moreover, in the second part of the study, aiming to find the peptide sequence that binds specifically to hGH, the peptide ligands were selected by phage display; additionally, computationally designed peptides and the peptides obtained from literature were tested to determine the interaction between the peptide ligand and hGH. In this context, the affinity and specificity of these peptides towards hGH were investigated using isothermal titration calorimetry and surface plasmon resonance analyses.

#### 4.1 Effect of Temperature on Cell Growth and Protein Production

Before starting bioreactor experiments, the effect of temperature on hGH production by *P.pastoris* was investigated in four shake flask experiments at different temperatures. The selected temperatures for investigation were T=25, 27, 30 and 32°C depending on the previous studies in literature. In these shake flask experiments the previously designed medium conditions (Açık, 2009) were used. After precultivation steps, the cells were harvested in production medium such that the initial  $C_x=0.08 \text{ g L}^{-1}$  ( $OD_{600}= 0.3$ ). The production was continued for 52 hours until the cell growth slows down for 30°C. For production, methanol inductions at t=24 and t=48 h of the bioprocess were done such that 1% (v/v) was present in the medium. For other three sets of experiments, the bioprocesses were continued aiming to reach the final cell concentration closer to 30°C case. In all sets, as co-substrate sorbitol was added to the production medium batch-wise at previously determined concentration of  $30 \text{ g L}^{-1}$ .

As can be seen from Figure 4.1, as the temperature decreases the growth rate decreases confirming the findings of Lin et al., (2007) and at 25°C, with a longer lag phase, until t=52 h cells could reach only one forth of the concentration achieved at 30°C. The highest cell concentration was obtained at 32°C, t=52 h as  $7 \text{ g L}^{-1}$ , which was 1.07-, 1.12- and 1.25- fold higher than the final cell concentrations obtained at 30°C, 27°C and 25°C, respectively.

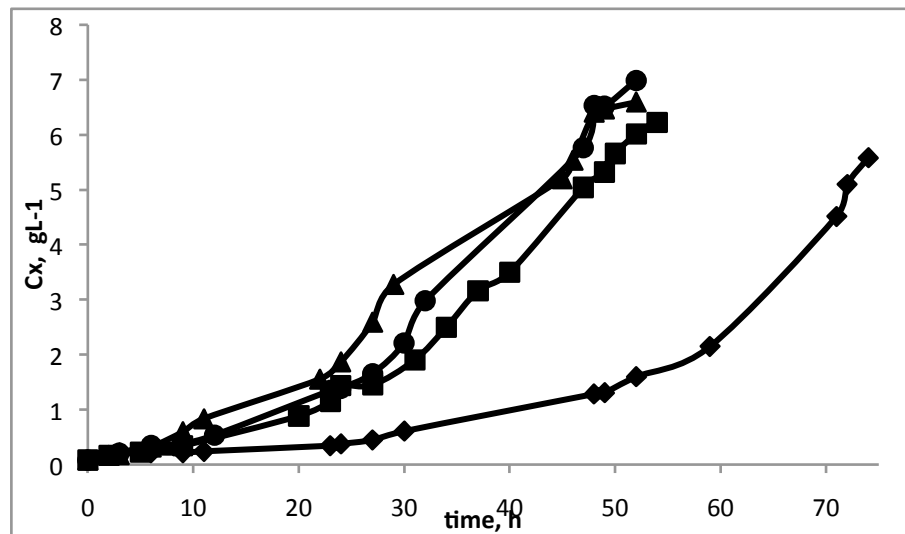


**Figure 4.1** Cell growth profiles at different temperatures; T=25°C (◆), T=27°C (■), T=30°C (▲) and T=32°C (●)

As much as its effect on cell growth, temperature is also an important parameter for protein production. Since the reactions on pathways that lead to protein formation are all temperature dependent, above or below the optimum temperature the production is negatively affected. In Figure 4.2 the affect of temperature on production at different times of the bioprocesses can be seen from SDS-PAGE results. In relation with the cell growth profiles, at the first 24 hours of the bioprocesses the product concentrations were lower. At T= 25°C, as the cells almost enter the exponential growth phase by t=47 h and until that period no product formation was observed.

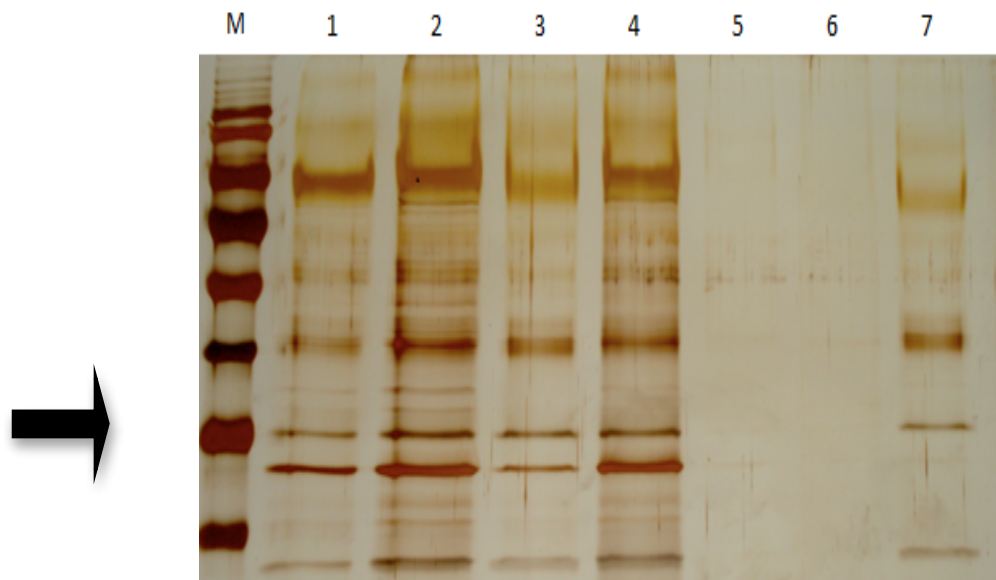


**Figure 4.2** Silver stained SDS-PAGE gel view of extracellular proteins produced by *Pichia pastoris* in laboratory scale air filtered shake bioreactor to observe the effect of temperature on rhGH production at different times of the bioprocesses; double band region indicated by arrow shows the two rhGH bands. Lane M: protein marker; Lane1: T=30°C-24h; Lane2: T=30°C-48h; Lane3: T=32°C-24h; Lane 4: T=32°C-48h; Lane5: T=25°C-24h; Lane6: T=25°C-48h; Lane7: T=25°C-72h

Together with the results of the T=27°C experiment, the final product concentrations of the four sets of experiments were compared in silver stained SDS-PAGE analysis and shown in Figure 4.3. From Figure 4.3, it can be concluded that for both rhGH production and cell growth 30 and 32°C are more suitable. However, considering the higher energy requirement to keep temperature constant throughout the processes, lower oxygen solubility at higher temperatures and possible effects of higher temperature on protein stability (Invitrogen, 2002), for continuing shake flask bioreactor and pilot scale bioreactor experiments 30°C was selected as the operation temperature.

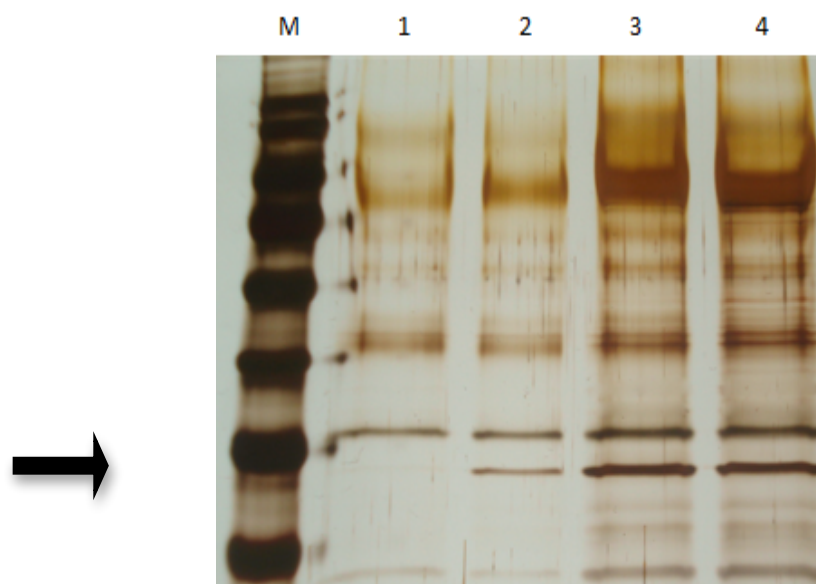


**Figure 4.3** Silver stained SDS-PAGE gel view of extracellular proteins produced by *Pichia pastoris* in laboratory scale air filtered shake bioreactor to observe the effect of temperature on final rhGH concentration; Lane M: protein marker; Lane1: T=25°C; Lane2: T=27°C; Lane3: T=30°C; Lane 4: T=32°C

#### 4.2 Effect of Tween-20/80 addition on Cell Growth and Production

In order to see the effect of the addition of Tween-20 and -80 to the medium, and to determine the effect of their concentration in the broth and understand whether Tween-20 or -80 could be used as an alternative or in addition to the co-substrate sorbitol. For this purpose, using the previously designed experimental conditions for air filtered shake flask bioreactors, the effect of Tween-80 addition and concentration on *P.pastoris* rhGH production process. Among eight different medium conditions, in six of the media sorbitol was continued to be used as co-substrate, in two other different Tween-80 concentrations of 0.1% and 0.2% (v/v) without sorbitol was used and in one set, Tween-20 was used instead of Tween-80 to compare the effect of these two surfactants on bioprocess. Tween-80 was added to the medium in the beginning of the experiment batch-wise and its

concentration in the media was kept between 0-0.2% depending on the literature studies. In all shake flask studies pulse methanol was added to the medium such that 1%(v/v) concentration was maintained every 24h. In Figure 4.4, the effect of these changes on cell growth profiles is shown. In comparison with only sorbitol case, while addition of 0.05% Tween-80 enhanced growth at a small extent, increasing Tween-80 concentration (0.1%, 0.15% and 0.2%) had negative effects on growth profiles which might be due to the toxic effects of this surfactant. In comparison of the effect of Tween-80 and Tween-20; Tween-20 inhibited growth at a higher extent at 0.2% concentration i.e 1.11-fold higher cell concentration was achieved by 0.2% Tween-80 addition than the case with 0.2% Tween-20 addition. Moreover, it was seen that without sorbitol as co-substrate, cell concentrations sharply decrease reaching approximately 1.7-fold less final cell concentration. The growth profiles were similar when only 0.2% or 0.1% Tween-80 was added.

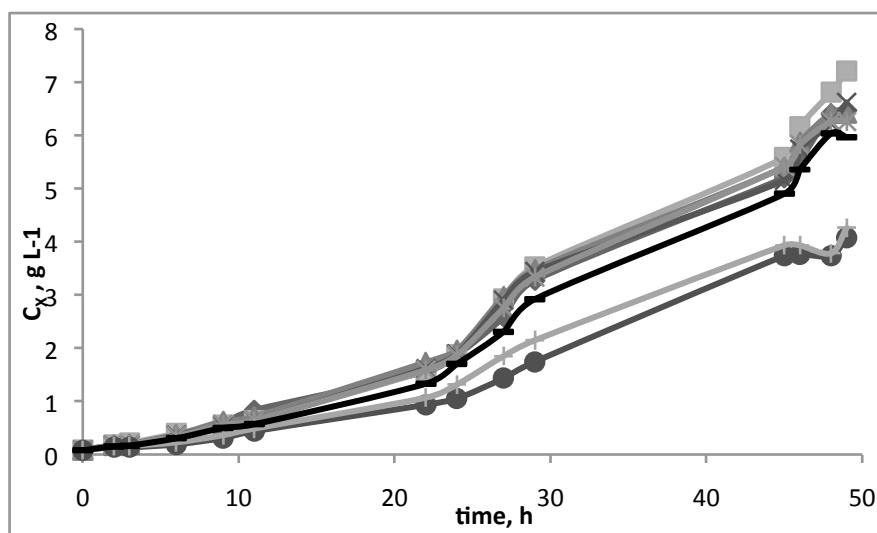


**Figure 4.4** The effect of Tween-80/20 (T-20 or T-80) surfactants on cell growth profiles of *P.pastoris* producing rhGH in air filtered shake flask bioreactors; Sorbitol only (◆); Sorbitol and 0.05%T-80 (■); Sorbitol and 0.1%T-80(▲); Sorbitol and 0.15%T-80 (x); Sorbitol and 0.2%T-80 (\*); 0.1%T-80 only (●); 0.2%T-80 only (○); Sorbitol and 0.2%T-20 (-)

The effect of Tween concentration on rhGH production is as much important as its effect on growth. The comparison of the total protein concentration data together with rhGH concentration are shown SDS-PAGE gel view in Figure 4.5. In comparison of only sorbitol case with Tween additions, almost equal product concentrations were achieved irrespective of the Tween concentration until 0.2% (Lanes 1,2,3 and 4) similar to the findings of Hao et al., (2007). From the figure it can also be clearly seen that, without sorbitol addition to the medium, production is also decreased to a great extent (Lanes 6 and 7) as oppose to findings of Apte-deshpande et al., (2009). Again Tween-20 inhibited product formation more than Tween-80 at 0.2% concentration (Lanes 5 and 8).

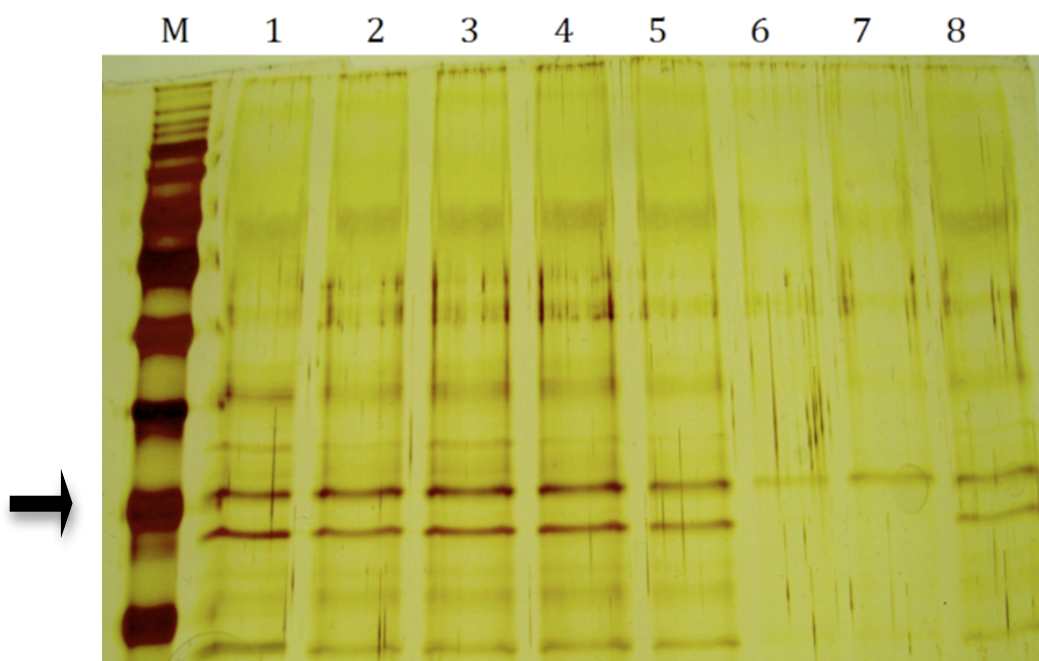


**Figure 4.5** Silver stained SDS-PAGE gel view of extracellular proteins produced by *Pichia pastoris* in laboratory scale air filtered shake bioreactor to observe the effect of Tween 20/80 on rhGH production Lane M: protein marker; Lane1: Only sorbitol; Lane2: Sorbitol and 0.05% T80; Lane3: Sorbitol and 0.1% T80; Lane 4: Sorbitol and 0.15% T80; Lane5: Sorbitol and 0.2% T80; Lane6: 0.1% T80; Lane7: 0.2% T80; Lane8: Sorbitol and 0.2% T20

These results showed that the inclusion of Tween in the medium can not be employed as an alternative to sorbitol (Lane 5 and 6). However in order to observe the effects of Tween concentration on high-density rhGH production more clearly, 0.05% (v/v) Tween-20 concentration could be studied in pilot scale bioreactor with batchwise 50 g L<sup>-1</sup> sorbitol added in the beginning of production phase and fed-batch methanol feeding. On the other hand, as the major goal of this study is to achieve optimum purification conditions by interacting rhGH and peptide ligands, the use of surfactants which might affect the interaction are not desirable. Therefore, in the following pilot scale bioreactor experiments using shake flask bioreactor studies' results, 30°C was selected as the operation temperature and Tween-20 or -80 were not added to the fermentation medium.

#### **4.3 Production of Human Growth Hormone by *Pichia pastoris* in Pilot Scale Bioreactor**

After determining the operation temperature, in laboratory scale air filtered shake flask bioreactors, in the first step of high-density fermentation, the effect of methanol feeding rate on cell growth were investigated in pilot scale bioreactor. In pilot scale bioreactor, with higher rate of agitation, proper oxygen feeding and controlled pH product formation and cell growth are enhanced as the oxygen transfer limitations decrease and product is kept more stable. Moreover, the pilot scale enables the fed-batch feeding rather than batch which is useful in keeping the medium components at desired level throughout the process, providing better growth and production conditions and decreasing by-product formation.

##### **4.3.1 Bioreactor Operation Parameters**

In order to construct an efficient bioprocess to obtain high productivity and yields, determining and controlling the ideal bioprocess operation parameters is crucial. In this study, where the main aim is to investigate the effects of methanol feeding rate and understand the effect of

sorbitol feeding strategy for the production of rhGH by *P. pastoris* cells, the temperature has decided to be controlled at 30°C, which was shown to be most suitable temperature considering both growth and production in previous experimental set.

In selection of the operation pH, as the optimum pH for the *P.pastoris* fermentation processes differ for different recombinant proteins, the previously conducted study by Bayraktar (2009) on three different pH values of pH=4.2, 5.0 and 6.0 was considered and pH=5.0 was used as the operation pH in the first set of experiments.

#### **4.3.2 Effect of Methanol Feeding Rate on Bioprocess Characteristics of *P.pastoris* Producing rhGH**

In the first set of bioreactor experiments, the effect of pre-determined methanol feeding rate on fermentation and oxygen transfer characteristics in rhGH production by *P.pastoris* Mut<sup>+</sup> strain, was investigated considering the cell growth and production of rhGH, AOX, by-products, protease, as well as oxygen transfer characteristics and process yields.

For that purpose the three methanol feeding rates MS=0.02 ( $\mu_0=0.02$  h<sup>-1</sup>), MS=0.03 ( $\mu_0=0.03$  h<sup>-1</sup>) and MS=0.04 ( $\mu_0=0.04$  h<sup>-1</sup>) in the existence of co-substrate 50 g L<sup>-1</sup> batch sorbitol in the medium were selected such that the specific growth rate ( $\mu$ ) was closer to the  $\mu$  values studied in literature.

As all experimental runs feeding strategy for the first three phases (GB, GFB and MT) were the same with batch-phase glycerol addition of 40 g L<sup>-1</sup>; glycerol fed-batch feeding with given parameters in Table 3.8 using (3.1) as shown by Figure 3.3 with slight differences in  $V_0$  due to volumetric loss in sampling of  $t=0$  h and in  $Cx_0$ .

In calculation of predetermined methanol feeding rates, (3.1) was used with the tabulated parameters in Table 3.8 and change in exponential

methanol feeding rates that depend on the specific growth rates of  $\mu_0=0.02 \text{ h}^{-1}$ ,  $\mu_0=0.03 \text{ h}^{-1}$  and  $\mu_0=0.04 \text{ h}^{-1}$ , are plotted in Figure 4.6.

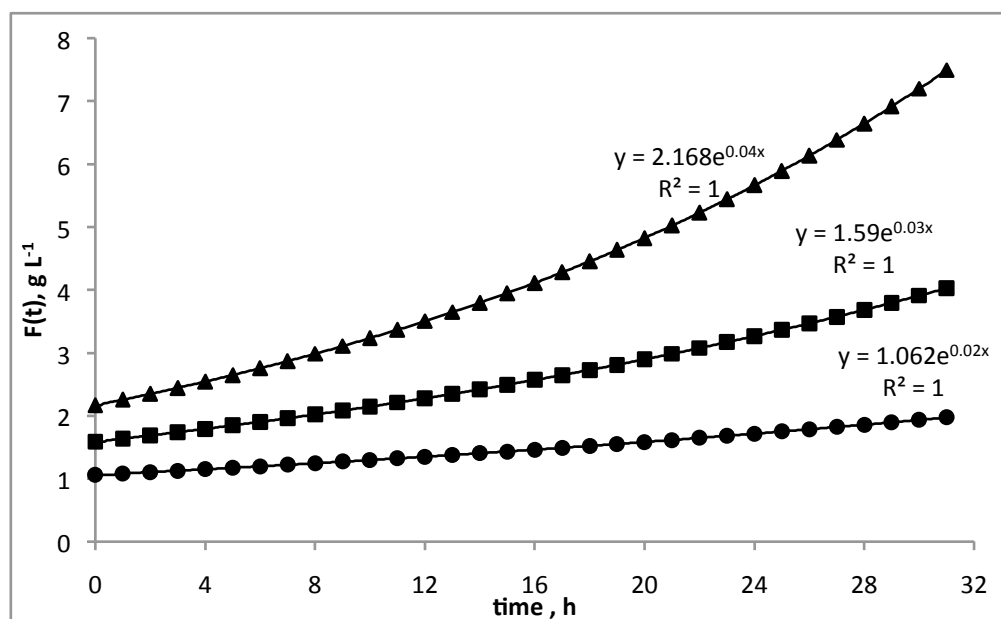


**Figure 4.6** The predetermined feeding profile for methanol, calculated for specific growth rates  $\mu_0=0.02 \text{ h}^{-1}$  (MS-0.02)(●);  $\mu_0=0.03 \text{ h}^{-1}$  (MS-0.03)(■); and  $\mu_0=0.04 \text{ h}^{-1}$  (MS-0.04)(▲)

#### 4.3.2.1 Effect of Methanol Feeding Rate on Sorbitol Consumption Rate

From these feeding profiles the sorbitol consumption and cell growth profiles were affected as shown in Figure 4.7. As mentioned, although the process was continued around 60 hours, and the production (induction) phase starts at around  $t=32 \text{ h}$  of the bioprocess, for simplicity in calculations and explanation the beginning of the production phase was taken as  $t=0 \text{ h}$ .

As methanol was never detected in the medium throughout the fermentation processes; similar to the findings of Jungo et al., (2007); Çelik et al., (2009) and Wang et al., (2009), it can be concluded that methanol and

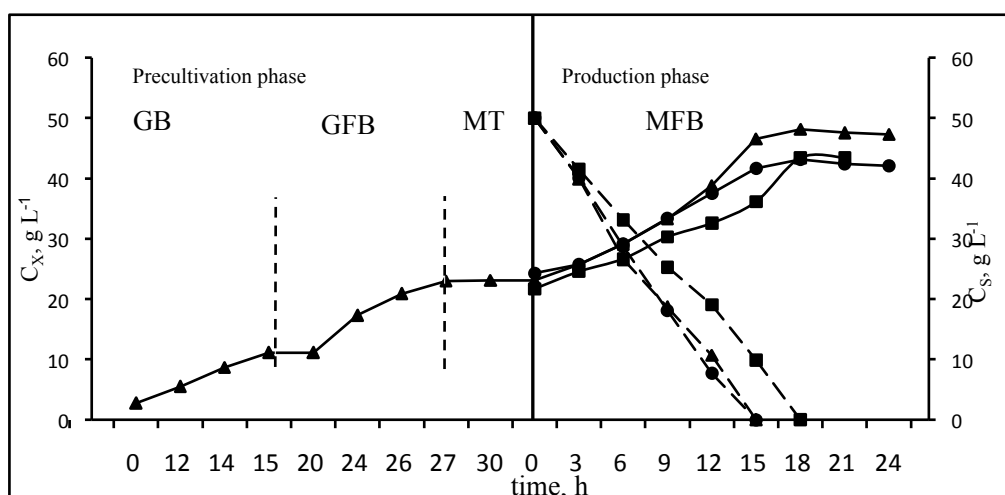


**Figure 4.7** Variation in cell (straight lines) and sorbitol (dashed lines) concentrations with cultivation time for different methanol feeding rates; MS-0.02 (■), MS-0.03 (●), MS-0.04 (▲).

sorbitol were consumed simultaneously. Sorbitol consumption started at the beginning of the production phase right after its addition to the medium and showed a linear relation with the cultivation time and totally utilized at  $t=15$  h for MS-0.03 and MS-0.04 conditions, and for MS-0.02 at  $t=18$  h.

In comparison of MS-0.03 and MS-0.02, it can be concluded that with the decrease in methanol feeding rate the intracellular reaction rates reduce leading to a decrease in sorbitol consumption rate. In order to understand the effect of methanol feeding for all operations in more detail, the specific rates of the bioprocess were calculated and tabulated in Table 4.1. From the tabulated data, it can be seen that while the specific methanol consumption rate,  $q_M$ , remained constant throughout the process, the specific sorbitol consumption rate,  $q_S$ , decreased with the cultivation time at all conditions. The highest value was obtained as  $q_S=0.17$   $gg^{-1}h^{-1}$  at  $t=0$  h at MS-0.04 condition.

**Table 4.1** Variations in specific rates throughout of the fermentation for MS-0.02, MS-0.03 and MS-0.04 conditions.

<b>time</b>	$\mu_t$	$q_s$	$q_M$	$q_{rhGH} * 1000$	$q_0$
h	$h^{-1}$	$h^{-1}$	$g\ g^{-1}\ h^{-1}$	$g\ g^{-1}\ h^{-1}$	$g\ g^{-1}\ h^{-1}$
<b>MS-0.02</b>					
0	0.044	0.129	0.047	0.004	0.061
3	0.039	0.114	0.044	0.408	0.077
6	0.036	0.101	0.043	-	0.075
9	0.031	0.078	0.040	0.316	0.069
12	0.029	0.079	0.040	-	0.065
15	0.05	0.088	0.038	0.127	0.055
18	0.028	0.073	0.034	0.121	0.048
21	0		0.036	-0.245	0.032
<b>MS-0.03</b>					
0	0.018	0.162	0.077	-	0.132
3	0.039	0.145	0.08	0.112	0.153
6	0.046	0.120	0.077	-	0.209
9	0.045	0.098	0.076	0.463	0.099
12	0.038	0.082	0.072	-	0.103
15	0.028	0.068	0.073	0.420	0.093
18	0.016		0.075	0.346	0.067
21	0		0.086	0.220	0.045
<b>MS-0.04</b>					
0	0.043	0.169	0.094	0.535	0.252
3	0.039	0.152	0.095	0.414	0.160
6	0.034	0.122	0.095	-	0.116
9	0.049	0.079	0.093	0.217	0.179
12	0.057	0.080	0.090	-	0.227
15	0.034	0.067	0.085	0.089	0.088
18	0.004		0.093	0.071	0.069
21	0		0.106	0.094	0.113

#### **4.3.2.2 Effect of Methanol Feeding Rate on Cell Growth**

The variations in cell concentration with the feeding strategy and the cultivation time are shown in Figure 4.9. Since the first three steps of the precultivation process were adjusted such that they were the same in for all experiments. Therefore they were plotted using of the data sets.

Owing to the existence of sorbitol, lag phase was eliminated, and the specific growth rates obtained were higher than the pre-determined ones i.e. for MS-0.02 2.5-fold, and for MS-0.03 and MS-0.04 1.5-fold (Table 4.1) similar to the results of Çelik et al., (2009) and Açık, (2009). In all operations, exponential growth phase was observed until sorbitol was totally consumed, pointing out the direct effect of sorbitol on cell growth. The highest cell concentration was obtained for MS-0.04 case as 48 g L<sup>-1</sup> and for MS-0.02 and MS-0.03 the final cell concentrations were the same as 43 g L<sup>-1</sup>.

#### **4.3.2.3 Effect of Methanol Feeding Rate on rhGH Production**

Since methanol is the inducer of rhGH production through AOX1 promoter, the methanol feeding rate is directly effective on production. The change in rhGH concentration throughout bioprocesses can be seen from Figure 4.8, rhGH concentration ( $C_{rhGH}$ ) increased with the cultivation time, and the highest values were reached at t=18, 24 and 24h of the MS-0.02, MS-0.03 and MS-0.04 conditions as both found by SDS-PAGE (data not shown) and capillary electrophoresis results (Figure 4.10). The highest rhGH concentration was reached at MS-0.03 condition as 270 mg L<sup>-1</sup>, which was 2.1- and 1.6-fold higher than those obtained at MS-0.02 and MS-0.04 cases respectively (Figure 4.9).

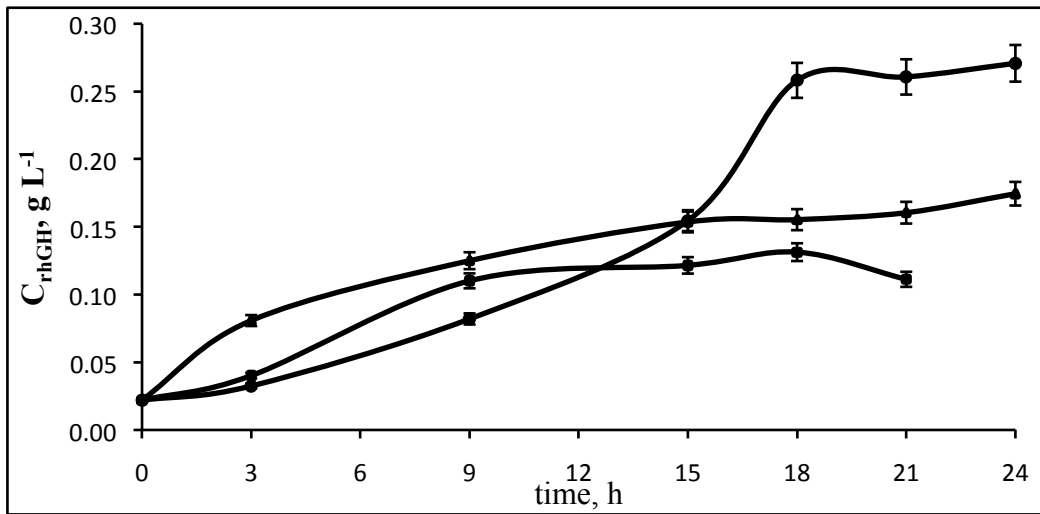


**Figure 4.8** Variation in rhGH concentrations with cultivation time for different methanol feeding rates; MS-0.02 (■), MS-0.03 (●), MS-0.04 (▲).

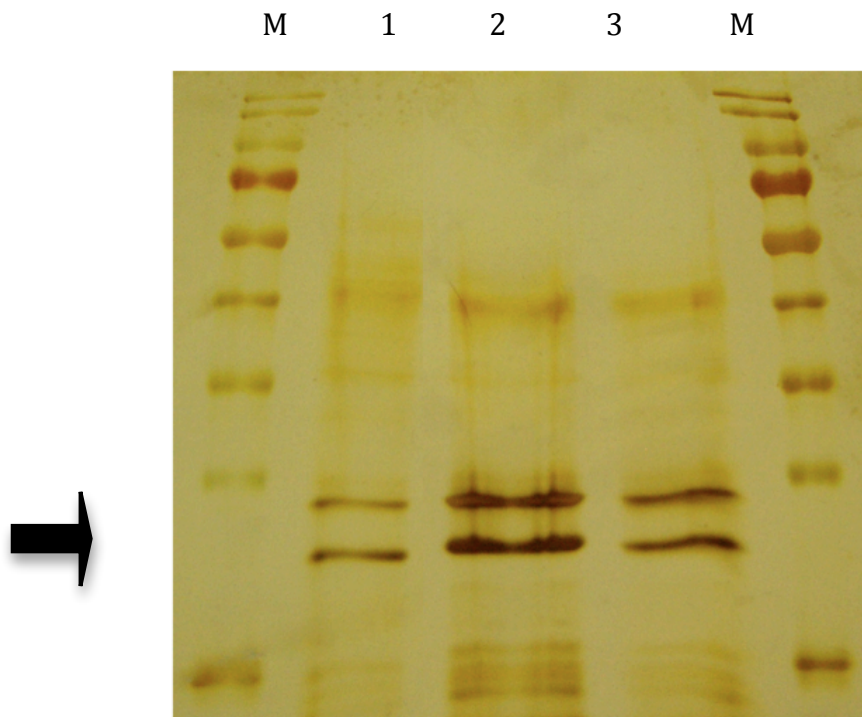


**Figure 4.9** Silver stained SDS-PAGE gel view of extracellular proteins for different methanol feeding rates. Lane M: protein marker; Lane1: MS-0.02; Lane2: MS-0.03; Lane3: MS-0.04

In comparison of the maximum rhGH concentration with the recent findings of Çelik et al., (2009) in which similar feeding strategy was employed for the production of highly glycosylated protein, recombinant human erythropoietin, by Mut<sup>+</sup> strain, 2.1-fold higher recombinant protein concentration was achieved. This is probably due to the fact the addition of glycans to the protein requires more energy than production of a non-glycosylated protein. Also, the comparison of the specific production rates of rhGH fermentation (Table 4.2) and the specific production rates of recombinant erythropoietin, it is clearly shown that higher specific production rates of non-glycosylated protein (rhGH) could be achieved under similar experimental conditions. Hence, when the total recombinant protein concentration (rhGH) was taken into account MS-0.03 condition is the most beneficial condition. However, it should also be noted that, at the beginning of production phase until t=15 h rhGH concentrations were higher under MS-0.04 condition compared to MS-0.03 condition due to higher AOX induction.

#### **4.3.3.4 Effect of Methanol Feeding Rate on Alcohol Oxidase Enzyme Production**

As mentioned earlier, alcohol oxidase (AOX) activity is associated with rhGH production and enzymatic activity of AOX is induced by methanol. Therefore, determination of AOX activity provides insight for understanding the relation between AOX and rhGH production. In Figure 4.10, the AOX activity profiles different methanol feeding rates throughout the processes were shown. In all three cases, similar AOX profiles were observed in which activity first increased and after reaching the highest value, started decreasing and finally remained unchanged as the growth reaches stationary phase. The highest AOX activities were obtained as 29 U g<sup>-1</sup> CDW at t=12 h, 41 U g<sup>-1</sup> CDW at t=15 h and 37 U g<sup>-1</sup> CDW at t=6 h at MS-0.02, MS-0.03 and MS-0.04, respectively. At the beginning of the fermentation specific AOX activity was the highest for MS-0.04, which resulted in higher rhGH

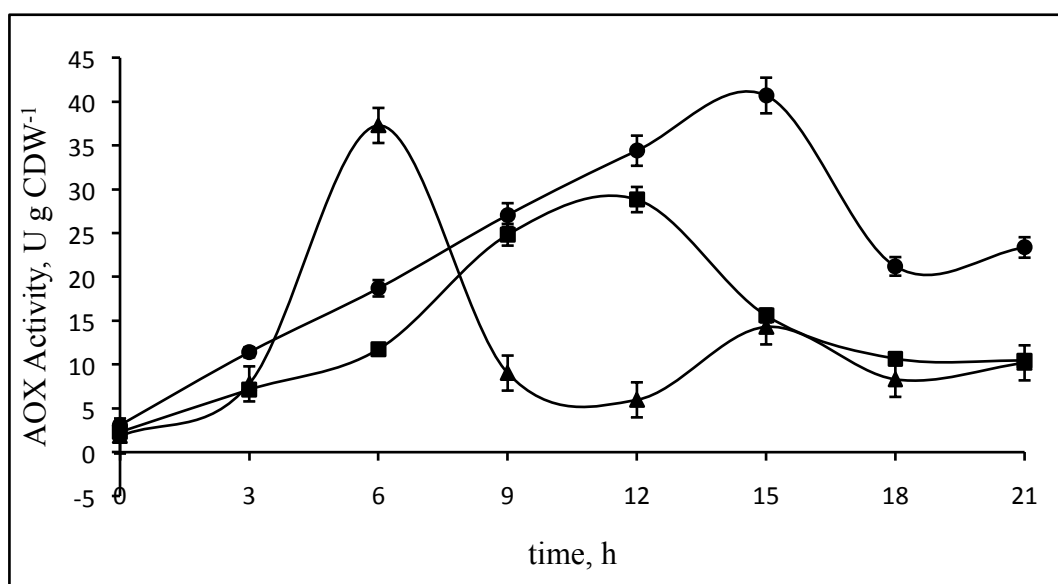


**Figure 4.10** Variation in AOX activity with cultivation time for different methanol feeding rates; MS-0.02 (■), MS-0.03 (●), MS-0.04 (▲).

concentration this case at the beginning. However, after  $t=15$  h, AOX activity reached its maximum value,  $41 \text{ U g}^{-1} \text{ CDW}$ , at  $t=15$  h for MS-0.03, where the highest rhGH concentration was achieved.

#### 4.3.2.5 Effect of Methanol Feeding Rate on Protease Production

Extracellular activities of alkali, neutral and acidic proteases were determined separately and their total activity is converted to concentration. As can be seen from Figure 4.11, the total protease concentrations were not much different from each other reaching the highest value around  $0.09 \text{ g L}^{-1}$ . As the most of the main parameters that are effective on protease concentration such as pH, temperature and dissolved oxygen concentration were kept the same for all cases. The slight differences between protease concentrations of the cases were mostly dependent on the methanol feeding rate as the values increased with increasing methanol-feeding rate, in parallel to the findings of Sinha et al., (2005).

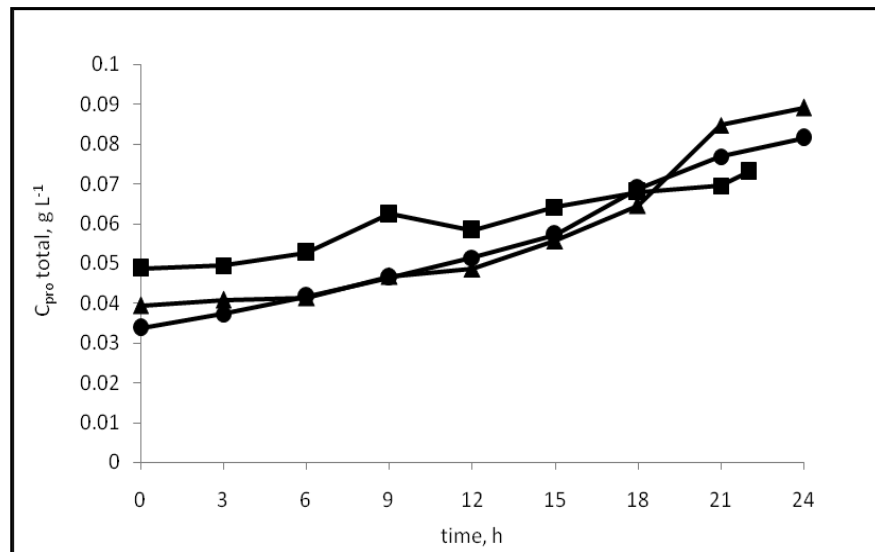


**Figure 4.11** Variation in total protease concentration activity with cultivation time for different methanol feeding rates; MS-0.02 (■), MS-0.03 (●), MS-0.04 (▲).

The protease concentration was slightly higher for MS-0.02 condition until  $t=18\text{h}$ , although the highest final protease concentration was seen at MS-0.04 case as  $0.09\text{ g L}^{-1}$ . Moreover, for this condition, maximum specific total protease production was calculated as  $1\text{ mg g}^{-1}\text{ CDW h}^{-1}$ .

#### 4.3.2.6 Effect of Methanol Feeding Rate on Amino Acid and Organic Acid Concentration Profiles

The variations of the amino and organic acid concentrations in the media give insight about the supply and demand of the metabolites those are regulated by the reactions of the metabolic pathways. Therefore, they were detected in the medium at several cultivation times of the process ( $t=3\text{ h}$ ,  $t=9\text{ h}$ ,  $t=15\text{ h}$  and  $t=21\text{ h}$ ) (Table 4.2).

**Table 4.2** Variations in amino acid concentrations\* with respect to time for different specific growth rates

<b>MS-0.02</b>				
	<b>t=3h</b>	<b>t=9h</b>	<b>t=15h</b>	<b>t=21h</b>
Asp	0.0158	0.0205	0.0163	0.0346
Asn	0.0362	0.0135	0.0244	0.0226
Gly	0.0350	0.0234	0.0189	0
His	0.0066	0.0052	0.0056	0
Pro	0	0	0	0
Val	0.0252	0.0274	0.0126	0
Met	0.0028	0.0031	0.0027	0.0051
Phe	0	0	0	0
Trp	0.0037	0.0024	0.0023	0.0027
Lys	0.0336	0.0181	0	0.0194
<b>Total</b>	<b>0.1588</b>	<b>0.0902</b>	<b>0.0828</b>	<b>0.0843</b>

<b>MS-0.03</b>				
	<b>t=3h</b>	<b>t=9h</b>	<b>t=15h</b>	<b>t=21h</b>
Asp	0.0126	0.0181	0.0274	0.0168
Asn	0.0152	0.0167	0.016	0.0082
Gly	0.0229	0.0182	0.016	0
His	0	0	0	0
Pro	0	0.0006	0.0005	0
Val	0.0319	0.0245	0	0.0049
Met	0.0049	0.0064	0.0077	0.0081
Phe	0.0028	0.0045	0.0043	0.0051
Trp	0	0.0009	0	0
Lys	0.0022	0.0183	0.0150	0.0140
<b>Total</b>	<b>0.0925</b>	<b>0.1082</b>	<b>0.0869</b>	<b>0.0571</b>

<b>MS-0.04</b>				
	<b>t=3h</b>	<b>t=9h</b>	<b>t=15h</b>	<b>t=21h</b>
Asp	0.0182	0.0198	0.0325	0.0293
Asn	0.0239	0.0307	0.0155	0.0137
Gly	0.0144	0.0337	0.0140	0.0131
His	0	0	0	0
Pro	0	0	0	0
Val	0.0315	0.0210	0	0
Met	0.0027	0.0029	0	0
Phe	0	0	0	0
Trp	0.0029	0.0026	0.0025	0.0030
Lys	0.0288	0.0308	0.0320	0
<b>Total</b>	<b>0.1225</b>	<b>0.1415</b>	<b>0.0964</b>	<b>0.0590</b>

\*Concentrations are in g L<sup>-1</sup> units.

The amino acids that were mainly detected in the fermentation medium are aspartic acid, asparagine, glycine, histidine, valine, methionine, tryptophan and lysine. Proline and phenylalanine were also detected in trace amounts for MS-0.03 condition. In none of the three conditions the amino acids which take part in the structure of rhGH, i.e. leucine (13.6%), serine (9.4%), glutamic acid (7.3%) and glutamine (6.8%) ,which make up rhGH, were detected in the medium. The initial reactions of the leucine biosynthesis pathway lead to valine (Çelik et al., 2010), final valine concentration was the highest for MS-0.03. Maximum amino acid concentration was achieved as 0.15 g L<sup>-1</sup> in MS-0.02 condition while for MS-0.03 and MS-0.04 cases the maximum concentrations of 0.11 g L<sup>-1</sup> and 0.14 g L<sup>-1</sup> were obtained respectively at t=9 h of the bioprocesses.

Related with the organic acid concentrations, for all the conditions formic,  $\alpha$ -ketoglutaric, citric, succinic and fumaric acids were the organics acids detected in the medium (Table 4.3). On the other hand, lactic acid, which is produced in case of oxygen limitation in the medium, was not detected in the medium in any condition. This is probably due to existence of co-substrate sorbitol that decreased the oxygen demand on methanol (Çelik et al., 2009). With an increase in the specific growth rate, the organic acid concentrations that were secreted to the medium increased, reaching the highest concentrations of 0.41 g L<sup>-1</sup>, 0.48 g L<sup>-1</sup>, and 0.80 g L<sup>-1</sup> in MS-0.02, MS-0.03 and MS-0.04 conditions respectively.

**Table 4.3** Variations in organic acid concentrations with respect to time for different specific growth rates in g L<sup>-1</sup>

Time, h	0	3	6	9	12	15	18	21	24
<b>MS-0.02</b>									
Formic acid	0.0611	0.1088	0.0884	0.1022	0.1109	0.1280	0.1598	0.1682	0.1979
$\alpha$ -keto glutaric acid	0.0094	0.0237	0.0248	0.0290	0.0237	0.0283	0.0281	0.0218	0.0209
Citric acid	0.0075	0.0091	0.0134	0.0158	0.0191	0.0226	0.0244	0.0269	0.0280
Fumaric acid	0.0010	0.0009	0.0011	0.0012	0.0013	0.0014	0.0016	0.0015	0.0014
Succinic acid	0.0000	0.0000	0.0293	0.0727	0.0854	0.1043	0.1225	0.1253	0.1160
<b>MS-0.03</b>									
Formic acid	0.0851	0.1163	0.1155	0.1299	0.1616	0.1743	0.2627	0.3015	0.3021
$\alpha$ -keto glutaric acid	0.0252	0.0269	0.0288	0.0319	0.0342	0.0364	0.0368	0.0402	0.044
Citric acid	0.0007	0.0007	0.0074	0.0089	0.0112	0.0145	0.0199	0.0201	0.0323
Fumaric acid	0.0002	0.001	0.001	0.0012	0.0014	0.0017	0.0017	0.0017	0.002
Succinic acid	0.0635	0.0721	0.0778	0.0751	0.0812	0.0882	0.0798	0.0815	0.0941
<b>MS-0.04</b>									
Formic acid	0.1155	0.2530	0.2853	0.2883	0.3746	0.4045	0.4582	0.4659	0.5350
$\alpha$ -keto glutaric acid	0.0216	0.0264	0.0359	0.0513	0.0565	0.0587	0.0612	0.0644	0.0769
Citric acid	0.0073	0.0072	0.0078	0.0081	0.0088	0.0097	0.0116	0.0124	0.0149
Fumaric acid	0.0010	0.0000	0.0010	0.0010	0.0010	0.0010	0.0010	0.0010	0.0011
Succinic acid	0.0000	0.0000	0.0926	0.1105	0.1490	0.1630	0.1640	0.1601	0.1767

The organic acid that was detected with the highest concentration for all cases was formic acid. In relation with formic acid, formaldehyde was never detected in the media. This is related with the fact that, formaldehyde is oxidized to formic acid or goes into assimilatory pathway and enters glycolysis. Moreover the concentration of formic acid was increased with respect to time, indicating methanol feed rate increased the formaldehyde formation through methanol utilization pathway, which was then oxidized to formic acid.

#### **4.3.2.7 Effect of Methanol Feeding Rate on Oxygen Transfer Characteristics of the Bioprocess**

OUR, OTR,  $K_{La}$ , OD, Da,  $\eta$  and the enhancement factor (E), during MFB were determined by Dynamic Method and are tabulated in Table 4.4.

As expected,  $K_{La}$  first increased at the beginning of the bioprocess ( $t=0-15h$ ), and then decreased with the cultivation time, the highest  $K_{La}$  values obtained were  $K_{La}= 0.09, 0.14, 0.15 \text{ s}^{-1}$  for MS-0.02, 0.03, and 0.04 conditions, respectively. This variation in  $K_{La}$  can be explained by the changes in rheological properties of the broth. Correlation suggested by Ryu et al. (1971) indicates that  $K_{La}$  is inversely proportional to apparent viscosity ( $\mu_{ap}$ ). When  $\mu_{ap}$  was calculated by using the cell concentration values according to the correlation of Raposa et al. (2006), it was seen that there was a sharp increase in apparent viscosity at  $t=12 \text{ h}$  for MS-0.03 and MS-0.04 and at  $t=15 \text{ h}$  for MS-0.02 which could be the reason of the  $K_{La}$  decrease at these hours. Furthermore, as the cells grow, they secrete metabolites and proteins to the extracellular medium, which results in a resistance zone for mass transfer, by limiting the contact area of the gas bubbles with the cells.

**Table 4.4** Variations in oxygen transfer parameters throughout the bioprocess for different growth rates

t	$K_{La}$	E	$OTR \times 10^3$	$OTR_{max} \times 10^3$	OUR $\times 10^3$	OD $\times 10^3$	Da	$\eta$
h	( $s^{-1}$ )	( $K_{La}/K_{La0}$ )	( $mol\ m^{-3}s^{-1}$ )	( $mol\ m^{-3}s^{-1}$ )	( $mol\ m^{-3}s^{-1}$ )	( $mol\ m^{-3}s^{-1}$ )		
<b>MS-0.02</b>								
0	0.060	5.41	12.48	19.2	11.6	36.6	1.9	0.32
3	0.077	6.94	17.33	24.6	16.4	58.5	2.4	0.28
6	0.083	7.48	18.73	26.6	17.4	67.5	2.5	0.26
12	0.084	7.57	19.93	26.9	18.5	90.0	3.3	0.21
15	0.090	8.11	19.95	29.0	18.3	48.8	1.7	0.37
18	0.090	8.11	19.80	29.0	18.0	89.4	3.1	0.20
21	0.052	4.67	12.77	16.6	12.2			
<b>MS-0.03</b>								
0	0.092	8.28	29.00	36.6	27.8	244.4	6.7	0.11
3	0.119	10.71	36.40	47.2	34.1	132.6	2.8	0.26
9	0.119	10.71	33.50	47.5	29	97.7	2.1	0.30
12	0.136	12.24	38.20	54.1	33.4	135.0	2.5	0.25
15	0.121	10.89	34.70	48.2	33.6	193.3	4.0	0.17
18	0.093	8.37	26.60	37.0	25.0	287.9	7.8	0.09
21	0.067	6.03	18.60	26.7	16.6			
<b>MS-0.04</b>								
3	0.097	8.75	53.94	68.0	35.8	130.3	1.9	0.27
6	0.095	8.56	48.69	66.5	29.3	117.9	1.8	0.25
9	0.110	9.91	59.41	77.0	51.7	150.0	1.9	0.34
12	0.147	13.24	80.21	102.9	76.6	188.6	1.8	0.41
15	0.090	8.11	53.08	63.0	35.4	145.1	2.3	0.24
18	0.070	6.31	39.89	49.0	29.0			

On the other hand, with the increase in cell concentration, oxygen uptake rate having a positive effect on  $K_{La}$ , increases due to increase in oxygen demand. That is, cell growth has a complex effect on  $K_{La}$ , however, after  $t=12$  h; effect of the properties of fermentation medium dominates over the effect of OUR on  $K_{La}$  and determines the decline of it throughout the bioprocess.

Other parameter, OTR is proportional to the difference between the saturated oxygen concentration and dissolved oxygen concentration in the

medium, and increased to an extent depending on the OUR. The highest OTR values obtained were  $OTR=19.9, 36.4, \text{ and } 80.2 \text{ mmol m}^{-3}\text{s}^{-1}$  at MS-0.02, 0.03, and 0.04 conditions, respectively, increasing with respect to the specific growth rate. The reason of this behavior might have been the driving force generated by the difference between the saturated and dissolved oxygen concentrations.

OUR depends on the biomass production and substrate consumption rates (Çalık et al., 1998). It had a tendency to increase at the beginning of the process with the increase in cell concentration, and then reached its maximum at  $t= 9\text{-}15 \text{ h}$  of the bioprocess, having OUR values for MS-0.02, 0.03, and 0.04 conditions as  $18.5, 34.1, 76.6 \text{ mmol m}^{-3}\text{s}^{-1}$  respectively.

To find out the limiting step of the growth process, OD and  $OTR_{\max}$  were calculated along the cultivation time. The relation between these maximum rates is defined as Da (Çalık et al., 1998). Throughout the experiments Da was higher than 1 with mostly an increasing profile with respect to cultivation time. In this range of Da, mass transfer resistances dominate over biochemical reaction resistances. The reason is that increase in oxygen demand due to high methanol feeding rate cannot be satisfied by oxygen transfer rate ( $OTR_{\max}$ ). As methanol consumption rate increased, OD started to increase for all runs (or vice versa), since methanol utilization pathway enhances oxygen demand. Owing to the fact that Da is directly proportional to OD, it also increased. The maximum Da values obtained were 3.3, 7.8 and 2.3 for MS-0.02, 0.03 and 0.04 operations, respectively. That is, the highest Da was observed at MS-0.03, where the metabolites (mainly rhGH) secreted to the medium were at the highest concentration. This can also be seen clearly at  $t=15 \text{ h}$ , at which the sharp increase in rhGH concentration leading to a transport limiting condition, Da increased sharply.

Furthermore,  $\eta$  took higher values at the beginning of the bioprocess, and then decreased (Table 4.4). As  $\eta$  decreased oxygen transport become

limited. For all conditions,  $\eta$  was less than 1, indicating oxygen was consumed below the maximum oxygen demand. The highest  $\eta$  values obtained are 0.32, 0.31 and 0.41 for MS-0.02, 0.03 and 0.04 conditions, respectively. The reason why the  $\eta$  was lower for MS-0.03 is the fact that although OD was expected to be higher for higher methanol feeding rates, metabolite secretion was fairly higher for MS-0.03 condition while cell concentrations were comparable to each other.

It was observed that there was an inverse relation between  $Da$  and  $\eta$ . In all operations, as  $\eta$  decreased,  $Da$  increased. When  $Da$  decreases and  $\eta$  approaches to 1, mass transfer resistances become negligible.

Moreover, during the biotransformation,  $K_{La}$  values obtained are different from those obtained under inert conditions (in the absence of the microorganism) ( $K_{La0}$ ). Therefore, for sufficient description of the OTR, defining enhancement factor ( $K_{La}/K_{La0}$ ) is necessary due to the presence of microorganisms. Since  $E$  is function of  $K_{La}$ , variation in  $E$  with the cultivation time is only due to the changes in  $K_{La}$ . Thus,  $E$  increased then decreased. The maximum  $E$  values obtained are 8, 12, and 13 for MS-0.02, 0.03, and 0.04 conditions, respectively.

#### **4.3.2.8 Effect of Methanol Feeding Rate on Yield Coefficients of the Bioprocess**

The overall yield of cells on total substrate ( $Y_{X/S}$ ), overall product on total substrate ( $Y_{rhGH/S}$ ) and overall yield of product formed per total cell generated ( $Y_{rhGH/X}$ ) were calculated. In addition, to determine the effect of methanol feeding rate, the overall yield of rhGH on methanol ( $Y_{rhGH/M}$ ) are considered for all operations and the overall yields are given in Table 4.5. For MS-0.03 condition  $Y_{X/M}$  was the lowest, whereas  $Y_{rhGH/M}$  was the highest. Maximum  $Y_{rhGH/M}$  attained at MS-0.03 was  $3.6 \text{ mg g}^{-1}$  which is close to MS-0.02 ( $Y_{rhGH/M}=3.01 \text{ mg g}^{-1}$ ), and 1.9-fold higher than that obtained in MS-0.04 operation. It can be concluded that for MS-0.03 operation the methanol fed

to the medium, mainly consumed for rhGH formation, rather than cell generation.

Similar to overall yields on methanol,  $Y_{X/S'}$  is the lowest and  $Y_{rhGH/S'}$  is the highest for MS-0.03. The lowest overall  $Y_{X/S'}$ ,  $0.15 \text{ g g}^{-1}$ , was achieved in MS-0.03; whereas, the highest overall  $Y_{rhGH/S'}$  and  $Y_{rhGH/X}$  were attained as 2.09 and  $13.97 \text{ g g}^{-1}$  respectively. On the other hand, at MS-0.02 and MS-0.04 conditions a 1.87-fold decrease in overall  $Y_{rhGH/S'}$  was observed. Overall  $Y_{rhGH/X}$  value also decreased 3.36-fold at MS-0.02 condition and 2.22-fold at MS-0.04 condition when compared to MS-0.03 condition.

**Table 4.5** Overall yield coefficients for different specific growth rates

<b>Operation condition</b>	$Y_{X/S'}$	$Y_{rhGH/S'}$	$Y_{rhGH/X}$	$Y_{rhGH/M}$
	$\text{g g}^{-1}$	$\text{mg g}^{-1}$	$\text{mg g}^{-1}$	$\text{mg g}^{-1}$
<b>MS-0.02</b>	0.27	1.12	4.16	3.01
<b>MS-0.03</b>	0.15	2.09	13.97	3.61
<b>MS-0.04</b>	0.19	1.16	6.30	1.88

#### 4.3.3 Effect of pH on Bioprocess Characteristics of *P.pastoris* Producing rhGH

In literature it was shown that different pH values were optimum for different recombinant proteins. In a recent study of our group, the effect of pH on rhGH production by *P.pastoris* was investigated in three sets of experiments, namely pH=4.2, pH=5.0 and pH=6.0 operation (Bayraktar, 2009). In the study it was indicated that at pH=6.0 the highest cell growth with almost no rhGH production was observed and at pH=4.2 operation with comparable growth rate to pH=5.0, lower rhGH concentration due to higher protease and lower AOX activity. The highest product formation rate and the

overall product yield on substrate and on cell was the highest for pH=5.0 compared with other two cases. Therefore, in order to understand after which pH the productivity and yields reach maximum and then start to decrease, an additional pH experiment was conducted at pH=5.5, with pre-determined methanol feeding rate for  $\mu_0=0.03 \text{ h}^{-1}$  and  $50 \text{ g L}^{-1}$  batch sorbitol addition at the beginning of production phase in order to convey the same experimental conditions as Bayraktar (2009).

#### 4.3.3.1 Cell growth and Sorbitol Consumption Profiles at pH=5.5

The cell growth and sorbitol utilization profiles are given in Figure 4.12. Sorbitol was utilized at almost a constant rate throughout the process at a higher rate compared with pH=6.0 and similar to pH=4.2 and 5.0, and totally depleted at  $t=15 \text{ h}$ . Moreover the final cell concentration was reached as  $C_x = 44.9 \text{ g L}^{-1}$ , which is slightly higher than pH=5.0 and pH=4.2 cases.

When the specific rates are considered similar to all other cases  $q_s$  was the highest in the beginning of the process and decreased in relation with increase in cell concentration (Table 4.6).

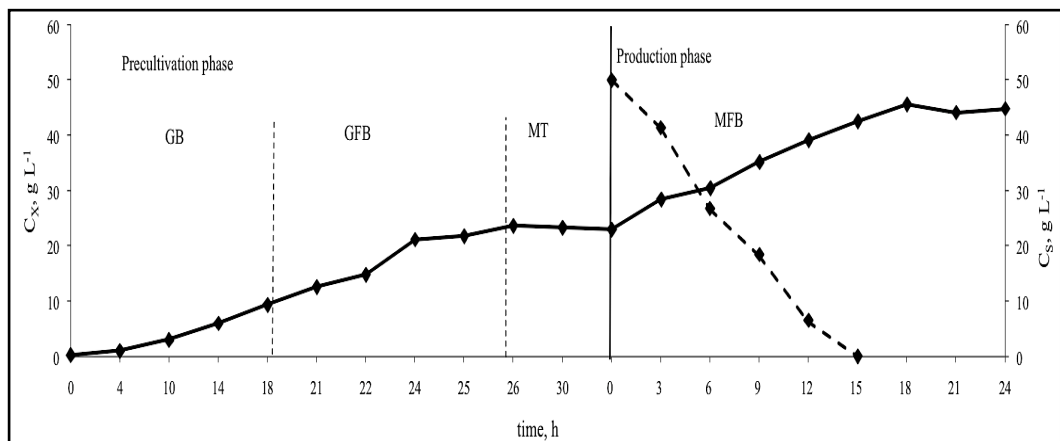


**Figure 4.12** Variation in cell (straight lines) and sorbitol (dashed lines) concentration with cultivation time for pH=5.5 condition.

Likewise,  $\mu$  was higher at the beginning of the process. Moreover, in order to understand the effects of pH on cell growth and production the overall yields were calculated.

For pH=5.5 case  $Y_{x/s}$  and  $Y_{p/s}$  were found as  $0.2 \text{ g g}^{-1}$  and  $10 \text{ mg g}^{-1}$  close to the results of pH=5.0 experiment (1.2-fold higher and 1.3-fold less, respectively).

**Table 4.6** Variations in specific rates throughout of the process at pH=5.5

<b>t</b> (h)	<b><math>\mu_t</math></b> (h <sup>-1</sup> )	<b><math>q_s</math></b> (g g <sup>-1</sup> h <sup>-1</sup> )	<b><math>q_M</math></b> (g g <sup>-1</sup> h <sup>-1</sup> )	<b><math>q_{rhGH}</math></b> (mg g <sup>-1</sup> h <sup>-1</sup> )	<b><math>q_0</math></b> (g g <sup>-1</sup> h <sup>-1</sup> )
0	0.054	0.151	0.070		0.063
3	0.044	0.137	0.062		0.145
6	0.037	0.126	0.063	0.380	0.140
9	0.041	0.096	0.060	0.221	0.043
12	0.031	0.078	0.059		0.043
15	0.025	0.025	0.059	0.420	0.091
18	0.006		0.060	-0.068	
21	-0.003		0.068	-0.068	
24	0.005		0.074	-0.014	0.003

#### 4.3.3.2 rhGH Production, AOX Activity and Protease Concentration Profiles at pH=5.5

As the major goal of this study is to obtain the higher product concentration, the investigation of production concentration is important. Since methanol pathway uses AOX promoter for induction of rhGH production AOX activity was also plotted together with concentration data (Figure 4.13). The highest  $C_{rhGH}$  value was attained at t=18 h as  $0.25 \text{ g L}^{-1}$  1.08 fold less than the highest resulting rhGH concentration (at pH=5.0 condition). The comparison of the maximum protein concentrations of all four cases was conducted on SDS-PAGE (Figure 4.14). Also another

important coefficient  $Y_{P/X}$  was calculated as  $1.9 \text{ mg g}^{-1}$ , 1.1-fold less than the value found in pH=5.0 condition. Different from the best-case pH=5.0, the highest AOX activity was seen closer to the beginning of the bioprocess as  $22 \text{ U g}^{-1} \text{ CDW}$ , and then decreased continuously. Although slightly lower AOX profile compared to pH=4.2 case was seen, at pH=5.5 higher product concentrations were achieved. This is probably due to the existence of higher concentration of proteases at pH=4.2 (Figure 4.13).

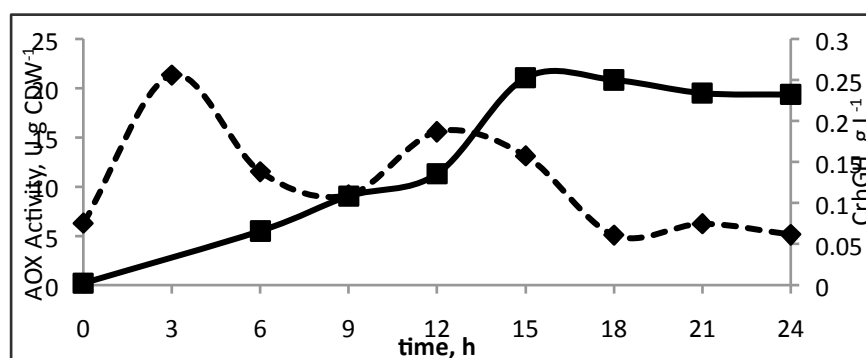


**Figure 4.13** Variation in rhGH concentration (straight lines) and AOX activity (dashed lines) with cultivation time for pH=5.5 condition

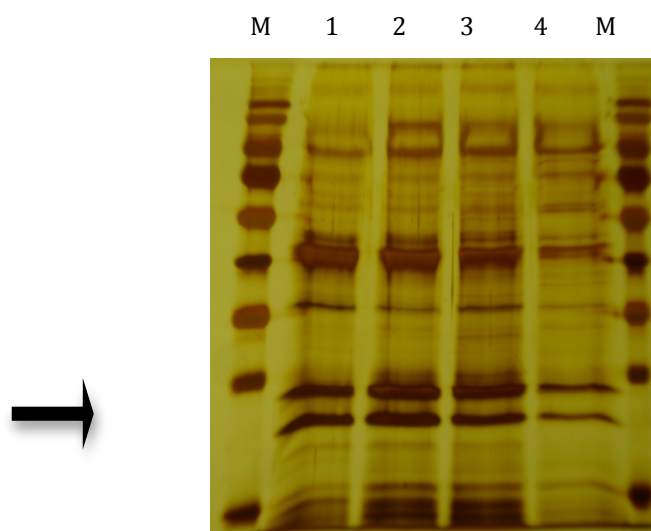


**Figure 4.14** Silver stained SDS-PAGE gel view of extracellular proteins for different pH values. Lane M: protein marker; Lane1: pH=4.2; Lane2: pH=5.0; Lane3: pH=5.5; Lane 4: pH=6.0

The acidic, basic and neutral protease concentration were calculated separately and then added up to get the total protease concentration (Figure 4.15). It was observed that at pH=5.5 the total protease concentration was the lowest at all times of the bioprocess with slowly increasing trend reaching  $C_{\text{rpo}}=0.062 \text{ g L}^{-1}$  final concentration, in comparison with the data from Bayraktar (2009)'s work.

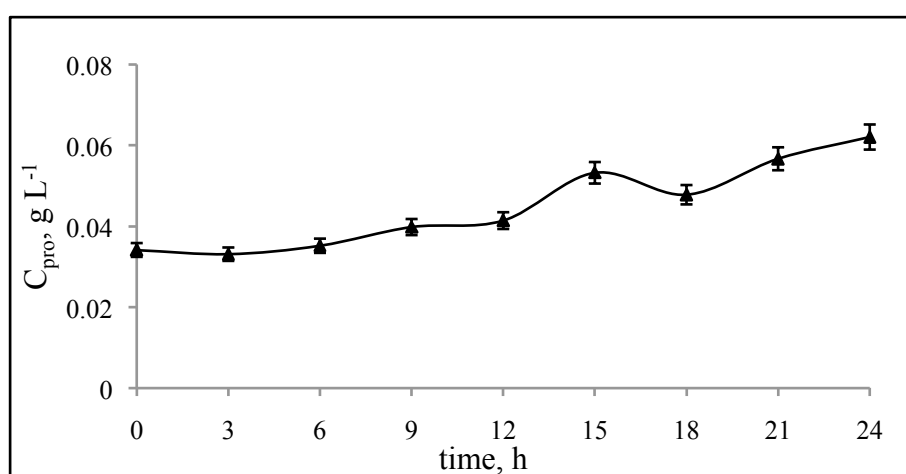


**Figure 4.15** Variation in protease concentration with fermentation time for pH=5.5 condition

#### 4.3.3.3 Organic Acid Concentrations at pH=5.5

Similar to the results of previous rhGH production experiments by *P.pastoris* formic, fumaric, glutaric, citric, and succinic acids were the organic acids detected in the medium; whereas, formaldehyde was not detected in the medium throughout the process. It is observed that amount of formic acid in the fermentation broth increased with the increase in cultivation time. On the other hand, in comparison with the previous pH experiments, fumaric and succinic acid concentrations in the medium increased with decreasing pH.

#### 4.3.3.4 Oxygen Transfer Characteristics of the rhGH Production Process at pH=5.5

$C_{D0}$  depends on the extent of the oxygen transfer rate (OTR) to the media and the oxygen uptake rate (OUR) of the cells. Throughout the process as oxygen concentration was kept at 20%, OUR was expected to be equal to OTR throughout the bioprocesses. Oxygen transfer parameters  $K_{La}$ , OUR, OTR, maximum possible oxygen transfer rate  $OTR_{max}$ , oxygen demand OD, and  $\eta$ , Da and E were calculated throughout the fermentations and are given in Table 4.7.

**Table 4.7** Variations in oxygen transfer parameters with the cultivation time at pH=5.5

t (h)	$K_{La}$ ( $s^{-1}$ )	E $K_{La}/K_{La0}$	$OTR \times 10^3$ ( $molm^{-3}s^{-1}$ )	$OTR_{max} \times 10^3$ ( $molm^{-3}s^{-1}$ )	$OUR \times 10^3$ ( $molm^{-3}s^{-1}$ )	OD $\times 10^3$ ( $molm^{-3}s^{-1}$ )	Da	$\eta$
0	0.053	4.8	15.1	20.6	12.6	32.5	1.6	0.39
3	0.125	11.37	37.2	48.8	35.9	114.5	2.3	0.31
6	0.13	11.85	38.8	50.8	36.9	140.1	2.8	0.26
9	0.052	4.68	16	20.1	13.1	44.4	2.2	0.29
12	0.051	4.64	15.9	19.9	14.7	65.3	3.3	0.22
15	0.114	10.36	35.4	44.5	33.8	186.3	4.2	0.18
24	0.044	4.1	12.1	17.1	1.3	38.6	2.3	0.03

Among the four pH conditions, generally the highest  $K_{La}$  values were obtained at pH=5.0. pH=5.5 was the case with second the highest  $K_{La}$  values close to pH=5.0 condition. This can be explained by the fact that at pH=5.0 and pH=5.5, rhGH and secreted metabolite concentrations (mainly rhGH) attained higher values, compared with other pH cases.

OUR that has a positive effect on  $K_{La}$ , depends mostly on the substrate consumption. As the substrate was consumed, oxygen demand increased related with product and cell formation reactions during the fermentation.

The highest OUR value achieved at pH=5.5 was  $37\text{mmol m}^{-3}\text{s}^{-1}$ , being the highest OUR among the four conditions. OTR, which is proportional to the difference between the saturated oxygen concentration and dissolved oxygen concentration in the medium, was increased to an extent depending on the OUR.

At  $t=3-18$  h,  $Da$  is slightly higher than 1.0, indicating that both the mass transfer and biochemical reaction resistances were effective; however, when rhGH concentration was sharply increased, oxygen demand cannot be satisfied by the oxygen transfer rate leading to higher  $Da$  values. The effectiveness factor,  $\eta$ , were lower than 0.4 for all the conditions, showing all four processes are oxygen transfer limited; i.e. cells were consuming lower oxygen than the oxygen demand (OD).

OD and  $Da$  are the theoretical values achieved without any resistance. In *Pichia pastoris* fermentations, high cell density can be achieved with the lower specific growth rates; thus, oxygen uptake rate (OUR) can not reach to OD and as  $OTR_{\max}$  changes proportional with  $K_{La}$ ,  $Da$  values  $\ll 1.0$ , are not expected. Therefore OD and  $Da$  values do not show that there is an oxygen limitation for the real system.

#### **4.3.4 Effect of sorbitol feeding strategy on Bioprocess Characteristics of *P.pastoris* Producing rhGH**

The previous studies in literature report that sorbitol is a non-repressing carbon source, which can be used as a co-substrate to enhance production and cell growth (Sreekrishna et al., 1997; Cos et al., 2006; Jungo et al. 2007b, Aık, 2009). Moreover, in the first set of experiments in which effect of methanol feeding rate was investigated, it was observed that cell concentration starts to increase without a lag phase and in all cases as soon as sorbitol was depleted at  $t=15\text{h}-18\text{h}$ , cell growth slows down and growth enters stationary phase and product formation decreases. It was also observed that cells utilize sorbitol at a constant rate irrespective of the cell

concentration. Therefore, as an additional experiment to the work done by Aık, (2009) in the following experiment sorbitol was added to the medium at 14 h for the second time right before depletion and also at  $t=31$  h right after a sharp increase in dissolved oxygen concentration was observed indicating sorbitol was totally consumed and growth was slowed down. The experiment was conducted at previously selected conditions of  $\text{pH}=5.0$ ,  $T=30^\circ\text{C}$  and  $\mu=0.03\text{h}^{-1}$ .

#### **4.3.4.1 Sorbitol Consumption and Cell Growth Profiles**

As mentioned considering the previous sorbitol consumption profiles in which the cells consume  $50\text{ g L}^{-1}$  sorbitol at almost a constant rate, regardless of cell concentration, sorbitol was added to the medium in three batches at  $t=0$  h,  $t=14$  h and  $t=31$  h aiming to provide  $50\text{g L}^{-1}$  sorbitol which is the maximum non-inhibiting sorbitol concentration as found by Aık, (2009).

The sorbitol consumption profile of the cells is plotted in Figure 4.16. Similar to the early work, sorbitol was consumed at a constant rate while exponential growth continued. At  $t=14$  h in sorbitol addition, the previous data was used and in calculation of the volume change until that time, ammonia solution added for keeping pH constant, methanol added at a predetermined exponential feeding and losses due to sampling were taken into account. However, as the sorbitol concentration  $t=14$  h was turned out to be slightly different from the value of the previous experiment,  $6\text{ g L}^{-1}$  extra sorbitol was observed in the medium right after sorbitol addition. The sorbitol was totally consumed at  $t=45$  h.

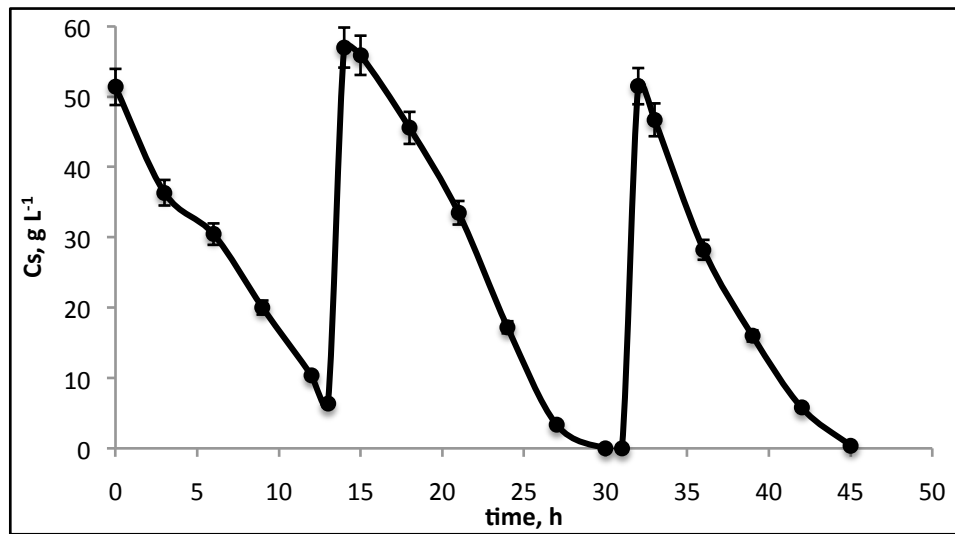


**Figure 4.16** Sorbitol consumption profile of *P.pastoris* producing rhGH

For the given sorbitol consumption profile cell growth profile is given in Figure 4.17. As done in all *P.pastoris* fermentation experiments, first three phases (GB, GFB, MT) were conducted achieving same growth profiles and methanol was added exponentially to initiate and continue the production phase.

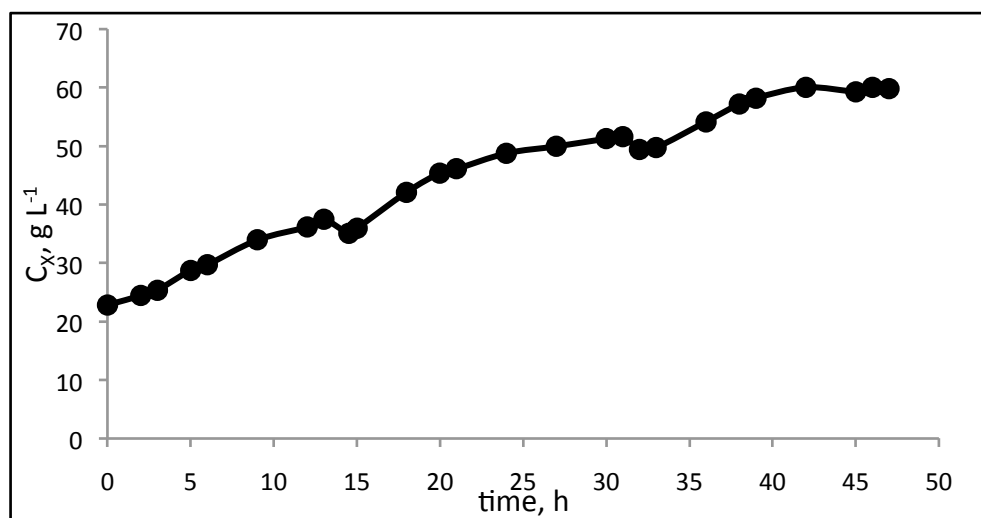


**Figure 4.17** Cell growth profile for *P.pastoris* producing rhGH

As seen from the figure, cell growth continued as long sorbitol existed in the medium. At  $t=14, 15$  h and  $t=31, 32$  h a decrease in cell concentrations was observed as expected. The reason for this is the sorbitol addition, which increased the volume of the bioprocess medium at an amount that cannot be neglected.

Moreover, when the specific rates of the process were calculated, it was seen that the specific growth rate increased each time sorbitol was added and was higher than  $0.03 \text{ h}^{-1}$ , due to the existence of sorbitol as co-substrate (Table 4.8). Specific sorbitol utilization rate increased each time after sorbitol addition and then decreased with the process time owing to the increase in cell concentration. Specific methanol utilization rate, on the other hand, remained almost constant at all times.

**Table 4.8** Variations in specific rates throughout the fermentation

<b>t</b> h	<b><math>\mu_t</math></b> $\text{h}^{-1}$	<b><math>q_s</math></b> $\text{g g}^{-1} \text{h}^{-1}$	<b><math>q_M</math></b> $\text{g g}^{-1} \text{h}^{-1}$	<b><math>q_{rp} \cdot 1000</math></b> $\text{g g}^{-1} \text{h}^{-1}$	<b><math>q_o</math></b> $\text{g g}^{-1} \text{h}^{-1}$
0	0.052	0.205	0.070	0.041	0.169
3	0.048	0.137	0.069	0.194	0.225
6	0.044	0.115	0.065	0.538	0.160
9	0.036	0.100	0.062		0.169
12	0.030	0.094	0.064	0.435	0.181
15	0.056	0.104	0.070		0.109
18	0.045	0.089	0.065	0.194	0.089
21	0.024	0.081	0.065		0.073
24	0.013	0.103	0.068	0.072	0.075
27	0.009	0.057	0.072		0.065
30	0.008	0.022	0.077	0.025	0.046
33	0.024	0.117	0.087	0.031	0.036
36	0.027	0.095	0.087		0.032
39	0.012	0.064	0.089	-0.155	0.022
42	0.006	0.028	0.094	-0.149	0.012
45	0.000	0.030	0.104	-0.152	0.020

#### 4.3.4.2 rhGH Production, AOX Activity and Protease Activity Profile

As seen from Figure 4.18 rhGH concentration increased until  $t=39$  h of the process at which the highest concentration of rhGH was achieved as  $C_{rhGH}=0.29 \text{ g L}^{-1}$   $t=39$  h. After that, the concentration started to decrease to  $C_{rhGH}=0.22 \text{ g L}^{-1}$  which is even below the value reached at  $t=18$  h.

In comparison of the highest value of rhGH reached with the findings of Acik, (2009) it was seen that the highest value of rhGH reached in this experiment at  $t=39$  h with three times pulse sorbitol feeding at  $t=0, 14$  and  $31$ h was lower than the rhGH concentration found at  $t=30$  h with twice sorbitol feeding (Acik, 2009) at  $t=0$  and  $9$  h of the process (MSS) and almost equal to the value obtained with single sorbitol feeding (Acik, 2009) at the beginning of the process (MS) (Figure 4.19).

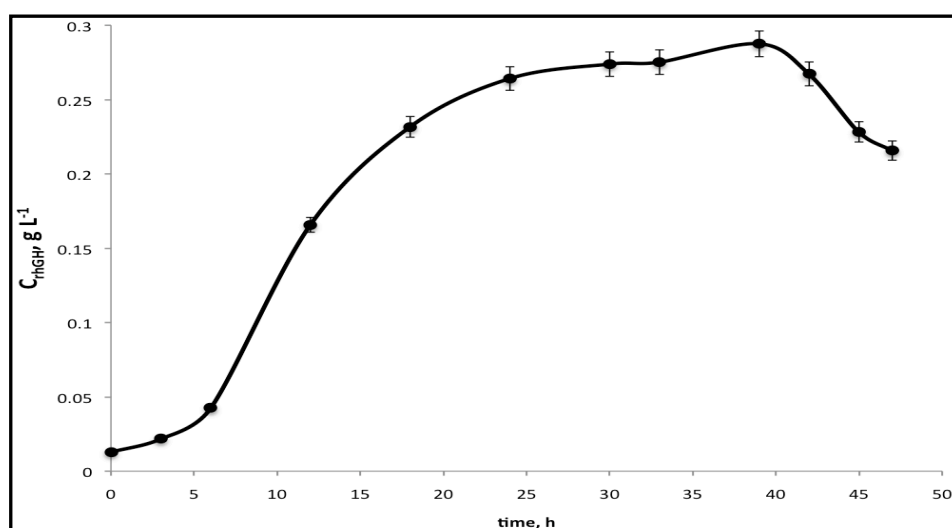


**Figure 4.18** Variation in rhGH concentration with fermentation time

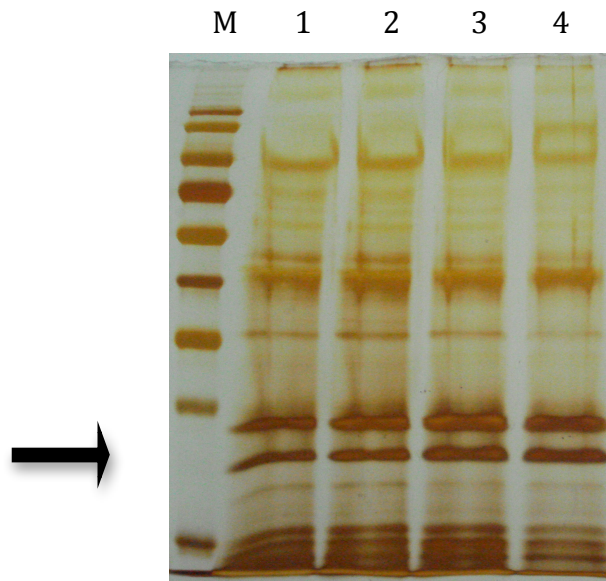


**Figure 4.19** Silver stained SDS-PAGE gel view of extracellular proteins for different feeding strategies. Lane M: protein marker; Lane1: Pure MeOH t=24h; Lane2:MS t=24h; Lane3: MSS t=30h; Lane 4: MSSS t=39h

When the AOX activity and protease concentration profiles are considered (Figure 4.20), the reasons for the decrease in product concentration become clear. Towards the end of the bioprocess, the AOX activity decreases to almost zero, and protease concentration continues to increase throughout the process with even higher rate between t=39-48 h. The final total protease concentration reached at the end of this process, is twice the concentration observed in Acik's study (2009) with single sorbitol feeding.

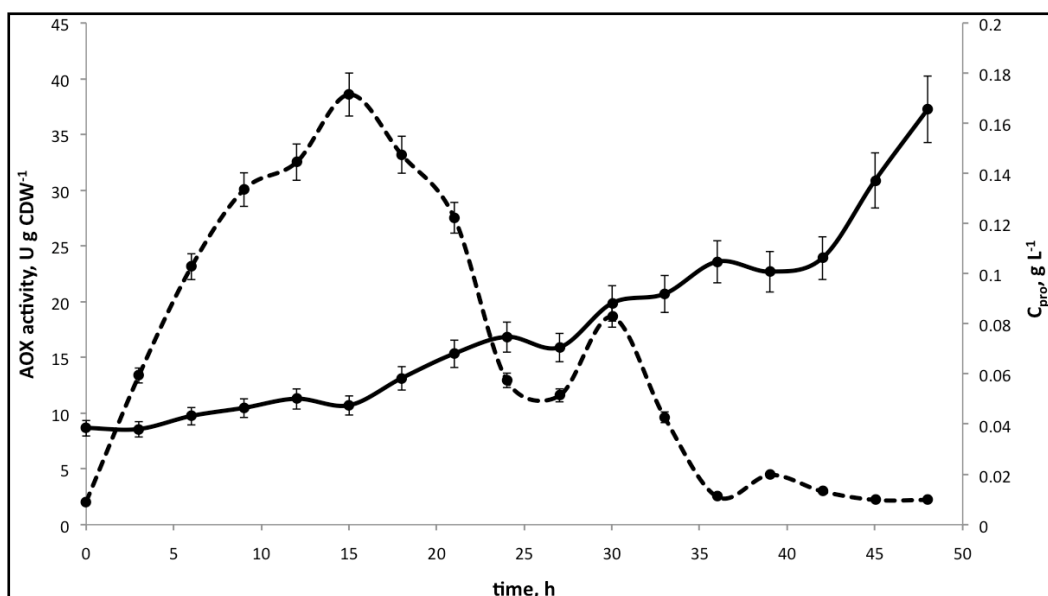


**Figure 4.20** Variation in protease concentration (straight lines) and AOX activity (dashed lines) with cultivation time

#### 4.3.5.3 Organic acid concentration

Similar to the findings of previous rhGH production experiments by *P.pastoris* formic, fumaric, glutaric, citric, and succinic acids were organic acids detected in the medium; whereas, formaldehyde was not detected in the medium throughout the process. It is observed that amount of organic acids in the fermentation broth increased with the increase in cultivation time. Fumaric acid concentrations were relatively low in comparison with other organic acids seen in the media (Table 4.9).

**Table 4.9** Organic acid concentrations throughout the process

time, h	Formic A.	Fumaric A.	Citric A.	Succinic A.	$\alpha$ -keto glutaric A.
0	0.0680	0.0004	0.0077	0.0445	0.0632
3	0.1100	0.0005	0.0077	0.0474	0.0632
6	0.1161	0.0003	0.0077	0.0339	0.0609
9	0.1207	0.0003	0.0077	0.0422	0.0568
12	0.1352	0.0004	0.0084	0.0504	0.0565
15	0.1784	0.0005	0.0115	0.0547	0.0769
18	0.1481	0.0004	0.0133	0.0477	0.0741
21	0.2059	0.0007	0.0157	0.0613	0.0981
24	0.2127	0.0012	0.0215	0.0754	0.0843
27	0.1286	0.0012	0.0223	0.0686	0.1254
30	0.3067	0.0017	0.0314	0.1254	0.1600
33	0.1811	0.0016	0.0233	0.0650	0.0935
36	0.3080	0.0016	0.0387	0.1081	0.1822
39	0.2876	0.0022	0.0459	0.1164	0.1923
42	0.3400	0.0021	0.0431	0.1253	0.1814
45	0.5318	0.0034	0.0675	0.1873	0.2463
48	0.4135	0.0026	0.0606	0.1801	0.2049

#### 4.3.5.4 Oxygen Transfer Characteristics

Oxygen transfer parameters  $K_{La}$ , OUR, OTR, maximum possible oxygen transfer rate  $OTR_{max}$ , oxygen demand OD,  $K_{La0}$  and  $\eta$ , Da and Ewere calculated throughout the fermentations and are given in Table 4.10. Throughout the process as oxygen concentration was kept at 20%, OUR was expected to be equal to OTR throughout the bioprocesses. From table it can be seen that this condition was mostly established through the process.

$K_{La}$  values first started to increase and then decrease mostly in relation with the increased concentration of cells and metabolites in the medium. As mentioned earlier, as the cells grow, they secrete metabolites and proteins to the extracellular medium, which results in a resistance zone for mass transfer, by limiting the contact area of the gas bubbles with the cells.

**Table 4.10** Oxygen transfer characteristics of the process

<b>t</b>	<b>K<sub>La</sub></b>	<b>E</b>	<b>OTR<sub>x</sub>10<sup>3</sup></b>	<b>OTR<sub>max</sub>X 10<sup>3</sup></b>	<b>OUR<sub>x</sub> 10<sup>3</sup></b>	<b>OD x10<sup>3</sup></b>	<b>Da</b>	<b>η</b>
(h)	(s <sup>-1</sup> )	K <sub>La</sub> /K <sub>La0</sub>	(mol m <sup>-3</sup> s <sup>-1</sup> )	(mol m <sup>-3</sup> s <sup>-1</sup> )	(mol m <sup>-3</sup> s <sup>-1</sup> )	(molm <sup>-3</sup> s <sup>-1</sup> )		
0	0.087	7.92	37.0	45.7	33.5	90.1	2.0	0.37
3	0.126	11.45	52.0	66.1	49.6	146.0	2.2	0.34
6	0.101	9.22	42.8	53.2	41.2	132.4	2.5	0.31
9	0.122	11.10	51.6	64.1	49.7	195.7	3.1	0.25
12	0.134	12.15	57.6	70.1	56.7	265.0	3.8	0.21
15	0.101	9.14	34.8	43.9	33.9	84.2	1.9	0.40
18	0.088	8.04	34.0	46.4	32.4	100.2	2.2	0.32
21	0.088	7.96	32.2	46.0	29.2	169.8	3.7	0.17
27	0.082	7.44	31.7	43.0	28.2	156.2	10.6	0.17
30	0.058	5.29	23.2	30.5	20.6	119.1	11.4	0.16
33	0.048	4.34	19.0	25.1	15.7	92.7	3.7	0.17
36	0.049	4.49	16.7	26.0	15.1	79.6	3.1	0.19
39	0.041	3.76	12.8	21.7	10.9	128.8	5.9	0.08
42	0.041	3.74	14.1	21.6	6.1	140.8	6.5	0.04
48	0.047	4.26	16.7	24.6	10.3			

OUR that has a positive effect on K<sub>La</sub> and depends mostly on the substrate consumption. The highest OUR value achieved at t=12 h was 56.7 mmol m<sup>-3</sup>s<sup>-1</sup>. OTR, was increased to an extent depending on the OUR.

At t=0-21 h, Da is slightly higher than 1.0, indicating that both the mass transfer and biochemical reaction resistances were effective; however, when rhGH concentration was sharply increased, oxygen demand cannot be satisfied by the oxygen transfer rate leading to higher Da values. The effectiveness factor, η, were lower than 0.4 for all the conditions, showing all four processes are oxygen transfer limited; i.e. cells were consuming lower oxygen than the oxygen demand (OD).

OD and Da are the theoretical values achieved without any resistance. Again as high cell density was achieved with the lower specific growth rates; thus, oxygen uptake rate (OUR) can not reach to OD and as  $OTR_{max}$  changes proportional with  $K_{La}$ , Da values  $\ll 1.0$ , are not expected. Therefore OD and Da values do not show that there is an oxygen limitation for the real system.

#### 4.4 Determination of peptides having affinity and selectivity towards hGH

##### 4.4.1 Experimental determination of hGH specific peptides: Phage Display

36 phage clones that show selectivity and affinity towards hGH were selected by phage display method following the procedure explained in Section 2.4.5. Equal concentrations,  $10^{11}$  pfu/ml, of each selected phage clone were incubated in hGH or BSA coated ELISA plates and ELISA assay was conducted. The absorbances are given in Figure 4.21.

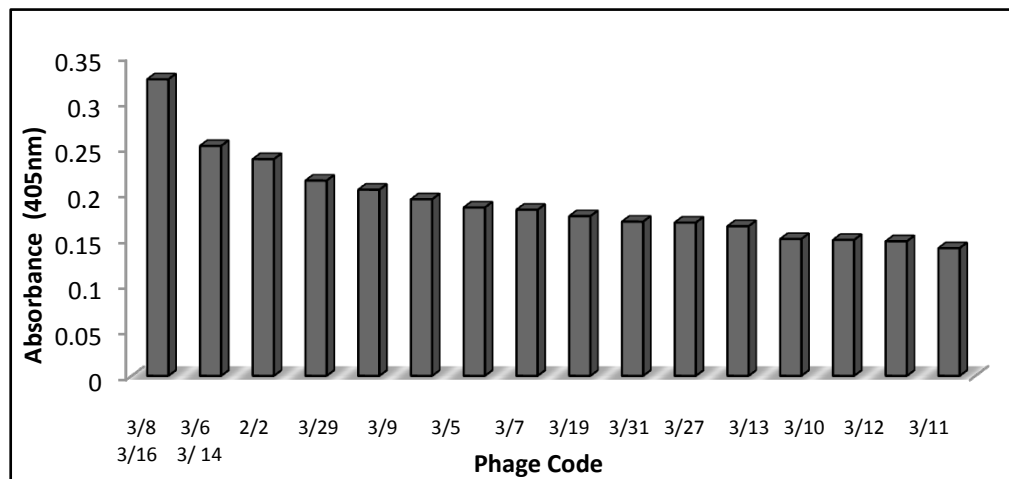


**Figure 4.21** Phage clones that bind to hGH in ELISA

As a result of the sequencing analyses; some of the phages showed the same peptide sequence, while mostly different sequences were obtained (Table 4.11). Which may indicate that each peptide interacts with a different region of hGH. The results of the sequencing analysis are given in Table 4.11. The additional information on the properties of these selected peptides is given in Appendix E.

**Table 4.11** Amino acid sequences of peptides that show affinity to hGH in phage-ELISA

Peptide Code	DNA Code	Amino Acid Sequence
3/8	AAGCAGACUCUCCGUCGGCG	KQTLPSA
3/6	ACUAUGUAUCUUACGUUUGAG	TMYLTFE
2/2-3/9	AGUUAUCCUCCGUUUACUUCU	SYPPFTS
3/5-3/11-3/27	CAUGCUAUUUAUCCGCGUCAU	HAIYPRH
3/7	GCGCGGACUGAGUUUUUUGUU	ARTEFFV
3/13	CUGCCGUUGACUCCGCUUCCG	LPLTPLP
3/10	UAUCUUACGAUGCCGACGCCU	YLTMPTP
3/19	AAGGUUUGGUUGUUGUCGACG	KVWLLST
3/29	UCGACGACUAAGUUGGCUUUG	STTKLAL
3/12-3/14-3/16	CAUUUUCAGACUCAUCCUACA	HFQTHPT

In addition to the peptides selected by phage display, Prof. Dr. Burak Erman's research group (Koç University) designed five peptides computationally. The amino acid sequences of the computationally designed peptides are given in Table 4.12 and additional information on properties of these peptides are given in Appendix E.

**Table 4.12** Amino acid sequences of computationally designed peptides

<b>Peptide Code</b>	<b>Amino Acid Sequence</b>
P-1	FSEEVFW
P-2	FEEEVFW
P-3	ESEEVFW
P-4	FEPHVFW
P-5	FSEEPFW

In another study, one sequence, selected by *in-vivo* phage display targeting insulin, was also shown to have an affinity towards hGH (Chen et al., 2006). Therefore, in addition to the peptide sequences listed in Tables 4.11 and 4.12, this literature peptide and two other peptides designed by Prof. Dr. Burak Erman's research group by modifying literature peptide were also used in this study (Table 4.13).

**Table 4.13** Amino acid sequences of literature and modified peptides

<b>Peptide Code</b>	<b>Amino Acid Sequence</b>
L	CSSSPSKHC
M-1	CSSKAAAHL
M-2	CSSAAAKHL

As mentioned earlier, for investigation of hGH-peptide interaction, isothermal titration calorimetry and surface plasmon resonance were used as they both have advantages and disadvantages as discussed. While for some peptides ITC was preferred, for some others considering the lower hGH-peptide concentration for the analysis SPR was used. Moreover, Prof. Dr. Burak Erman's research group estimated the binding energies ( $\Delta G$ ) for the selected peptides. The experiments conducted with the selected peptides and their estimated binding energies are listed in Table 4.14.

**Table 4.14** Experiments conducted by ITC and SPR and their computationally estimated ( $\Delta G$ ) values

Peptide Code	SPR	ITC	$\Delta G$ (kcal mol <sup>-1</sup> )
P-1	+	+	-8.55
P-2	+	+	-8.05
P-3	-	+	-7.99
P-4	-	+	-7.93
P-5	-	+	-7.07
L	-	+	-6.59
M-1'	-	-	-8.56
M-2'	-	-	-
3/8	+	+	-7.26
3/6	-	+	-7.06
2/2-3/9	+	+	-7.85
3/5-3/11-3/27	-	+	-7.19
3/7	-	+	-3.34
3/13*	-	-	-
3/10*	-	-	-
3/19	+	+	-6.76
3/29	-	+	-
3/12-3/14-3/16	-	+	-

Peptides with (-) both for SPR and ITC did not dissolve in buffers tried.

\*Due to their very high hydrophobicity peptides 3/10 and 3/13 were not used in experiments

#### 4.4.2 Isothermal Titration Calorimetry Studies

The results of the ITC studies are given in Appendix F. All the experiments were performed at T=30°C aiming to mimic the tertiary structure and stability of the rhGH produced by *P.pastoris* using standard hGH solution. Among all sets of experiments conducted with various peptides at different pH values, in different buffers of various molarity, the peptide that was given in previous literature study (Chen et al., 2006) was shown to have a low strength binding affinity towards hGH at pH=9, in 30mM Tris buffer (Figure 4.24). The reason for choosing pH=9 as the operation pH was due to the result of previous experiment conducted at same concentrations, but different pH of pH=7.0. Although at pH=7, no

binding profile was observed, at the end of the experiments the final solution was in suspension form. Therefore, the result was thought such that the aggregate formation might be an indication of interaction, for which the binding energy could not be calculated by ITC due to non-homogeneity. As a solution to this problem pH of the final solution was changed (lowered and increased) until no aggregate formation was observed, at pH=8.5-9 the particles started to dissolve. So, further experiment was conducted at pH=9.

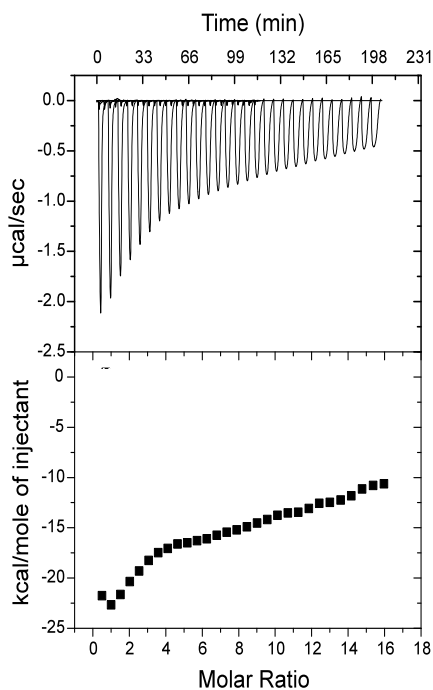


**Figure 4.22** ITC diagram for titration of  $15\mu\text{M}$  hGH with  $1.07\text{ mM}$  L. peptide

For this binding profile the peptide dilution and macromolecule dilution experiments were performed (Figure 4.23 a and b).

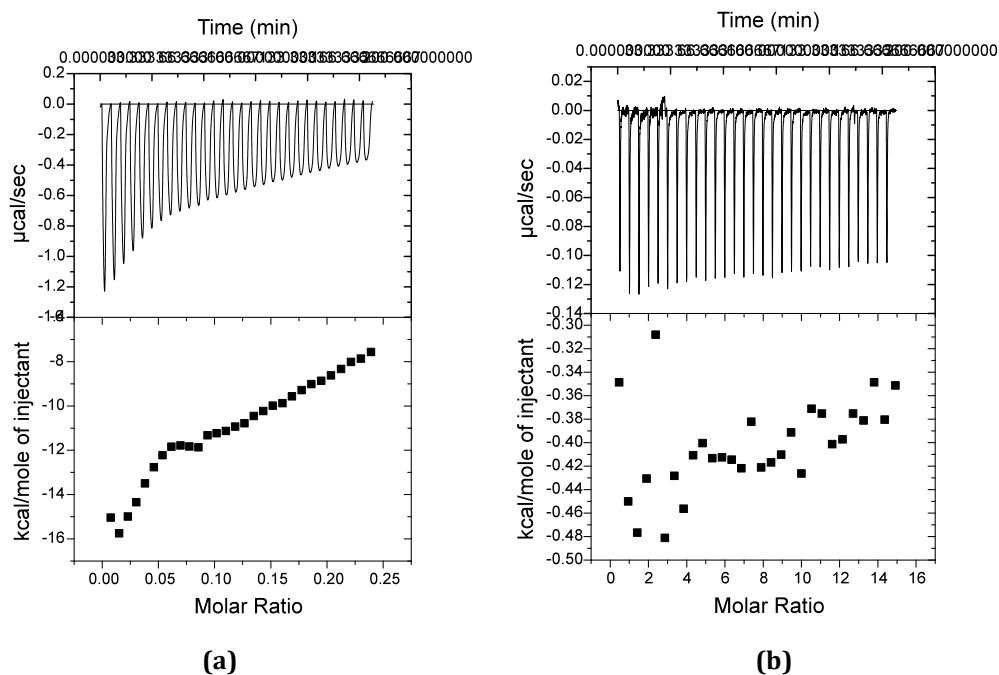


**Figure 4.23** Dilution experiments for literature peptide; (a) 1.07mM peptide titrated onto buffer; (b) buffer titrated onto 15 $\mu\text{M}$  hGH

The subtraction of peptide dilution experiment (Figure 5.23 a) from actual titration experiment (Figure 4.22) results in the energy profile that arose only from hGH-peptide interaction. Therefore, assuming 1-site binding and using Origin 7.5 software data fitting was conducted and given in Figure 4.24.

According to this fitting profile, the binding energies calculated by the program are found as number of binding sites  $n=0.967$ ,  $K_a=1.21 \cdot 10^3 \text{ M}^{-1}$ ,  $\Delta H=-3.88 \cdot 10^5 \text{ cal/mol}$ ,  $\Delta S=-1.27 \cdot 10^3 \text{ cal/mol.K}$ . The  $\Delta G$  term can be calculated from (2.32) and the negative sign of  $\Delta G$  indicates that the binding is spontaneous. The negative sign of  $\Delta H$ , which is the resultant energy of all formation/breaking of bonds during interaction, points out that the binding reaction is favored by the enthalpy.

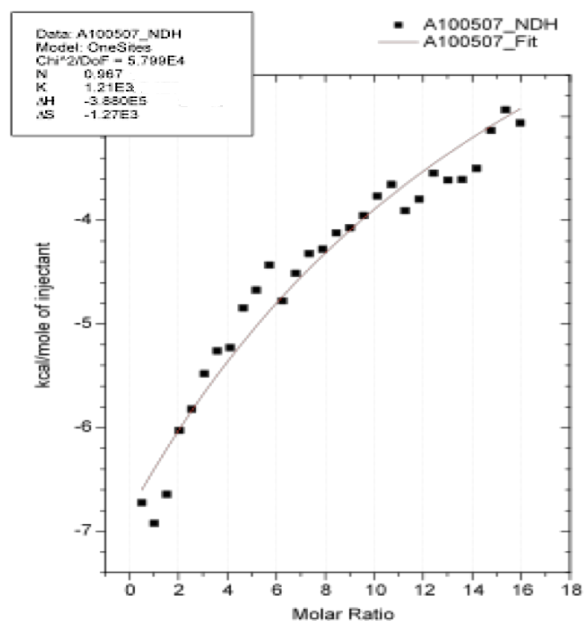


**Figure 4.24** Data fitting for hGH-peptide binding at pH=9.0

The negative sign of the entropy on the other hand shows that entropy does not favor binding. Therefore it can be said that the interaction is enthalpically driven. By looking at  $K_a$  value, the binding is shown to be a result of low strength affinity, which is affected by pH of the medium.

#### 4.4.3 Surface Plasmon Resonance Studies

Due to the lower amount and lower concentration of sample requirement, surface plasmon resonance was employed as an alternative to ITC. As this process is a rather a time-consuming process and requires higher amount of substrate in comparison to ITC, prior to the experiments ELISA results (Figure 4.21) and HPLC results (Appendix G) were taken into account for the selection of peptide that was to be used in SPR studies. From ELISA results, the highest affinity showing phage's peptide sequence 3/8 & 2/2-3/9 and from HPLC results 3/19 peptides were selected for SPR.

Moreover, the designed peptides P-1 and P-2 were selected for SPR analysis prior to ITC analysis of the designed peptide set.

The SPR analysis was performed as described in Section 3.5.1 after SAM was formed on the sensor surface the surface preparation steps before binding gave similar trends for all experimental runs (Figure 4.25).

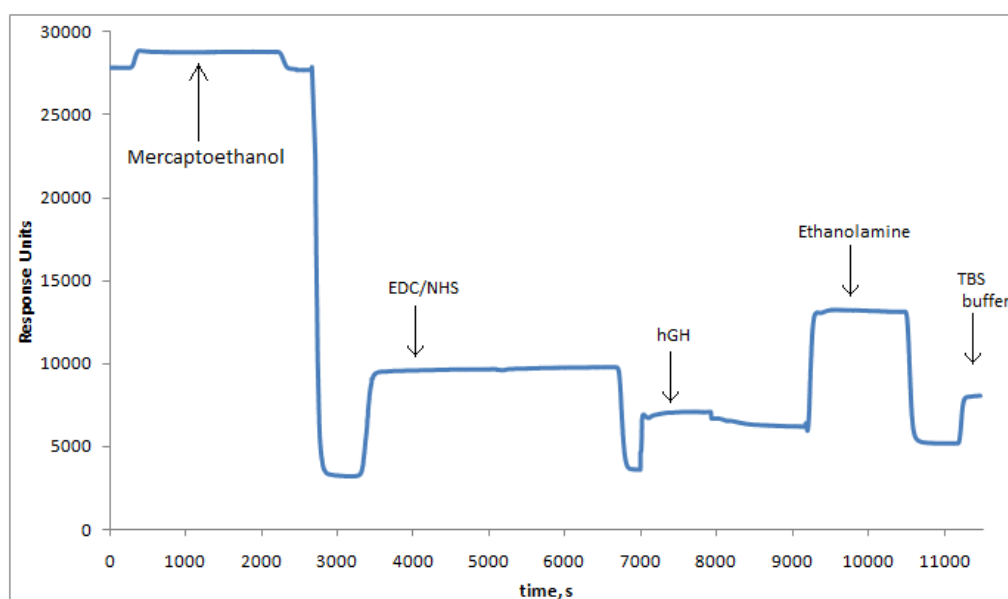


**Figure 4.25** SPR sensogram showing steps involved prior to peptide binding

In preliminary studies for determination binding interaction between hGH and P-1, P-2; it was observed that both peptides bind to the control surface (surface without hGH) with similar affinity profile to the actual experiment (Appendix H). Therefore, considering the probability that the peptides show affinity towards ethanolamine further interaction analyses of those peptide set was performed with ITC.

Moreover, experiments with peptides 3/8 and 22/39 gave similar results such that the binding and control profiles showed similar profiles (Appendix H). Therefore glycine or BSA were tried using peptide 2/2-3/9 as

alternative molecules to cover the hGH unbound surface. The results revealed that, while glycine had no use for understanding the peptide-hGH interaction, the peptide showed less affinity towards BSA than it showed to hGH (Appendix H). Therefore in further studies with peptides that show affinity towards ethanolamine, BSA can be tried for the first instance.

As 3/19 was shown to have an affinity towards hGH in preliminary HPLC studies, this peptide was also used in SPR analyses. The control experiments did not show affinity toward ethanolamine but bound to hGH. Therefore, the results of the binding analysis at different concentrations of 0.05, 0.075, 0.100, 0.135 and 0.250 are plotted in Figure 4.26.

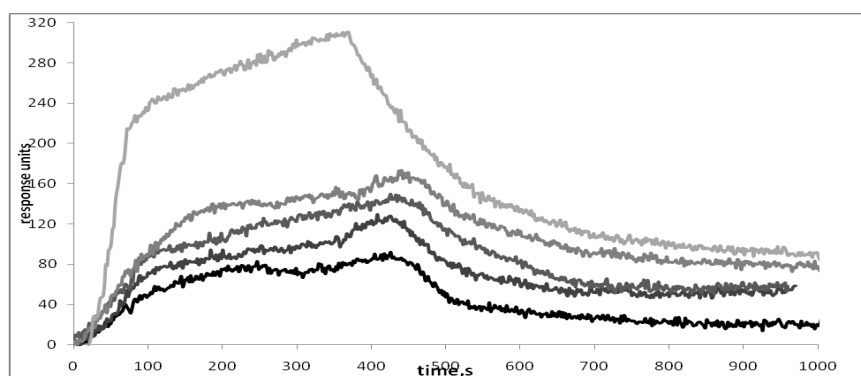


**Figure 4.26** SPR sensogram for peptide 3/19 at different peptide concentrations in increasing order of  $C_p = 0.05, 0.075, 0.100, 0.135$  and  $0.250 \text{ mg mL}^{-1}$

In order to calculate the affinity constant  $K_a$  and  $K_d$ , 1:1 interaction was assumed and simple Langmuir interaction model (Eqn. 2.28) was fit to adsorption part of each of the profiles and the  $k_{\text{obs}}$  values were obtained and plotted with respect to ligand concentration in Figure 4.27. Using Eqn. (2.26) the linear fit to this plot resulted in  $K_a = 9.6 \times 10^3 \text{ M}^{-1}$ , i.e.  $K_D \sim 10^{-4} \text{ M}$ , was

calculated, which is higher than that calculated for the literature peptide with ITC.

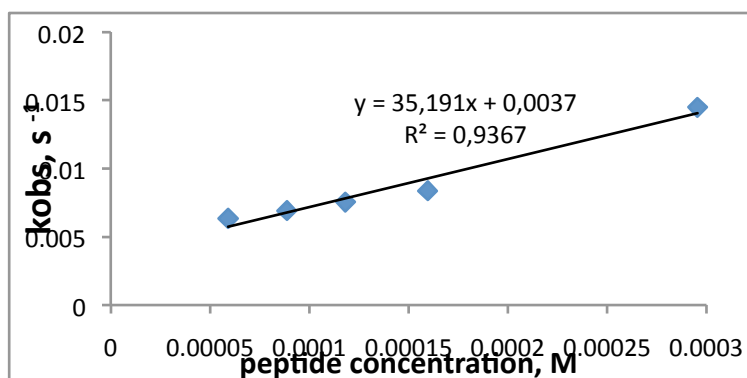


**Figure 4.27**  $k_{obs}$  vs peptide 3/19 concentrations

In addition to these, in order to check for the strength of interaction of standard hGH and antibody was analyzed. For that purpose, ITC experiment was performed by titration of hGH onto hGH monoclonal antibody (mouse). The data fitting showed binding strength of  $K_D \sim 5 \cdot 10^{-8}$  M, with an exothermic interaction.

## CHAPTER 5

### CONCLUSION

In this study, it was aimed to investigate the operation conditions that lead to higher recombinant human growth hormone, rhGH production by *Pichia pastoris* and to select the peptide ligands that show affinity and selectivity towards hGH, and to determine the interaction strength and specificity of rhGH with the selected peptides.

In the first part of the study, the influence of temperature (T=25, 27, 30 and 32°C) and Tween-20/80 addition at various concentrations were investigated in air filtered shake bioreactor experiments. Moreover, except two sets, in which the effect of Tween-20 on production alone was investigated, 30g L<sup>-1</sup> sorbitol was added batchwise at the beginning of production stage. As a result of this study it was observed that at lower temperatures both the growth rate and production decreases. Therefore considering hGH production and cell growth and the higher energy requirement to keep temperature constant throughout the processes, lower oxygen solubility at higher temperatures and possible negative effects of higher temperature on protein stability 30°C is the best condition. Moreover, Tween-20/80 cannot be employed as an alternative to co-substrate sorbitol.

In the second part, bioreactor experiments were performed to investigate the effect of pre-determined exponential methanol-feeding rates  $\mu=0.02, 0.03$  and  $0.04 \text{ h}^{-1}$ , which mainly depends upon the aimed specific cell growth rate, on rhGH production in pilot scale bioreactor.

- Among three cases of different methanol feeding rates (MS-0.02, MS-0.03 and MS-0.04) the highest rhGH production was obtained at MS-0.03 condition as 270 mg L<sup>-1</sup>, which is 2.1- and 1.6- fold higher than MS-0.02 and MS-0.04 cases, respectively.

- For MS-0.03 condition biochemical reactions are directed to product formation rather than cell generation as  $Y_{P/X}$  and  $Y_{P/S}$  was the highest for this condition.

- Despite the fact that rhGH concentration was the highest for MS-0.04 condition until t=15 h, after that time a sharp increase reaching higher rhGH concentrations were observed for MS-0.03 condition. Considering rhGH concentration profile, feeding strategy can be further improved by first employing MS-0.04 feeding rate and starting from t=15 h shifting to MS-0.03 feeding strategy. Also this improvement can be useful in improvement of AOX activity.

In the additional study to Bayraktar's work (2009), pH=5.5 was selected as the experimental condition, the mid-point between pH=5.0 in which the highest rhGH concentration was achieved, and pH=6.0 in which the lowest rhGH and the highest cell concentrations were obtained, to understand after which pH metabolic pathways prefer cell growth rather than production.

- pH=5.5 showed similar process characteristics to pH=5.0 condition rather than pH=6.0.

- Although slightly lower AOX profile compared to pH=4.2 case was seen, at pH=5.5 higher product concentrations were achieved probably due to the existence of higher concentration of proteases at pH=4.2.

- For achieving desired product formation and cell growth rates with lower protease concentration; achieving higher yields for the production of rhGH by *P.pastoris* the medium pH should be kept strictly between 5.0 and 5.5.

In addition to Aık's (2009) study, batch sorbitol addition to the medium was repeated three times at t=0 h, at t=14 h right before sorbitol depletion and at t=31 h right after sorbitol was totally depleted, to observe the effect of sorbitol majorly on cell growth and rhGH production profiles.

- The addition of batch sorbitol to the medium for the second/third time, enhanced cell growth and hence increased the duration of production period. AOX activity showed significant increase each time after sorbitol addition. However, as the process time increased, the protease concentration in the extracellular media increased and AOX activity decreased. Therefore, increasing the production period after a certain point (~30h) has no use in achieving higher product concentrations with higher yields. There sorbitol could be added twice to the medium at the beginning of the production phase and when the highest AOX activity was observed.

In the third part of this study, the peptide ligands that show affinity towards hGH were selected from phage display peptide library, computationally designed peptides and one other peptide obtained from the study of Chen et al., (2006). The strength and thermodynamic characteristics of peptide-hGH interaction were investigated by surface plasmon resonance and isothermal titration calorimetry.

- Among the peptides investigated by ITC, the peptide sequence CSSSPSKHC, obtained from literature (Chen, 2006), was shown to have a low binding affinity towards hGH with  $K_a = 1.21 \cdot 10^3 \text{ M}^{-1}$  at pH=9, while at pH=7, no binding was observed at the same concentrations. Therefore, in further studies the effect of pH on hGH-Literature peptide should be investigated.

- In SPR studies, the peptide, KVVLLST, selected by phage display showed binding profile at different peptide concentrations upto 0.25mg mL<sup>-1</sup> above which undissolved particles were observed in the solution. To the profiles obtained, single-site binding was assumed and fitting resulted in  $K_d = 1 \cdot 10^{-4} \text{ M}$ . However, due to low solubility of the peptide, no results were

obtained from ITC studies. Therefore, the peptide sequence can be further modified to increase hydrophilicity without loss of affinity and ITC studies with higher peptide concentration should be conducted to gain deeper insight in thermodynamics of binding.

## REFERENCES

- Abdel-Meguid S.S., Shieh H.S., Smith W.W., Dayringer H.E., Violand B.N., Bentle L.A., 1987. Three-dimensional structure of a genetically engineered variant of porcine growth hormone. *Proceedings of National Academy of Sciences USA*. 84:6434–6437.
- Abraham T., Lewis R.N., Hodges R.S., and McElhaney R.N., 2005. Isothermal titration calorimetry studies of the binding of the antimicrobial peptide gramicidin S to phospholipid bilayer membranes. *Biochemistry* 44: 11279-11285.
- Açık E., 2009. Effects of carbon sources and feeding strategies on recombinant human growth hormone production by metabolically engineered *Pichia pastoris*, Thesis of Master of Science of Middle East Technical University, Ankara
- Aitken S.M., Turnbull J.L., Percival M.D., and English A. M., 2001. Thermodynamic analysis of the binding of aromatic hydroxamic acid analogues to ferric horseradish peroxidase. *Biochemistry* 40, 13980-13989.
- Alam S. M., Treavers P.J., Wung J.L., Nasholds W., Redpath S., 1996. T-cell receptor affinity and thymocyte positive selection. *Nature* 381: 616-620
- Alam S.M , Morimoto M., Yoshizato H., Fyjikawa T., Furukawa K., Tanaka M., Nakashma K., 1998. Expression and purification of a mutant human growth hormone that is resistant to proteolytic cleavage by thrombin, plasmin and human plasma in vitro. *Journal of Biotechnology*. 65:183-190.
- Anderka O., Boyken J., Aschenbach U., Batzer A., Boscheinen O., Schmoll D., 2008. Biophysical characterization of the interaction between hepatic glucokinase and its regulatory protein impact of physiological and pharmacological effectors. *Journal of Biological Chemistry* 283: 31333–31340.
- Andujar-Sanchez M., Jara-Perez V., Camara-Artigas A., 2007. Thermodynamic determination of the binding constants of angiotensin-converting enzyme inhibitors by a displacement method. *FEBS Letters* 581:3449–3454.
- Apte-Deshpande A., Rewanwar S., Kotwal P., Raiker V.A., Padmanabhan S., 2009. Efficient expression and secretion of recombinant human growth hormone in the methylotropic yeast *Pichia pastoris*: potential applications for other proteins. *Biotechnology Applied Biochemistry*. 54:197-205.
- Arouri A., Garidel P., Kliche W., Blume A., 2007. Hydrophobic interactions are the driving force for the binding of peptide mimotopes and Staphylococcal

protein A to recombinant human IgG1. *European Biophysics Journal* 36:647-660.

Banerjee T., Kishore N., 2006. Binding of 8-anilinonaphthalene sulfonate to dimeric and tetrameric concanavalin A: energetics and its implications on saccharide binding studied by isothermal titration calorimetry and spectroscopy. *J Phys Chem B Condens Matter Mater Surf Interfaces Biophys* 110, 7022-7028.

Bayraktar E., 2009. Effects of pH on human growth hormone production by *Pichia pastoris* considering the expression levels of regulatory genes, Thesis of Master of Science of Middle East Technical University, Ankara

Battersby J.E., Mukku V.R., Clark R, Hancock W.S., 1995. Affinity purification and micro characterization of recombinant DNA derived human growth hormone isolated from an in vivo model. *Analytical Chemistry*. 67:447-455.

Baulieu E., Kelly P. A., 1990. "HORMONES from molecules to disease", 1<sup>st</sup> Ed. Hermann Press, France

Bertini I., Calderone V., Fragai M., Giachetti A., 2007. Exploring the subtleties of drug-receptor interactions: The case of matrix metalloproteinases. *Journal of the American Chemical Society* 129: 2466–2475.

Bewley T.A., Brovetto-Cruz J., Li C.H., 1969. Human Pituitary Growth Hormone. *Physicochemical Investigations of the Native and Reduced-Alkylated Protein*. *Biochemistry*. 8(12): 4701-4708

Bewley T.A., Li C.H., 1972. Circular dichroism studies on human pituitary growth hormone and ovine pituitary lactogenic hormone. *Biochemistry*. 11(5):884-888.

Binkley S. A., 1994. *Endocrinology*. 1<sup>st</sup> Ed. Harper Collins College Publishers, New York.

Boltovets P.M., Snopok B.A., Boyko V.R., Shevchenko T.P., Dyachenko N.S., Shirshov Y.M., 2004. Detection of plant viruses using surface plasmon resonance via complexing with specific antibodies. *Journal of Virology Methods* 121:101-106

Bondeson K., Frostell-Karlsson A., Fägerstam L., Magnussin G., 1993. Lactose repressor operator-DNA interactions: kinetic analysis by surface plasmon resonance biosensor. *Analytical Biochemistry*. 214:245-251

Boniface J.J., and Davis M.M., 1994. The kinetics of binding of peptide/MHC complexes to T-cell receptors: application of surface plasmon resonance to a low affinity measurement. *Methods in Enzymology* 6:168-176

Braden B.C., Poljak R.J. 1995. Structural features of the reactions between antibodies and protein antigens. *Journal of the Federation of American*

Societies for Experimental Biology 9: 9-16.

Bratkovič T., 2010. Progress in phage display: evolution of the technique and its application. Cellular and Molecular Life Sciences. 67: 749-767.

Buczek P., Horvath M.P., 2006. Structural reorganization and the cooperative binding of single-stranded telomere DNA in *Sterkiella nova*. Journal of Biological Chemistry 281: 40124-40134.

Chatterjee A., Moulik S.P., Majhi P.R., Sanyal S.K., 2002. Studies on surfactant-biopolymer interaction. I. Microcalorimetric investigation on the interaction of cetyltrimethylammonium bromide (CTAB) and sodium dodecylsulfate (SDS) with gelatin (Gn), lysozyme (Lz) and deoxyribonucleic acid (DNA). Biophysical Chemistry 98:313-327.

Cooper A., McAlpine A., Stockley P. G., 1994. Calorimetric studies of the energetics of protein-DNA interactions in the *E. coli* methionine repressor (MetJ) system. FEBS Letters 348: 41-45.

Cao Z., Suljak S.W., Tan W., 2005. Molecular beacon aptamers for protein monitoring in real-time and in homogeneous solutions. Current Proteomics. 2: 31-40.

Catzel D., Lavlevski H., Marquis C.P., Gray P.P., Van Dyk D., Mahler S.M., 2003. Purification of recombinant human growth hormone from CHO cell culture supernatant by Gradiflow preparative electrophoresis technology. Protein Expression and Purification 32:126-134.

Cereghino G.P.L. and Cregg J., 1999. Applications of yeast in biotechnology: protein production and genetic analysis. Current Opinion in Biotechnology. 10:422-427

Cereghino J.L., Cregg J.M., 2000. Heterologous protein expression in the methylotrophic yeast *P.pastoris*. FEMS Microbiology Reviews. 24:45-66.

Cereghino G.P.L., Cereghino J.L., Ilgen C., and Cregg J.M., 2002. Production of recombinant proteins in fermenter cultures of the yeast *Pichia pastoris*. Current Opinion in Biotechnology. 13:329-332.

Chen Y., Shen Y., Guo X., Zhang C., Yang W., Ma M., Liu S., Zhang M., Wen L-P., 2006. Transdermal protein delivery by coadministered peptide identified via phage display. Nature Biotechnology Letters. 24 (4): 455-460.

Chen L., Wang Q., Hou W., 2009., The utilization of BSA-modified chip on the investigation of ligand/protein interaction with surface plasma resonance. Africal Journal of Biotechnology. 8(24):7148-7155

Clackson T., Wells J.A., 1994. In vitro selection from protein and peptide libraries. Trends in Biotechnology. 12: 173-184.

Clackson T., Ultsch M.H., Wells J.A., de Vos A.M., 1998. Structural and

Functional analysis of the 1:1 Growth hormone: Receptor complex reveals the molecular basis for Receptor affinity. *Journal of Molecular Biology*. 277: 1111-1128

Clonis Y.D., Lowe C.R., 1981. Affinity chromatography on immobilized triazine dyes. Studies on the interaction with multinucleotide-dependent enzymes. *Biochimica et Biophysica Acta* 659: 86–98.

Clonis Y.D., Stead V., Lowe C.R., 1987. Novel cationic triazine dyes for protein purification. *Biotechnology Bioengineering* 30: 621–627.

Clonis, Y., 1990. Process Affinity Chromatography. Separation processes in Biotechnology. Asenjo J.A. (Ed.). 1<sup>st</sup> Ed., Marcel Dekker Inc., New York.

Cos O., Serrano A., Montesinos J.L., Ferrer P., Cregg J.M., Valero F., 2005 Combined effect of the methanol utilization (Mut) phenotype and gene dosage on recombinant protein production in *Pichia pastoris* fed-batch cultures. *Journal of Biotechnology*. 116 321-335

Cos O., Ramon R., Montesinos J.L., Valero F., 2006. Operational Strategies, monitoring and control of heterologous protein production in the methylotropic yeast *Pichia pastoris* under different promoter: A review. *Microbial Cell Factories*. 5:17-38.

Cwirla S.E., Peters E.A., Barrett R.W., Dower W.J., 1990. Peptides on phage: A vast library of peptides for identifying ligands. *Proceedings of the National Academy of Sciences*. 87: 6318-6382.

Çalık P., Çalık G., Özdamar T.H., 1998. Oxygen transfer effects in serine alkaline protease fermentation by *Bacillus licheniformis*: use of citric acid as carbon source. *Enzyme and Microbial Technology*. 23:451-461.

Çalık P., Çalık G., Özdamar T.H., 1998. Oxygen transfer strategy and its regulation effects in serine alkaline protease production by *Bacillus licheniformis*. *Biotechnology Bioengineering*. 69:301-311.

Çalık P., Özdamar T.H., 2001. Carbon sources affect metabolic capacities of *Bacillus* species for the production of industrial enzymes: theoretical analyses for serine and neutral proteases and  $\alpha$ -amylase. *Biochemical engineering*. 1:61-81.

Çalık P., Çalık G., Takaç S., Özdamar T.H., 1999. Metabolic Flux Analysis for Serine Alkaline Protease Fermentation by *Bacillus licheniformis* in a Defined Medium: Effects of the Oxygen Transfer Rate, *Biotechnology and Bioengineering*, 64:151-167.

Çalık P., Balci O., Ozdamar T.H., 2010. Human growth hormone specific aptamer identification using oligonucleotide ligand evolution method. *Protein Expression and Purification*. 69(1):21-28.

- Çelik E., Çalık P., Halloran S.M., Oliver S.G., 2007. Production of recombinant erythropoietin from *Pichia pastoris* and its structural analysis. *Journal of Applied Microbiology*. 103:2084-2094.
- Çelik E., 2008. Bioprocess development for therapeutical protein production. Ph.D. Thesis, METU, Ankara.
- Çelik E., Çalık P., Oliver S.G., 2009. Fed-batch methanol feeding strategy for recombinant protein production by *Pichia pastoris*. *Yeast* 26:474-484.
- Çelik E., Çalık P., Oliver S.G., 2010. Metabolic flux analysis for recombinant protein production by *Pichia pastoris* using dual carbon sources: Effects of methanol feeding rate. *Biotechnology and Bioengineering*. 105(2):317-329.
- Daly R., Hearn M.T.W., 2005. Expression of heterologous proteins in *Pichia pastoris*: a useful experimental tool in protein engineering and production. *Journal of Molecular Recognition*, 18: 119–138.
- Dam T.K., Brewer C. F., 2002. Thermodynamic studies of lectin-carbohydrate interactions by isothermal titration calorimetry. *Chemical Reviews* 102: 387-429.
- Dam T. K., Brewer C.F., 2004. Multivalent protein-carbohydrate interactions: isothermal titration microcalorimetry studies. *Methods in Enzymology* 379: 107-128 .
- D'Aquino J.A., Freire E., Amzel L.M., 2000. Binding of Small Organic Molecules to Macromolecular Targets: Evaluation of Conformational Entropy Changes. *PROTEINS:Structure, Function and Genetics Suppl.* 4:93-107.
- De Vos A.M., Ultsch M., Kossiakoff A. A., 1992, Human growth hormone and extracellular domain of its receptor: Crystal structure of the complex. *Science* . 255: 306-312
- Deleeuw L., Tchernatynskaia A.V., Lane A.N., 2008. Thermodynamics and specificity of the Mbp1-DNA interaction. *Biochemistry*47: 6378-6385.
- Denizli A., Salih B., Kavakli C., Piskin E., 1997. Dye-incorporated poly(EGDMA-HEMA) microspheres as specific sorbents for aluminumremoval. *Journal of Chromatography B* 698: 89–96.
- Dexheimer T.S., Stephen A.G., Fivash M.J., Fisher R.J., Pommier Y., 2010., The DNA binding and 3'-end preferential activity of human tyrosyll-DNA phosphoesterase. *Nucleic Acids Research*. 38(7): 2444-2452
- Dormitzer P.R., Ulmer J. B., Rappuoli, R., 2008. Structure-based antigen design: A strategy for next generation vaccines. *Trends in Biotechnology* 26: 659–667.
- Ecamilla-Trevino L.L., Viader-Salvado J.M., Barrera-Saldana H.A., Guerrero-Olazarán M., 2000. Biosynthesis and secretion of recombinanthuman growth

hormone in *Pichia pastoris*. *Biotechnology Letters* 22(2):109 – 114.

Edwards P.R., Gill A., Pollard-Knight D.V., Hoare M., Buckle P.E., et al, 1995. kinetics of protein-protein interactions at the surface of an optical biosensor. *231: Analytical Biochemistry* .210-217

Eftink M.R., Anusiem A.C., Biltonen R.L., 1983. Enthalpy entropy compensation and heat capacity changer for protein-ligand interactions: General thermodynamic models and data for the binding of nucleotides to ribonuclease A. *Biochemistry*. 22:3884-3896.

Ek B.A., Cistola D.P., Hamilton J.A., Kaduce T.L., Spector A. A., 1997. Fatty acid binding proteins reduce 15-lipoxygenase-induced oxygenation of linoleic acid and arachidonic acid. *Biochimica et Biophysica Acta* 1346: 75-85.

Erickson J.A., Jalaie M., Robertson D.H., Lewis R.A., Vieth M., 2004. Lessons in molecular recognition: The effects of ligand and protein flexibility on molecular docking accuracy. *Journal of Medicinal Chemistry*. 47 (1):45-55.

Evans H.M., Long J.A., 1921. The effect of the anteriorlobe administered intraperitoneally upon growth, maturity and oestrus cycles of the rat. *Anatomical Record*. 21:62-63.

Eurwilaichitr L., Roytroku R., Suprosongsin C., Manitchotpisit P., Panyim S., 2002. Glutamic acid and alanine spacer is not necessary for removal of MF $\alpha$ -1 signal sequence fused to the human growth hormone produced from *Pichia pastoris*. *World Journal of Microbiology and Biotechnology*. 18 : 493-495.

Falconer R.J., Penkova A., Jelesarov I., Collins B.M., 2010. Survey of the year 2008: application of isothermal titration calorimetry. *Journal of Molecular Recognition*. DOI:10.1002/JMR.1025

Fang Y., Tong G.C., Means G. E., 2006. Structural changes accompanying human serum albumin's binding of fatty acids are concerted. *Biochimica et Biophysica Acta* 1764: 285-291.

Fisher R.J., Fivash M.J., 1994. Surface plasmon resonance based methods for measuring the kinetics and binding affinities of biomolecular interactions. *Current Opinions in Biotechnology* 5:389-395

Fisher H.F., Singh N., 1995. Calorimetric Methods for Interpreting Protein-Ligand Interactions. *Methods In Enzymology* 259(9): 194-221.

Franchi E., Maisano F., Testori S.A., Galli G., Toma S., Parente L., Ferra, F., Grandi G., 1991. A new human growth hormone production process using a recombinant *Bacillus subtilis* strain. *Journal of Biotechnology*. 18: 41-54.

Gedig E., 2008. Surface Chemistry in SPR Technology, *Handbook of Surface Plasmon Resonance*, 1<sup>ST</sup> Ed. , Ed by. Schasfoort R.B.M., Tudos A.J., The Royal

Society of Chemistry, Thomas Graham House, Science Park, Milton Road, Cambridge UK.

Georgiou G., Valax P., 1996. Expression and correctly folded proteins in *E. coli*. *Current Opinion in Biotechnology*. 7 (2):190-197.

Glaser R.W., Hausdorf G., 1996. Binding kinetics of antibody against HIV p24 core protein measured with real-time biomolecular interaction analysis suggest a slow conformational change in antigen p24. *Journal of Immunological Methods*. 189:1-14

Goeddel D.V., Heyneker H.L., Hozumi T., Arentzen R., Itakura K., Yansura D.G., Ross M.J., Miozzari G., Crea R., Seeburg P.H., 1979. Direct expression in *Escherichia coli* of a DNA sequence coding for human growth hormone. *Nature*, 281:544-548.

Goldstein B., Dembo M., 1995. Approximating the effects of diffusion on reversible reactions at the cell surface : ligand- receptor kinetics. *Biophysical Journal* 68: 1222-1230

Goodyear C.S., Silverman G.J., 2005. Phage display methodology for the study of protein-protein interactions. *Protein-Protein Interactions*. 2<sup>nd</sup> E.d.; Golemis E.A. and Adams P.D., Cold Spring Harbor Laboratory Press, Cold Spring Harbor , NY, USA.

Gray G.L., Bladridge J.S., McKeown K.S., Heyneker H.L., Chang, C.N., 1985. Periplasmic production of correctly processed human growth hormone in *Escherichia coli* natural and bacterial signal sequences are interchangeable. *Gene*.29(2-3):247-254.

Guo M-J., Zhuang Y-P., Chu J., Zhang S-L., Xiong A-S., Peng R-H., Yao Q-H., 2007. Production and purification of a novel thermostable phytase by *Pichia pastoris* FPY34. *Process Biochemistry*. 42:1660-1665.

Han Y., Gras S., Forde G.M., 2009. Binding properties of peptidic affinity ligands for plasmid DNA capture and detection. *AIChE Journal* 55(2): 505-515.

Hansen L.D., Christensen J.J., Izatt R.M., 1965. Entropy titration:A calorimetric method for the determination of  $\Delta G$ ,  $\Delta H$ , and  $\Delta S$ . *Journal of Chemical Society, Chemical Communications* 3: 36-37.

Hao Y., Chu J., Wang Y., Zhuang Y., Zhang S., 2007. The inhibition of aggregation of recombinant human consensus interferon- $\alpha$  mutant during *Pichia pastoris* fermentation. *Applied Microbiology and Biotechnology*. 74: 578- 584.

Haq I., 2002. Thermodynamics of drug-DNA interactions. *Archives of Biochemistry Biophysics* 403:1-15.

- Higgins D.R., Cregg J.M., 1998. *Pichia* protocols. Methods in Molecular Biology 103. Humana Press, Totowa, New Jersey
- Hilt W., Wolf D.H., 1992. Stress-induced proteolysis in yeast. Molecular Microbiology. 6:2437-2442.
- Hohenblum H., Gasser B., Maurer M., Borth N., Mattanovich D., 2004. Effects of gene dosage, promoters, and substrates on unfolded protein stress of recombinant *Pichia pastoris*. Biotechnology and Bioengineering.85(4): 367–375.
- Holmberg A., Blomstergren A., Nord O., 2005. The biotin-streptavidin interaction can be reversibly broken using water at elevated temperatures. Electrophoresis26 (3): 501–510.
- Holst B., Bruun, A.W., Kiellandbrand M.C., Winther J.R., 1996. Competition between folding and glycosylation in the endoplasmic reticulum. EMBO Journal.15: 3538–3546.
- Hong F., Meinander N.Q., Jonsson L.J., 2002. Fermentation strategies for improved heterologous expression of laccase in *Pichia pastoris*. Biotechnology and Bioengineering. 79(4):438-449.
- Hoyer W., Hard T., 2008. Interaction of Alzheimer's  $\beta$ -peptidewith an engineered binding, protein–thermodynamics and kinetics of coupled folding-binding. Journal of Molecular Biology378: 398–411.
- Hsiung H.M., Mayne N.G., Becker G.W., 1986. High-level expression, efficient secretion and folding of human growth hormone in *Escherichia coli*. Biotechnology, 4:991-995.
- Inan M., Chiruvolu V., Eskridge K.M., Vlasuk G.P., Dickerson K., Brown S., Meagher M.M., 1999. Optimization of temperature-glycerol-pH conditions for a fedbatch fermentation process for recombinant hookworm (*Ancylostoma caninum*) anticoagulant peptide(AcAP-5) production by *Pichia pastoris*. Enzyme and Microbial Technology 24(7): 438-445.
- Inan M., Meagher M.M., 2001. Non-repressing carbon sources for alcohol oxidase (AOX1) promoter of *Pichia pastoris*. Journal of Bioscience and Bioengineering.92(6): 585-589.
- Invitrogen, 2002. *Pichia* fermentation process guidelines. [www.invitrogen.com](http://www.invitrogen.com) retrieved, may 2009.
- Jackola D.R., Blackburn C., Sveum M., Rosenberg A., 2008. Entropy-favored human antibody binding reactions with a non-infectious antigen. Molecular Immunology 45: 1494–1500.
- Jacobsen B., Gårdsvoll H., Funch G.J., Østergaard S., Barkholt V., Ploug M., 2007. One-step affinity purification of recombinant urokinase-type

plasminogen activator receptor using a synthetic peptide developed by combinatorial chemistry. *Protein Expression and Purification* 52: 286-296

Jahic M., Viede A., Charoenrat T., Teeri T., Enfors S.O., 2006. Process technology for production and recovery of heterologous proteins with *Pichia pastoris*. *Biotechnology Progress*. 22: 1465-1473.

Jahic M., Wallberg F., Bollok M., Garcia P., Enfors S.O., 2003. Temperature limited fed-batch technique for control of proteolysis in *Pichia pastoris* bioreactor cultures. *Microbial Cell Factories*, 2:6.

Jayasena S.D., 1999. Aptamers: an emerging class of molecules that rival antibodies in diagnostics. *Clinical Chemistry*. 45:1628-1650.

Jelesarov I., Bosshard H.R., 1999. Review: isothermal titration calorimetry and differential scanning calorimetry as complementary tools to investigate energetics of biomolecular recognition. *Journal of Molecular Recognition*. 12:3-18.

Jost P.J., Harbottle R.P., Knight A., Miller A.D., Coutelle C., Schneider H., 2001. A novel peptide, for targeting of human epithelia. *FEBS Letters*. 489:263-269.

Jungo C., Rerat C., Marison I.W., von Stockar U., 2006. Quantitative characterization of the regulation of the synthesis of alcohol oxidase and of the expression of recombinant avidin in a *Pichia pastoris* Mut<sup>+</sup> strain. *Enzyme Microbial Technology*. 39 (4): 936-944.

Jungo C., Marison I.W., von Stockar U., 2007a. Mixed feeds of glycerol and methanol can improve the performance of *Pichia pastoris* cultures: A quantitative study based in concentration gradients in transient continuous cultures. *Journal of Biotechnology*. 128 (4):824-837.

Jungo C., Schenk J., Pasquier M.M., Marison I.W., von Stockar U., 2007b. A quantitative analysis of the benefits of mixed feeds of sorbitol and methanol for production of recombinant avidin with *Pichia pastoris*. *Journal of Biotechnology*. 131:57-66.

Karlsson R., Michealsson A., Mattson L., 1991. Kinetic analysis of monoclonal antibody-antigen interactions with new biosensor based analytical system. *Journal of Immunological Methods*. 145: 229-240

Karlsson R., Falt A., 1997. Experimental design for kinetic analysis of protein-protein interaction with surface plasmon resonance biosensors. *Journal of Immunological Methods*. 200:121-133

Kasimova R.M., Kristensen S.M., Howe P.W.A., Christensen T., Matthiesen F., Petersen J., Sorensen H.H.M., Led J.J., 2002. NMR studies of the backbone flexibility and structure of human growth hormone: a comparison of high and low pH conformations. *Journal of Molecular Biology*. 318:679-695.

Kato C., Kobayashi T., Kudo T., Frusetto T., Murakami Y., Tanaka T., Baba H., Oishi T., Ohtsuka E., Ikehera M., Yanagida T., Keto H., Moriyama S., Horikoshi K., 1987. Construction of an excretion vector and extracellular production of human growth hormone from *Escherichia coli*. *Gene*, 54: 197-202.

Kelly R.F., O'Connell M.P., 1994. Thermodynamic analysis of an antibody functional epitope. *Biochemistry*. 32(27):6828- 6835

Khodabandeh M., Yakhchali B., Rahimi M., Vaseli N., Jahromi Z. M., Zomorrodipour A., Deezagi A., Majd S. A., Sanati M. H., 2003. Purification of large quantities of biologically active recombinant human growth hormone. *Iranian Journal of Biotechnology*. 1(4): 207-209.

Kim M., Park K., Jeong E.J., Shin Y.B., Chung B.H., 2006. Surface plasmon resonance imaging analysis of protein-protein interactions using on-chip-expressed capture protein. *Analytical Biochemistry*. 226:175-181

Kiovunen E., Wang B., Ruoslahti E., 1994. Isolation of a highly specific Ligand for the  $\alpha_5\beta_1$  integrin from a phage display library. *Journal of Cell Biology* 124(3):373-380.

Kirk R. E., Othmer D. F., 1994. *Encyclopedia of Chemical Technology*, 4<sup>th</sup> Ed., the Interscience Encyclopedia Inc., New York.

Kobayashi K., Kuwae S., Ohya T., Ohda T., Ohyama M., Tomomitsu K., 2000. High level secretion of recombinant human serum albumin by fedbatch fermentation of the methylotrophic yeast, *Pichia pastoris*, based on optimal methanol feeding strategy. *Journal of Bioscience and Bioengineering*. 90:280-288.

Komolov K.E., Senin I.I., Philippov P.P., Koch K.W., 2006. Surface plasmon resonance study of G.protein-eceptor coupling in a lipid bilayer free system. *Analytical Chemistry*. 78:1228-1234

Kopchick J.J., 2003. History and Future of Growth Hormone Research. *Hormone Resolutions* . 60 (Suppl 3): 103-112.

Kresheck G.C., Vitello L.B., Erman J.E., 1995. Calorimetric studies on the interaction of horse ferricytochrome c and yeast cytochrome c peroxidase. *Biochemistry*. 34:8398-8405.

Krysiak R., Gdula-Dymek A., Bernardska-Czerwinska B.O., 2007. Growth Hormone Therapy in Chilren and Adults, *Pharmacological Reports*, 59:500-516.

Labrou N.E., 2003. Design and selection of ligands for affinity chromatography. *Journal of Chromatography B*. 790: 67-78.

- Ladbury J.E. and Chowdhry B.Z., 1996. Sensing the heat: the application of isothermal titration calorimetry to thermodynamic studies of biomolecular interactions. *Chemistry and Biology*. 3:791-801.
- Liedberg B., Nylander C., Lundström, 1983. Surface plasmon resonance for gas detection and biosensing. *Sensors and Actuators* 4:299-304
- Li C.H., Evans H.M., 1944. The isolation of pituitary growth hormone. *Science*. 99:183-184.
- Li Z., Xiong F., Lin Q., d'Anjou M., Daugulis A.J., Yang D.S.C., Hew C.L., 2001. Low-temperature increases the yield of biologically active herring antifreeze protein in *Pichia pastoris*. *Protein Expression and Purification*. 21: 438-445.
- Li J., Feng J., Dang Q., Qiao Y., Zhao J., Zhang S., Sun H., Wen X., Yuan Z., 2009, Affinity adsorption mechanism studies of adsorbents for oligopeptides using model polymer. *Polymer* 50 :1602-1608
- Liesisene J., Racaityte K., Morkeviciene M., Valancius, Bumelis B., 1997. Immobilized metal affinity chromatography of human growth hormone-Effect of ligand density. *Journal of Chromatography A*. 764(1):27-33.
- Lin J., Panigraphy D., Trinh L.B., Folkman J., Shiloach J., 2000. Production process for recombinant human angiostatin in *Pichia pastoris*. *Journal of Industrial Microbiology and Biotechnology* . 24:31-35.
- Lin H., Kim T., Xiong F., Yang X., 2007. Enhancing the production of fc-fusion protein in fed-batch fermentation of *Pichia pastoris* by design of experiments. *Biotechnology Progress*. 23:621-625.
- Lin K., Wey M., Kan L., Shiuan D., 2009. Characterization of the interactions of lysozyme with DNA by surface plasmon resonance and circular dichroism spectroscopy. *Applied Biochemistry Biotechnology*. 158:631-641.
- Love J.C., Estroff L.A, Kriebel J.K., Nuzzo R.G., Whitesides G.M., 2005. Self assembled monolayers of thiolates on metals as a form of nanotechnology. *Chemical Reviews*. 105:1103-1116
- Löfås S., McWhirter A., 2006. The art of immobilization for SPR sensors. *Series on Chemical Sensors and Biosensors* 4:117-151.
- Macauley-Patrick S., Fazenda M.L., McNeil B., Harvey L.M., 2005. Heterologous protein production using the *Pichia pastoris* expression system. *Yeast*. 22,:249-270.
- Martial J.A., Hallewell R.A., Baxter J.D., Goodman H.M., 1979. human growth hormone: complementary DNA cloning and expression in bacteria. *Science*. 205: 602-607.
- Mbrabet N.T., Vijaylakshmi M.A., 2002. Immobilized metal-ion chromatography: from phenomenological hallmarks to structure based

molecularinsights. In: Vijaylakshmi, M.A. (Ed.), Biochromatography. Theory and Practice. Taylor and Francis, New York.

Mondal K., Gupta M.N., 2006. The affinity concept in bioseparation: evolving paradigms and expanding range of applications. Biomolecular engineering. 23:59-76.

Mourez M., Kane R.S., Mogridge J., Metallo S., Deschatelets P., Sellman B.R., Whitesides G.M., Collier R.J., 2001. Designing a polyvalent inhibitor of anthrax toxin. Nature Biotechnology 19: 958-961.

Mudhivartha V. K., Bhambhani A., Kumar C.V., 2007. Novel enzyme/DNA/inorganic nanomaterials: A new generation of biocatalysts. Dalton Transactions 5483–5497.

Mukhija R., Rupa P., Pillai D., Garg L.C., 1995. High-level production and one-step purification of biologically active human growth hormone in *Escherichia coli*, Gene 165(2): 303–306.

Murphy K.P., Freire E., 1992. Thermodynamics of structural stability and cooperative behavior in proteins. Advance in protein chemistry. 43:313-361.

Nakayama A., Ando K., Kawamura K., Mita I., Fukazawa K., Hori M., Honjo M., Furutani Y., 1988. Efficient secretion of the authentic mature human growth hormone by *Bacillus subtilis*. Journal of Biotechnology. 8: 123-134.

Nam Y., Chang J.C., Wheeler B.C., Brewer G.J., 2004. gold-coated microelectrode array with thiol linked self assembled monolayers for engineering neuronal cultures. IEEE Transactions on Biomedical Engineering. 51(1):158-165.

Nielsen J., Villadsen J., 1994. Bioreaction Engineering Principles, 1<sup>st</sup> Ed. Plenum Press, New York.

Nielsen J., Villadsen J., Liden G., 2003. Bioreaction Engineering Principles. 2<sup>nd</sup> Ed. Plenum press, New York.

Nienhaus G.U., 2005. Protein-Ligand interactions: methods and applications. Methods in molecular biology 305. Humana Press, Totowa NJ.

Oliviera J.E., Soares C.R.J. Prezi C.N., Gimbo E., Camargo I.M.C., Morganti L., Bellini M.H., Affonso R., Arkaten R.R., Bartolini P., Ribela M.T.C.P., 1999. High-yield purification of biosynthetic human growth hormone secreted in *Escherichia coli* periplasmic space. Journal of Chromatography A. 852:441-450.

Orman M.A., Çalık P., Çelik E., Halloran S.M., Çalık G., Özdamar T.H., 2008. Expression system for biosynthesis and purification of recombinant human growth in *Pichia pastoris* and structural analysis by MALDI-ToF mass spectrometry. Biotechnology Progress. 24 (1): 221-226

Orman M.A., Çalık P., Özdamar T.H., 2009. The influence of carbon sources on recombinant-human-growth-hormone production by *Pichia pastoris* is dependent on phenotype: A comparison of Mut<sup>s</sup> and Mut<sup>+</sup>. *Biotechnology and Applied Biochemistry*. 52 (3): 245-255

Özdamar T.H., Senturk B., Yilmaz O.D., Çalık G., Çelik E., Çalık P., 2009. Expression system for recombinant human growth hormone production by *Bacillus subtilis*. *Biotechnology Progress*. 25(1): 75-84.

Papalia G.A., Baer M., Luehrsen K., Nordin H., Flynn P., Myszka D.G., 2006,. High-resolution characterization of antibody fragment/antigen interactions using Biocore T100. *Analytical Biochemistry*. 359(1):112-119

Patel N., Davies M. C., Hartshorne M., Heaton R. J., Roberts C.J., Tendler S. J. B., Williams P. M. 1997.*Langmuir*.13: 6485-6490.

Patra A.K., Mukhopadhyay R., Mukhija R., Krishnan A., Garg L.C. Garg, Panda A.K., 2000. Optimization of inclusion body solubilization and renaturation of recombinant human growth hormone from *Escherichia coli*, *Protein Expression and Purification* 17: 182–192.

Pellequer J.L., Van Regenmortel M.H.V., 1993. Measurement of kinetic binding constants of viral antibodies using new biosensor technology. *Journal of Immunological Methods*. 166:133-143

Pizarro J.C., Normand B.V., Riottot M.M., Budkowska A., Bentley G.A., 2001. Structural and functional characterization of a monoclonal antibody specific for the preS1 region of hepatitis B virus, *FEBS Letters* 509: 463-468

Pla I.A., Damasceno L.M., Vanelli T., Ritter G., Batt C.A., Shuler M.L., 2006. Evaluation of Mut<sup>+</sup> and Mut<sup>s</sup>*Pichia pastoris* phenotypes for high levels extracellular scFv Expression under Feedback Control of the Methanol Concentration., *Biotechnology Progress*. 22: 881-888.

Plantz B.A., Sinha J., Villarete L., Nickerson K.W., Schlegel V.L., 2006. *Pichia pastoris* fermentation optimization: Energy state and testing a growth-associated model. *Applied Microbiology and Biotechnology*. 72(2): 297-305.

Ploug M., Østergaard S. Gårdsvoel H., Kraovalski K., Holst-Hansen C., Holm A., Ossowski L., Danø K., 2001. Combinatorial Chemistry, Identification of Functional Epitopes and Inhibitory Effect on Cancer Cell Intravasation. *Biochemistry* 40:12157-12168.

Pollet J., Delpont F., Janssen K.P.F., Jans K., Maes G., Pfeiffer H., Wevers M., Lamertyn J., 2009, *Biosensors and Bioelectronics* 25(4):864-869

[www.pnas.org](http://www.pnas.org), Proceedings of the National Academy of Sciences, retrieved 19.05.2010

Raemaeker R.J.M., de Muro L., Gatehouse J.A., Fordham-Skelton A.P., 1999.

Functional phytohaemagglutinin (PHA) and Galanthus nivalis agglutinin (GNA) expressed in *Pichia pastoris*: correct N-terminal processing and secretion of heterologous protein expressed using the PHA-E signal peptide. *European Journal of Biochemistry*. 265: 394–403.

Ramon R., Ferrer P., Valero F., 2007. Sorbitol co-feeding reduces metabolic burden caused by the overexpression of a *Rhizopus oryzae* lipase in *Pichia pastoris*. *Journal of Biotechnology*. 130: 39-46.

Ramsden J.J., Bachmanova G.G., Arcakova A.I., 1996. Immobilization of proteins to lipid bilayers. *Biosensors and Bioelectronics*. 11:523-528

Raposo S., Lima-Costa M.E, 2006. Rheology and shear stress of *Centaurea calcitrapa* cell suspension cultures grown in bioreactor. *Biotechnology Letters* 28:431-438.

Ravelet C., Grosset C., Peyrin E., 2006. Liquid chromatography, electrochromatography and capillary electrophoresis applications of DNA and RNA aptamers. *Journal of Chromatography A*. 1117 (1):1-10.

Reya-Tonetti G., Perotti N.I., 1999. Rapid screening of textile dyes employed as affinity ligands to purify enzymes from yeast. *Biotechnology Applied Biochemistry* 29:151–156.

Romanos M.A., Scorer C.A., Clare J.J., 1992. Foreign gene expression in yeast: a review. *Yeast*. 8: 423–488.

Romig T.S., Bell C., Drolet D.W., 1999. Aptamer affinity chromatography: combinatorial chemistry applied to protein purification. *Journal of Chromatography B*. 731:275-284.

Roselin L.S., Lin M-S., Lin P-H., Chang Y., Chen W-Y., 2010. Recent trends and some applications of isothermal titration calorimetry in biotechnology. *Bio-Technology Journal*. 5: 85-98.

Roy I., Gupta M.N., 2000. Purification of alkaline phosphatase from chicken intestine by expanded-bed affinity chromatography on dye-linked cellulose. *Biotechnology Applied Biochemistry* 32: 81–87.

Rusmini F., Zhong Z., Feijen J., 2007. Protein Immobilization strategies for protein biochips. *Biomacromolecules* . 8(6):1775-1789

Ryu D.Y., Humphrey A.E., Fuchs R., 1971 Effect of surface aeration on scale-up producers for fermentation processes. *Industrial and Engineering Chemistry-Process design and Development*.

Sambrook J., Russell D.W. , 2001. *Molecular Cloning: a laboratory manual* 3<sup>rd</sup> Ed. Cold Spring Harbor Laboratory Press, Cold Spring Harbor New York

Sandler I.S., 1999. *Chemical and Engineering Thermodynamics*. 3<sup>rd</sup> Ed. John Wiley and Sons. Hoboken NJ, USA

- Schubert F., Zettl H., Häfner W., Krauss G., Kraysch G., 2003. Comparative thermodynamic analysis of DNA-protein interactions using surface plasmon resonance and fluorescence correlations spectroscopy. *Biochemistry* 42: 10288-10294
- Schuck P., 1997. Use of surface plasmon resonance to probe the equilibrium and dynamic aspects of interactions between biological macromolecules. *Annual review of biophysics and biomolecular structure* 26(1): 541-566
- Scott J.K., Smitt G.P., 1990. Searching for peptide ligands with an epitope library. *Science*. 249 :386-390.
- Scragg A.H., 1988. *Biotechnology for engineers: biological systems in technological processes*. 1<sup>st</sup> Ed. Ellis Horwood, Michigan
- Shankaran D.R., Gobi K.V., Miura N., 2007. Recent advancements in surface plasmon resonance immunosensors for detection of small molecules of biomedical, food and environmental interest. *Sensors and Actuators B* 121: 158-177
- Shin N.K., Kim D.Y., Shin C.S., Hong M.S., Lee J., Shin H.C., 1998. High-level production of human growth hormone in *Escherichia coli* by a simple recombinant process. *Journal of Biotechnology*, 62: 143-151.
- Shuler M.L., Kargi F., 2002. *Bioprocess Engineering: Basic Concepts*, 2<sup>nd</sup> Ed., Prentice Hall Inc., USA.
- Sibirny A.A., Ubiyvovk V.M., Gonchar M.V., Titorenko V.I., Voronovsky A.Y., Kapultsevich Y.G., Bliznik K.M., 1990. Reaction of direct formaldehyde oxidation to CO<sub>2</sub> are not essential for energy supply of yeast methylotropic growth. *Archives of Microbiology* 154:566-575
- Singh S.M., Sharma A., Pande A.K., 2009. High throughput purification of recombinant human growth hormone using radial flow chromatography. *Protein Expression and Purification*. 68(1):54-59.
- Sinha J., Plantz B.A., Zhang W., Gouthro., Shlegel V., Liu C-P., Meagher M.M., 2003. Improved production of recombinant ovine interferon- $\tau$  by Mut<sup>+</sup> strain of *Pichia pastoris* using an optimized methanol feed profile. *Biotechnology Progress*. 19:794-802.
- Sinha J., Plantz B.A., Inan M., Meagher MM., 2004. Causes of proteolytic degradation of secreted recombinant proteins produced in methylotropic yeast *Pichia pastoris*: case study with recombinant ovine interferon- $\tau$ . *Biotechnology and Bioengineering*. 89:102-112.
- Smith G.P., 1985. Filamentous fusion phage: Novel expression vectors that display cloned antigens onto the virion surface. *Science*. 228: 1315-1317.
- Sottriffer C.A., Flader W., Cooper A., Rode, B.M. 1999. Ligand binding by

antibody IgE Lb4: Assessment of bindingsite preferences using microcalorimetry, docking, and freeenergy simulations. *Biophysical Journal* 76: 2966–2977.

Soykut E.A., Dudak F.C., Boyaci I.H., 2008. Selection of staphylococcal enterotoxin B(SEB) binding peptide using phage display technology. *Biochemical and Biophysical Research Communications*. 370:104-108

Sreekrishna K., Brankamp R.G., Kroop K.E., Blankenship D.T., Tsay J.T., Smith P.L., Wierschke J.D., Subramaniam A., Birkenberger L.A., 1997. Strategies for optimal synthesis and secretion of heterologous proteins in the methylotrophic yeast *Pichia pastoris*. *Gene*. 190: 55-62.

Stettner J., Winkler A., 2010. Characterization of self-assembled monolayers on gold by thermal desorption. *Langmuir*.

Stites W.E., 1997, Protein-Protein Interactions: Interface structure, binding thermodynamics and mutational analysis. *Chemical Reviews* 97:1233-1250.

Stratton J., Chiruvolu V., Meagher M., 1998. High cell density fermentation. *Methods in Molecular Biology: Pichia protocols*. Ed by Higgins D.R. and Cregg J.M. Humana press, Totowa NJ.

Subramaniam A., Irudayaraj J., Ryan T., 2006. A mixed self-assembled monolayer based surface plasmon immunosensor for detection of E.Coli O157:H7, *Biosensors and Bioelectronics* 21:998-1006

Sundstrom M., Lundqvist T., Rodin J., Giebel L.B., Milligan D., Norstedt G., 1996. Crystal structure of and antagonist mutant of human growth hormone , G120R, in Complex with its receptor at 2.9Å resolution . *The Journal of Biological Chemistry* . 271(50):32197-32203

Tabandeh F., Shojaosadeti A.A., Zomorodipour A., Khodabandeh M., Saneti M.H., Yakhchali B., 2004. Heat-induced production of human growth hormone by high cell density cultivation of recombinant *Escherichia coli*. *Biotechnology Letters*, 26: 245-250.

Terpe K., 2003. Overview of tag protein fusions: from molecular and biochemical fundamentals to commercial systems. *Applied Microbiology and Biotechnology*. 60:523–533.

Thorpe E.D., d'Anjou M.C., Daugulis A.J., 1999. Sorbitol as a non-repressing carbon source for fed batch fermentation of recombinant *Pichia pastoris*. *Biotechnology Letters* 21:669-672.

Tombelli S., Minunni A., Mascini A., 2005. Analytical applications of aptamers. *Biosensors and Bioelectronics*. 20:2424-2434.

- Trevino L.L., Viader-Salvado J.M., Barrera-Saldana H.A., Guerrero-Olazaran, M., 2000. Biosynthesis and secretion of recombinant human growth hormone in *Pichia pastoris*. *Biotechnology Letters*. 22: 109-114.
- Tritos N.A., Mantzoros C.S., 1998. Recombinant human growth hormone: old and novel uses. *American Journal of Medicine*. 105(1):44-57.
- Ueda E.K.M., Gout P.W., Morganti L., 2003. Current and prospective applications of metal ion-protein binding. *Journal of Chromatography A*. 988: 1-23.
- Valezquez-Campoy A., Ohtaka H., Nezami A., Muzammil S., Freire E., 2004. Isothermal Titration Calorimetry. *Current Protocols in Cell Biology*. Suppl 23: 17.8.1-17.8.24.
- Van der Werve P.A., Barclay A.N. 1996. Analysis of cell-adhesion molecule interactions using surface plasmon resonance. *Current Opinion in Immunology* 8: 257-261.
- Van Regenmortel M.H.V., Altschuh D., Pellequer J., Richalet-Secordel P., Saunal H., 1994. Analysis of viral antigens using biosensor technology. *Methods: companion Methods in Enzymology*. 6:177-187
- Walker G.M., 1998. *Yeast: Physiology and Biotechnology*. 1<sup>st</sup> Ed. John Wiley & Sons Inc., New York.
- Wang G., De J., Schoeniger J.S., Roe D.C., Carbonell R.G., 2004. A hexamer peptide ligand that binds selectively to staphylococcal enterotoxin B: isolation from a solid phase combinatorial library. *Journal of Peptide Resolutions*. 64:51-64.
- Wang G., Salm J.R., Gurgel P.V., Carbonell R.G., 2005. Small peptide ligands for affinity separations of biological molecules. *Chemical Engineering: Trends and Developments*, 1<sup>st</sup> Ed. John Wiley and Sons Ltd. The Atrium, Southern Gate, Chichester, West Sussex PO19 8SQ, England
- Wang Z., Wang Y., Zhang D., Li., Hua Z., Guocheng D., Chen J., 2010. Enhancement of cell viability and alkaline polygalacturonate lyase production by sorbitol co-feeding with methanol in *Pichia pastoris* fermentations. *Biosource Technology*. 101: 1318-1323.
- Werten M.W.T., van den Bosch T.J., Wind R.D., Mooibroek H., de Wold F.A., 1999. High-yield secretion of recombinant gelatins by *Pichia pastoris*. *Yeast*. 15: 1087-1096.
- White C.E., Kempf N.M., Komives E.A., 1994. Expression of highly disulfide-bonded proteins in *Pichia pastoris*. *Structure* 2 (11): 1003-1005.
- Wilchek M., Bayer E.A., 1990. Applications of avidin-biotin technology: literature survey. *Methods in Enzymology*. 184: 14-45.

- Wiseman T., Williston S., Brandt J.F., NinL.N., 1989. Rapid measurement of binding constants and heats of binding using a new titrationcalorimeter. *Analytical Biochemistry*. 179:131-137.
- Wobbe L., Zimmermann D., Wißbrock M., Urman S., Sewald K., Malešević, Sewald N., 2006. Intergrin  $\alpha_5\beta_1$ : a new purification strategy based on immobilized peptides. *Journal of Peptide Research*. 66(Suppl.1):22-29
- Wolthers K.R., Lou X., Toogood H.S., Leys D., Scrutton N.S., 2007. Mechanism of coenzyme binding to human methioninesynthase reductase revealed through the crystal structureof the FNR-like module and isothermal titration calorimetry. *Biochemistry* 46:11833–11844.
- Wood R. W., 1902. XLII. On a remarkable case of uneven distribution of light in a diffraction grating spectrum. *Philosophical Magazine Series 6*, 4 (21): 396-402
- Wood R.W., 1912 XXVII. Diffraction gratings with controlled groove form and abnormal distribution of intensity. *Philosophical Magazine Series 6*, 6 (134):310-317
- Wu D., Hao Y-Y., Chu J., Zhuang Y-P., Zhang S-L., 2008. Inhibiton of degradation and aggregation of recombinant human consensus interferon- $\alpha$  mutant expressed in *Pichia pastoris* with complex medium in biorector. *Applied Microbial and Cell Physiology*. 80: 1063-1071.
- Xie W.Z., Wang D., Du H.W., 2002. Analysis of antigen-antibody interactions on protein microarrays. *Progress in Biochemistry and Biophysics*. 29(2):311-315
- Xie J., Zhou Q., Du P., Gan R., Ye Q., 2005. Use of different carbon sources in cultivation of recombinant *Pichia pastoris* for angiostatin production. *Enzyme and Microbial Technology*. 36:210-216.
- Yang W., Wu H., Barbas C.F., 1995. Surface plasmon resonance based kinetic studies of zinc finger-DNA interactions. *Journal of Immunological Methods*. 183: 175-82
- Yang X., Li X., Prow T.W., Reece L.M., Bassett S.E., Luxon B.A., HerzogN.K., Aronson J., Shope R.E., Leary J.F., Gorenstein D.G., 2003. Immuno-fluorescence assay and flow-cytometry selection of bead boundaptamers. *Nucleic Acid Resolutions* 3: e54.
- Yang G., Zhou H., Lu Y., Lin Y., Zhou S., 2004. Comparing expression of different forms of human DNA topoisomerase I in *Pichia pastoris*. *Enzyme and Microbial Technology*. 34(2):139-146.
- Yang H., Gurgel P.V., Carbonell R.G., 2006. Hexamer peptide affinity resins that bind the Fc-Region of human immunoglobulin G. *Peptide Resolutions*. 66(Suppl1) 120-137.

Zhang W., Bevins M.A., Plantz B.A., Smith L.A., 2000. Modeling *Pichiapastoris* growth on methanol and optimizing the production of a recombinant protein, the heavy-chain fragment C of Botulinum Neurotoxin, Serotype A. *Biotechnology and Bioengineering*. 70 (1): 1-8.

Zhang Q., Tao M.L., Shen W.D., Zhou Y.Z., Ding Y., Ma Y., Zhou W.L., 2004. Immobilization of L-asparaginase on the microparticles of the natural silk sericin protein and its characteristics. *Biomaterials*. 25(17): 3751-3759

## APPENDIX A

### BUFFERS AND STOCK SOLUTIONS

#### Fermentation Medium

<b>Antifoam</b>	10 % (v/v) antifoam solution, prepared with dH <sub>2</sub> O. Can be autoclaved once.
<b>Base</b>	25 % NH <sub>3</sub> OH (Sigma). No need to sterilize.
<b>1 M potassium phosphate, pH 6.0</b>	56.48 g KH <sub>2</sub> PO <sub>4</sub> , 14.8 g K <sub>2</sub> HPO <sub>4</sub> was dissolved in dH <sub>2</sub> O and the volume made upto 500 mL. The pH was controlled. The buffer was autoclaved and stored at room temperature.

#### AOX Assay Solutions

<b>Yeast Lysis Buffer</b>	2% Triton X-100, 1% SDS, 100 mM NaCl, 10 mM Tris-Cl-pH8.0, 1mM Na <sub>2</sub> EDTA. The solution was autoclaved and stored at room temperature.
<b>1 M potassium phosphate, pH=7.5</b>	1M KH <sub>2</sub> PO <sub>4</sub> , 1M K <sub>2</sub> HPO <sub>4</sub> was dissolved in dH <sub>2</sub> O and titer KH <sub>2</sub> PO <sub>4</sub> with K <sub>2</sub> HPO <sub>4</sub> while controlling pH. The buffer was autoclaved and stored at room temperature.

#### SDS-PAGE Solutions

<b>10%(w/v) APS (Ammonium PerSulfate)</b>	Add 0.1g APS to 1 mL dH <sub>2</sub> O , freshly prepared.
<b>1.5 M Tris-HCl, pH=8.8</b>	36.3 g Tris base was dissolved in 150 mL dH <sub>2</sub> O and pH was adjusted to 8.8 with 6N HCl. The buffer was made up to 200 mL with dH <sub>2</sub> O. The buffer was autoclaved and stored at 2-8°C.

<b>0.5 M Tris-HCl, pH=6.8</b>	12.1 g Tris base was dissolved in 150 mL dH <sub>2</sub> O and pH was adjusted to 6.8 with 6N HCl. The buffer was made up to 200 mL with dH <sub>2</sub> O. The buffer was autoclaved and stored at 2-8°C.
<b>Resolving Buffer (12%) (for 2 gels)</b>	3.4mL dH <sub>2</sub> O, 4mL 30% Acrylamide-bis, 2.5 mL 1.5M Tris-HCl pH=8.8, 100µL 10%SDS, prior to gel preparation add 50µL APS and 5µL N,N,N',N'-Tetramethylethylenediamine .
<b>Stacking Buffer (5%) (for 2 gels)</b>	2.8mL dH <sub>2</sub> O, 0.85mL 30% Acrylamide-bis, 1.25 mL 0.5M Tris -HCl pH=6.8, 50µL 10%SDS, prior to gel preparation add 25µL APS and 5µL N,N,N',N'-Tetramethylethylenediamine
<b>4 x Sample Loading Buffer for SDS-PAGE</b>	200 mM Tris-HCl, pH 6.8; 40% glycerol; 6% SDS; 0.013% Bromophenol blue; 10% 2-mercaptoethanol. Distributed into microcentrifuge tubes and stored at -20°C.
<b>5x SDS-PAGE Running Buffer</b>	15 g Tris Base, 72 g glycine, 5 g SDS, dH <sub>2</sub> O to 1 liter. The buffer was stored at 2-8°C and diluted 1:5 with dH <sub>2</sub> O prior to use.
<b>Fixer Solution</b>	Mix 150 mL methanol + 36 mL acetic acid + 150 µL 37% formaldehyde and complete to 300 mL with distilled water. This solution can be used several times.
<b>Pretreatment Solution</b>	Dissolve 0.08 g sodium thiosulphate (Na <sub>2</sub> S <sub>2</sub> O <sub>3</sub> .5H <sub>2</sub> O) in 400 mL distilled water by mixing with a glass rod. Take 8 mL and set aside for further use in developing solution preparation.
<b>Silver Nitrate Solution</b>	Dissolve 0.8 g silver nitrate in 400 mL distilled water and add 300 µL 37% formaldehyde
<b>Developing Solution</b>	Dissolve 9 g potassium carbonate in 400 mL distilled water. Add 8 mL from pretreatment solution and 300 µL 37% formaldehyde.
<b>Stop Solution</b>	Mix 200 mL methanol + 48 mL acetic acid and complete to 400 mL with distilled water

### Protease Assay solutions

<b>Borate buffer (for Alkali proteases)</b>	2.381 g Boraks ( $\text{Na}_2\text{B}_4\text{O}_7 \cdot 10 \text{H}_2\text{O}$ ) dissolved in 250 ml $\text{dH}_2\text{O}$ . pH is adjusted to 10 by 1 M NaOH (6-7 ml) and add $\text{dH}_2\text{O}$ till 500 ml. Filter and store at $+4^\circ\text{C}$ .
<b>0.05 M Sodium Acetate buffer (for acidic proteases)</b>	Dissolve 0.713 ml acetic acid in 25 ml total $\text{dH}_2\text{O}$ . Dissolve 2.052 g sodium acetate in 50 ml $\text{dH}_2\text{O}$ . Titrate sodium acetate solution with acetic acid solution to pH 5.0, and final V= 50 ml. Then dilute to 500 ml. Autoclave and store at $+4^\circ\text{C}$ .
<b>0.05 M Sodium Phosphate Buffer (for neutral proteases)</b>	Dissolve 6.70 g $\text{Na}_2\text{HPO}_4 \cdot 7\text{H}_2\text{O}$ in 50 ml $\text{dH}_2\text{O}$ . Dissolve 3.90 g $\text{NaH}_2\text{PO}_4 \cdot 2\text{H}_2\text{O}$ in 50 ml $\text{dH}_2\text{O}$ . Titrate till pH 7.0, and final V= 50 ml. Then dilute to 500 ml. Autoclave and store at room temperature.

### Phage Display Solutions

<b>LB Medium</b>	Add 20mL LB broth to 1 L $\text{dH}_2\text{O}$ . Autoclave, store at room temperature
<b>IPTG/Xgal Stock</b>	Mix 1.25 g IPTG (isopropyl- $\beta$ -D-thiogalactoside) and 1g Xgal (5-Bromo-4-chloro-3-indolyl- $\beta$ -D-thiogalactoside). Solution can be stored at $-20^\circ\text{C}$ .
<b>IPTG/Xgal Plates</b>	Add 35mL LB agar to 1 L $\text{dH}_2\text{O}$ . Autoclave, cool to $<70^\circ\text{C}$ , add 1mL IPTG/Xgal stock per 1L and pour on to petri dishes. Store plates at $4^\circ\text{C}$ in dark.
<b>Top Agar</b>	Per liter: 10g Bacto-Tryptone, 5g Yeast Extract, 5g NaCl, 7g Bacto-Agar. Keep in microwave until homogeneous mixture is obtained, dispense into glass tubes with cotton lids into 4mL aliquots before it solidifies. Autoclave, store at room temperature, melt in microwave as needed.
<b>Blocking Buffer</b>	0.1M $\text{NaHCO}_3$ (pH=8.6), 5mg/mL BSA, 0.02% $\text{NaN}_3$ . Filter sterilize, store at $4^\circ\text{C}$ .
<b>1M Tris-HCl, pH=9.1</b>	16.13 g Tris base was dissolved in 90 mL $\text{dH}_2\text{O}$ and pH was adjusted to 9.1 with 6N HCl. The buffer is made up to 100 mL with $\text{dH}_2\text{O}$ . The buffer was autoclaved and stored at $2-8^\circ\text{C}$ .

<b>0.2 M Glycine-HCl, pH=2.2, 1mg/mL BSA</b>	Dissolve 1.5g Glycine and 100mg BSA in 90mL dH <sub>2</sub> O and adjust pH to 2.2 with 6N HCl. The buffer was made up to 100 mL with dH <sub>2</sub> O. The buffer was autoclaved and stored at room temperature.
<b>TBS</b>	50mM Tris-HCl (pH=7.5), 150mM NaCl, Autoclave, store at room temperature
<b>PEG/NaCl</b>	20% (w/v) polyethylene glycol-8000, 2.5M NaCl. Autoclave, mix well to combine separated layers while still warm. Store at room temperature.
<b>ABTS Stock</b>	Dissolve 22mg of azino-bis (3ethylbenzothiazole sulfonic acid)diammonium salt in 100mL of 50mM sodium citrate, pH=4.0. Filter sterilize and store at 4°C in dark.

## APPENDIX B

### CALIBRATION CURVES

#### Calibration Curve for Bradford Assay

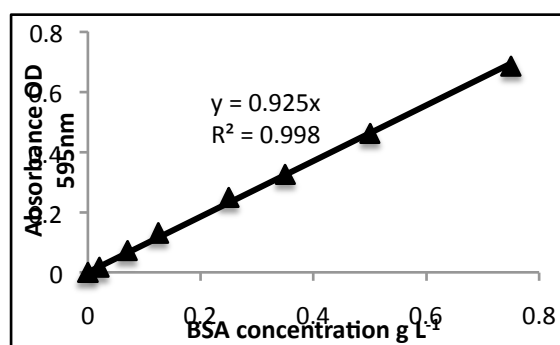


Figure B.1 Standard curve for Bradford Assay

#### Calibration Curve for Methanol Concentration

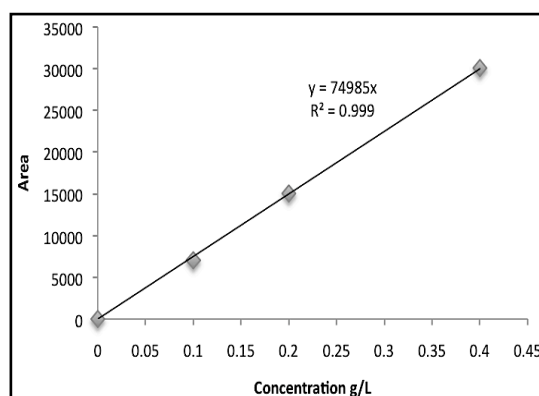


Figure B.2 HPLC Analysis: calibration curve obtained for methanol concentration

### Calibration Curve for Sorbitol Concentration

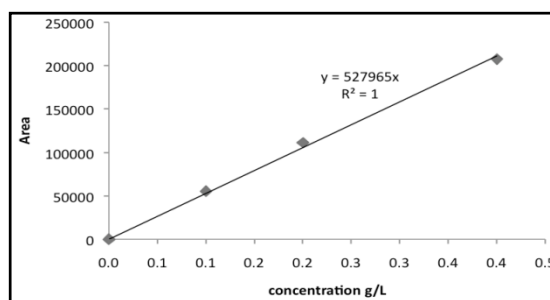


Figure B.3 HPLC Analysis: Calibration curve for sorbitol concentration

### Calibration Curves for Organic Acid Concentrations performed by HPLC

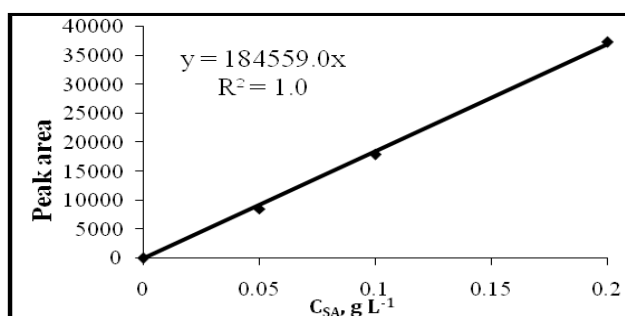


Figure B.4 Calibration curve for succinic acid concentration

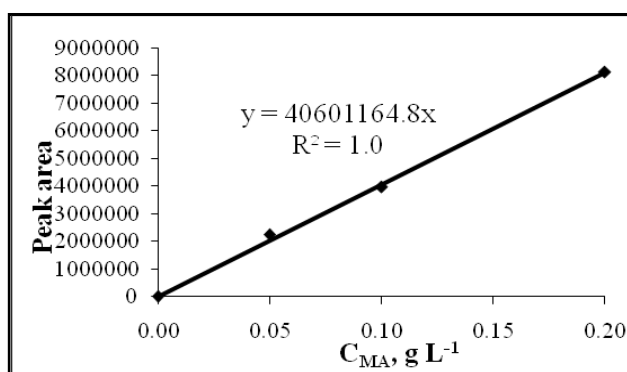
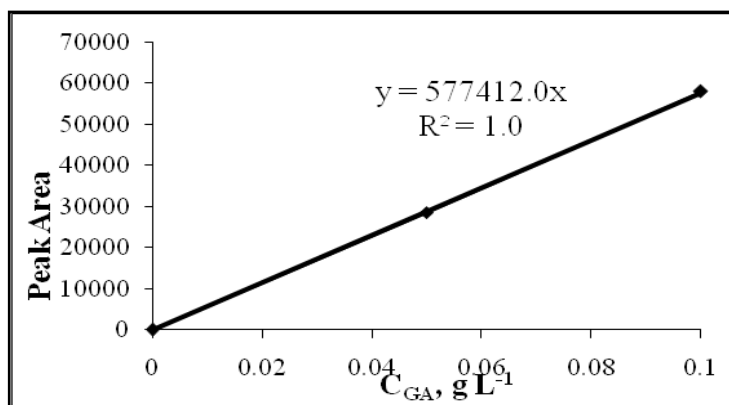
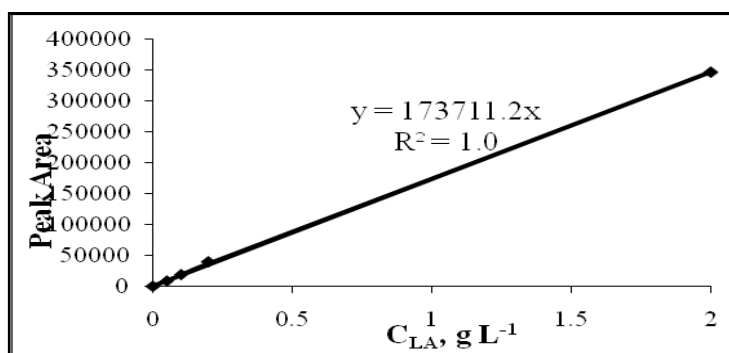


Figure B.5 Calibration curve for maleic acid concentration



**Figure B.6** Calibration curve for glutaric acid concentration



**Figure B.7** Calibration curve for lactic acid concentration

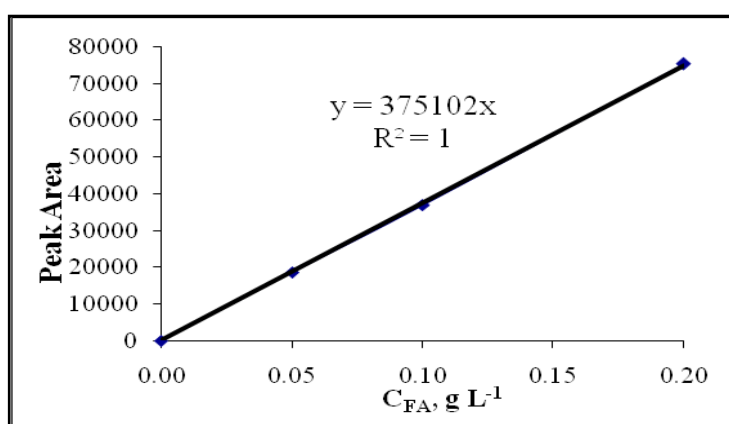


**Figure B.8** Calibration curve for formic acid concentration

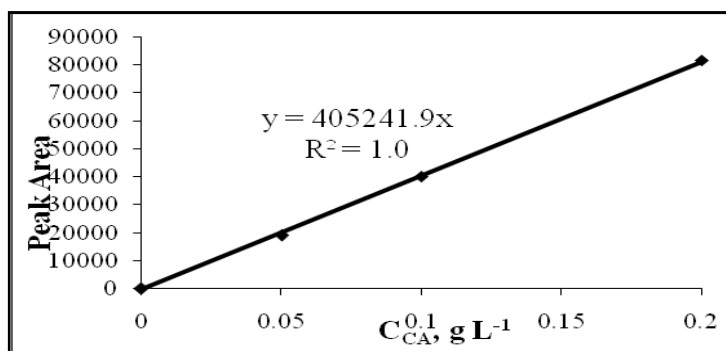


**Figure B.9** Calibration curve for citric acid concentration

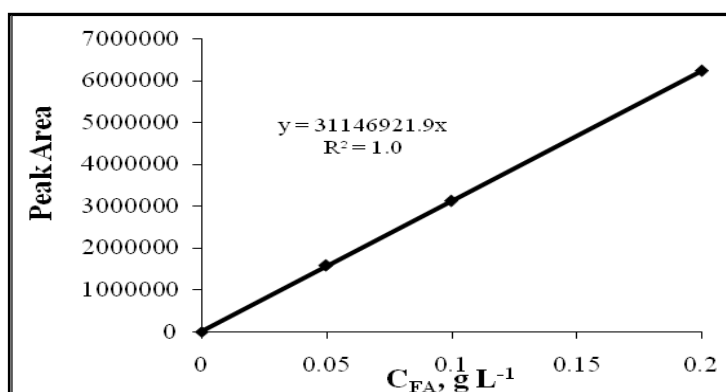


**Figure B.10** Calibration curve for fumaric acid concentration

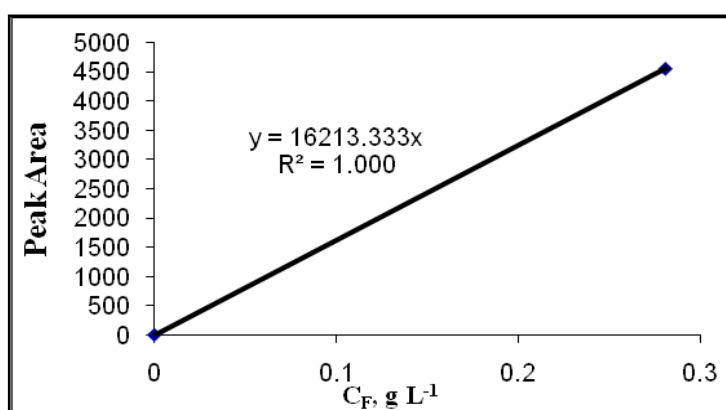


**Figure B.11** Calibration curve for formaldehyde concentration

## APPENDIX C

### ELECTROPHEROGRAM OF hGH STANDARD

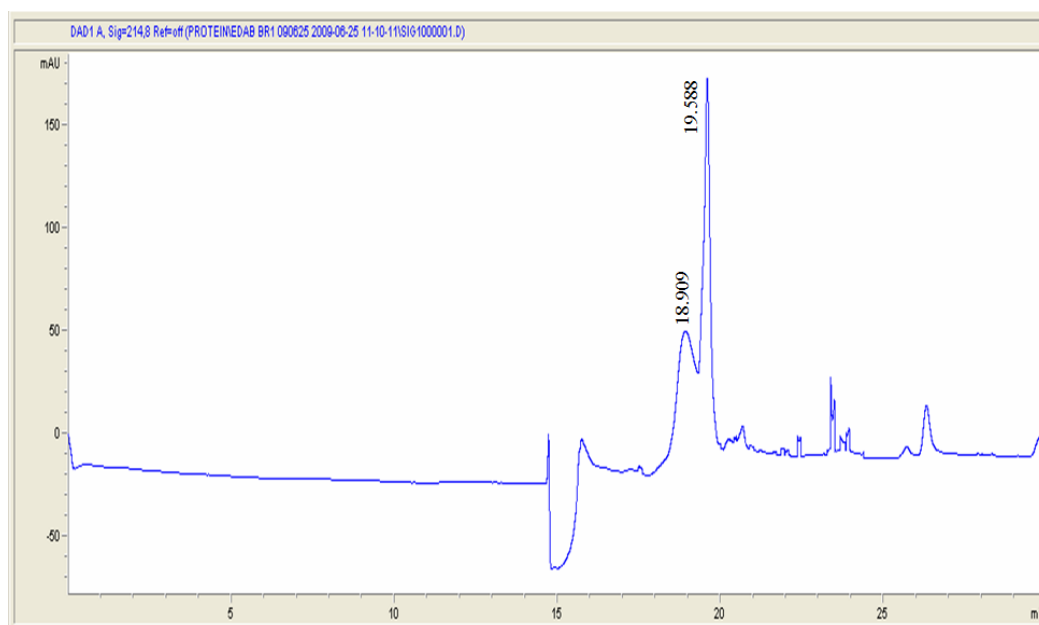


**Figure C.1** Electropherogram of 0.05 g L<sup>-1</sup> hGH standard

## APPENDIX D

### MOLECULAR WEIGHT MARKER

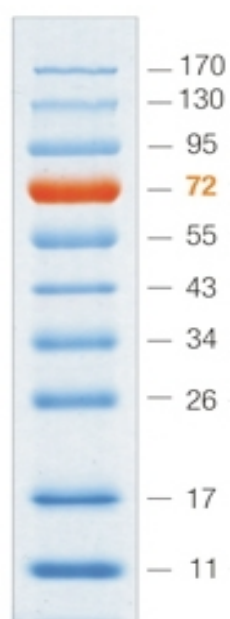


**Figure D.1** PageRuler™ Prestained Protein Ladder (Fermentas)

## **APPENDIX E**

### **PROPERTIES OF SELECTED PEPTIDES**

The properties of the peptides that were selected/used in determination of their affinity towards hGH are given in Table E.1.

**Table E.1** Properties of selected peptides for interaction determination towards hGH

Peptide Code	Amino Acid Sequence	# of residues	Molecular Weight	Net charge at pH=7	pI	Average hydrophilicity	Ratio of hydrophilic residues to hydrophobic residues (%)
P-1	FSEVFW	7	1169.3	-3.0	0	-0.5	43
P-2	FEVEFW	7	1211.4	-4.0	0	-0.1	43
P-3	ESEVFW	7	1151.3	-4.0	0	0.3	57
P-4	FEPHFW	7	1187.4	-1.9	3.3	-1.1	14
P-5	FSEPFW	7	1167.3	-3.0	0	-0.3	43
L	CSSSPSKHC	9	935.0	1.0	8.3	0.2	56
M-1	CSSKAAHL	9	887.0	1.0	9.0	-0.1	33
M-2	CSSAAKHL	9	887.0	1.0	9.0	-0.1	33
3/8	KQTLPSA	7	734.9	1.0	10.1	0.1	43
3/6	TMYLTFE	7	904.1	-1.0	3.3	-0.8	14
2/2-3/9	SYPPFTS	7	797.9	0.0	5.9	-0.7	29
3/5-3/11-3/27	HAIYPRH	7	893.0	1.2	9.8	-0.4	14
3/7	ARTEFFV	7	869.0	0	7.0	-0.2	29
3/13	LP L T L P L P	7	749.9	0	6.0	-0.8	0
3/10	Y L T M P T P	7	822.0	0	5.9	-0.9	0
3/19	K V W L L S T	7	846.0	1.0	10.1	-0.8	29
3/29	S T T K L A L	7	732.9	1.0	10.1	-0.2	29
3/12-3/14-3/16	H F Q T H F T	7	866.9	2.0	8.0	-0.6	14

## APPENDIX F

### ISOTHERMAL TITRATION CALORIMETRY RUNS

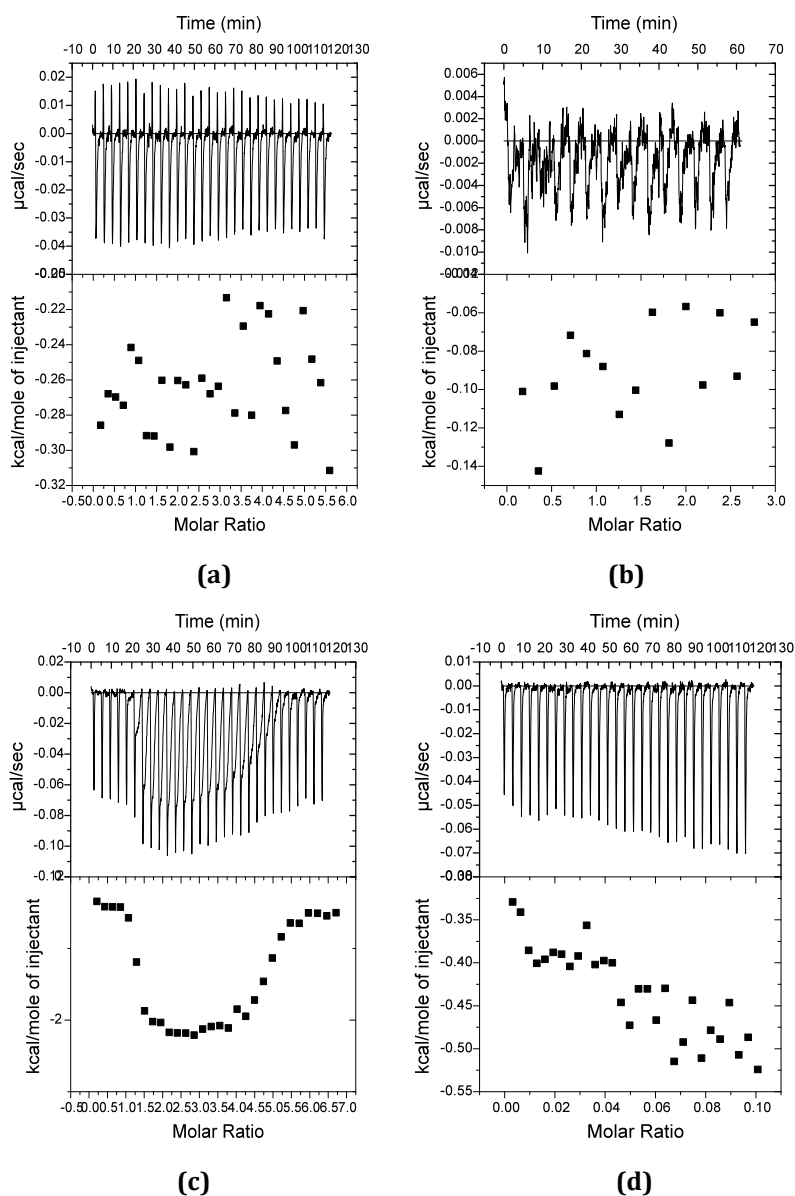


**Figure F.1** (a)  $20\mu\text{M}$  hGH+ $500\mu\text{M}$  P-1, in pH=7, 10mM Phosphate Buffer (PB)  
 (b)  $20\mu\text{M}$  hGH+ $500\mu\text{M}$  P-3, in pH=7 10mM PB  
 (c)  $15\mu\text{M}$  hGH+ $450\mu\text{M}$  P-4, in pH=7 10mM PB+100mM NaCl  
 (d) Dilution Buffer+  $450\mu\text{M}$  P-4, in pH=7 10mM PB +10mM NaCl

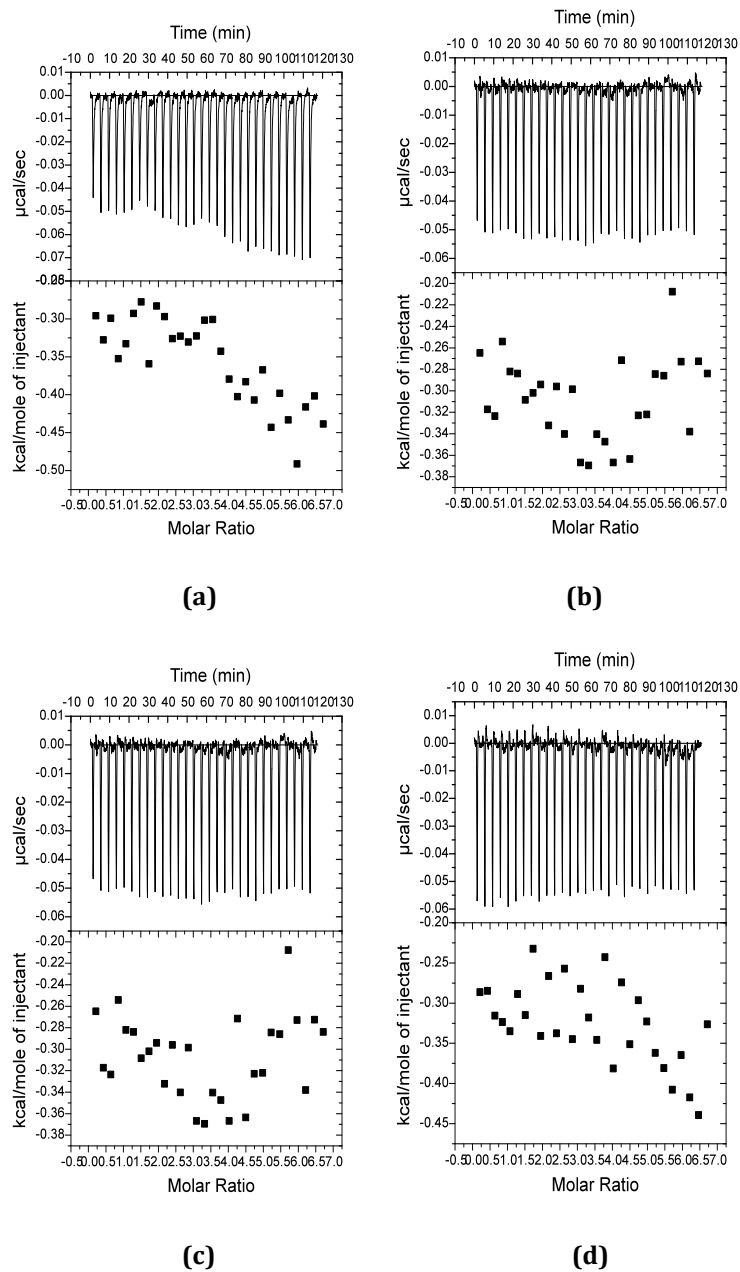
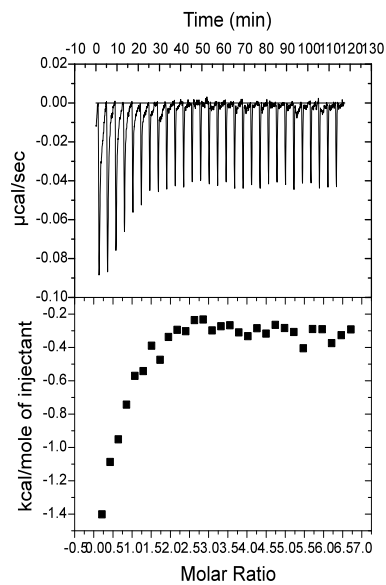
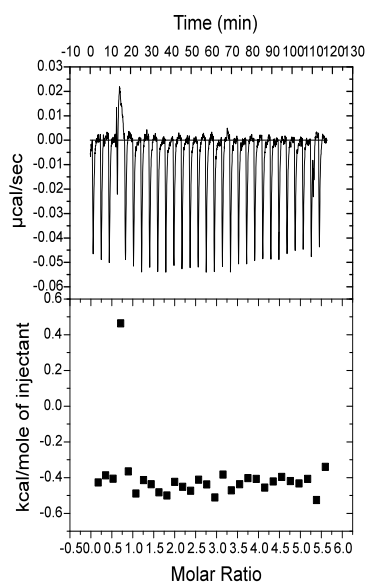


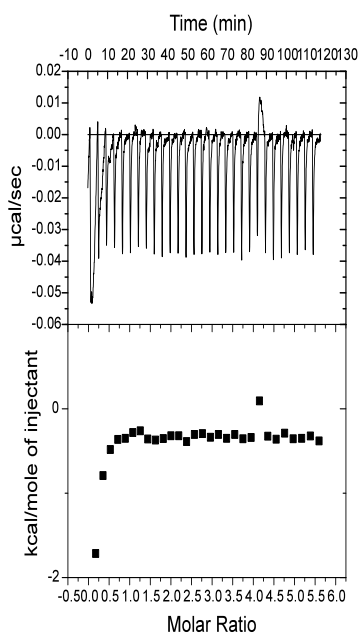
**Figure F.2** (a) 20 $\mu$ M hGH+600 $\mu$ M P-5, in pH=7 10mM PB+100mM NaCl  
 (b) 15  $\mu$ M hGH+450  $\mu$ M P-4, in pH=3.5 10mM citrate Buffer (CB)+100 mM NaCl  
 (c) 15  $\mu$ M hGH+450  $\mu$ M P-4, in pH=4.5 10mM CB+100 mM NaCl  
 (d) 15  $\mu$ M hGH+450  $\mu$ M P-4, in pH=5.5 10mM CB+100 mM NaCl



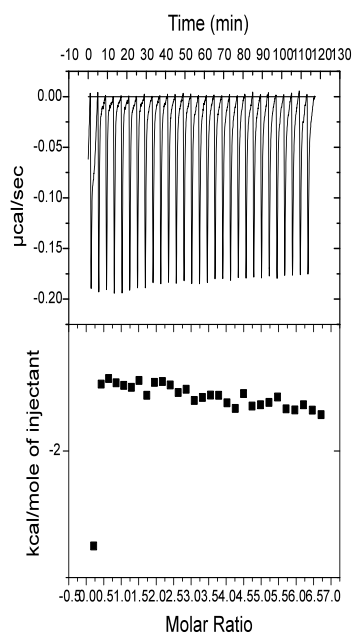
(a)



(b)

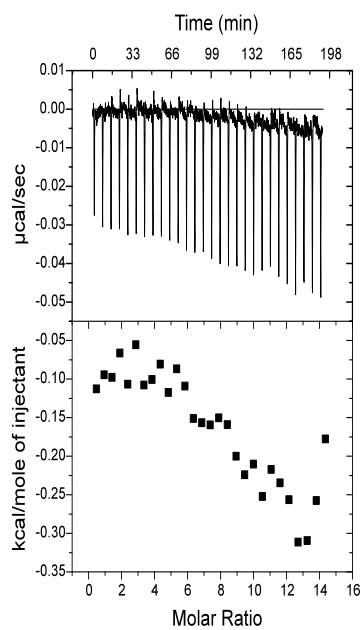


(c)

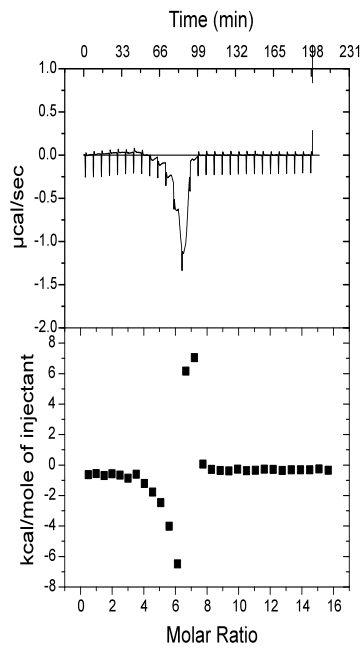


(d)

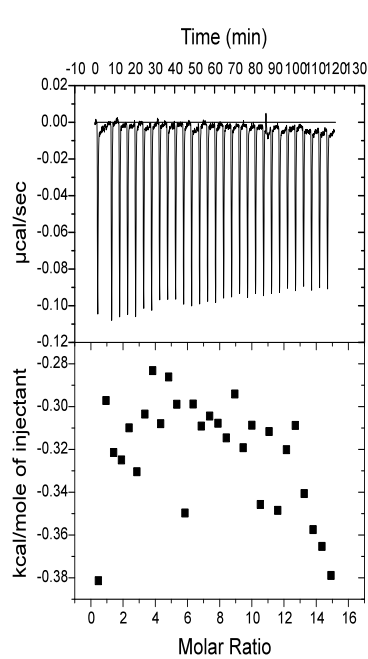
**Figure F.3** (a)  $15\mu\text{M}$  hGH+ $450\mu\text{M}$  L, in pH=7.5 PBS Buffer  
 (b)  $18\mu\text{M}$  hGH+ $450\mu\text{M}$  L, in pH=7.5 30mM HEPES Buffer  
 (c)  $18\mu\text{M}$  hGH+ $395\mu\text{M}$  L, in pH=5.5 30 mM HEPES Buffer  
 (d)  $15\mu\text{M}$  hGH+ $450\mu\text{M}$  L, in pH=6.5 30mM Tris- Buffer



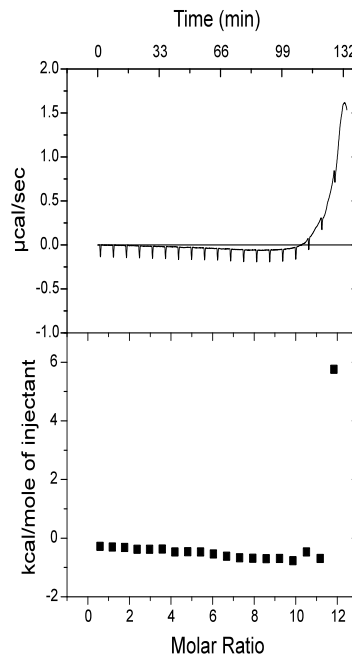
(a)



(b)

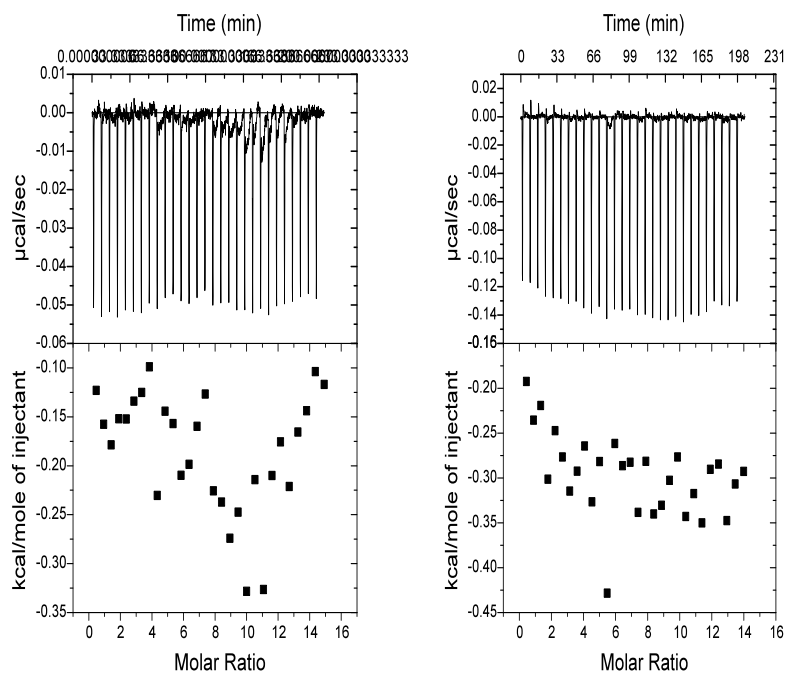


(c)



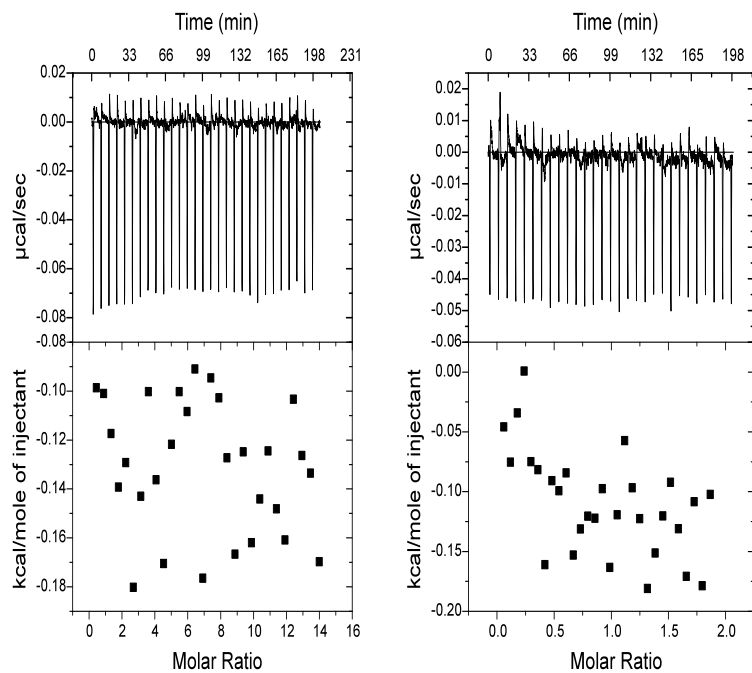
(d)

**Figure F.4** (a)  $15\mu\text{M}$  hGH+ $1.3\text{mM}$  3/8, in pH=7.5  $30\text{mM}$  HEPES+ $50\text{mM}$  NaCl  
 (b)  $15\mu\text{M}$  hGH+ $1\text{mM}$  3/6, in pH=7.5  $30\text{mM}$  Tris+ $50\text{mM}$  NaCl  
 (c)  $18\mu\text{M}$  hGH+ $1.15\text{mM}$  3/7, in pH=7.5  $30\text{mM}$  Tris+ $50\text{mM}$  NaCl  
 (d)  $15\mu\text{M}$  hGH+ $1.27\text{mM}$  2/2-3/9, in pH=7.5  $30\text{mM}$  Tris+ $50\text{mM}$  NaCl



(a)

(b)



(c)

(d)

**Figure F.5** (a)  $15\mu\text{M}$  hGH +  $1\text{ mM}$  3/8, in pH=8.5  $30\text{mM}$  Tris +  $50\text{mM}$  NaCl  
 (b)  $20\mu\text{M}$  hGH +  $1.34\text{mM}$  3/8, in pH=7.5 TBS  
 (c)  $20\mu\text{M}$  hGH +  $1\text{mM}$  3/5, in pH=7.5 TBS  
 (d)  $15\mu\text{M}$  hGH +  $1.27\text{mM}$  2/2-3/9, in pH=7.5 TBS

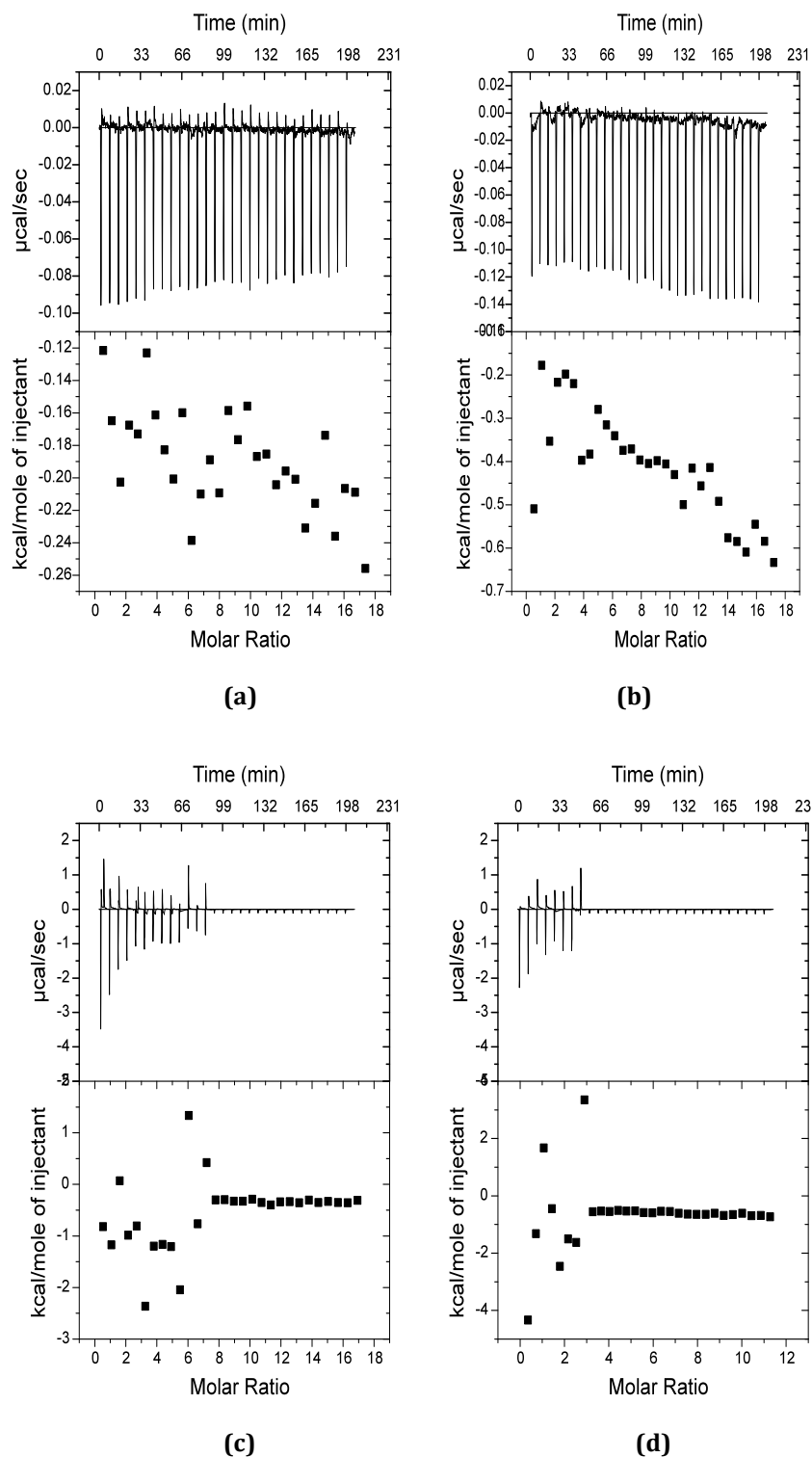


**Figure F.6** (a)  $15\mu\text{M hGH} + 1.115\text{ mM } 3/29$ , in pH=7.5 TBS  
 (b)  $15\mu\text{M hGH} + 1.035\text{ mM } 3/16$ , in pH=7.5 TBS  
 (c)  $15\mu\text{M hGH} + 1.153\text{ mM } 3/31$ , in pH=7.5 TBS  
 (d)  $15\mu\text{M hGH} + 0.756\text{ mM } 3/31$ , in pH=7.5 TBS

## APPENDIX G

### HPLC RESULTS FOR hGH-Peptide Binding

**Table G.1** Conditions for HPLC system for interaction analyses

Column	: Hydrophilic gel filtration column, 5 $\mu$ m
Column dimensions	: 4.6 $\times$ 250 mm
System	: Size exclusion chromatography
Mobile phase	: 50mM TBS Buffer
Mobile phase flow rate	: 0.6 mL/min
Column temperature	: 30°C
Detector type and wavelength	: Agilent 1100 UV detector, 280 nm
Detector temperature	: 30°C
Injection volume	: 50 $\mu$ L
Analysis period	: 15 min

**Table G.2** Preliminary HPLC study for detection of hGH and phage display selected peptides' interaction

	Concentration	Area	Retention time	Height
<b>hGH</b>	0.2 mg mL <sup>-1</sup>	648,4	4,817	28,1
<b>3/6</b>	0.2 mg mL <sup>-1</sup>	2001,5	5,354	91,9
<b>Complex</b>	peak 1	647	4,814	29
	peak 2	2002,8	5,345	92
<b>hGH</b>	0.2 mg mL <sup>-1</sup>	650,3	4,813	26,4
<b>3/19</b>	0.05 mg mL <sup>-1</sup>	1646,8	7,854	38,6
<b>Complex</b>	peak 1	794	4,826	30,6
	peak 2	1486,1	7,891	34,6
<b>hGH</b>	0.2 mg mL <sup>-1</sup>	650,3	4,813	26,4
<b>3/31</b>	0.05 mg mL <sup>-1</sup>	2021,2	6,992	59,5
<b>Complex</b>	peak 1	662,3	4,816	27,1
	peak 2	2032,4	7,035	60,6
<b>hGH</b>	0.2 mg mL <sup>-1</sup>	650,3	4,813	26,4
<b>3/5</b>	0.2 mg mL <sup>-1</sup>	1011,2	8,494	7,9
<b>Complex</b>	peak 1	694,3	4,816	27,5
	peak 2	973,5	8,494	7,1

**NOTE:** Peptides peaks for 3/8, 3/7, 3/16 and 3/29 were not observed by HPLC even at higher peptide concentrations, 1mg mL<sup>-1</sup>.

## APPENDIX H

### SURFACE PLASMON RESONANCE RUNS

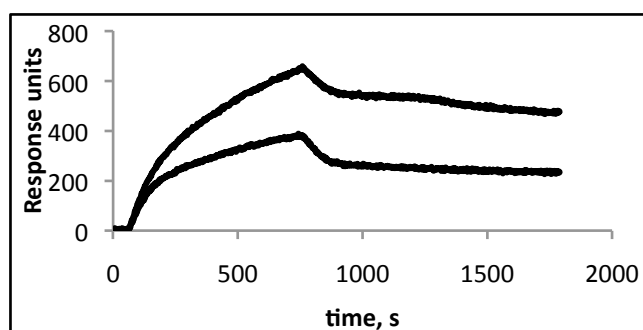


**Figure H.1** Sensogram for P-1 binding to hGH  $C_p=0.75 \text{ mg mL}^{-1}$ , upper curve: control, lower curve: actual run

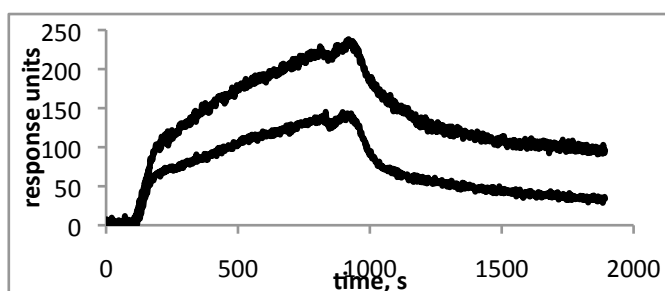


**Figure H.2** Sensogram for P-1 binding to hGH  $C_p=0.25 \text{ mg mL}^{-1}$ , upper curve: control, lower curve: actual run

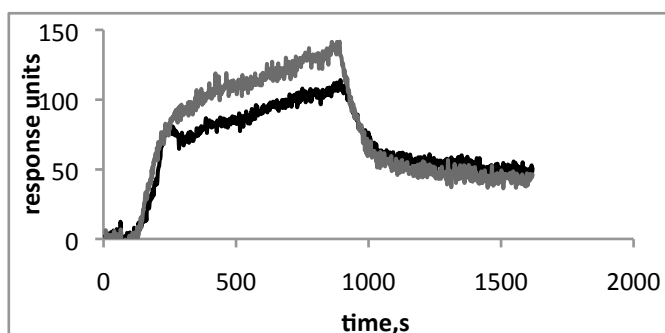


**Figure H.3** Sensogram for P-2 binding to hGH  $C_p=0.25 \text{ mg mL}^{-1}$ , upper gray curve: control, lower black curve: actual run

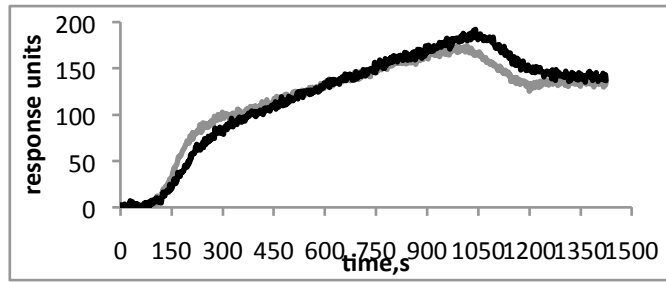


**Figure H.4** Sensogram for 3/8 binding to hGH  $C_p=0.1 \text{ mg mL}^{-1}$ , gray curve: control, black curve: actual run

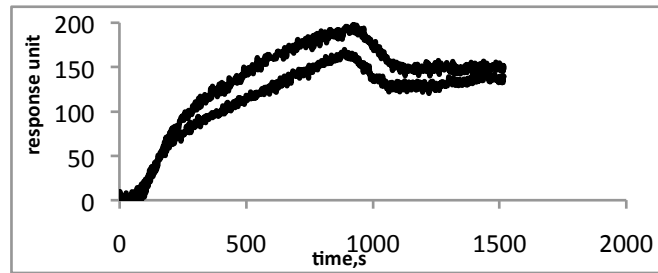


**Figure H.5** Sensogram for 2/2-3/9 binding to hGH  $C_p=0.2 \text{ mg mL}^{-1}$ , upper curve: control 1M ethanolamine, lower curve: actual run hGH attached to the surface

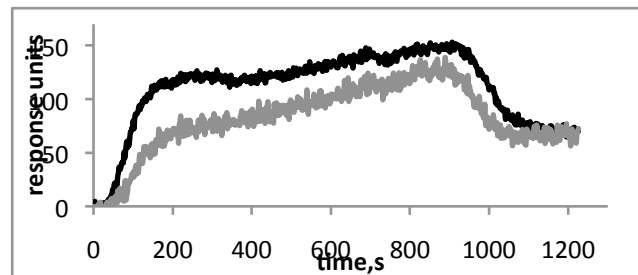


**Figure H.6** Sensogram for 2/2-3/9 binding to hGH  $C_p=0.15 \text{ mg mL}^{-1}$ , upper curve: control 10M glycine, lower curve: actual run hGH attached to the surface

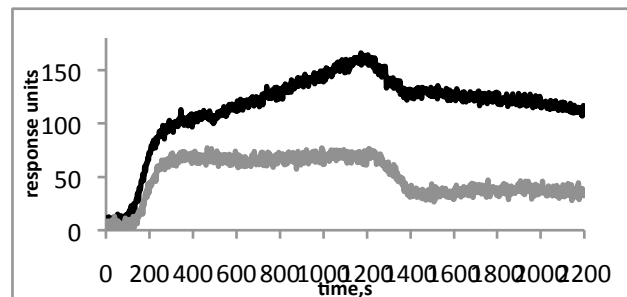


**Figure H.7** Sensogram for 2/2-3/9 binding to hGH  $C_p=0.15 \text{ mg mL}^{-1}$ , upper curve: actual run hGH attached to the surface, lower curve: control  $0.25 \text{ mg mL}^{-1}$  BSA actual run hGH attached to the surface